Calhoun
Institutional Archive of the Naval Postgraduate School

**Calhoun: The NPS Institutional Archive**

**DSpace Repository**

Theses and Dissertations 1. Thesis and Dissertation Collection, all items

1963

# The acquisition, reduction, and analysis of turbulence data associated with PA configuration approaches to carrier landings.

Oldmixon, W. J.

Princeton University

http://hdl.handle.net/10945/11553

*Downloaded from NPS Archive: Calhoun*

DUDLEY KNOX LIBRARY

Calhoun is the Naval Postgraduate School's public access digital repository for research materials and institutional publications created by the NPS community. Calhoun is named for Professor of Mathematics Guy K. Calhoun, NPS's first appointed -- and published -- scholarly author.

Dudley Knox Library / Naval Postgraduate School
411 Dyer Road / 1 University Circle
Monterey, California USA 93943

http://www.nps.edu/library

NPS ARCHIVE
1963
OLDMIXON, W.

# PRINCETON UNIVERSITY

## DEPARTMENT OF AERONAUTICAL ENGINEERING

Library
U. S. Naval Postgraduate School
Monterey, California

DUDLEY KNOX LIBRARY
NAVAL POSTGRADUATE SCHOOL
MONTEREY CA 93943-5101

[redacted]

# THE ACQUISITION, REDUCTION, AND ANALYSIS OF TURBULENCE DATA ASSOCIATED WITH PA CONFIGURATION APPROACHES TO CARRIER LANDINGS

by

W. J. Oldmixon, Lieutenant, USN

Report No. 653 July 1963

Submitted in partial fulfillment of the requirements for the degree of Master of Science in Engineering from Princeton University, 1963.

Library
U. S. Naval Postgraduate School
Monterey, California

# ACKNOWLEDGEMENTS

The author wishes to express his appreciation and gratitude to Professor Edward Seckel, of the Department of Aeronautical Engineering of Princeton University, whose ideas and suggestions form the basis of this investigation.

Appreciation is also expressed to Mr. Martin Lamers, of the Netherlands, whose suggestions and material assistance were essential to the completion of this study.

Finally, the author wishes to thank all those members of the Forrestal staff whose instructions and suggestions regarding the operation and use of the necessary electronic equipment greatly facilitated the progress of the data analysis.

# TABLE OF CONTENTS

| | | Page |
|---|---|---|
| | SUMMARY | i |
| | LIST OF TABLES | ii |
| | LIST OF FIGURES | iii |
| | NOMENCLATURE | iv |
| I | INTRODUCTION | 1 |
| II | EQUIPMENT AND PROCEDURE | 3 |
| III | DISCUSSION AND ANALYSIS | 10 |
| IV | RESULTS | 36 |
| V | CONCLUSIONS AND RECOMMENDATIONS | 40 |
| VI | REFERENCES | 41 |
| | TABLES | 42 |
| | FIGURES | |

# SUMMARY

An analysis was made of flight test data to obtain information representing the atmospheric turbulence inputs to the test aircraft. The basis of the method was the use of the linearized equations of motion of the aircraft, with the addition of certain terms representing the aerodynamic effects of the turbulence on the aircraft.

These equations were set up on an analog computer and verified by the technique of matching transient response flight data. Then, through the use of a feedback system, the desired turbulence quantities were obtained as system outputs. Inputs to the system were the aircraft response and control deflections, obtained from the flight test data.

The method was found to be valid, assuming the aircraft analogue was correct. The resulting data appeared suitable for further analysis to determine its statistical qualities.

# LIST OF TABLES

Page

I RECORDED FLIGHT TEST DATA QUANTITIES 42

II RECORDED FLIGHT DATA QUANTITIES, TELEMETERING CHANNELS UTILIZED 44

III WIND CONDITIONS DURING CARRIER TEST APPROACHES (Headwind and Crosswind Components) 45

IV RMS VALUES OF TURBULENCE QUANTITIES 46

# LIST OF FIGURES

1. F4B LONGITUDINAL ANALOG
2. F4B LATERAL ANALOG
3. AILERON - SPOILER CALIBRATION CURVES
4. MATCHED RUDDER RESPONSE
5. MATCHED RESPONSE TO RUDDER DOUBLET
6. MATCHED RESPONSE TO AILERON DOUBLE STEP
7. MATCHED STABILATOR PULSE RESPONSE
8. MATCHED RESPONSE TO STABILATOR DOUBLET
9. MATCHED RESPONSE TO STABILATOR PULSE
10. NAVION PRELIMINARY ANALYSIS CIRCUIT
11. INITIAL LATERAL GUST ANALYSIS CIRCUIT
12. FINAL LATERAL GUST ANALYSIS CIRCUIT
13. SIMULATED $\beta_g$ INPUT AND ANALOG RESPONSE QUANTITIES
14. SIMULATED $\beta_g$ QUANTITY REPRODUCTIONS
15. LONGITUDINAL GUST ANALYSIS CIRCUIT
16. through 31. LATERAL AND LONGITUDINAL GUST QUANTITIES
32. INITIAL BURBLE ENCOUNTER FOR VARIOUS APPROACHES
33. LATERAL AND LONGITUDINAL GUST PLOT

# NOMENCLATURE

| | |
|---|---|
| PA | Power approach |
| $C_L$ | Lift coefficient, lift/qS |
| $C_m$ | Pitching moment coefficient, pitching moment/qS |
| $C_\ell$ | Rolling moment coefficient, rolling moment/qSb |
| $C_n$ | Yawing moment coefficient, yawing moment/qSb |
| $C_y$ | Lateral force coefficient, lateral force/qS |

$$C_{L_\alpha} = \frac{\partial C_L}{\partial \alpha}$$

$$C_{m_\alpha} = \frac{\partial C_m}{\partial \alpha}$$

$$C_{\ell_\beta} = \frac{\partial C_\ell}{\partial \beta}$$

$$C_{n_\beta} = \frac{\partial C_n}{\partial \beta}$$

$$C_{y_\beta} = \frac{\partial C_y}{\partial \beta}$$

$$C_{\ell_p} = \frac{\partial C_\ell}{\partial (pb/2V)}$$

$$C_{n_p} = \frac{\partial C_n}{\partial (pb/2V)}$$

$$C_{\ell_r} = \frac{\partial C_\ell}{\partial (rb/2V)}$$

$$C_{y_r} = \frac{\partial C_y}{\partial (rb/2V)}$$

$$C_{m_{d\alpha}} = \frac{\partial C_m}{\partial \left( \frac{d\alpha}{d\,t/\tau} \right)}$$

$$C_{L_{\delta_s}} = \frac{\partial C_L}{\partial \delta_s}$$

$$C_{m_{\delta_s}} = \frac{\partial C_m}{\partial \delta_s}$$

$$C_{y_{\delta_r}} = \frac{\partial C_y}{\partial \delta_r}$$

$$C_{\ell_{\delta_r}} = \frac{\partial C_\ell}{\partial \delta_r}$$

$$C_{n_{\delta_r}} = \frac{\partial C_n}{\partial \delta_r}$$

$$C_{\ell_{\delta_a}} = \frac{\partial C_\ell}{\partial \delta_a}$$

$$C_{n_{\delta_a}} = \frac{\partial C_n}{\partial \delta_a}$$

$$C_{n_r} = \frac{\partial C_n}{\partial (rb/2V)}$$

$$C_{y_p} = \frac{\partial C_y}{\partial (rb/2V)}$$

$$C_{m_{d\theta}} = \frac{\partial C_m}{\partial \left( \frac{d\theta}{d\,t/\tau} \right)}$$

| | |
|---|---|
| $I_x$ | moment of inertia about x axis, slug - $ft^2$ |
| $I_y$ | moment of inertia about y axis, slug - $ft^2$ |
| $I_z$ | moment of inertia about z axis, slug - $ft^2$ |
| S | wing area, $ft^2$ |
| V | true airspeed, ft/second |
| $V_o$ | initial airspeed, ft/second |
| W | aircraft weight |
| H | pitching moment of inertia parameter = $\frac{2I_y}{m\mu c^2}$ |

| | |
|---|---|
| b | wing span, ft. |
| c | wing chord, ft. |
| $\bar{c}$ | mean aerodynamic chord, ft. |
| g | acceleration due to gravity, $ft/sec^2$ |
| h | aircraft altitude, ft. |
| m | aircraft mass, slugs |
| n | normal acceleration, $a_z/g$ |
| $a_z$ | normal acceleration, $ft/sec^2$ |
| $a_y$ | lateral acceleration, $ft/sec^2$ |

p = $\dot{\varphi}$ = rolling velocity, radians/sec.

q = $\dot{\theta}$ = pitching velocity, radians/sec.

r = $\dot{\psi}$ = yawing velocity, radians/sec.

t = time, seconds

u = longitudinal velocity perturbation

v = lateral velocity perturbation

w = normal velocity perturbation

# I INTRODUCTION

In accordance with a proposal submitted to the Bureau of Naval Weapons, the James Forrestal Research Center at Princeton University in late 1962 undertook an investigation into the lateral flying qualities of operational Navy aircraft in the PA configuration approach to carrier landings.

As noted in Reference 1, the official proposal, it is typical that during this type of approach the lateral stability and control characteristics of some high performance aircraft deteriorate with increasing angle of attack and decreasing airspeed. This is common in many current sweptwing aircraft. The situation is aggravated by the added difficulty of approach and landing on aircraft carriers, where the pilot is required to maintain a flightpath with extremely narrow tolerances. The difficulty is further compounded by natural atmospheric disturbances, and those caused by the airflow about the carrier hull and superstructure, which are often encountered in the final few seconds prior to touch-down.

It was therefore proposed that a flying qualities research program be conducted at Princeton, utilizing a variable stability aircraft to obtain pilot opinion ratings. The approach to a carrier was to be simulated as closely as possible, including effects of the forementioned atmospheric disturbances. These turbulence effects were to take the form of recorded signals applied as inputs to the electronic servos driving the control surfaces of the variable stability aircraft. It was therefore considered desirable to represent the turbulence as accurately as possible

since this factor would probably have an important effect on pilot rating in this particular investigation.

To this end, a suitably instrumented Navy fighter aircraft from the Naval Air Test Center, Patuxent River, Maryland, made a series of actual carrier approaches under varying conditions of wind velocity across the deck and cross wind component. Recordings were made of the aircraft response in five degrees of freedom, together with recordings of the various control surface deflections. These data were analyzed on an analog computer setup of the aircraft equations of motion. By a process to be described, it was possible to determine the atmospheric disturbance information in a form suitable for application to the variable stability aircraft.

This report is concerned with the first phase of this research project: the acquisition, reduction, and analysis of the flight test data associated with the carrier approaches made by the Naval Air Test Center aircraft.

## II EQUIPMENT AND PROCEDURE

### 1) FLIGHT TEST EQUIPMENT

The data acquisition flights were flown in an F4B fighter aircraft piloted by Navy test pilots from the Naval Air Test Center. The F4B (Phantom II) is a two-place, swept-wing, high-performance interceptor manufactured by the McDonnell Aircraft Corporation of St. Louis. It is powered by two General Electric J-79 turbojet engines, each producing a maximum of 17,000 pounds thrust at sea level.

The aircraft was completely instrumented for the data acquisition by the Instrumentation Branch of the Flight Test Division, Naval Air Test Center. The rear cockpit seat was removed from the aircraft to provide space for the instrumentation package. A summary of the flight instrumentation follows:

Power Supply: The basic aircraft power package was utilized as the instrumentation power source. This consisted of the normal 28 volt DC supply, and 115 volt, 400 cycle AC source.

Sensing and Transducing: The physical quantities measured by the instrumentation system are shown in Table I. Potentiometer type transducers were chosen in order to provide compatibility with the telemetering system. The potentiometers provided signals of adequate magnitude, and through their excitation source also provided zero and full scale reference voltage for the telemetering unit.

Table I also lists the basic instrument used in the measurement of each quantity. The rate gyros which sensed the various angular velocities, and the potentiometers which measured the required position angles,

were all types commonly used in flight test instrumentation. It should be noted that the actual control surface deflections were measured rather than simple stick and pedal deflections, due to the non-linear characteristics of the stability augmentation system. Use of the actual deflections permitted the aircraft equations of motion to be written in simple form.

Airspeed and altitude were measured by W. O. Leonard force balance type transducers. These units were located on the lower shelf of the rear cockpit instrumentation sled, as shown in Reference 2. The transducers, operating on the force balance principle, provided linear outputs for airspeed and altitude without the use of cams, function gears, shunts, etc. The force sensors were isolated from the output devices, thus minimizing response to transients. As a result, the units were characterized by a pressure accuracy of up to .1%. In the case of the altimeter this meant accuracy to within three inches for a two hundred foot aircraft altitude.

Lateral and normal acceleration were sensed by Donner model 4310 linear accelerometers installed with a range of ± .5 G and ± 2.0 G, respectively. These units exhibited natural frequencies much higher than the test aircraft, thus precluding resonance problems. Their response was essentially flat to 8 cps. It was determined, however, during installation, that some H. F. system noise was being passed by the accelerometer. In order to eliminate this noise, a low pass filter was therefore designed and installed between the accelerometer output and the telemetering unit.

The filter, designed for a 5 cps corner frequency, eliminated the high frequency noise but provided essentially flat response over the

expected aircraft response range, which was estimated to be no higher than 1 cps, well above the Dutch roll frequency.

A schematic of the filter circuit is shown below, together with a sketch of the filter frequency response characteristic:

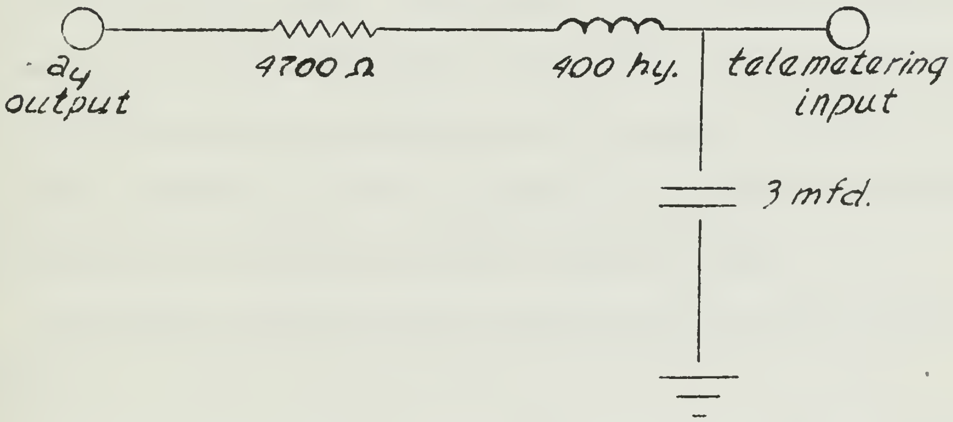

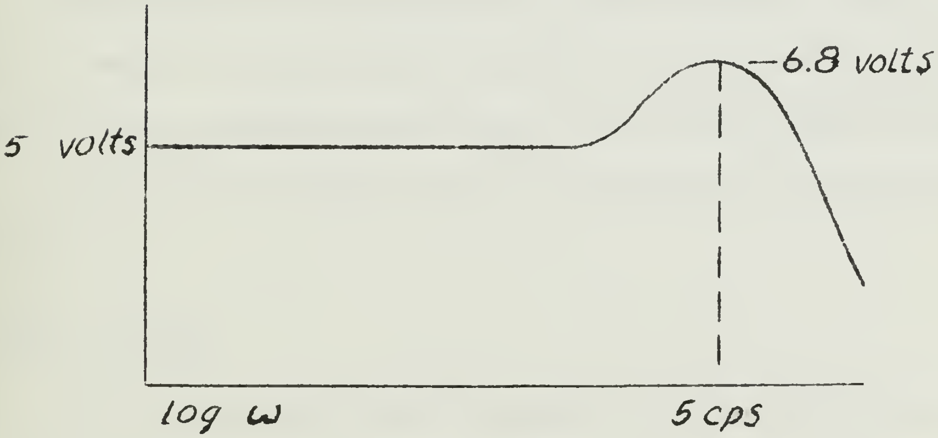

Telemetering and Recording: Telemetering equipment of the pulse width type was installed in the aircraft as part of the instrumentation package. This equipment, manufactured by the Applied Science Corporation of Princeton (ASCOP), was the manufacturer's D Series Pulse Width Multicoder-Telemeter, capable of sampling up to 43 channels at a sampling rate

of 20 times per channel per second, using a Model DSG20 Commutator-Gear Box.

Since each channel was sampled 20 times per second, it was felt that good fidelity would be obtained with input frequencies as high as the 2 to 5 cps range. Many of the measured quantities were sampled on each of two or three channels, and in these cases it was felt that good reproduction was assured at all frequencies encountered in the investigation. Table II lists the measured quantities and the number of sampling channels used for each. For those quantities sampled in more than one channel, the sampling was, as far as possible, equally spaced in time.

The sampled data were then converted into PW data by the Model DKH-I Keyer.

The pulse width information was then recorded directly in the aircraft by means of an Ampex Model 800 tape transport which was mounted, together with its associated power supply, in the rear cockpit installation.

Provisions were also made for simultaneous voice recording by the test pilot.

## 2) GROUND EQUIPMENT

The following units were available at the Forrestal Research Center for analysis of the flight test data:

Magnetic Tape Recorder: An Ampex Model 309C dual track, three speed tape recorder was available for playback of the recorded flight data, and also for use in the preliminary analysis studies which were conducted.

Telemetering Ground Station: The telemetering unit used for decoding the taped pulse width flight test data was the ASCOP M Series PW

Ground Station. This unit continuously sampled the recorded pulse width information and converted this data into continuous voltage form. The information in this form was then compatible with the analog computer for analysis purposes.

GEDA Analog Computer: The basic tool in the analysis process was the Model L3 (GEDA) linear electronic differential analyzer, manufactured by the Goodyear Aircraft Corporation. This computer provided twenty-four automatically stabilized DC computing amplifiers, each with an open loop gain of greater than $5 \times 10^7$, and with negligible drift. The computer incorporated an automatic error indicator, and had a guaranteed accuracy of 1%. There were provisions for accurately setting computer board potentiometers using a special null indicator.

Data Recorder: Visual presentation of data was made possible by a Sanborn Model 154-100B four channel recorder. This instrument had a very high natural frequency (42 cps), and low frequency response flat to zero cps.

## 3) INSTRUMENT CALIBRATION

Calibration of the flight test instrumentation was conducted by the Instrumentation Branch of the Flight Test Division, Naval Air Test Center. The calibration charts are shown in Reference 2. All gradients were determined to be essentially linear within the range of measured data encountered during the test flights.

## 4) PROCEDURE

Data Acquisition:

In December, 1962, the instrumented F4B aircraft, piloted by a Navy test pilot, made a series of thirty-three landing approaches to the aircraft carrier USS Enterprise. These approaches and landings were made over a span of five separate flights. The heading and speed of the carrier were varied during the course of the series to provide a number of different conditions of wind velocity across the deck, and cross wind component. The wind conditions for each approach are shown in Table III.

It was expected that the most severe turbulence conditions would be experienced in the presence of a "right to left" crosswind. This was due to the extremely turbulent flow about the carrier "island" being directed into the path of an approaching aircraft, usually at the critical point occurring a few seconds prior to touchdown. It was felt that by making the approaches under varying wind conditions, it would be possible to obtain turbulence data which would be representative of the full range of severity normally encountered. As noted in Reference 3, the turbulence "burble" associated with the Enterprise was probably the extreme, due to the very boxlike design of the ship's "island".

The Naval Air Test Center provided facilities aboard the Enterprise for tape playback after each test flight. On the spot assessment of data quality was thus possible, and minor adjustments were made, as necessary, in the instrumentation.

## Aircraft Calibration:

Since the basis of a successful analysis of the flight test data was to be the setup of the aircraft equations of motion on the analog computer, it was necessary, as the next step, to obtain a valid set of equations representing the F4B aircraft in the PA configuration. The basic method used was the matching, on the computer, of transient response flight test data. The method will be discussed in some detail in a subsequent section.

To this end, two additional flights were made of the test aircraft for the purpose of obtaining transient response data. The aircraft was flown in the PA configuration, and pilot control inputs of the pulse, step, and doublet types were made. The aircraft response was recorded as before.

In order to prevent stability augmentation equipment inputs to the system, these units were made inoperative during the transient response data runs.

## Data Analysis:

Having thus acquired the necessary flight test data, the actual analysis was then conducted at the Forrestal Research Center. This analysis is discussed in detail in the following section of this report.

## III DATA ANALYSIS: DESCRIPTION AND DISCUSSION

The first step in the data analysis was the determination of a valid set of differential equations representing the F4B aircraft in the PA configuration. It was assumed that the motions of the aircraft while approaching a carrier in this configuration could be described by the usual linear equations. This assumption seemed valid since the final part of a typical carrier approach, where the turbulence effects are normally most severe, is basically a constant power, constant airspeed, shallow descent to a touchdown; the aircraft motions are approximately perturbations from the steady state glide path.

The resulting equations are shown below, written in dimensional form for compatibility with the flight data and analog computer. For convenience, the terms of each equation have been divided by the coefficient of the highest appropriate derivative. The assumption was also made that the aircraft forward velocity remained essentially constant during the runs, thus eliminating the drag equation, and also eliminating longitudinal velocity terms from the remaining equations.

Longitudinal:

(1) lift equation:

$$\dot{\alpha} - \dot{\theta} + \left[ \frac{C_{L_\alpha}}{2\,\tau} \right] \alpha + \left[ \frac{C_{L_{\delta_s}}}{2\tau} \right] \delta_s = 0$$

(2) pitch equation:

$$\ddot{\theta} - \left[ \frac{C_{m_{d\theta}}}{H\tau} \right] \dot{\theta} - \left[ \frac{C_{m_{d\alpha}}}{H\tau} \right] \dot{\alpha} - \left[ \frac{C_{m_\alpha}}{H\tau^2} \right] \alpha - \left[ \frac{C_{m\delta_s}}{H\,\tau^2} \right] \delta_s = 0$$

(3) normal acceleration: $a_z = -C_{L_\alpha}\left(\frac{V_0}{2\tau}\right)\alpha + C_{L_{\delta_s}}\left(\frac{V_0}{2\tau}\right)\delta_s$

Lateral:

(4) side force: $$\dot{\beta} - \left[\frac{C_{y_\beta}}{2\tau}\right]\beta + \dot{\psi} - \left[\frac{C_{y_r}}{4\mu}\right]\dot{\psi} - \left[\frac{C_L}{2\tau}\right]\varphi - \left[\frac{C_{y_p}}{4\mu}\right]\dot{\varphi} - \left[\frac{C_{y_{\delta_a}}}{2\tau}\right]\delta_a - \left[\frac{C_{y_{\delta_r}}}{2\tau}\right]\delta_r = 0$$

(5) roll equation: $$\ddot{\varphi} - \left[\frac{C_{\ell_p}}{2J_x\tau}\right]\dot{\varphi} - \left[\frac{C_{\ell_r}}{2J_x\tau}\right]\dot{\psi} - \left[\frac{\mu C_{\ell_\beta}}{J_x\tau^2}\right]\beta - \left[\frac{\mu C_{\ell_{\delta_a}}}{J_x\tau^2}\right]\delta_a - \left[\frac{\mu C_{\ell_{\delta_r}}}{J_x\tau^2}\right]\delta_r = 0$$

(6) yaw equation: $$\ddot{\psi} - \left[\frac{C_{n_r}}{2J_z\tau}\right]\dot{\psi} - \left[\frac{C_{n_p}}{2J_z\tau}\right]\dot{\varphi} - \left[\frac{\mu C_{n_\beta}}{J_z\tau^2}\right]\beta - \left[\frac{\mu C_{n_{\delta_a}}}{J_z\tau^2}\right]\delta_a - \left[\frac{\mu C_{n_{\delta_r}}}{J_z\tau^2}\right]\delta_r = 0$$

These uncoupled sets of equations were then separately mechanized on the GEDA analog computer. Schematic circuit diagrams of the two setups are shown in Figures 1 and 2.

All factors in these equations were known accurately, except for the various stability derivatives. Approximate values for the derivatives, for the PA configuration, were obtained from a report of the McDonnell Aircraft Corporation. These values determined the initial potentiometer settings for the computer setups. Shown below is a list of the various quantities utilized in the initial formulation of the aircraft equations for the PA configuration:

$V_o$ = 134 knots = 224 feet per second

$W$ = 34000 lbs.

$\alpha_o$ = 16 degrees

$C_{L_o}$ = 1.1

$\rho$ = .002378 slug/ft$^3$

$b$ = 39 feet

$S$ = 530 feet$^2$

$\bar{c}$ = 16 feet

$I_x$ = 23880 slug - ft$^2$

$I_y$ = 121007 slug - ft$^2$

$I_z$ = 131177 slug - ft$^2$

$C_{L_\alpha}$ = 3.05/radian

$C_{m_\alpha}$ = -.19

$C_{m_{\delta_s}}$ = -.421

$C_{L_{\delta_s}}$ = +.328

$C_{m_{d\theta}}$ = -.023

$C_{m_{d\alpha}}$ = -.0095

$C_{\ell_\beta}$ = -.240

$C_{\ell_{\delta_a}}$ = +.055

$C_{\ell_{\delta_r}}$ = -.010

$C_{\ell_p}$ = -.285

$C_{\ell_r} = +.225$

$C_{n_\beta} = +.205$

$C_{n_{\delta_a}} = -.006$

$C_{n_{\delta_r}} = -.075$

$C_{n_p} = +.036$

$C_{n_r} = -.330$

$C_{y_\beta} = -.625$

$C_{y_{\delta_r}} = +.125$

$C_{y_p} = +.950$

$C_{y_r} = +.780$

The equations of motion based on these values are as follows:

Longitudinal:

1. $\dot{\alpha} - \dot{\theta} + .406\ \alpha + .0436\ \delta_s = 0$

2. $\ddot{\theta} + .162\ \dot{\theta} + .067\ \dot{\alpha} + .357\ \alpha + .792\ \delta_s = 0$

3. $n + 2.81\ \alpha - .311\ \delta_s = 0$

Lateral:

4. $-\dot{\beta} - .0832\ \beta - .990\ \dot{\psi} + .0109\ \dot{\varphi} + .139\ \varphi + .0166\ \delta_r = 0$

5. $-\ddot{\varphi} - 1.25\ \dot{\varphi} + .986\ \dot{\psi} - 12.2\ \beta - .510\ \delta_r + 2.80\ \delta_a = 0$

6. $-\ddot{\psi} - .264\ \dot{\psi} + .0288\ \dot{\varphi} + 1.89\ \beta - .693\ \delta_r - .0556\ \delta_a = 0$

Improving the validity of these equations as representations of the aircraft thus required a more accurate determination of the stability

derivatives. This was accomplished by a transient response curve fitting technique, such as outlined in Reference 4, and described in detail in Reference 5. The mathematical basis for the validity of the method is found in Reference 6.

For this method a number of the transient response runs were selected by reference to Sanborn recordings of the aircraft response. The selection was made on the basis of freedom from telemetering dropouts, and relative freedom from apparent extraneous inputs, such as turbulence effects. These response curves were of the rudder pulse, rudder doublet, aileron step, aileron doublet, stabilator pulse, and stabilator doublet types.

Transparent overlays were made from the Sanborn records, incorporating the scale changes necessary to provide agreement with the scaling of the computer outputs. It was then possible, by means of the ground station equipment, to apply voltages to the aircraft analogue representing the actual aircraft control motions, as forcing functions to either the longitudinal or lateral sets, as appropriate. Sanborn recordings of the analog responses were made, all to the same scale as the transparent overlays. The two sets of data were compared, and by an iteration procedure, the potentiometer settings representing the various stability derivatives were changed until close agreement was attained between flight response and analog response.

In the lateral case the matched quantities were roll rate and yaw rate. It was found that a close match to the flight data could be fairly rapidly obtained by corrections to those derivatives which had major effects on the important lateral response parameters, i.e., Dutch roll

period and damping, initial roll and yaw magnitudes, spiral stability. Improvements to the initial match were obtained by a systematic iteration procedure, varying the potentiometer settings in turn until the desired match resulted.

In the initial study of the lateral responses it was immediately apparent that the flight data was not ideal. During even the best runs, the aircraft obviously had not been in steady flight at the instant of the control inputs; there were initial conditions which had to be considered in the matching process. By means of the analog initial condition circuitry it was possible to apply to the computer, as initial conditions, the actual flight data response in roll rate and yaw rate existing at the instant of control deflection. This was considered to be an improvement but it was noted that since the lateral equations represented a fourth order system, two additional initial conditions, $\beta$ and $\varphi$, for example, were necessary for accurate solution. These were not available and some error was thus to be expected. In the iteration procedure it was found that the best matches were obtained with flight data where the aircraft was very close to steady state flight conditions at the time of control deflection. This was to be reasonably expected since in these cases all initial conditions were approximately zero.

It was also apparent from observation of the flight data that some atmospheric turbulence existed during the tests. This, of course, could not be accounted for in the matching process, and was thus a source of error. For this reason the smoothest runs were selected for the matching process.

It was noted also that during the various transient response runs there were inadvertent inputs of those control surfaces which theoretically were being held in the neutral position. These inputs were also played into the analog.

It can be seen from Table I that only the left hand aileron and spoiler were instrumented for deflection measurement. Since the equations of motion as formulated on the computer were written in terms of aileron inputs, which are the sum of right and left aileron deflection, it was necessary to derive some function of left spoiler deflection which might be utilized as equivalent right aileron deflection. To this end, a calibration run was made to determine the relationship between aileron and spoiler deflection. The results were of the form shown in Figure 3. The relationship between the two was shown to be approximately linear. Therefore, it was possible to express right aileron as a linear function of the recorded spoiler deflection. The aileron signal fed to the analog was:

$$\delta_a = \delta_{a_L} + \delta_{a_R} = \delta_{a_L} - K\,\delta_{sp_L} \tag{7}$$

It can be seen from Figure 3 that each aileron exhibited a small upward deflection range of approximately three degrees. This property was ignored in determining the proportionality constant between aileron and spoiler. It was felt that the upward deflections were primarily for the purpose of assisting the effect of the spoiler deflections on the same wing. In the slightly open position the spoilers were assumed to be relatively ineffective in disrupting the airflow, and the small upward aileron deflection made up for the deficiency, thus maintaining system linearity.

By means of the analog limiter circuits, the voltages representing these upward aileron deflections were eliminated from the computer inputs.

It should be noted that in spite of the turbulence and initial condition problems, it was possible to obtain good matches between flight data and analog output. The accurate determination of all the various stability derivatives would probably have been difficult because of these problems, but the primary interest here was the matching of aircraft response. This could be done by matching the important lateral parameters mentioned previously. Since these parameters are primarily controlled by relatively few of the derivatives, it was possible to obtain a good match even though some of the derivatives might have been in error.

It should also be noted that since the instrumentation used in obtaining data for this matching was the same as subsequently used during the actual carrier approaches, then to the extent that any instrumentation errors would have caused false matching, the effect would tend to be cancelled during the actual approach data acquisition.

Shown below are the circuits utilized to provide inputs to the analog from the recorded data. By means of appropriate potentiometer settings the quantities were all scaled correctly for compatibility with the analog setup. Biasing of all quantities to the correct zero position was done by adjusting the biasing knobs of the ground station while referring to voltmeter readings of the various tape outputs.

Shown in Figures 4, 5, and 6 are some of the matched transient response curves. It is to be noted that the aileron step inputs were used primarily to match initial roll rate amplitude. It was felt that the aircraft

was out of the linear range shortly after application of an aileron step and this precluded any additional useful matching.

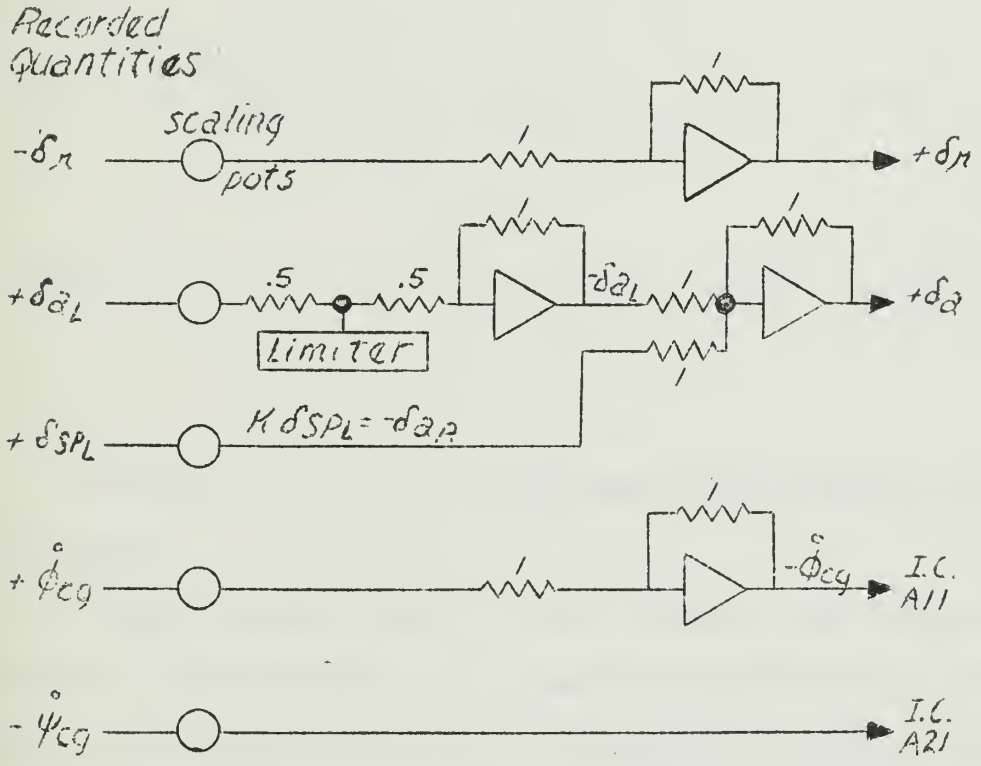
Recorded Quantities
scaling pots
$-\delta_r$
$+\delta_r$
$+\delta_{a_L}$
.5
.5
Limiter
$-\delta_{a_L}$
$+\delta_a$
$+\delta_{sp_L}$
$K\delta_{sp_L} = -\delta_{a_R}$
$+\dot{\phi}_{cg}$
$-\dot{\phi}_{cg}$
I.C. A11
$-\dot{\psi}_{cg}$
I.C. A21
1

The longitudinal responses were matched by comparing pitch rate and normal acceleration. The method utilized and the problems encountered were similar to those discussed in reference to the lateral equations. The phugoid mode was not visibly excited in any of the transient runs and, therefore, the matching was confined solely to the short period oscillations. The matching iteration procedure converged much more rapidly than in the lateral case. This was to be expected since in this longitudinal approximation there were only two degrees of freedom and, consequently, fewer controlling derivatives to be adjusted.

Shown below are the input circuits to the longitudinal analog:

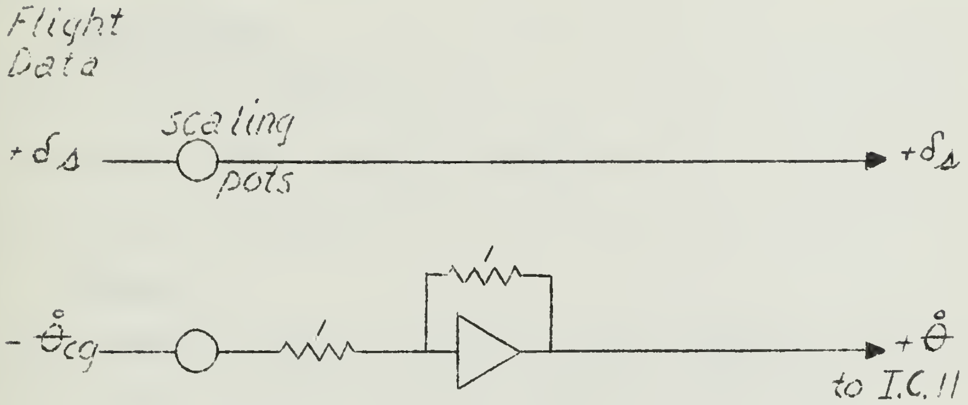

In Figures 7, 8, and 9 are shown some of the matched transient response curves.

It should be noted that the initial matching, both longitudinally and laterally, showed a number of discrepancies between the actual aircraft response and the analog response which was based on the stability derivatives obtained from the McDonnell report. In the lateral case the analog response showed a predicted Dutch roll period of approximately 4.5 seconds, with neutral damping. As can be seen in Figures 4 and 5, the aircraft actually exhibited a well damped Dutch roll of about a 3 second period. Longitudinally, the major discrepancy was in the apparent degree of aircraft static stability, which was considerably greater than the predicted value.

These discrepancies are illustrated more clearly by reference to the final equations of motion which resulted from the matching process. If these equations, which are shown below, are compared term by term with the

original set, the changes which had to be made during the matching are apparent.

Longitudinal:

(8) $\dot{\alpha} - \dot{\theta} + .472\ \alpha + .0436\ \delta_s = 0$

(9) $\ddot{\theta} + .838\ \dot{\theta} + .067\ \dot{\alpha} + 9.00\ \alpha + 4.50\ \delta_s = 0$

(10) $n + 3.25\ \alpha - .311\ \delta_s = 0$

Lateral:

(11) $-\dot{\beta} - .0956\ \beta - .990\ \dot{\psi} + .0110\ \dot{\varphi} + .140\ \varphi + .0209\ \delta_r = 0$

(12) $-\ddot{\varphi} - 2.48\ \dot{\varphi} - .984\ \dot{\psi} - 15.8\ \beta + .497\ \delta_r + 5.48\ \delta_a = 0$

(13) $-\ddot{\psi} - .569\ \dot{\psi} + .0288\ \dot{\varphi} + 3.38\ \beta - .674\ \delta_r - .061\ \delta_a = 0$

It can be seen that in the lateral set the directional stability and yaw damping, which are the primary parameters affecting Dutch roll period and damping, respectively, were each approximately doubled in the matching process. Longitudinally, it can be seen that the static stability was also increased considerably during the matching. Although the high value of $C_{m_\alpha}$, which finally produced a good match, was probably unrealistic it at least indicated that the predicted value was too low. It is noted again that accurate determination of each stability derivative was by no means assured. However, the aircraft response curves were fairly accurately matched, and this was the important point for purposes of this investigation.

With the equations of motion of the aircraft thus formulated, the next step was the actual analysis of the flight data to obtain the turbulence information. Preliminary studies were made to determine the feasibility of the proposed method of solution. For these studies the lateral equations of the Navion aircraft, as obtained from Reference 5,

were set up on the analog computer. The basis of the method was the well-known feedback principle:

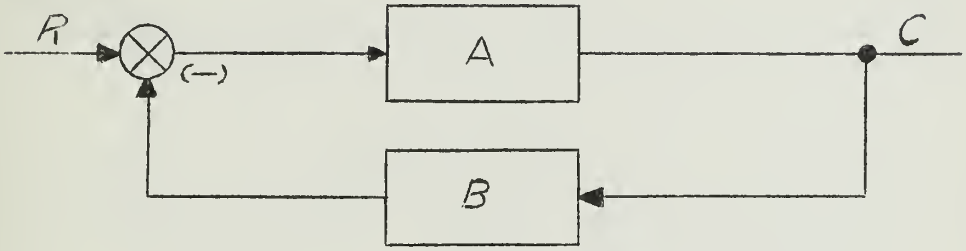

From the above diagram, $C/R = A/(1 + AB)$. If A, the forward loop gain, is very much greater than unity, then,

$$\frac{C}{R} \approx \frac{1}{B}$$

If B were an aircraft transfer function, e.g., $\dot{\varphi}/\delta_a$, then,

$$\frac{C}{R} \approx \frac{1}{\dot{\varphi}/\delta_a} \approx \frac{\delta_a}{\dot{\varphi}}$$

It seemed possible, then, that if known aircraft response in roll rate, for example, were fed into such a circuit at "R", where "B" was the aircraft transfer function as set up on the analog computer, then the circuit output at "C" would be a voltage representing the aileron deflection which had caused the roll response.

The validity of this theory was tested by recording on tape the analog response in $\dot{\varphi}$, $\dot{\psi}$, and $\beta$, to an arbitrary sequence of voltages representing aileron inputs to the system. This was accomplished by connecting a potentiometer to the appropriate points of the analog circuit and, in effect, "flying" the aircraft in the lateral modes. The previously discussed feedback circuit was then connected as shown below:

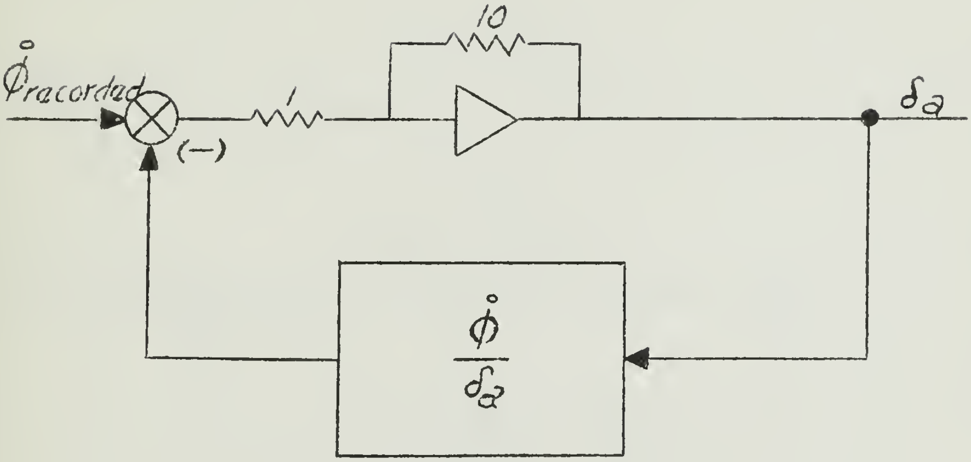

The taped response in roll rate was then played into the circuit at "R" and the output "C" was compared with the original aileron signals. The match was excellent with forward loop gains as low as 10. Below this value the reproduction decreased in accuracy since $(C/R) \approx (1/B)$ was no longer a good approximation.

The next logical step was to study the effects of two control inputs, both aileron and rudder. Again the analog was "flown", this time with aileron and rudder. The same aircraft response quantities were again taped. The analysis circuit was similar to the previous case, with the addition of another loop. The circuit is shown below in block diagram form. The taped responses in $\dot{\varphi}$ and $\dot{\psi}$ were played into the circuit at R and R' respectively, and the outputs at C and C' were compared with the original $\delta_a$ and $\delta_r$. Again the match was excellent, down to forward loop gains of 10.

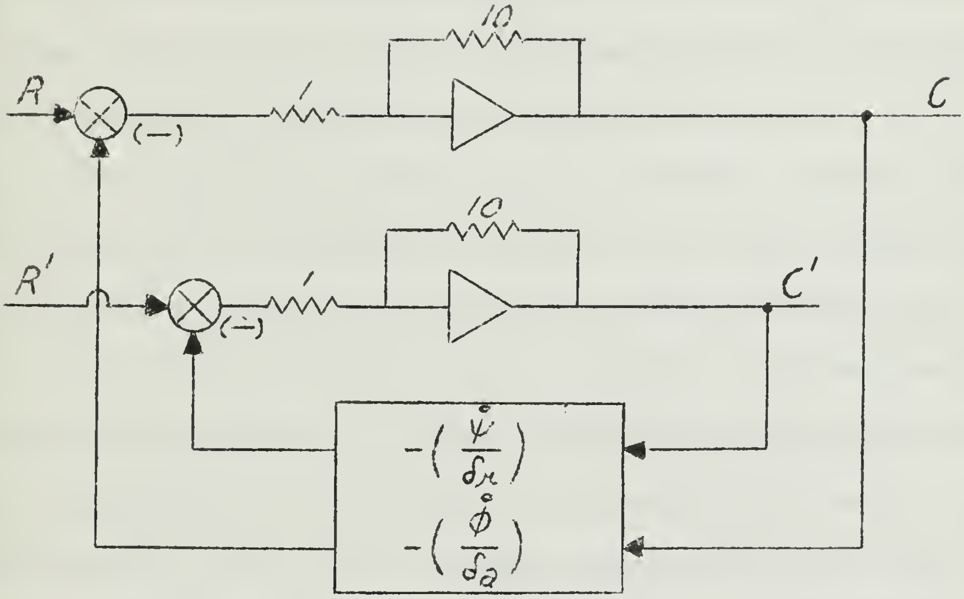
10
R
(−)
1
C
10
R'
1
C'
(−)
$-\left(\frac{\dot{\psi}}{\delta_r}\right)$
$-\left(\frac{\dot{\phi}}{\delta_a}\right)$

Figure 10 shows a more detailed schematic of this last analysis circuit. It was important to provide negative feedback in the loops in order to maintain system stability.

The results of this preliminary study pointed up the uniqueness of the solutions to the aircraft equations of motion. A given combination of aileron and rudder inputs results in a unique combination of roll, yaw, and sideslip response.

Originally, it had been proposed that this exact analysis method be employed in the study of the flight test data. In the lateral case, for example, aircraft response in roll rate and yaw rate were to be applied to a similar analysis circuit, where the analog would be of the F4B. From the resulting outputs of $\delta_r$ and $\delta_a$ then would have been subtracted the recorded flight test control deflections. The difference would be an aileron and rudder signal representing the turbulence input to the F4B.

This information, suitably modified to account for the difference in control power between F4B and Navion, might then be applied to the variable stability aircraft as a simulation of the turbulence input.

The longitudinal analysis would be similar. Aircraft response in pitch rate would be applied to the appropriate circuit and the output $\delta_s$ would yield an equivalent $\delta_s$ representing the turbulence input.

This method, however, obviously neglects the linear perturbations of aircraft motion due to turbulence, those motions along the aircraft axes. It assumes that the atmospheric turbulence effects may be described accurately by the resulting moments about the aircraft axes. For purposes of this research project reasonably valid simulation may be attained based on this concept.

However, in the interest of more accurate gust simulation, it was decided to conduct some initial research into the possibility of obtaining turbulence data which might be expressed in five degrees of freedom, thus including any lateral and normal acceleration effects. In addition, the possibility existed that some qualitative information concerning the character of the turbulence itself might result from such a study.

It was known that it is possible to visualize the atmosphere through which the aircraft moves as being in motion at some steady mean value, with random turbulent fluctuations superimposed. These random velocities may be considered as inputs to the aircraft linear system, which may respond in six degrees of freedom. The velocity inputs are assumed small, permitting linearization of the resulting aerodynamic forces.

As outlined in Reference 7, it is convenient to introduce these inputs into the equations of motion in the form of velocity components $u_g$, $v_g$, and $w_g$ (subscript "g" standing for gust). If it is assumed that the gust wavelengths are all large relative to the aircraft dimensions, then the gradient, or velocity variation, of these gusts across the length and span of the aircraft may be considered essentially linear. It can be shown that under this assumption the effects of the gust components and their gradients are aerodynamically equivalent to perturbations in angle of attack, sideslip, roll rate, yaw rate, and pitch rate. These are noted as $\alpha_g$, $\beta_g$, $\dot{\varphi}_g$, $\dot{\psi}_g$, $\dot{\theta}_g$.

The aircraft equations of motion incorporating the modified variables thus become:

Longitudinal:

$$(14)\quad \dot{\alpha} - \dot{\theta} + \frac{C_{L\alpha}}{2\,\tau}(\alpha + \alpha_g) + \frac{C_{L\delta_s}}{2\tau}\delta_s = 0$$

$$(15)\quad \ddot{\theta} - \frac{C_{n_{d\theta}}}{H\tau}(\dot{\theta} + \dot{\theta}_g) - \frac{C_{n_{d\alpha}}}{H\tau}\dot{\alpha} - \frac{C_{n_\alpha}}{H\tau^2}(\alpha + \alpha_g) - \frac{C_{n_{\delta_s}}}{H\tau^2}\delta_s = 0$$

Lateral:

$$(16)\quad \dot{\beta} - \frac{C_{y_\beta}}{2\,\tau}(\beta + \beta_g) + \dot{\psi} - \frac{C_{y_r}}{4\,\mu}(\dot{\psi} + \dot{\psi}_g) + \frac{C_\ell}{2\tau}\varphi - \frac{C_{y_p}}{4\,\mu}(\dot{\varphi} + \dot{\varphi}_g)$$

$$- \frac{C_{y\delta_a}}{2\tau}\delta_a - \frac{C_{y\delta_r}}{2\tau}\delta_r = 0$$

$$(17)\quad \ddot{\varphi} - \frac{C_{\ell_p}}{2J_x\tau}(\dot{\varphi} + \dot{\varphi}_g) - \frac{C_{\ell_r}}{2J_x\tau}(\dot{\psi} + \dot{\psi}_g) - \frac{\mu C_{\ell_\beta}}{J_x\tau^2}(\beta + \beta_g) - \frac{\mu C_{\ell\delta_a}}{J_x\tau^2}\delta_a - \frac{\mu C_{\ell\delta_r}}{J_x\tau^2}\delta_r = 0$$

$$(18)\quad \ddot{\psi} - \frac{C_{n_r}}{2J_z\tau}(\dot{\psi} + \dot{\psi}_g) - \frac{C_{n_p}}{2J_z\tau}(\dot{\varphi} + \dot{\varphi}_g) - \frac{\mu C_{n_\beta}}{J_z\tau^2}(\beta + \beta_g) - \frac{\mu C_{n\delta_a}}{J_z\tau^2}\delta_a - \frac{\mu C_{n\delta_r}}{J_z\tau^2}\delta_r = 0$$

With the gust terms rearranged to point out their role as forcing functions, the equations are written as:

Longitudinal:

$$(19)\quad \dot{\alpha} - \dot{\theta} + \frac{C_{\ell_\alpha}}{2\tau}\alpha + \frac{C_{L\delta_s}}{2\tau}\delta_s + \frac{C_{\ell_\alpha}}{2\tau}\alpha_g = 0$$

$$(20)\quad \ddot{\theta} - \frac{C_{n_{d_\theta}}}{H\tau}\dot{\theta} - \frac{C_{n_{d_\alpha}}}{H\tau}\dot{\alpha} - \frac{C_{n_\alpha}}{H\tau^2}\alpha - \frac{C_{n\delta_s}}{H\tau^2}\delta_s - \frac{C_{n_{d\theta}}}{H\tau}\dot{\theta}_g - \frac{C_{n_\alpha}}{H\tau^2}\alpha_g = 0$$

Lateral:

$$(21)\quad \dot{\beta} - \frac{C_{y_\beta}}{2\tau}\beta + \dot{\psi} - \frac{C_{y_r}}{4\mu}\dot{\psi} + \frac{C_L}{2\tau}\varphi - \frac{C_{y_p}}{4\mu}\dot{\varphi} - \frac{C_{y\delta_a}}{2\tau}\delta_a - \frac{C_{y\delta_r}}{2\tau}\delta_r - \frac{C_{y_\beta}}{2\tau}\beta_g - \frac{C_{y_r}}{4\mu}\dot{\psi}_g - \frac{C_{y_p}}{4\mu}\dot{\varphi}_g = 0$$

$$(22)\quad \ddot{\varphi} - \frac{C_{\ell_p}}{2J_x\tau}\dot{\varphi} - \frac{C_{\ell_r}}{2J_x\tau}\dot{\psi} - \frac{\mu C_{\ell_\beta}}{J_x\tau^2}\beta - \frac{\mu C_{\ell\delta_a}}{J_x\tau^2}\delta_a - \frac{\mu C_{\ell\delta_r}}{J_x\tau^2}\delta_r - \frac{C_{\ell_p}}{2J_x\tau}\dot{\varphi}_g - \frac{C_{\ell_r}}{2J_x\tau}\dot{\psi}_g - \frac{\mu C_{\ell_\beta}}{J_x\tau^2}\beta_g = 0$$

$$\ddot{\psi} - \frac{C_{n_r}}{2J_z\tau}\dot{\psi} - \frac{C_{np}}{2J_z\tau}\dot{\varphi} - \frac{\mu C_{n\beta}}{J_z\tau^2}\beta - \frac{\mu C_{n\delta_a}}{J_z\tau^2}\delta_a - \frac{\mu C_{n\delta_r}}{J_z\tau^2}\delta_r - \frac{C_{n_r}}{2J_z\tau}\dot{\psi}_g - \frac{C_{np}}{2J_z\tau}\dot{\varphi}_g - \frac{\mu C_{n\beta}}{J_z\tau^2}\beta_g = 0 \tag{23}$$

It is to be noted that these equations are not valid for short wavelength gust components.

However, it can be shown that the effect on aircraft response of the higher frequency gust components is negligible. For example, the effective gust frequency, $\omega_g$, may be expressed by:

$$\omega_g = \frac{V_o}{\lambda}$$

where $\lambda$ is the gust wavelength. For a short $\lambda$, say equivalent to the aircraft wingspan, $\omega_g$ is on the order of 5 cps, for the F4B in the PA configuration. This is very much higher than the aircraft natural oscillatory frequencies and consequently the aircraft response is negligible.

In addition, for gust wavelengths of this order, and shorter, the aircraft begins to "average out" the gust velocities, with the resulting net gust acting on the airframe being near zero. Thus, for these higher frequency components there is a compounded attenuation - that due to the aircraft dynamic characteristics, and that due to the cancelling effect just described.

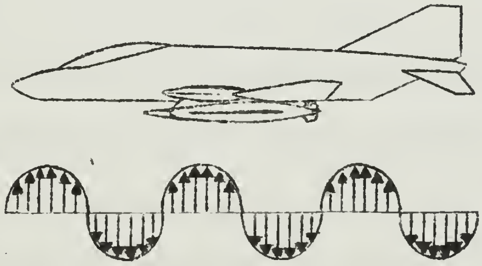

It should be noted that if the F4B were to respond dynamically to the higher frequencies, this last effect, that of cancelling, would cause some error if the acquired turbulence information were applied to the study of an aircraft differing greatly in size from the F4B. It is quite possible that the aircraft in question might respond to those gusts which were cancelled by the F4B and were thus missing from the acquired data. However, all aircraft which will be simulated by the variable stability Navion, for this investigation, are similar in size to the F4B, and therefore could be expected to "average" the gusts in the same manner.

With these modified equations of motion in mind, it was desired to obtain, as a solution, the various gust quantities. The method, although based on the previously discussed feedback principle, can probably be best described by a single degree of freedom example. For this purpose it is assumed that the aircraft can respond only in roll, and that the only gust quantity present is $\dot{\varphi}_g$. The equation of this system is then:

$$(24) \quad \ddot{\varphi} - \frac{C_{\ell_p}}{2J_x\tau}\dot{\varphi} - \frac{\mu C_{\ell_{\delta_a}}}{J_x\tau^2}\delta_a - \frac{\mu C_{\ell_{\delta_r}}}{J_x\tau^2}\delta_r - \frac{C_{\ell_p}}{2J_x\tau}\dot{\varphi}_g = 0$$

This equation is set up on the analog computer and a feedback circuit is connected as shown on page 29.

The output of the forward loop amplifier is defined as $-\dot{\varphi}_g$, and this quantity, modified by the appropriate proportionality constant, is used as an analog forcing function. The recorded values of $-\delta_r$ and $-\delta_a$ are also used to force the computer setup. The following equation, which expresses the aircraft response, is satisfied at point A:

$$\dot{\varphi}_{\text{recorded}} = \dot{\varphi}_{\text{control response}} + \dot{\varphi}_{\text{gust response}}$$

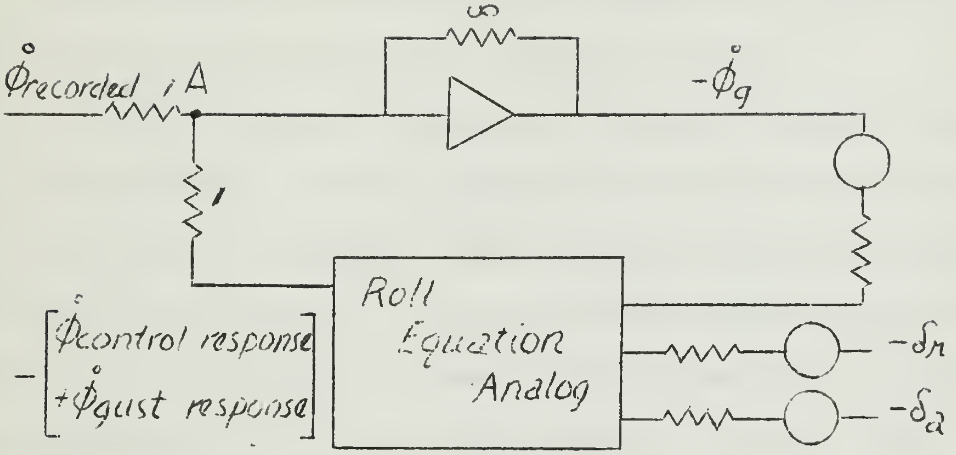
$\infty$
$\dot{\phi}_{recorded}$
1
A
$-\dot{\phi}_g$
1
Roll Equation Analog
$-\left[\begin{matrix}\dot{\phi}_{control\ response}\\ +\dot{\phi}_{gust\ response}\end{matrix}\right]$
$-\delta_r$
$-\delta_a$

Assuming that the circuit is dynamically stable, then the $-\dot{\varphi}_g$ quantity actually appears at the amplifier output. This circuitry is similar to those previously discussed.

The more complicated circuit which was proposed to solve the entire lateral set is shown in detail in Figure 11. It is, however, based on the same ideas. The three equations which are satisfied at the forward loop amplifier inputs are:

$$\beta_{recorded} - \beta_g - \beta_{gust\ response} - \beta_{control\ response} = 0$$

$$\dot{\varphi}_{recorded} - \dot{\varphi}_{gust\ response} - \dot{\varphi}_{control\ response} = 0$$

$$\dot{\psi}_{recorded} - \dot{\psi}_{gust\ response} - \dot{\psi}_{control\ response} = 0$$

It is to be noted that in the case of $\beta$, the recorded quantity from the tape was based on an accelerometer measurement and, thus, contained the quantity $\beta_g$, in addition to $\beta_{gust\ response}$, the aircraft response to $\beta_g$. Therefore, to satisfy the above equation, the $\beta_g$ was fed back to the amplifier input. In the case of $\dot{\phi}$ and $\dot{\psi}$, the aircraft response only was included in the measured response since the sensors were rate

gyros. Approximately infinite resistance feedback was therefore provided around the forward loop amplifiers in these two channels.

It was discovered, however, that the circuit shown in Figure 11 was not satisfactory. During operation of the circuit the output quantity $-\beta_g$ exhibited a divergence. This indicated some positive feedback within the multiloop system. It can be seen that there were nine loops through the aircraft analog. It seemed probable that the $-\beta_g$ output was controlled primarily by the loop through amplifier 9 which is shown below schematically:

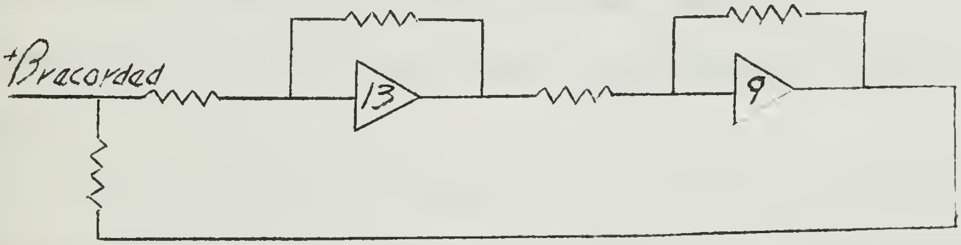

This circuit obviously provides positive feedback and is thus unstable. This problem emphasized the point that although the equations were physically satisfied in the circuit as shown, it was necessary to insure system stability in the electronic sense. A study of the circuit showed that there were additional unstable loops, but that their effect was minor compared to the effect of the stable loops which fed back to the same points.

In order to provide stability, the analysis circuit was modified to the form shown in Figure 12. The difference here is that the $-\beta_g$ quantity input to the analog is now taken directly from the recorded data. The analog circuit was modified to maintain satisfaction of the equations of

motion. Circuit stability was now attained since the unstable - $\beta_g$ loop through amplifier 9 was now eliminated.

To test the validity of the analyzer circuit, a preliminary study was made in which the aircraft analogue was forced by a ficticious $\beta_g$ quantity as obtained from a potentiometer output. The aircraft response in roll rate, yaw rate, and sideslip was recorded on tape. It is to be noted that the recorded sideslip was made the sum of the analog $\beta$ response and the forcing function, $\beta_g$. This was to provide similarity to the actual flight data where, as previously mentioned, the $\beta$ response was based on an accelerometer measurement. These recorded responses were then played into the analyzer circuit in an attempt to duplicate the original forcing function.

Figure 13 shows the original forcing function and the recorded aircraft responses. When these responses were played back into the analyzer circuit, the $\dot{\varphi}_g$ and $\dot{\psi}_g$ outputs were essentially zero, as expected. The $\beta_g$ output was found to be a good reproduction of the input wave form, although there was a very low frequency oscillation superimposed on the trace. This is shown in Figure 14(a), where the solid line is a tracing of the original $\beta_g$ input. It was determined experimentally that this low frequency drift was strongly affected by the biasing adjustment of the tape output from the ground station equipment. Careful adjustment of the bias practically eliminated the drift; but since this method would not be feasible with actual flight test data, another method was sought. It was decided to utilize a high pass filter to eliminate the low frequency oscillation. This was connected as shown:

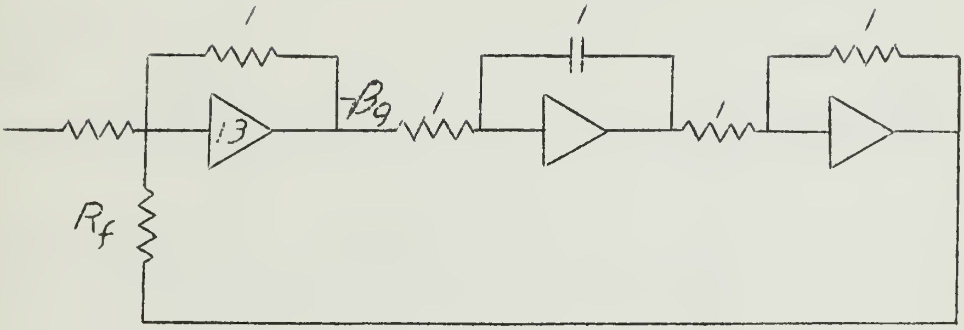

Since the use of such a filter would result also in the attenuation of some of the higher frequencies, the corner frequency was selected on the basis of compromise between minimum attenuation and minimum divergence. The results are shown in Figure 14 (b), (c), and (d). A corner frequency of 1/44 cps, as provided by $R_f$ = 7 meg Ω, seemed to give the best reproduction.

Throughout this discussion it has been assumed that the aircraft response data were available in the form of $\beta$, $\dot{\varphi}$, and $\dot{\psi}$. It can be seen from Table I that lateral acceleration, $a_y$, was recorded during the flight tests, rather than sideslip. It was necessary to obtain $\beta$ from this data by means of the following form of the side force equation:

$$(25) \quad +\beta = \frac{m}{(\rho/2)V_o^2 S}\,\frac{1}{C_{y_\beta}}\,a_y - \frac{C_{y_p}}{C_{y_\beta}}\,\frac{b}{2V_o}\,\dot{\varphi} - \frac{C_{y_r}}{C_{y_\beta}}\,\frac{b}{2V_o}\,\dot{\psi} - \frac{C_{y_{\delta_r}}}{C_{y_\beta}}\,\delta_r$$

The summing and scaling circuit utilized to solve this equation for application to the analyzer is shown below:

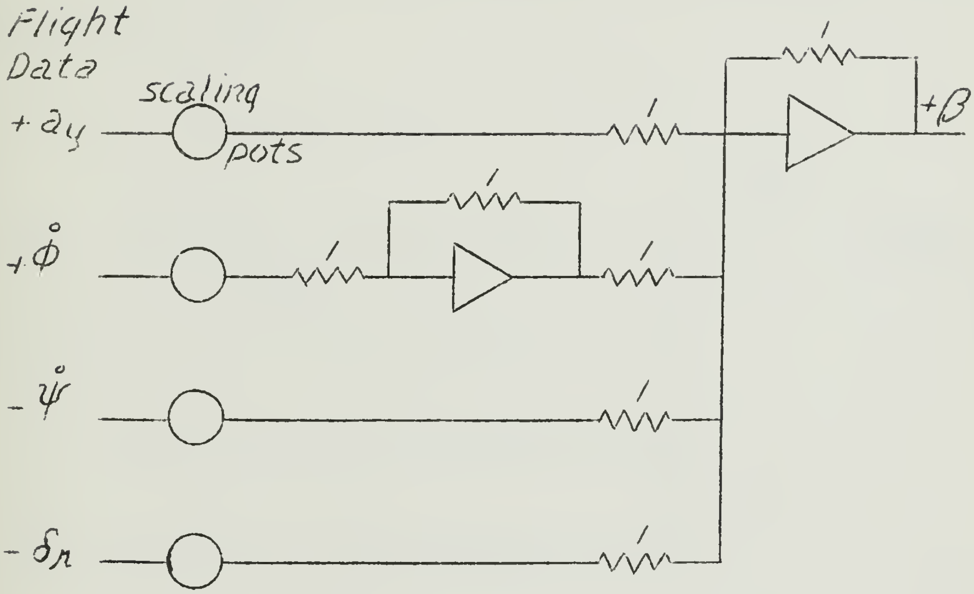

Since an accurate representation of β depended on reliable values of $C_{y_\beta}$, $C_{y_r}$, $C_{y_p}$, and $C_{y_{\delta_r}}$, and since these derivatives were not involved in the previous matching process, it was necessary to check their validity. The method used was to compare the quantity $a_y$ from the flight data with the derived $a_y$ obtained by summing the appropriate analog outputs in response to a rudder pulse. The results are shown in Figures 4, 5, and 6. It was felt that the matching was accurate enough to justify the use of β, as obtained from equation 25. The resulting equation for $a_y$ is:

$$(26)\quad +a_y = \frac{(\rho/2)V_o^2S}{m} C_{y_\beta}\,\beta + \frac{(\rho/2)V_o^2S}{m}\,\frac{b}{2V_o}\,C_{y_p}\,\dot{\varphi} + \frac{(\rho/2)V_o^2S}{m}\,\frac{b}{2V_o}\,C_{y_r}\,\dot{\psi}$$

$$+\frac{(\rho/2)V_o^2S}{m} C_{y_{\delta_r}}\,\delta_r$$

The summing and scaling circuit for obtaining $a_y$ for the matching process is shown below:

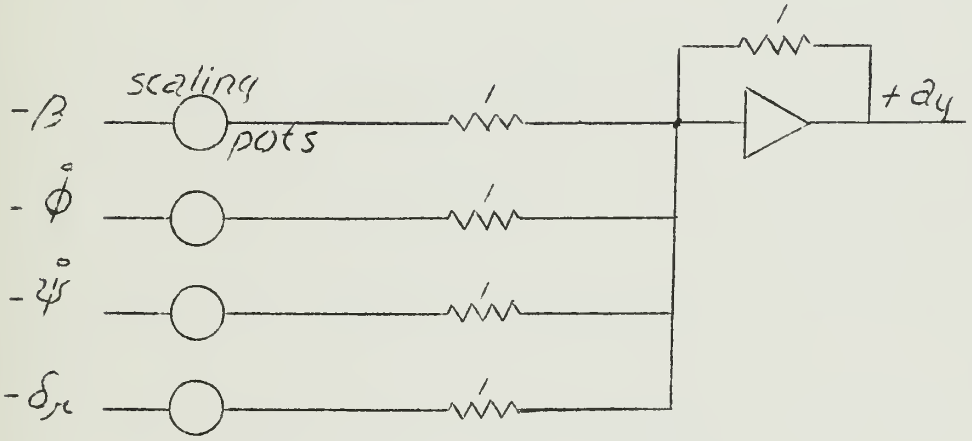

The analyzer circuit designed for use with the longitudinal equations was based on the same principles which governed the lateral circuit. The schematic of this circuit is shown in Figure 15. The following equations were satisfied at the inputs to the forward loop amplifiers:

$$\dot{\theta}_{\text{aircraft response}} = \dot{\theta}_{\text{gust response}} + \dot{\theta}_{\text{control response}}$$

$$\alpha_{\text{aircraft response}} = \alpha_{\text{gust}} + \alpha_{\text{gust response}} + \alpha_{\text{control response}}$$

It should be noted that the reliability of the analyzer output was probably improved if the aircraft maintained a very steady, smooth flight path during the carrier approaches. The reason for this is that with the aircraft responses very small, the aircraft analogue, in the analyzer feedback loops, was relatively inactive. This was beneficial since

the analogue had known inaccuracies. It was therefore desirable that the aircraft stability augmentation equipment be operative as an aid in maintaining steady flight during the carrier approaches.

## IV RESULTS

The next step in the data analysis was to play into the analyzer circuits the appropriate quantities from the flight test tape recordings. Of the five flight test tapes, one was determined to be virtually unusable due to superimposed noise. The four remaining tapes were each played into the analyzer and Sanborn recordings were made of the five gust quantities for each carrier approach. Also recorded for reference purposes were the aircraft response in five degrees of freedom and the various control deflections.

Figures 16 through 31 are reproductions of gust quantities from the lateral and longitudinal analyzers. Also shown are traces of aircraft response and control deflection. Aircraft altitude also appears on the recordings as an aid in orientation. It was apparent from the traces that some drift was still present in the $\beta_g$ channel, probably due to incorrect biasing at the ground station output. Further increase of the filter corner frequency was not practical due to the extensive attenuation of the higher frequency components.

Those approaches which are missing from the set of Sanborn recordings were unusable due to the effects of "dropouts" during the analyzer operation. As mentioned previously, the tape of the second flight, containing approaches 8 through 13, was completely unusable due to poor quality of recorded information.

Study of the traces revealed a number of points. It was expected that if the analyzer circuits were completely valid the output gust

quantities would be completely random in character, reflecting the nature of the actual turbulence. However, Figure 19, for example, shows that there were occasional sections of the various gust traces which were periodic in character. Conversely, many of the remaining traces, Figure 16 for example, appear quite random. Some of the oscillations appearing were of the approximate character of the aircraft short period and Dutch roll occillation. The implication here was that the F4B analogue was not completely accurate. As a result, some of the aircraft response characteristics appeared in the analyzer output.

In spite of the apparent imperfections in the turbulence data, some qualitative information was immediately available. The records showed that for all approaches there was a marked increase in the magnitude of the gust quantities in the few seconds prior to aircraft touchdown. This was a verification of the existence of the turbulent "burble" immediately astern of an aircraft carrier deck.

In order to detect any additional trends in the turbulence quanitites, the RMS value of each quantity for each approach was determined with the aid of the following circuit, which included the Donner Model 3751 Function Generator:

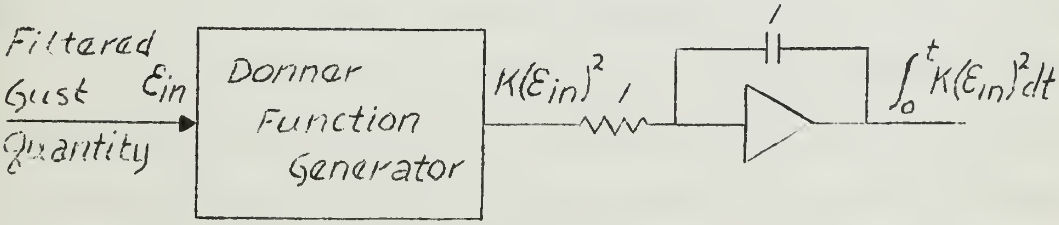

$$\text{(27)} \qquad \text{RMS} = \sqrt{\frac{1}{Kt} \int_0^t K(\epsilon_{in}^2)\,dt}$$

In order to eliminate the effect of any DC bias or low frequency oscillations, the various gust quantities were channeled through a high pass filter prior to entry into the above circuit. A corner frequency of .20 cps was selected for the filter, since it was felt that frequencies below this would probably not have a significant effect on pilot opinion.

The RMS values of the various quantities were tabulated and are shown in Table II. Omissions in the Table were due to the effects of telemetering dropouts. These tabulated values do not include the effect of the final "burble". No apparent trends were determined from study of the RMS tabulation, except for an indication of the general level of each quantity. These levels remained approximately constant during the course of the approaches, indicating that atmospheric conditions also generally remained the same.

It was also noted, with reference to Table III that the angular velocity gust quantities, $\dot{\varphi}_g$, $\dot{\psi}_g$, and $\dot{\theta}_g$ were all of approximately the same magnitude. The angular quantities $\beta_g$ and $\alpha_g$ were also approximately equal. This was a strong indication that the turbulence away from the immediate vicinity of the ship was indeed isotropic, as is normally assumed.

It was expected that the magnitude of the gust quantities within the "burble" would be a reflection of the existing relative wind conditions over the carrier deck. Although no formal tabulation was made of the RMS values of the gust quantities within the "burble", study of the traces

revealed that these RMS values were approximately doubled in the final three seconds of each approach. There was no apparent difference in the character of the "burbles" with varying relative wind conditions.

It was noted, however, from study of the gust traces that the "burble" was initially encountered at varying distances from the ship. Figure 32 shows the point of entering the "burble" for all of the approaches represented by Figures 16 through 31. It is interesting to note that those points furthest from the carrier were in the presence of high relative wind, with no x-wind component. Those points nearer the ship were with less wind velocity. Finally, those points appearing 2 and 3 seconds prior to touchdown were in the presence of "right to left" x-wind, indicating that the turbulence trail was being blown across the flightpath at this point.

In Figure 33 are plotted the pertinent lateral mode data from a typical approach. The increase in the magnitude of the gust quantities in the final few seconds before touchdown is apparent. However, it was also noted that the gust quantities at this point had some periodic characteristics. In addition, the oscillations are approximately of the same period as the aircraft roll and yaw response. In fact, in the case of $\dot{\varphi}$ and $\dot{\varphi}_g$, the oscillations are exactly 180° out of phase. Because of apparent "impurities" such as this in the turbulence data it was felt that a more detailed statistical analysis of the data should be made to determine its true spectral character. Such an analysis is beyond the present scope of this project.

## V CONCLUSIONS AND RECOMMENDATIONS

Based on the results of this investigation, it is concluded that:

1. Accurate representations of the atmospheric turbulence may be obtained by the analysis method described in the report, assuming that the aircraft analogue is valid.
2. The consistent similarity in the magnitude of the angular velocity gust quantities, and the similarity in the magnitudes of gust angular quantities, as shown in Table IV, indicated that the turbulence away from the immediate vicinity of the carrier was isotropic in character.
3. The atmospheric turbulence in the vicinity of an aircraft carrier is characterized by a strong "burble" in the vicinity of the approach end of the carrier deck. It is not possible, based on these results, to give a quantitative description of this turbulence although it appeared that the character of the "burble"did not vary noticeably with changing relative wind conditions. However, the point at which the "burble" is initially encountered is a function of the relative wind conditions.

It is recommended that:

1. A detailed spectrum analysis be made of the turbulence quantities resulting from this investigation, in order that undesirable portions of the spectrum be eliminated, making the information suitable for application to the variable stability Navion.
2. A further statistical analysis of this data be made to determine quantitatively the character of its components.
3. An investigation be conducted into the applicability of this analysis circuit for the general solution of complex inverse transfer function problems.

## VI REFERENCES

1. Seckel, Edward: Proposal for Research on PA Configuration Lateral Flying Qualities. Princeton University, Department of Aeronautical Engineering, April 23, 1962.

2. Whorl, Vernon: Wake Study Instrumentation Calibration Charts. Naval Air Test Center, Patuxent River, Maryland, Flight Test Division, December, 1962.

3. Ringleb, Friedrick O.: Studies of the Air Flow over an Aircraft Carrier. Naval Air Engineering Laboratory, U. S. Naval Air Material Center, Philadelphia, Pennsylvania, 7 September 1962.

4. McRuer, D. T., et. al.: Dynamics of the Airframe. Norair Division, Northrop Aircraft Corporation, Hawthorne, California, September 1952.

5. Adams, R. C., et. al.: An Investigation of the Feasibility of Obtaining Lateral Stability Derivatives for a Linear Aircraft by Matching Analog Computer Transient Response to Flight Test Data. Princeton University, Department of Aeronautical Engineering, Report No. 384, June 1957.

6. Klein, H., and Sedney, R.: Some Basic Concepts for Analyzing Dynamic Flight Test Data, Journal of the Aeronautical Sciences, November 1953.

7. Etkin, Bernard: Dynamics of Flight, Stability and Control. John Wiley & Sons, Inc., New York, 1959.

## TABLE I

## RECORDED FLIGHT TEST DATA QUANTITIES

| QUANTITY | SYMBOL | SENSOR |
|---|---|---|
| Roll rate, c.g. | $\dot{\varphi}_{cg}$ | Humphrey rate gyro, Model 01-0238 |
| Pitch rate, c.g. | $\dot{\theta}_{cg}$ | Humphrey rate gyro, Model 01-0238 |
| Yaw rate, c.g. | $\dot{\psi}_{cg}$ | Humphrey rate gyro, Model 01-0238 |
| Roll rate, seat | $\dot{\varphi}_{seat}$ | Minn.-Honeywell rate gyro, Model JG 7005A4-9 |
| Pitch rate, seat | $\dot{\theta}_{seat}$ | Minn.-Honeywell rate gyro, Model JG 7005A4-9 |
| Yaw rate, seat | $\dot{\psi}_{seat}$ | Minn.-Honeywell rate gyro, Model JG 7005A4-9 |
| Pitch and roll rate, vertical gyro | $\dot{\theta}_{VG}$<br>$\dot{\varphi}_{VG}$ | Minn.-Honeywell rate gyro, Model JG 7044A4 |
| Lateral acceleration | $a_y$ | Donner linear accelerometer, Model 4310 |
| Normal acceleration | $a_z$ | Donner linear accelerometer, Model 4310 |
| Rudder deflection | $\delta_r$ | 2 K Ω, modified, spring loaded, selsyn potentiometer |
| Left aileron defl. | $\delta_{a_L}$ | IRC 2 K Ω dual, spring loaded, potentiometer |
| Left spoiler defl. | $\delta_{s_L}$ | Bournes 4 inch linear potentiometer |
| Stabilator defl. | $\delta_s$ | 2 K Ω, modified, spring loaded, selsyn potentiometer |
| Rudder pedal defl. | $\delta_{ped}$ | spring loaded, modified selsyn potentiometer |
| Lateral stick defl. | $\delta_{stick,\ lat}$ | spring loaded, modified selsyn potentiometer |

TABLE I
(Continued)

| QUANTITY | SYMBOL | SENSOR |
|---|---|---|
| Longitudinal stick | $\delta_{stick,\ long}$ | spring loaded, modified selsyn potentiometer |
| Left and right throttle position | $\delta_{T_R}$, $\delta_{T_L}$ | spring loaded, modified selsyn potentiometers |
| Airspeed | $V_o$ | W. O. Leonard Model 50-2100 |
| Altitude | h | W. O. Leonard Model 50-2000-9 |

## TABLE II

## RECORDED FLIGHT DATA QUANTITIES, TELEMETERING CHANNELS UTILIZED

| QUANTITY | CHANNELS UTILIZED |
|---|---|
| Roll rate, cg | 3 |
| Pitch rate, cg | 3 |
| Yaw rate, cg | 3 |
| Roll rate, seat. | 3 |
| Pitch rate, seat. | 3 |
| Yaw rate, seat. | 3 |
| Pitch rate, vertical gyro | 1 |
| Roll rate, vertical gyro | 1 |
| Lateral acceleration | 2 |
| Normal acceleration | 2 |
| Rudder deflection | 2 |
| Left aileron deflection | 2 |
| Left spoiler deflection | 2 |
| Stabilator deflection | 2 |
| Rudder pedal deflection | 1 |
| Lateral stick deflection | 1 |
| Longitudinal stick deflection | 1 |
| Left throttle | 1 |
| Right throttle | 1 |
| Airspeed | 1 |
| Altitude | 1 |

## TABLE III

## WIND CONDITIONS DURING CARRIER TEST APPROACHES

(Headwind and Crosswind Components)

| APPROACH NUMBER | RELATIVE HEADWIND (KNOTS) | RELATIVE CROSSWIND (KNOTS) |
|---|---|---|
| 1 | 36 | 0 |
| 2 | 36 | 0 |
| 3 | 36 | 0 |
| 4 | 36 | 0 |
| 5 | 36 | 0 |
| 6 | 36 | 0 |
| 7 | 36 | 0 |
| 8 | 19 | 0 |
| 9 | 19 | 0 |
| 10 | 19 | 0 |
| 11 | 29 | 0 |
| 12 | 26 | 0 |
| 13 | 37 | 0 |
| 14 | 31 | 0 |
| 15 | 28 | 0 |
| 16 | 26 | 0 |
| 17 | 25 | 0 |
| 18 | 25 | 0 |
| 19 | 25 | 0 |
| 20 | 23 | 0 |
| 21 | 23 | 0 |
| 22 | 23 | 0 |
| 23 | 23 | 0 |
| 24 | 26 | 0 |
| 25 | 24 | 7 1/2 right |
| 26 | 28 | 5 right |
| 27 | 24 | 5 right |
| 28 | 27 | 5 right |
| 29 | 35 | 0 |
| 30 | 34 | 6 right |
| 31 | 34 | 5 right |
| 32 | 34 | 9 right |
| 33 | 30 | 5 right |

## TABLE IV

## RMS VALUES OF TURBULENCE QUANTITIES

| APPROACH | $\alpha_g$ (degrees) | $\dot{\theta}_g$ (deg/sec) | $\beta_g$ (degrees) | $\dot{\varphi}_g$ (dec/sec) | $\dot{\psi}_g$ (deg/sec) |
|---|---|---|---|---|---|
| 1 | 2.21 | 3.06 | 1.94 | 2.88 | 3.39 |
| 2 | 2.21 | 2.78 | 1.69 | - | - |
| 3 | 2.39 | 2.89 | 1.47 | 2.77 | 4.18 |
| 4 | 2.21 | 3.41 | - | 2.89 | 3.88 |
| 5 | 2.16 | 2.72 | 1.75 | 3.19 | 3.55 |
| 6 | 2.16 | 2.77 | 1.66 | 3.27 | 3.75 |
| 7 | 2.16 | 3.17 | 1.79 | 3.27 | 3.73 |
| 8 | | | | | |
| 9 | | | | | |
| 10 | | DATA UNUSABLE | | | |
| 11 | | | | | |
| 12 | | | | | |
| 13 | | | | | |
| 14 | 1.64 | - | 1.86 | 2.70 | 3.76 |
| 15 | - | 3.60 | 2.03 | 2.71 | 3.66 |
| 16 | 1.66 | - | - | 3.34 | - |
| 17 | 1.63 | 2.69 | - | - | - |
| 18 | 1.53 | 3.17 | 1.97 | - | 3.11 |
| 19 | 1.43 | 2.99 | 1.97 | 3.03 | 3.66 |
| 20 | - | - | 1.56 | 3.34 | 4.25 |
| 21 | - | 2.97 | - | 2.93 | 3.34 |
| 22 | 2.32 | 2.97 | 1.44 | 3.33 | 4.24 |
| 23 | - | 3.17 | - | 3.22 | 3.66 |
| 24 | 2.31 | 3.14 | 1.61 | 3.51 | 3.89 |
| 25 | 2.41 | 2.89 | 1.57 | 2.95 | 3.48 |
| 26 | 2.09 | 3.34 | - | 3.04 | 3.78 |
| 27 | - | 3.16 | 1.77 | - | 3.21 |
| 28 | - | - | - | - | - |
| 29 | 2.51 | - | 1.67 | 2.84 | - |
| 30 | 2.23 | 3.17 | 1.98 | 3.14 | 3.76 |
| 31 | 2.09 | 3.27 | 1.91 | 2.86 | 3.89 |
| 32 | 2.43 | 3.17 | 2.10 | 2.99 | 3.67 |
| 33 | 2.20 | 3.27 | 2.10 | 3.04 | 3.83 |

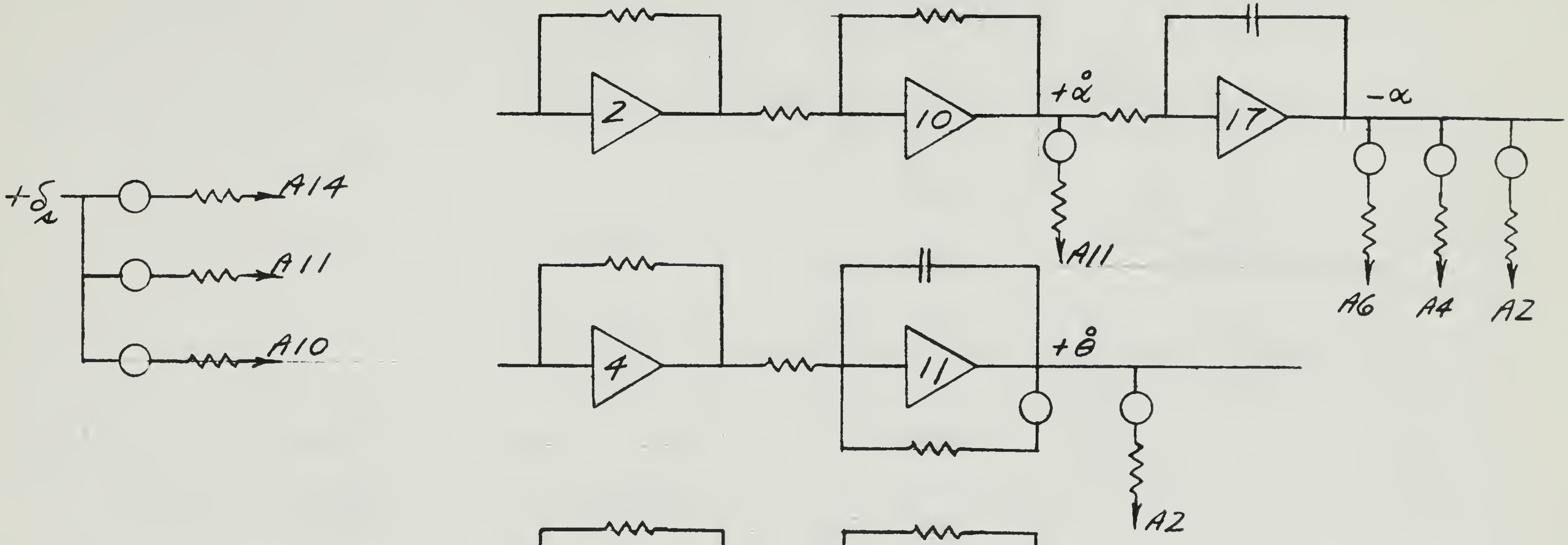
$+\delta_e$
A14
A11
A10
2
10
17
$+\dot{\alpha}$
$-\alpha$
A11
A6
A4
A2
4
11
$+\dot{\theta}$
A2
6
14
$+n$

FIG. 1
F4B LONGITUDINAL ANALOG

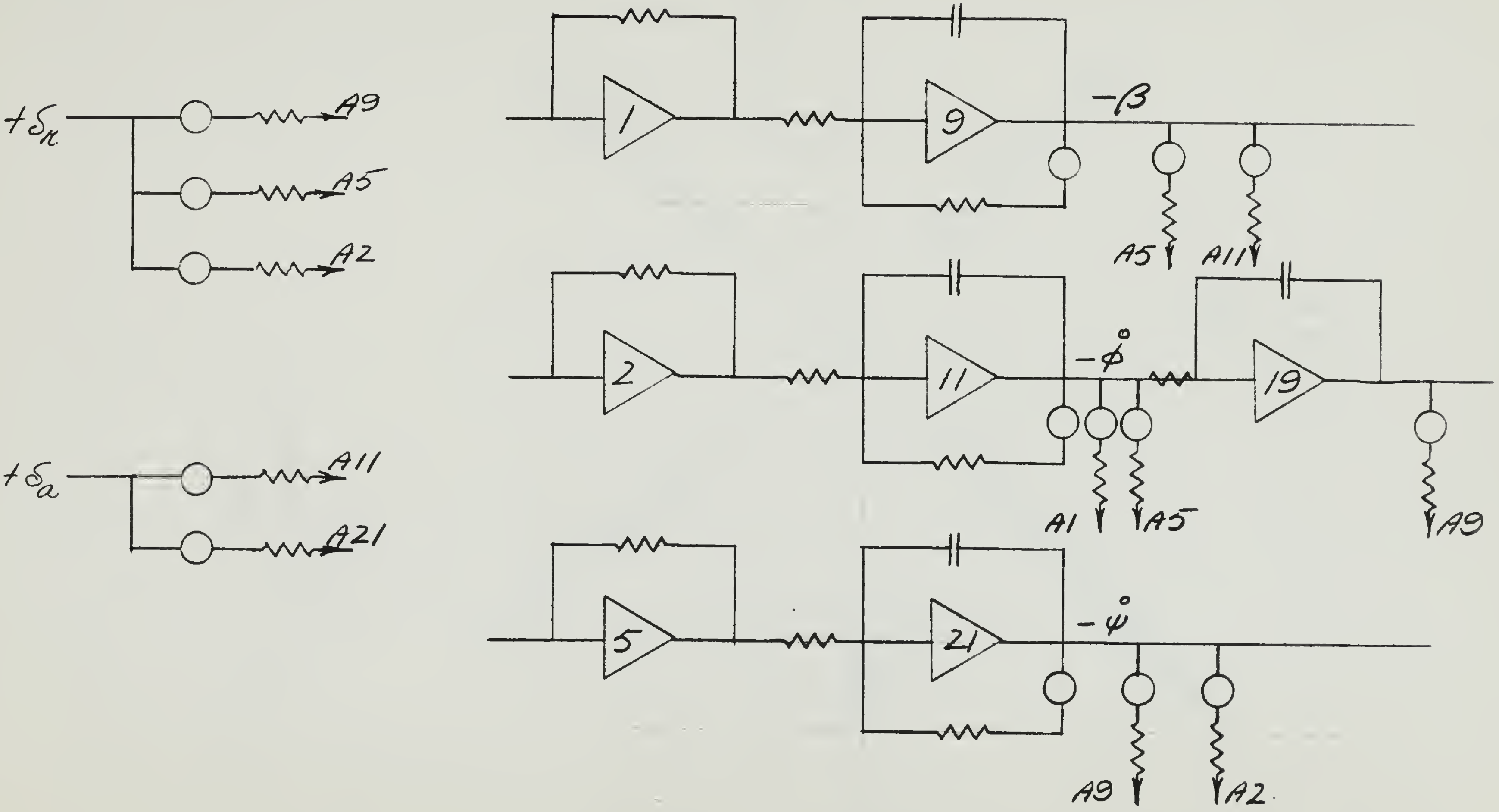
$+\delta_r$
A9
A5
A2
$+\delta_a$
A11
A21
1
9
$-\beta$
A5
A11
2
11
$-\dot{\phi}$
19
A1
A5
A9
5
21
$-\dot{\psi}$
A9
A2

FIG. 2
F4B LATERAL ANALOG

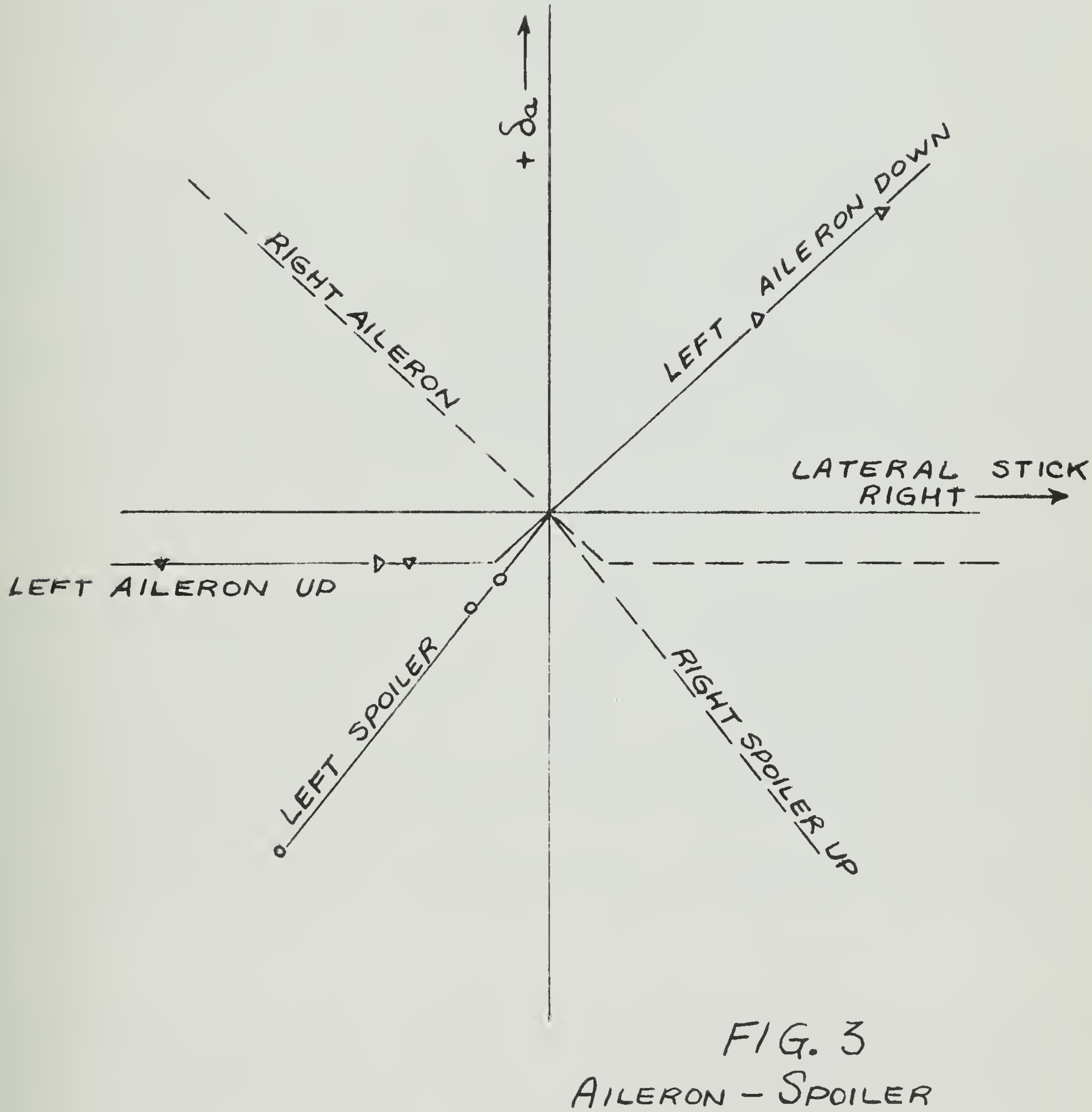

FIG. 3
AILERON – SPOILER
CALIBRATION CURVES

SANBORN Recording Permapaper

Fig. 4
Matched Rudder Response

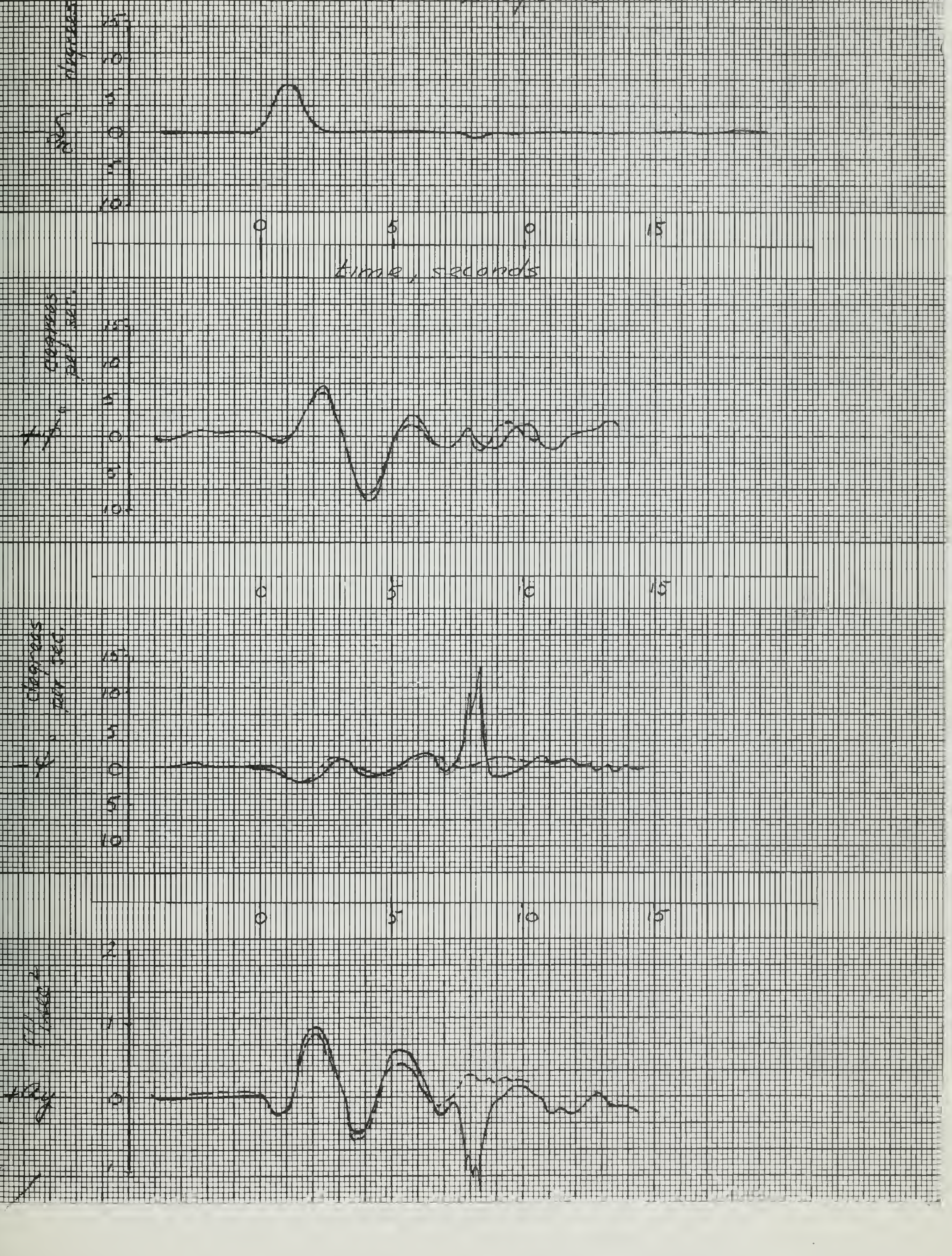

Fig. 5

Matched Response to Rudder Doublet

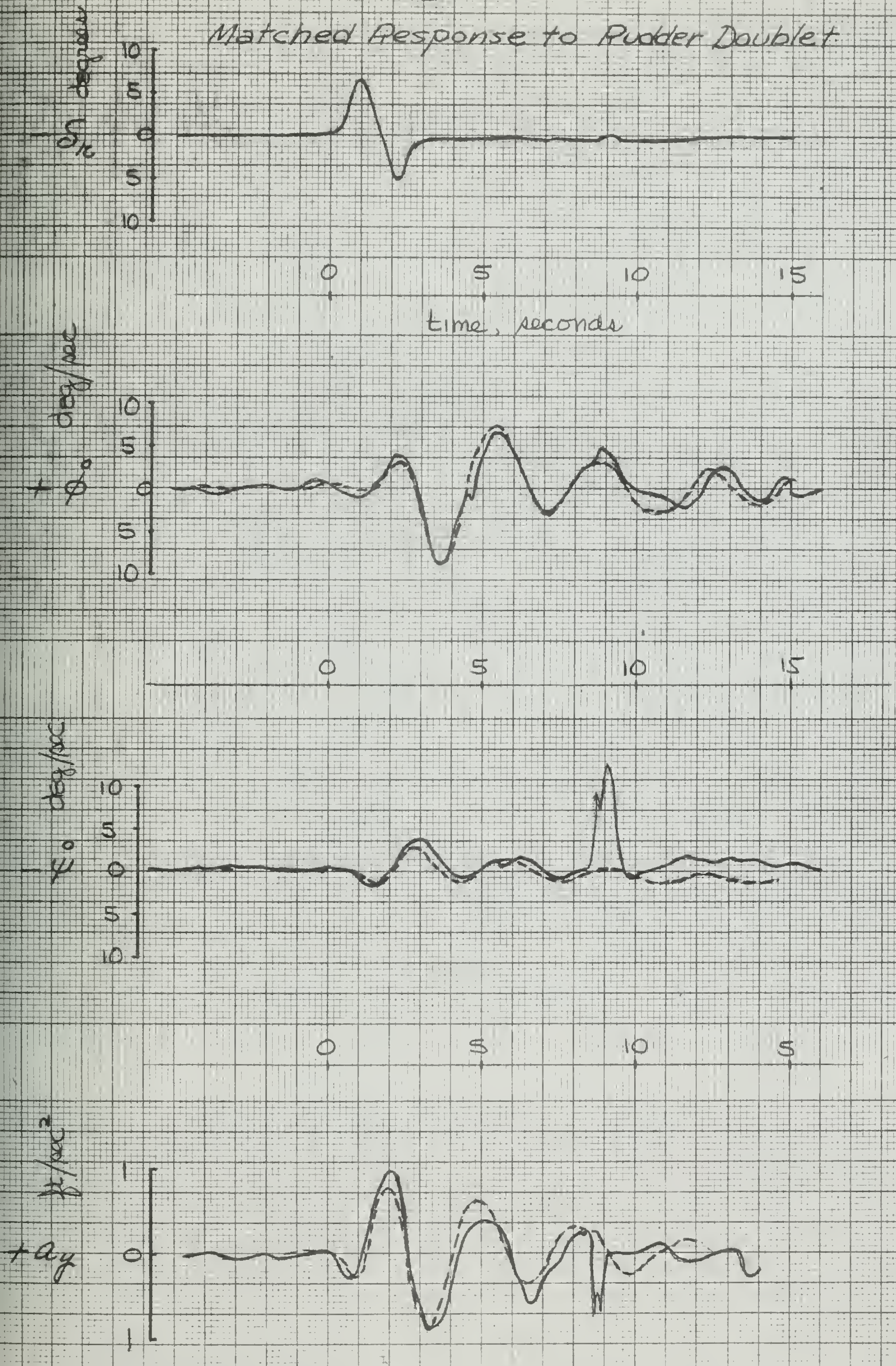

GRAPHIC CONTROLS CORPORATION | RECORDING CHARTS

BUFFALO, NEW YORK PRINTED IN U.S.A

Fig. 6

Matched Response to Aileron Double Step

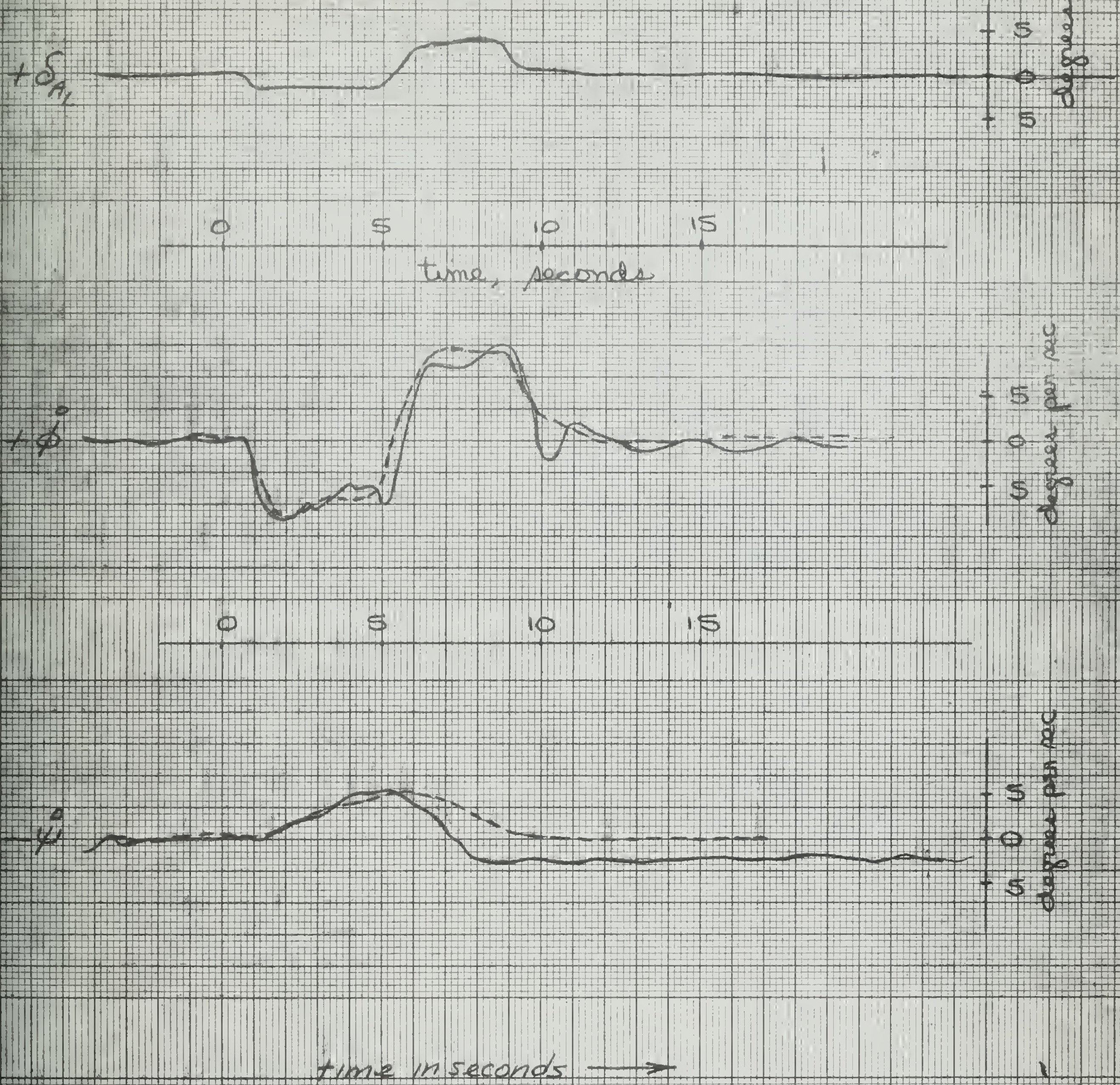

Fig. 7

Matched Stabilator Pulse Response

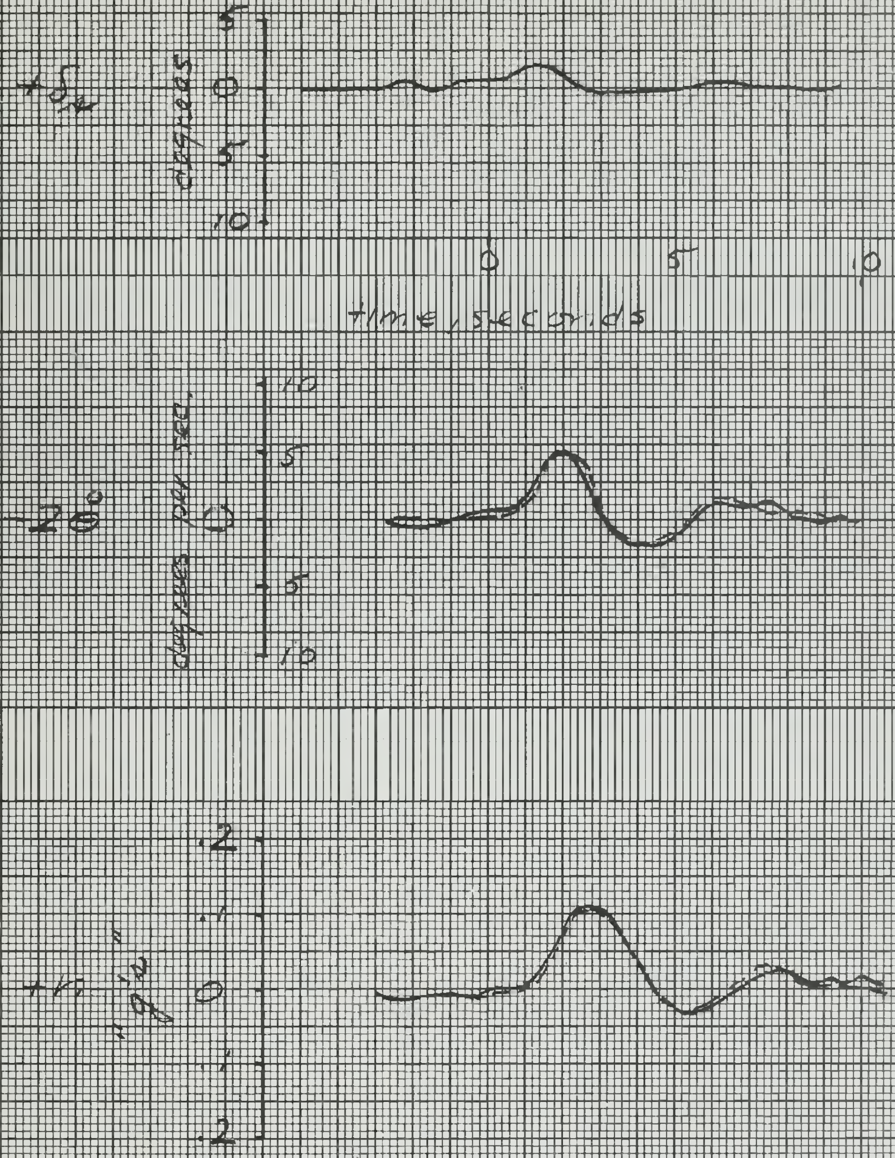

Recording Permapaper

SANBORN Recording Permapaper

Fig. 8

Matched Response to Stabilator Doublet

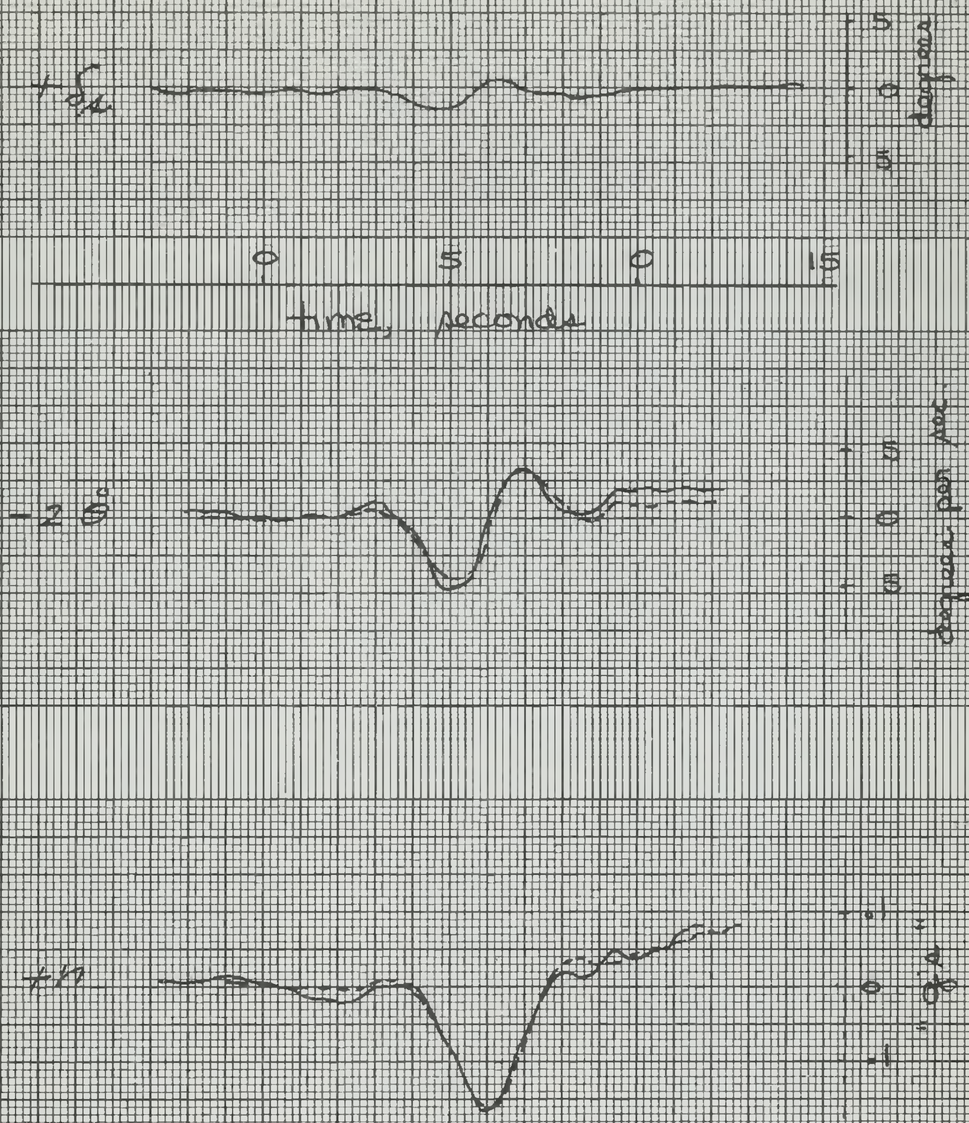

SANBORN *Recording Permapaper*

Fig. 9

Matched Response to Stabilator Pulse

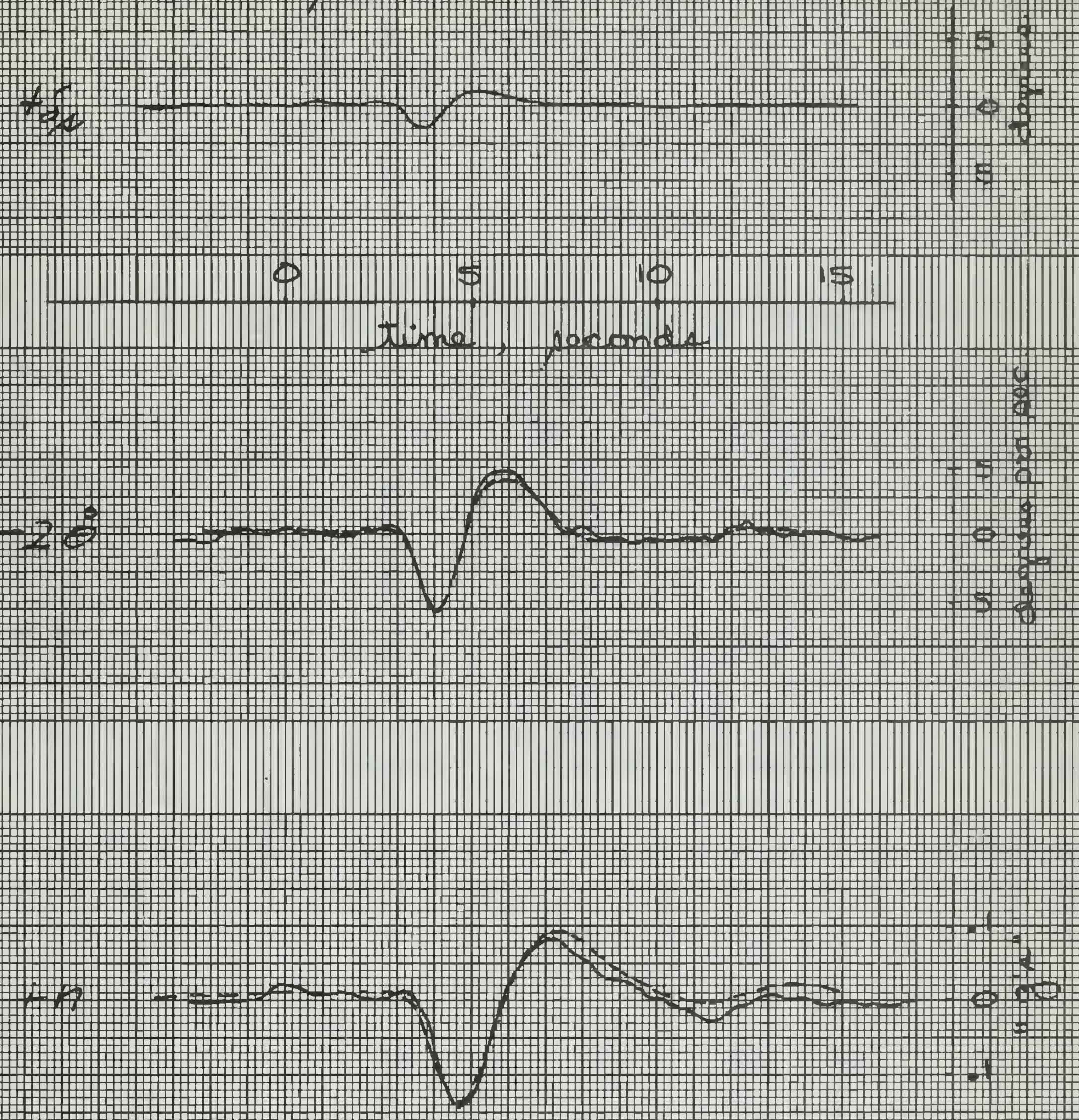

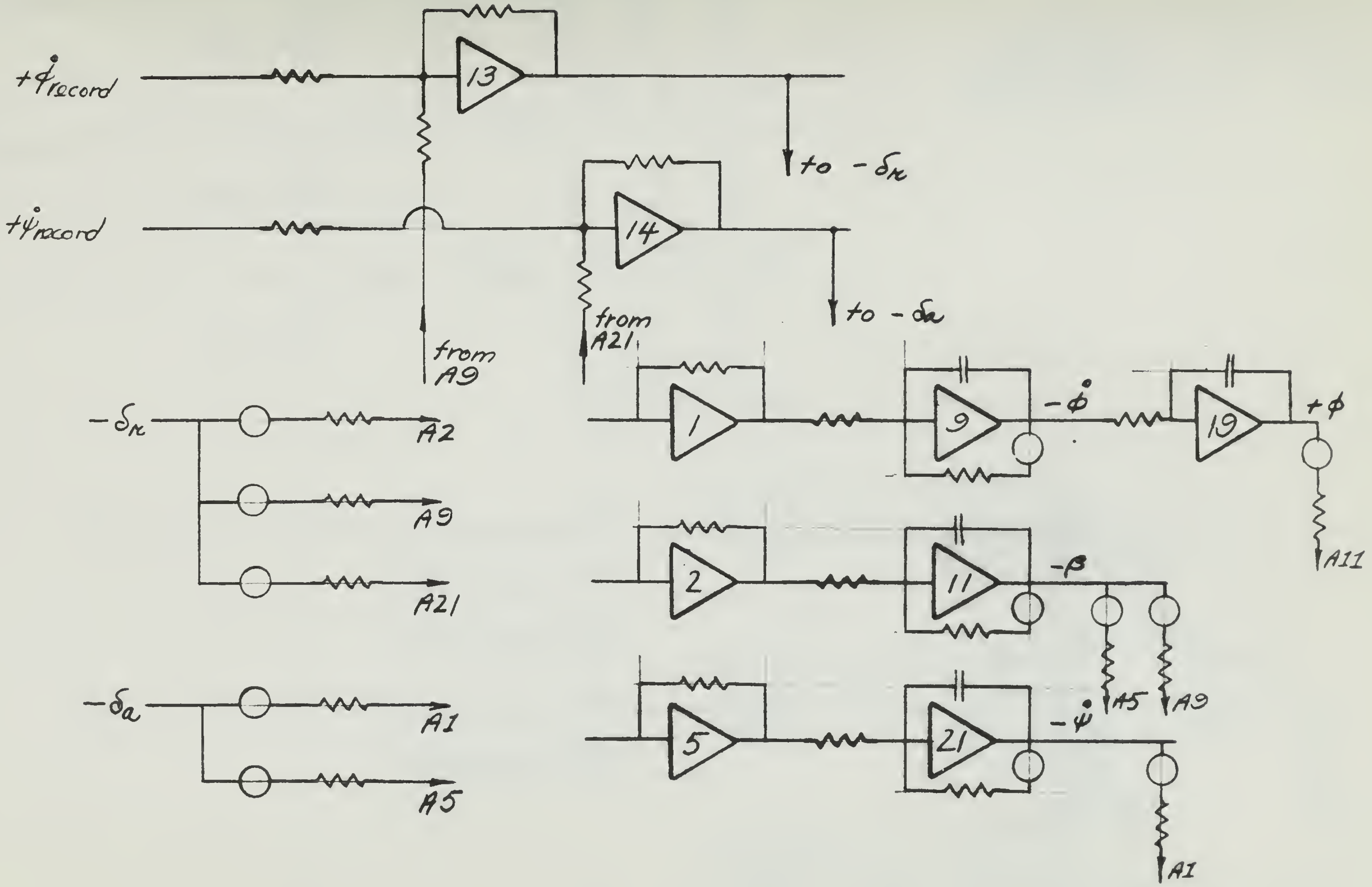

$+\dot{\phi}_{record}$
$+\dot{\psi}_{record}$
13
14
to $-\delta_r$
to $-\delta_a$
from A9
from A21
$-\delta_r$
A2
A9
A21
$-\delta_a$
A1
A5
1
2
5
9
11
21
19
$-\dot{\phi}$
$+\phi$
$-\beta$
$-\dot{\psi}$
A11
A5
A9
A1

FIG. 10

NAVION PRELIMINARY ANALYSIS CIRCUIT

FIG. 11
INITIAL LATERAL
GUST ANALYSIS CIRCUIT

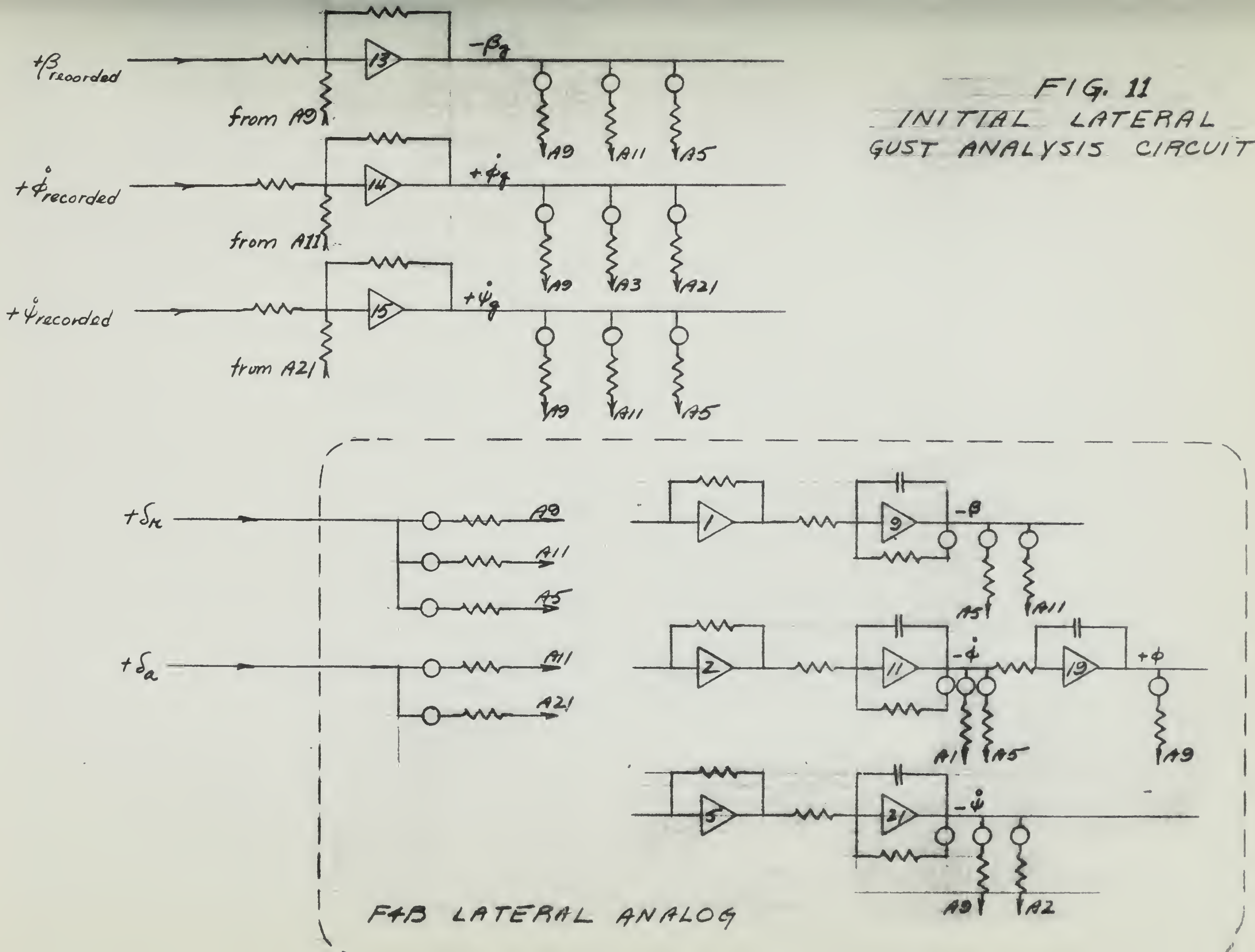
$+\beta_{recorded}$
$+\mathring{\phi}_{recorded}$
$+\mathring{\psi}_{recorded}$
from A9
from A11
from A21
13
14
15
$-\beta_g$
$+\dot{\phi}_g$
$+\dot{\psi}_g$
A9
A11
A5
A9
A3
A21
A9
A11
A5
$+\delta_r$
$+\delta_a$
A9
A11
A5
A11
A21
1
2
5
9
11
21
19
$-\beta$
$-\dot{\phi}$
$+\phi$
$-\dot{\psi}$
A5
A11
A1
A5
A9
A9
A2
F4B LATERAL ANALOG

FIG. 12

FINAL LATERAL
GUST ANALYSIS CIRCUIT

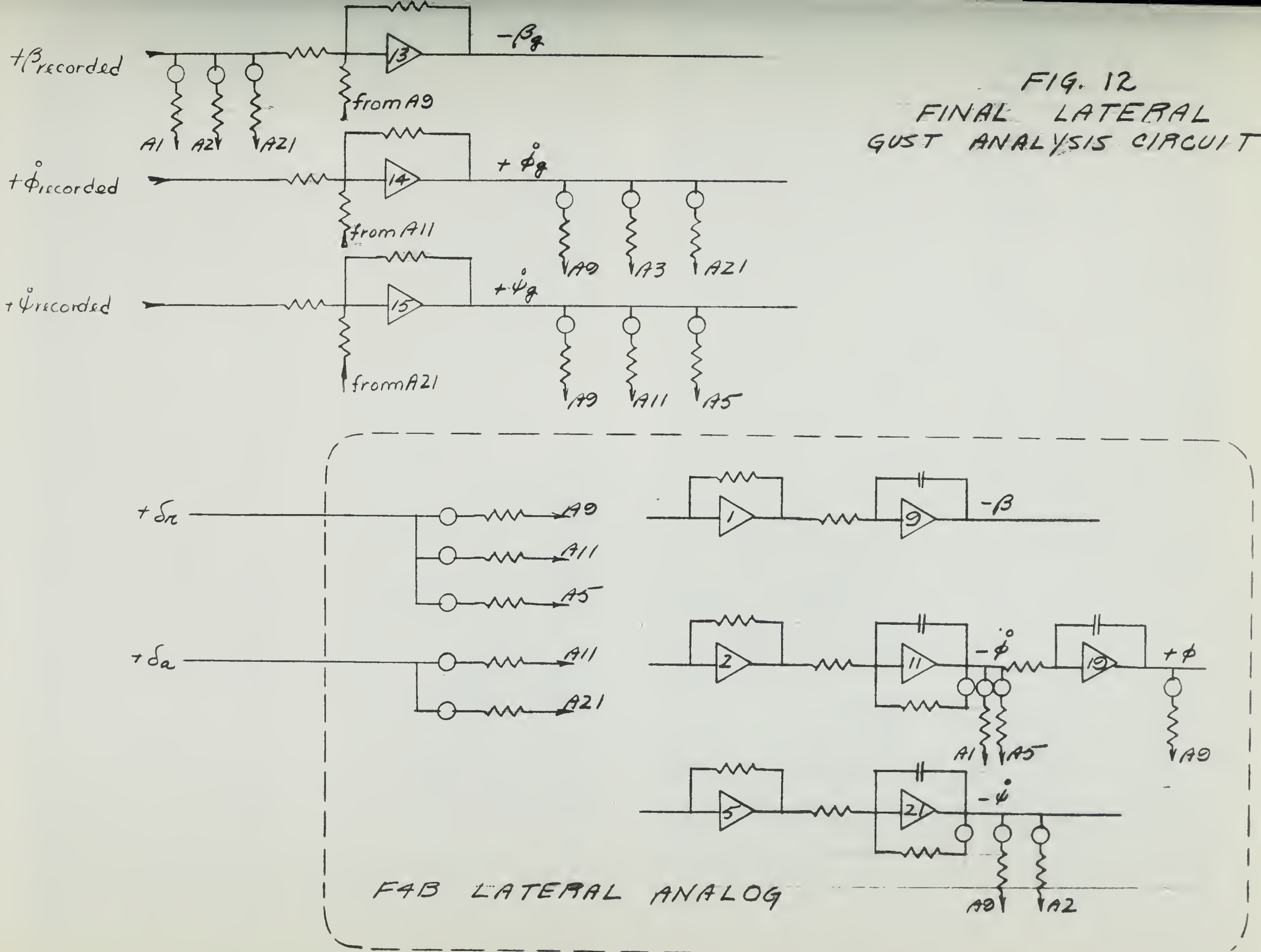
+β recorded
+φ̊ recorded
+ψ̊ recorded
A1
A2
A21
from A9
from A11
from A21
13
14
15
−β g
+ φ̊ g
+ ψ̊ g
A9
A3
A21
A9
A11
A5
+δr
+δa
A9
A11
A5
A11
A21
1
9
−β
2
11
−φ̇
19
+φ
A1
A5
A9
5
21
−ψ̇
A9
A2
F4B LATERAL ANALOG

Fig. 13

SIMULATED $\beta_g$ INPUT AND ANALOG RESPONSE QUANTITIES

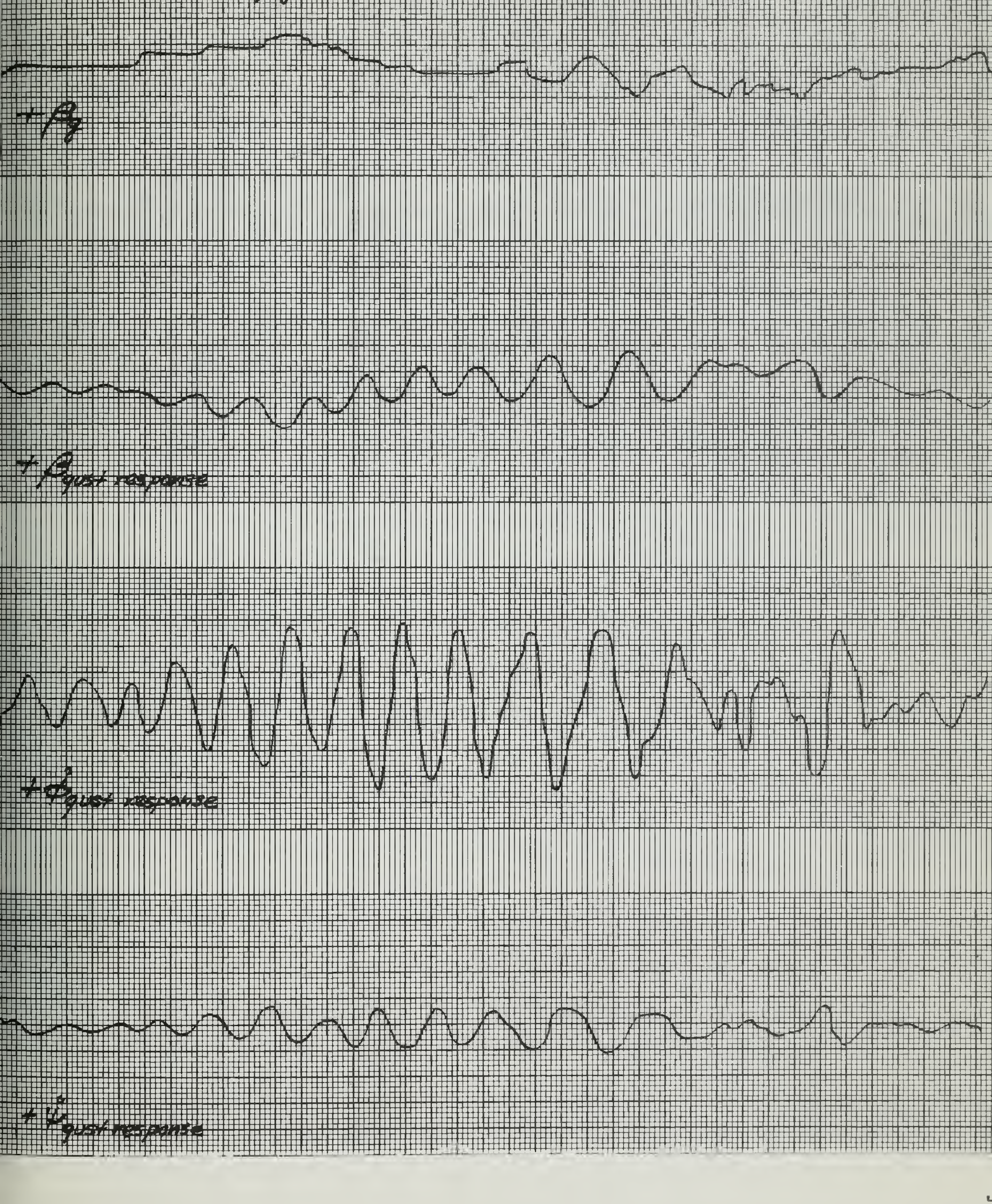

SANBORN Recording Permapaper

Fig. 14

Simulated $R_q$ Quantity Reproductions

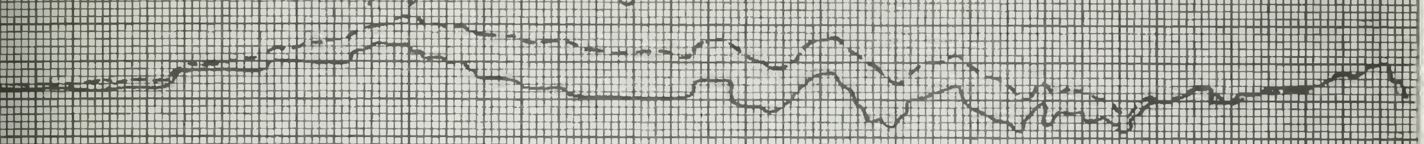

(a) $R_f = \infty$

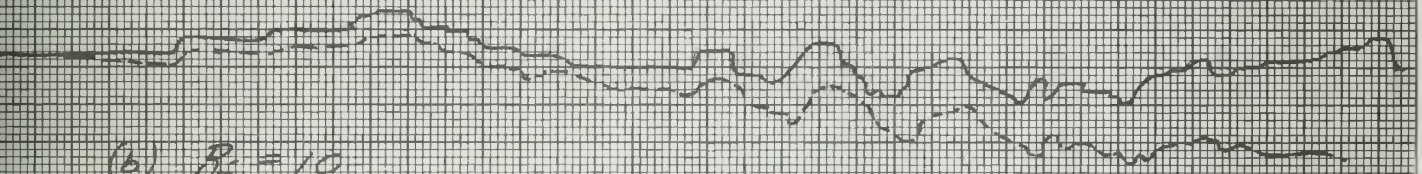

(b) $R_f = 10$

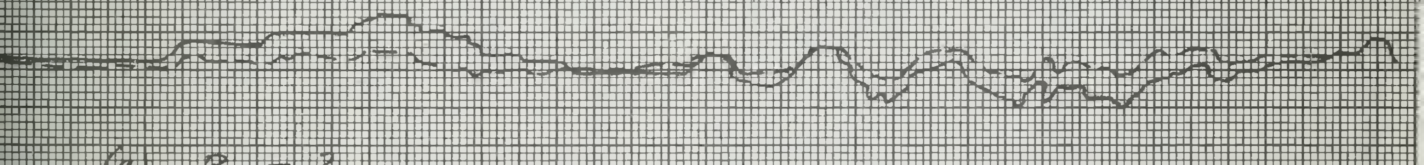

(c) $R_f = 2$

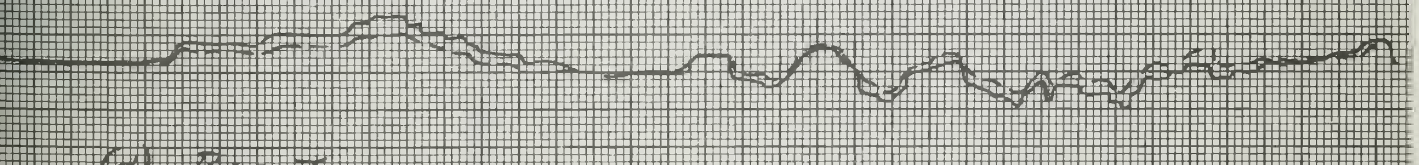

(d) $R_f = 7$

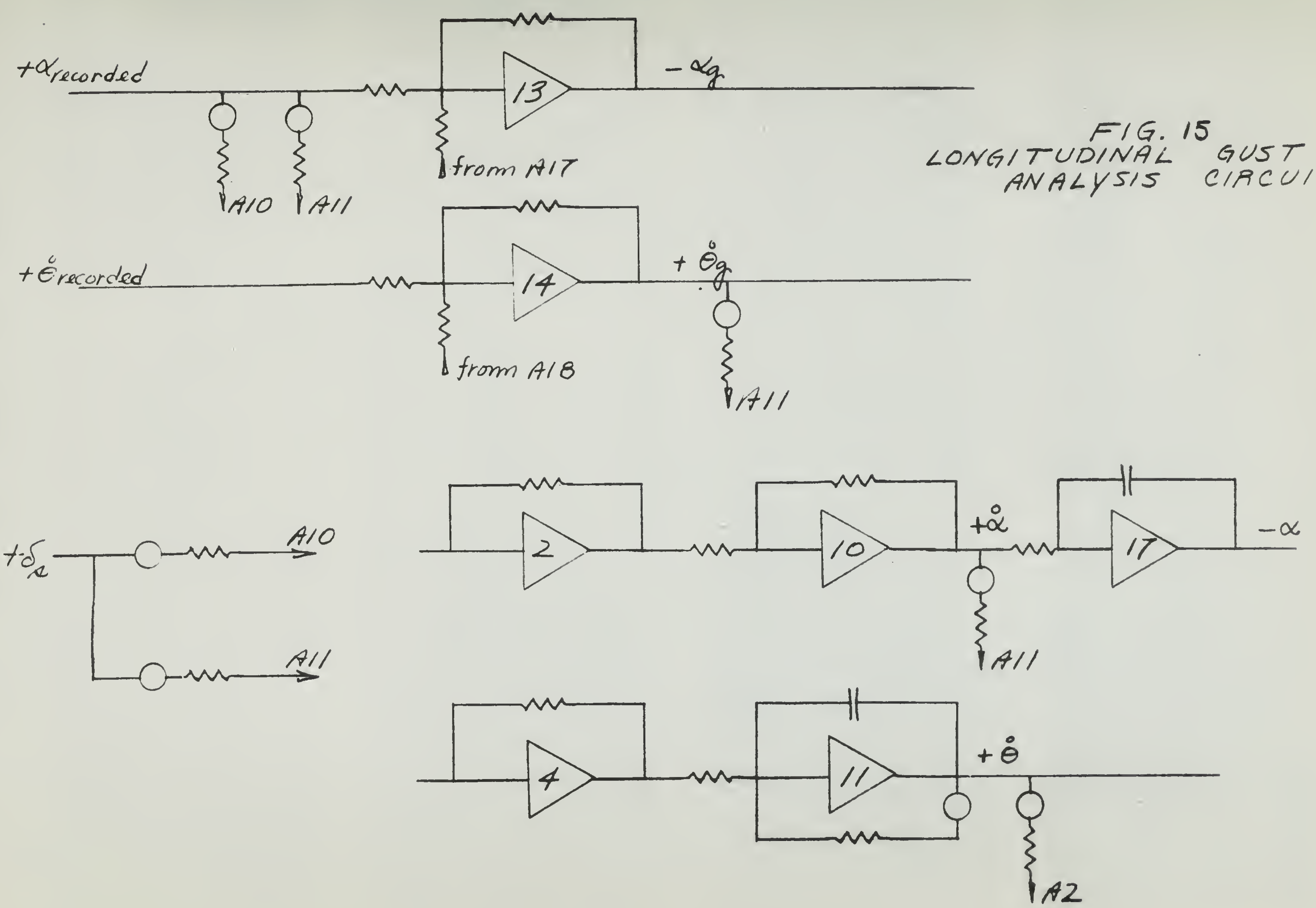
$+\alpha_{recorded}$
A10
A11
13
from A17
$-\alpha_g$
$+\mathring{\theta}_{recorded}$
14
from A18
$+\mathring{\theta}_g$
A11
$+\delta_e$
A10
A11
2
10
$+\mathring{\alpha}$
A11
17
$-\alpha$
4
11
$+\mathring{\theta}$
A2

FIG. 15
LONGITUDINAL GUST
ANALYSIS CIRCUIT

Lateral and Longitudinal Gust Quantities

RECORDING CHARTS GRAPHIC CONTROLS CORPORATION

Approach No 1

FIG 16A

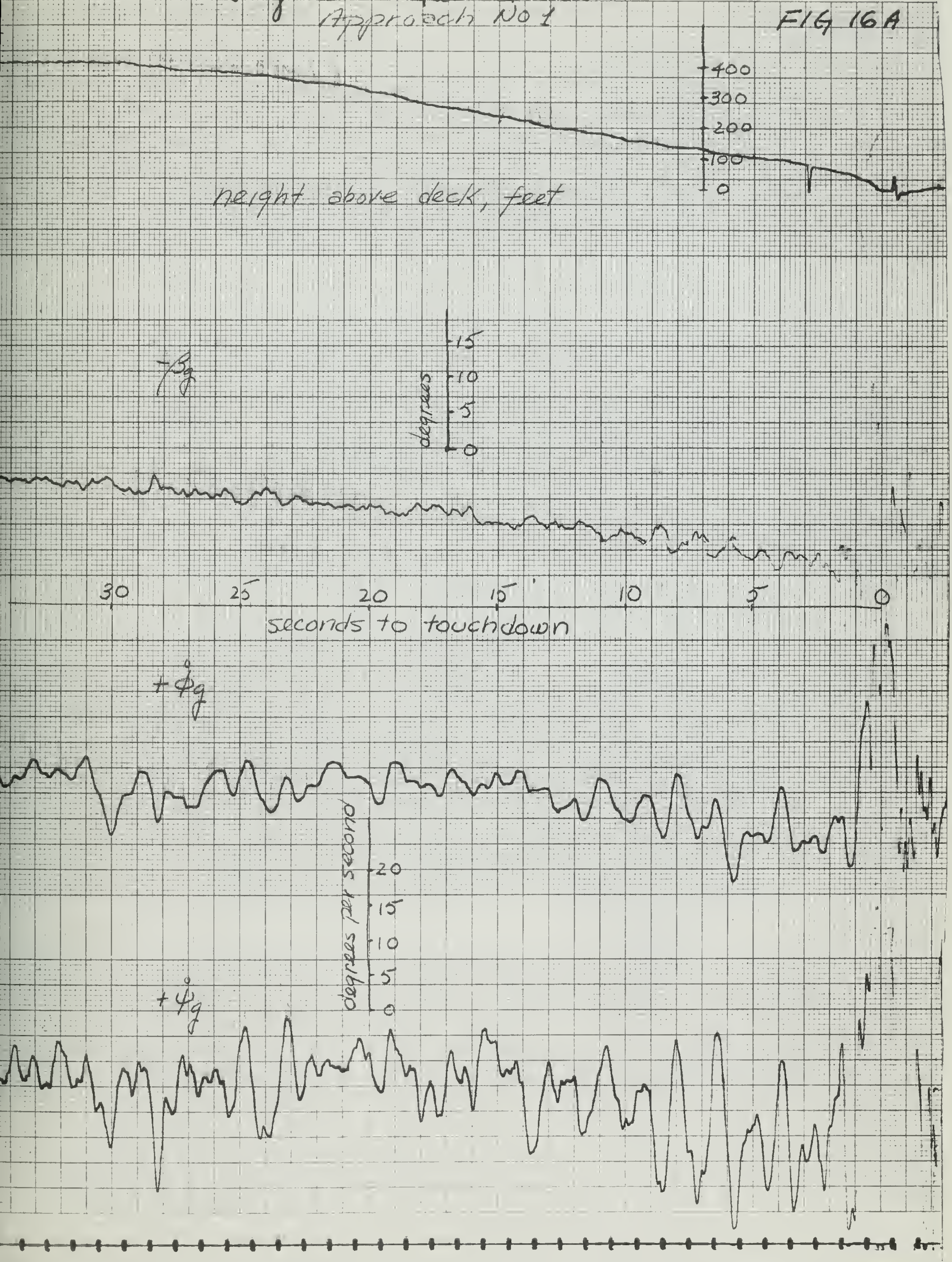

BUFFALO, NEW YORK PRINTED IN U S A

Approach No. X1

FIG 16B

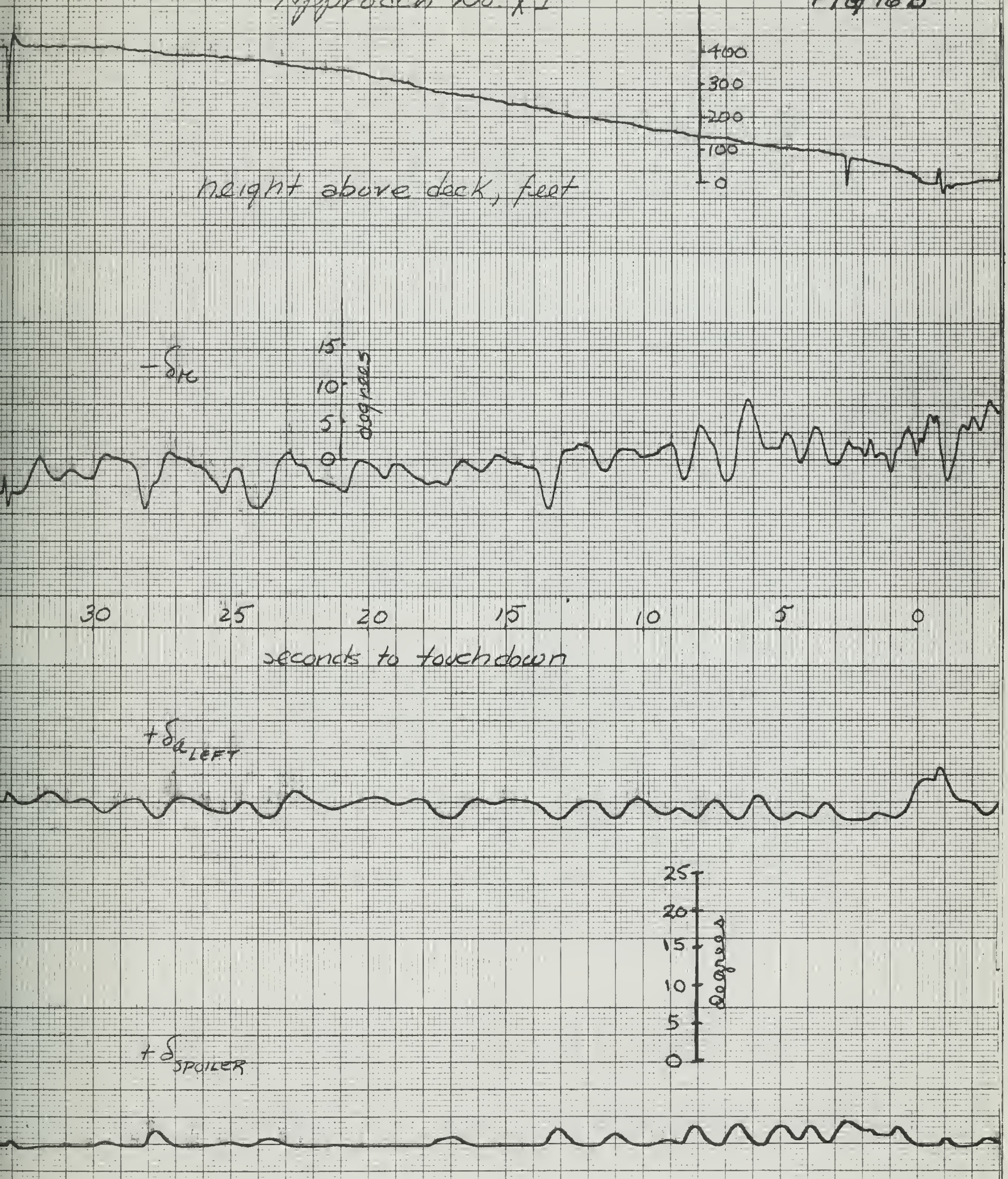

Approach No.#1

FIG 16C

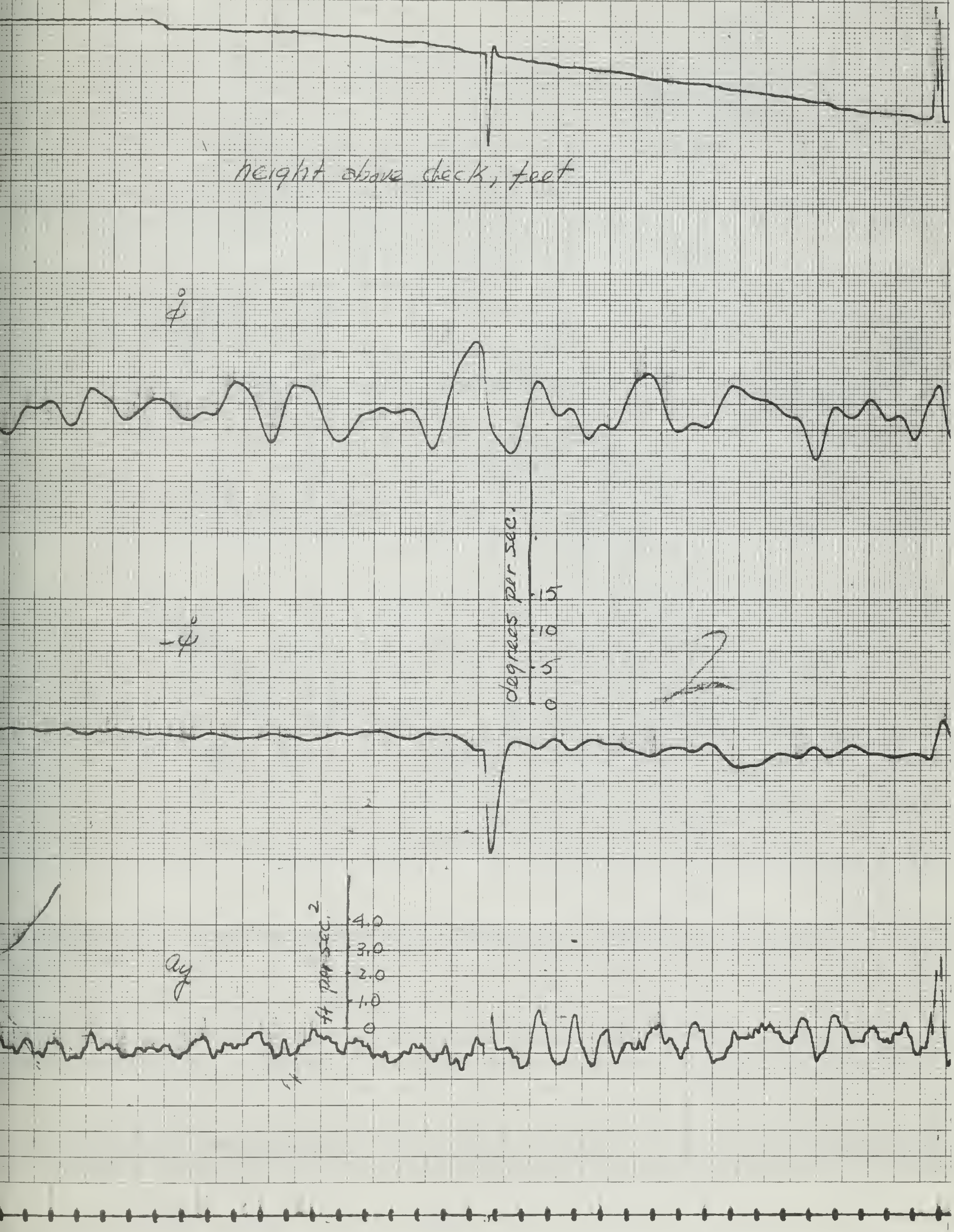

RECORDING CHARTS | GRAPHIC CONTROLS CORPORATION | BUFFALO, NEW YORK PRINTED IN

Approach No 1

FIG 16 D

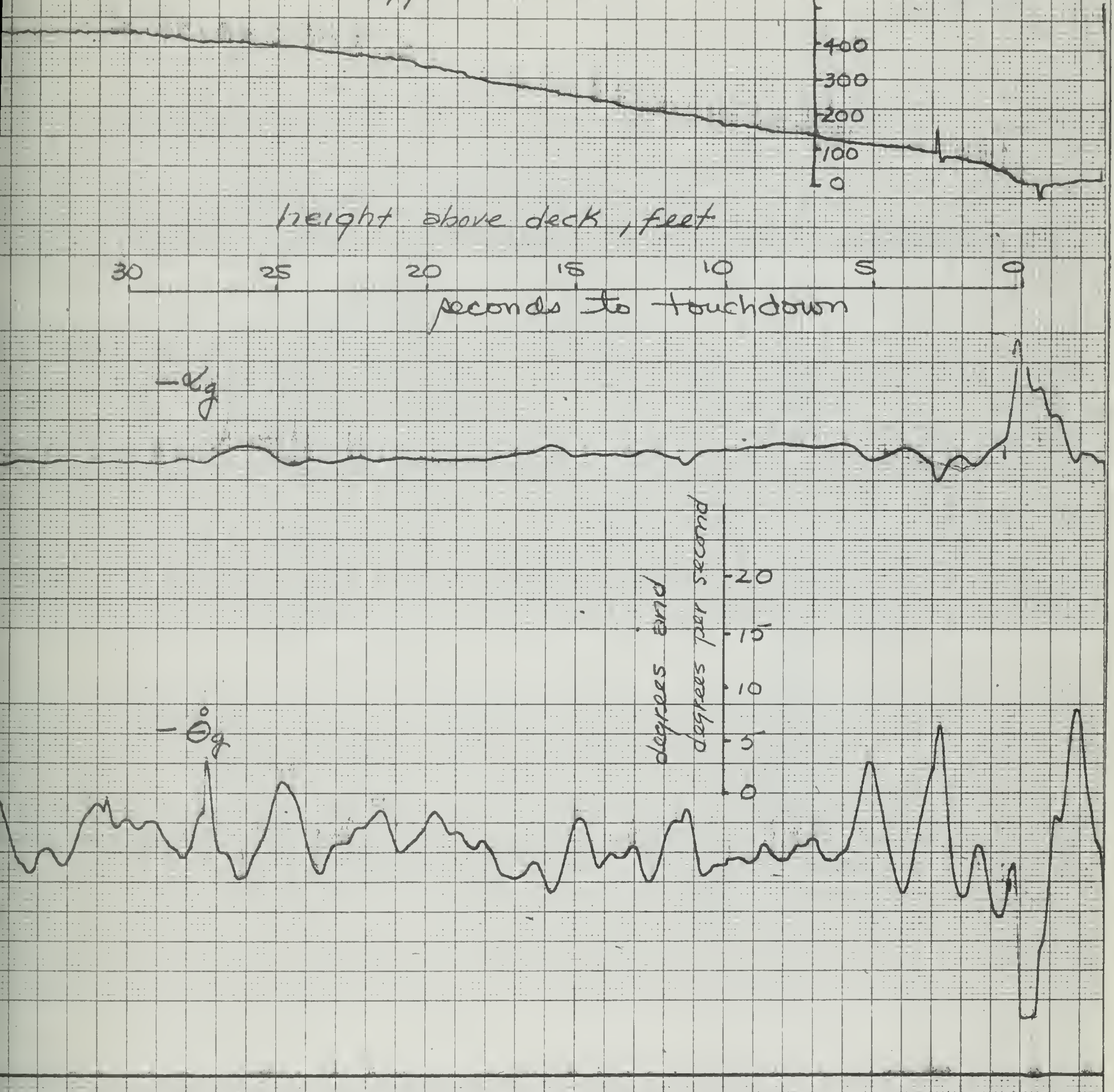

PRINTED IN U.S.A

G RECORDING CHARTS

Approach No. 1

FIG 16E

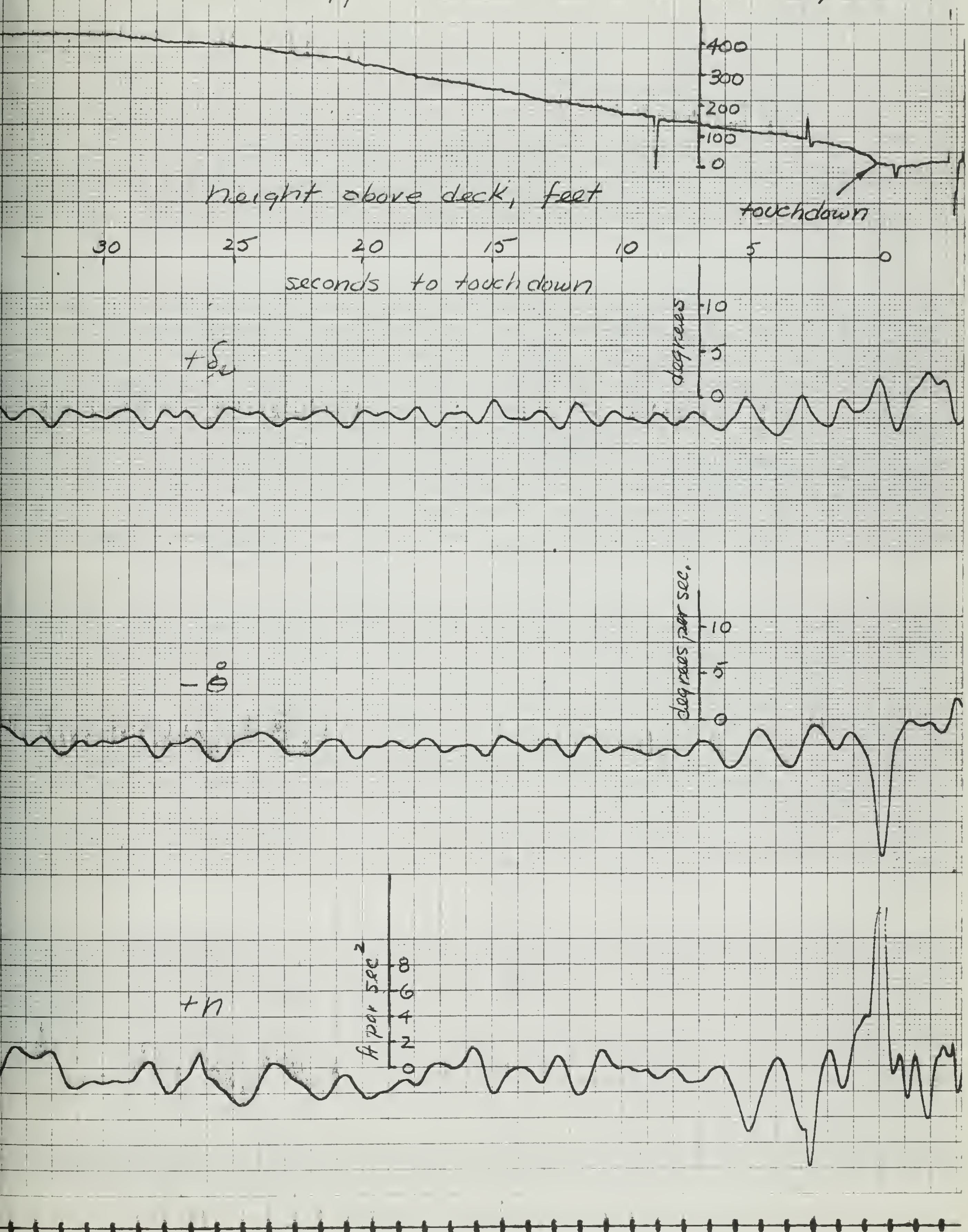

SA

Lateral and Longitudinal Gust Quantities

approach No 4

RECORDING CHARTS GRAPHIC CONTROL

Fig. 17A

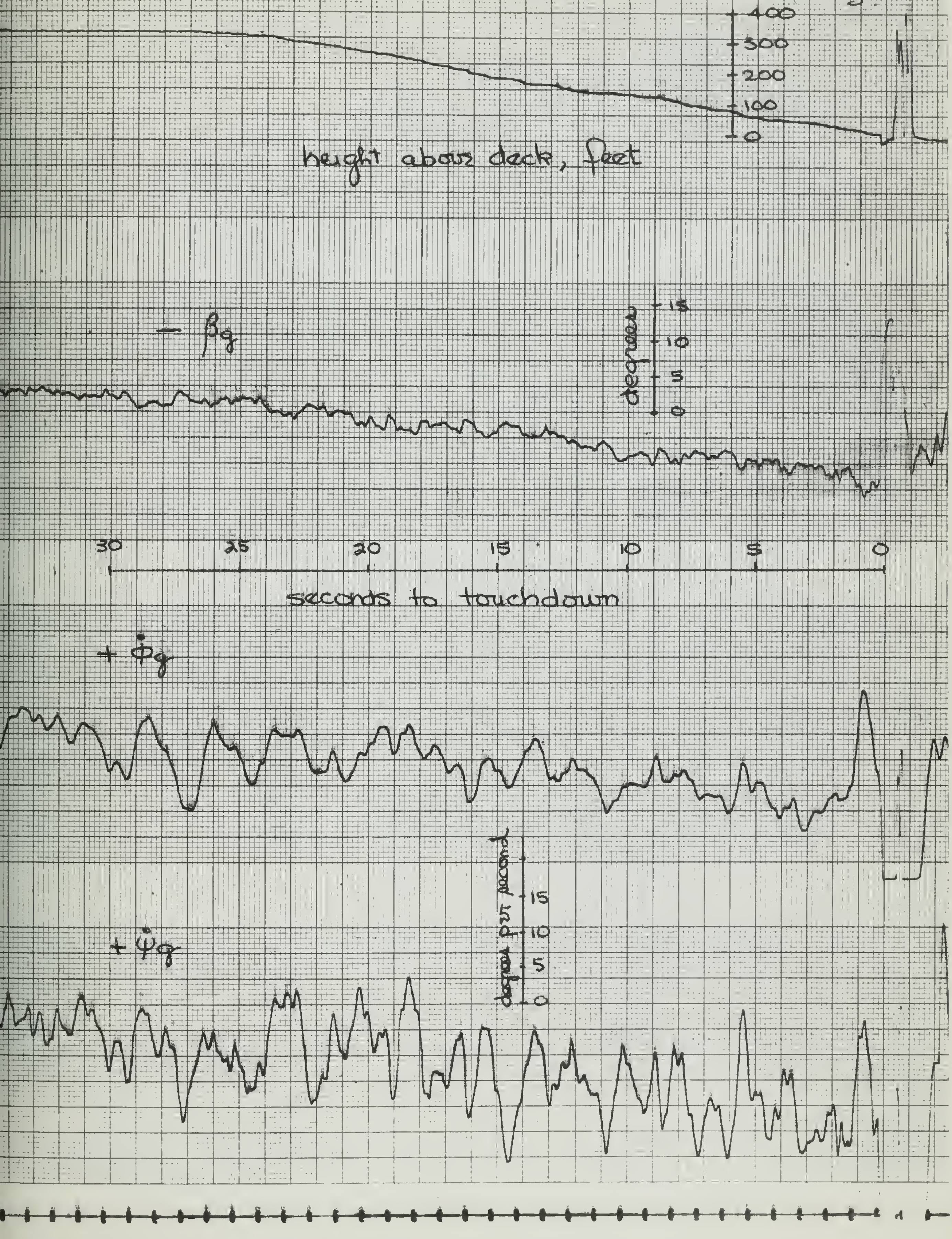

Approach No. 4

Fig 17 B

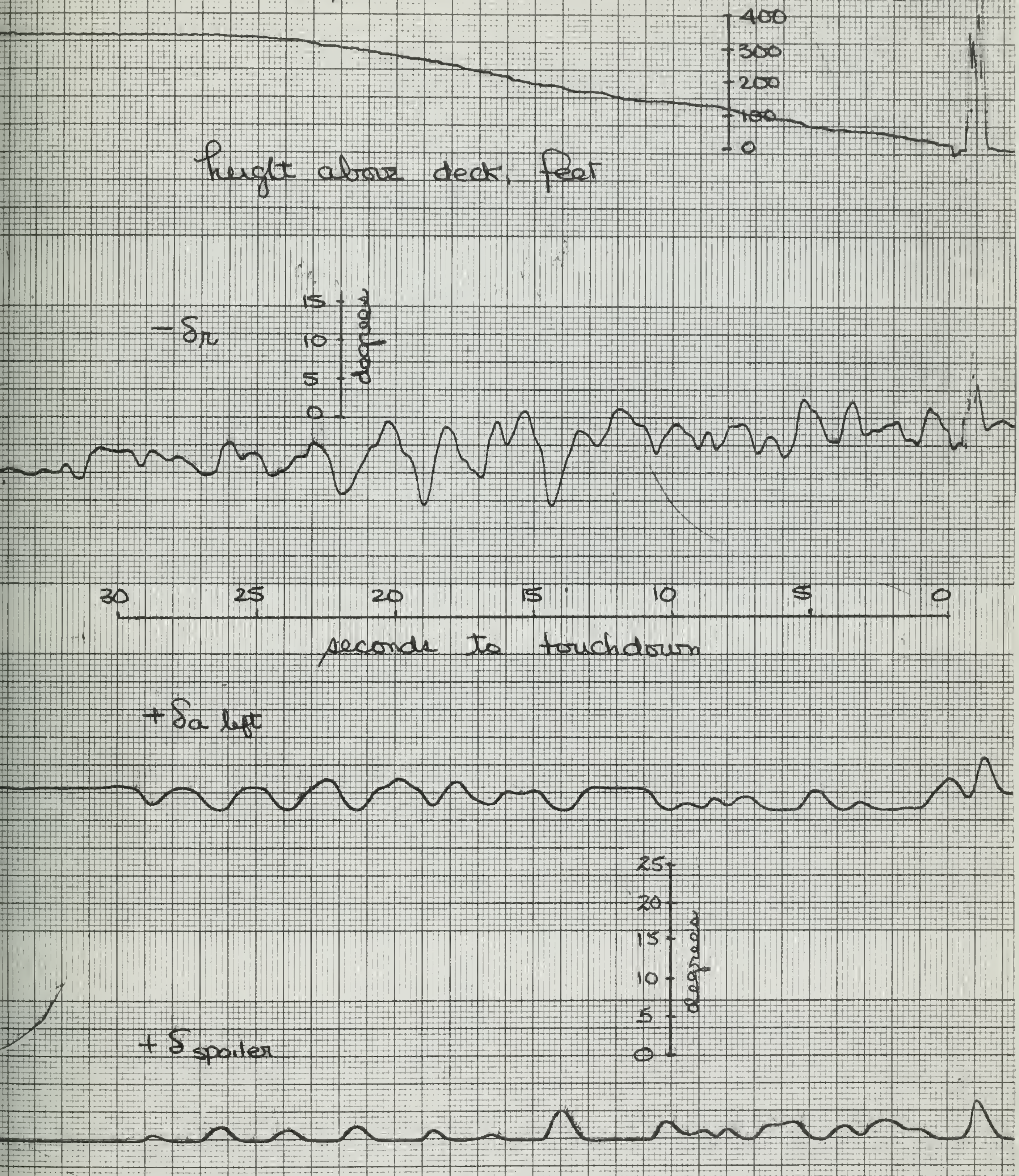

Fig. 17 C

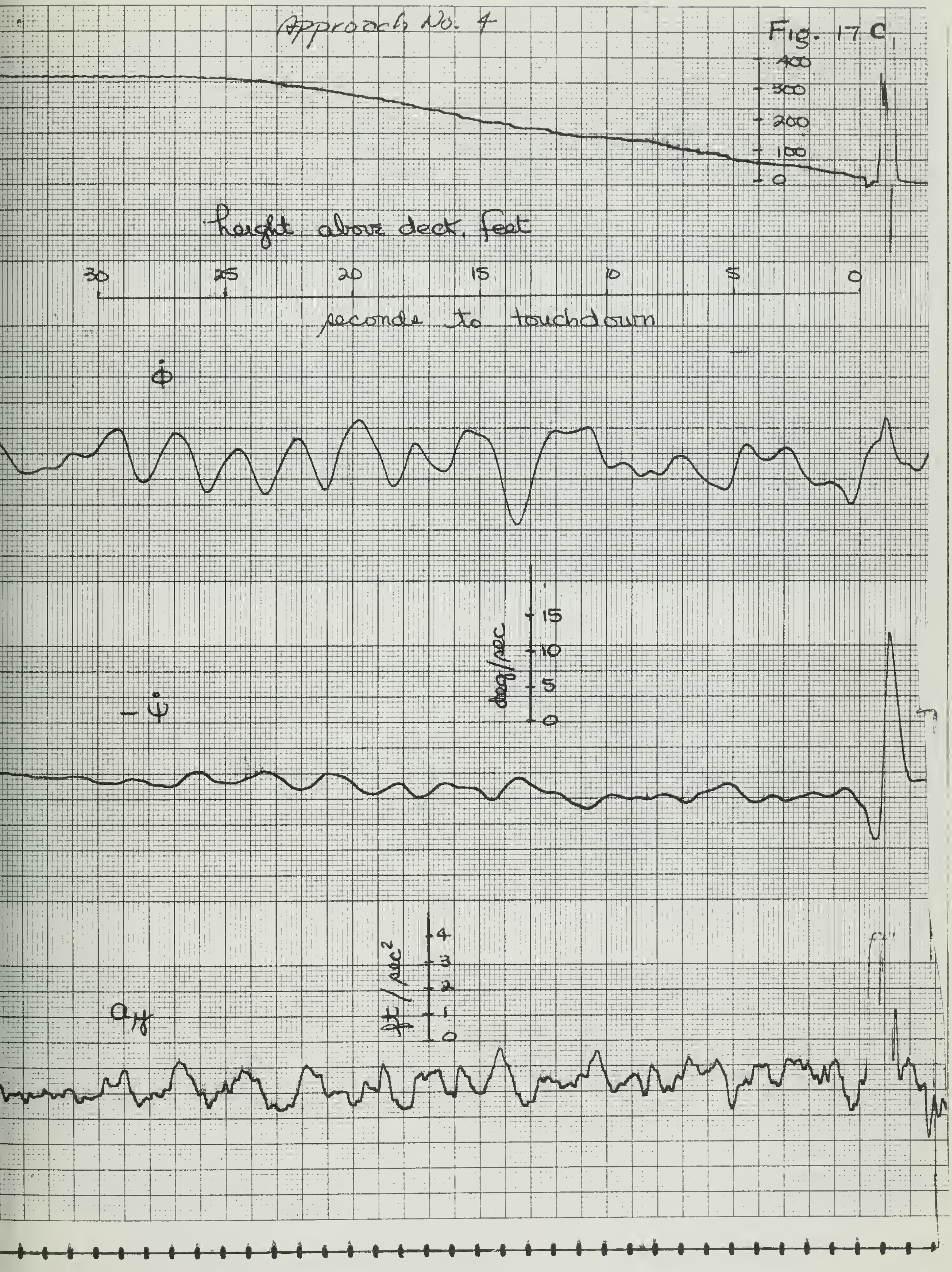
Approach No. 4
400
300
200
100
0
height above deck, feet
30
25
20
15
10
5
0
seconds to touchdown
$\dot{\Phi}$
$-\dot{\Psi}$
deg/sec
15
10
5
0
$a_y$
ft/sec²
4
3
2
1
0

RECORDING CHARTS | GRAPHIC CONTROLS CORPORATION | BUFFALO, NEW

Fig. 17 D

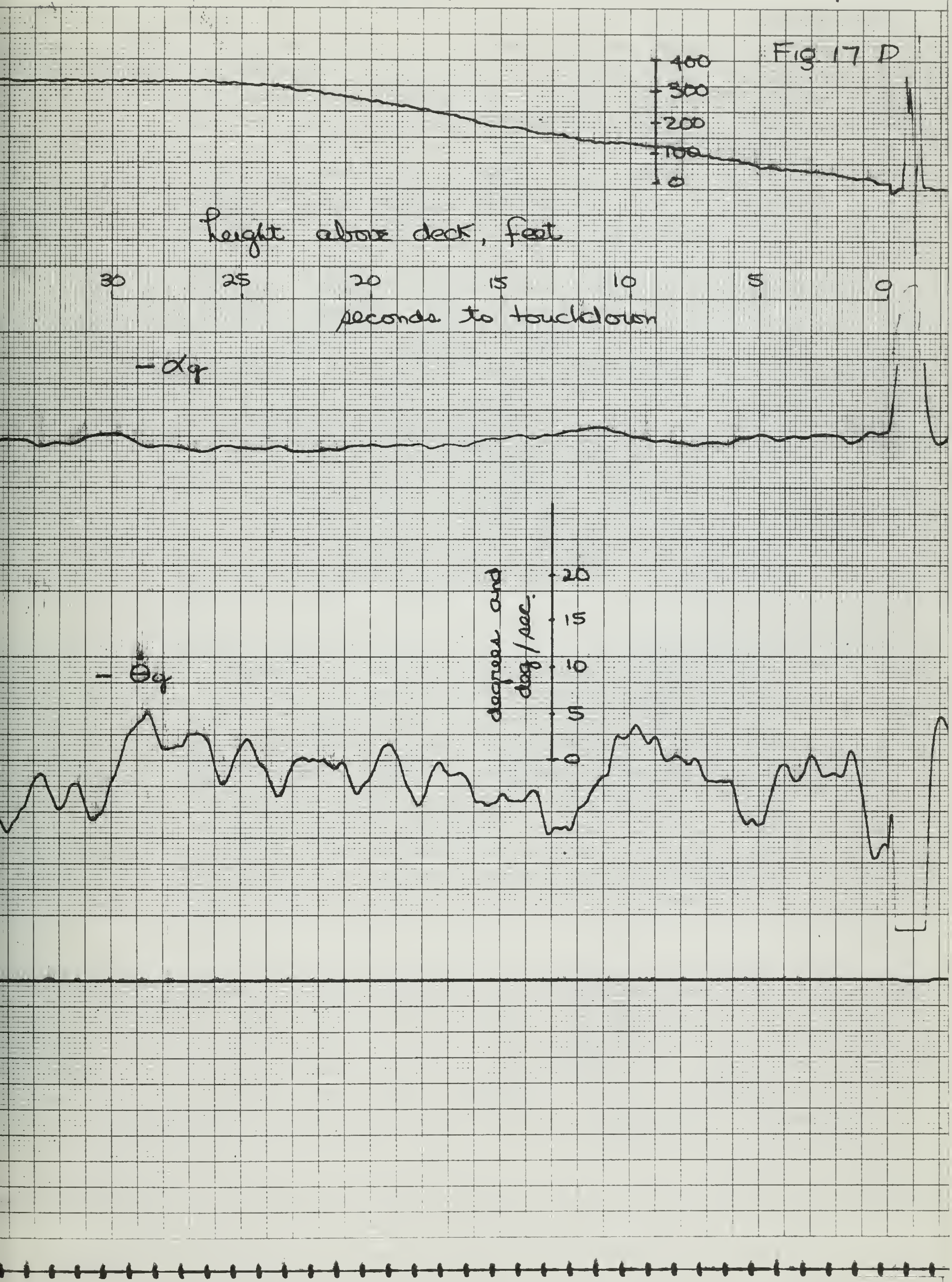

BUFFALO, NEW YORK PRINTED IN U.S.A

Fig. 17 E

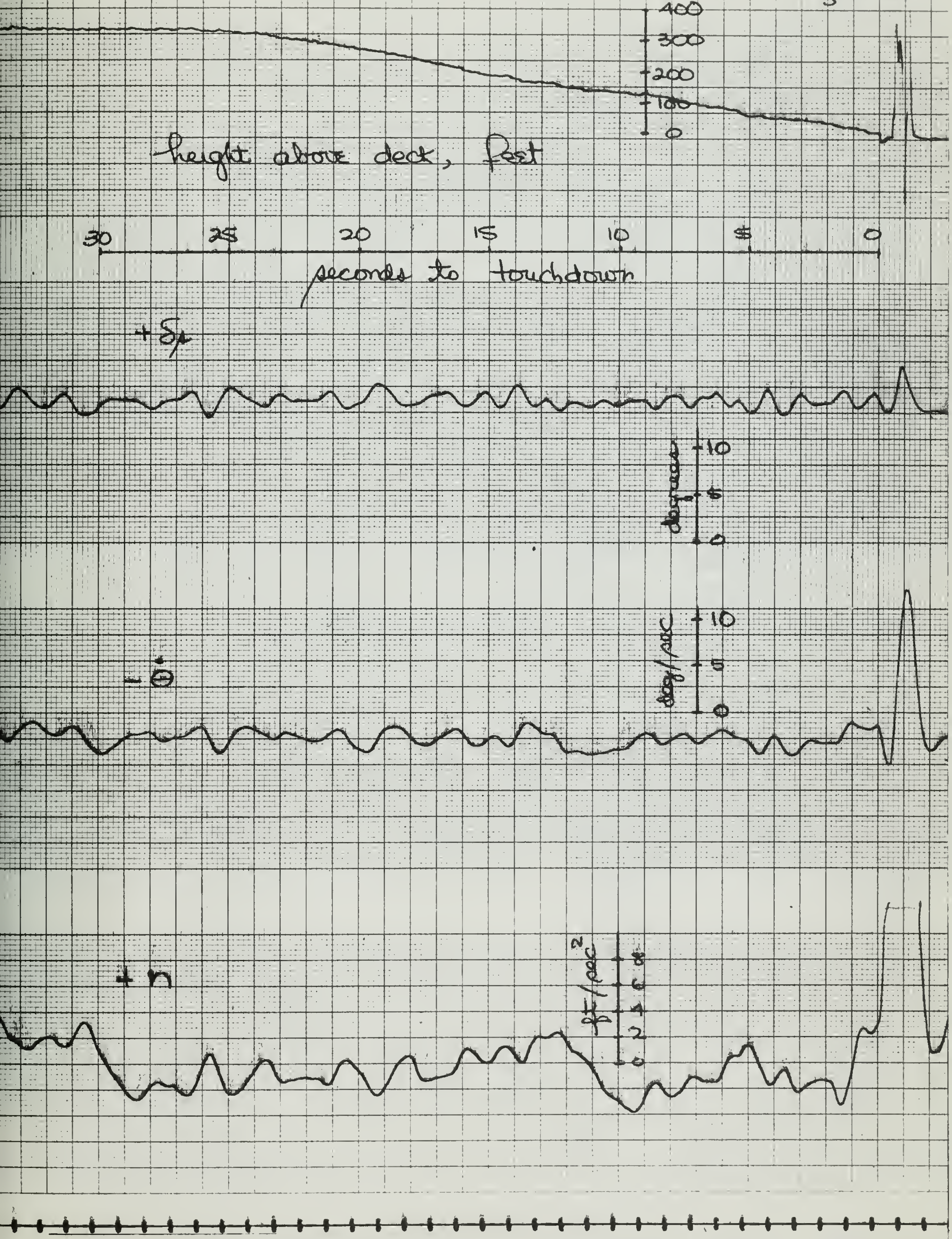

PRINTED IN U.S.A

G RECORDING CHARTS

Lateral and Longitudinal Gust Quantities

Approach No 5

Fig. 18A

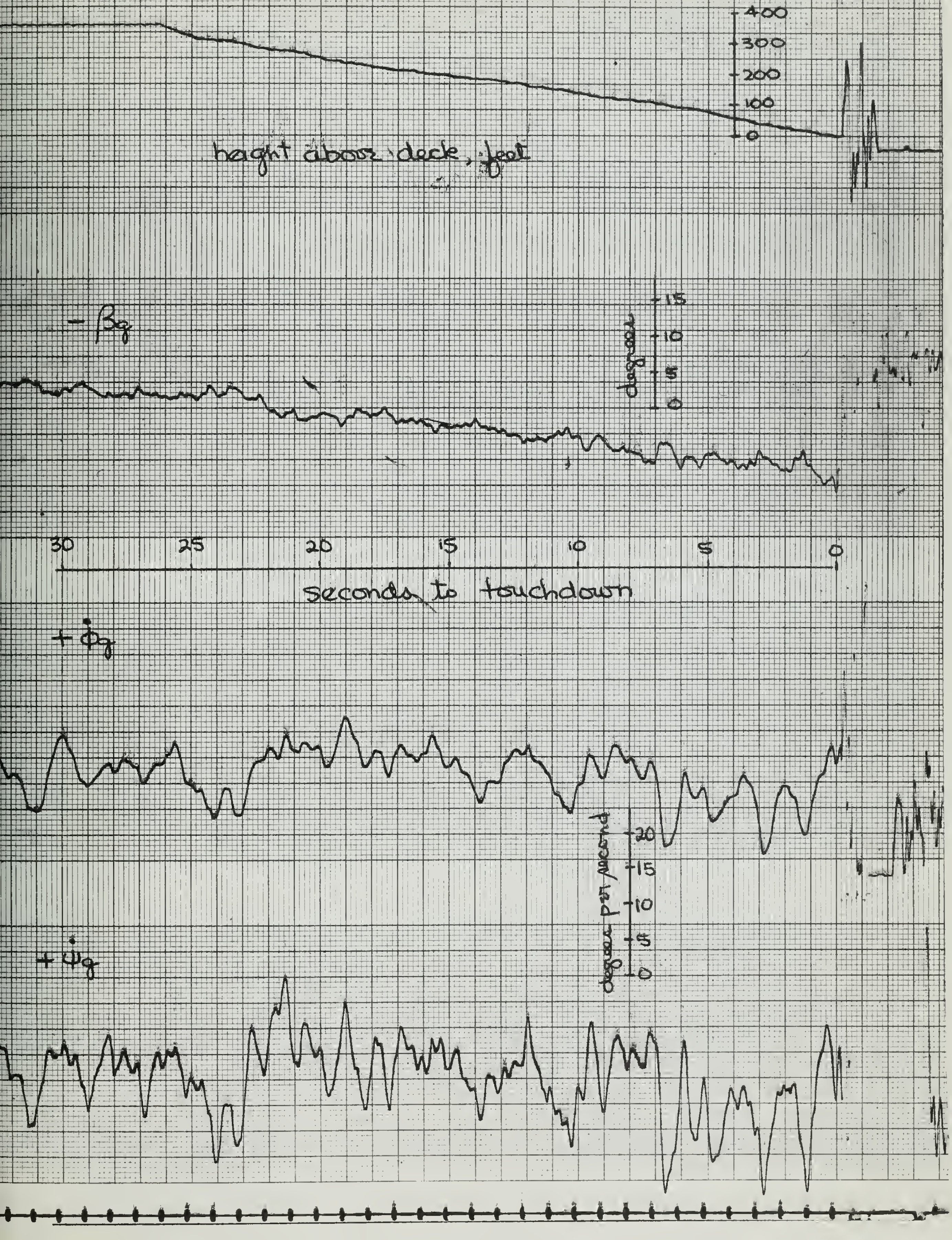

Fig. 18 B

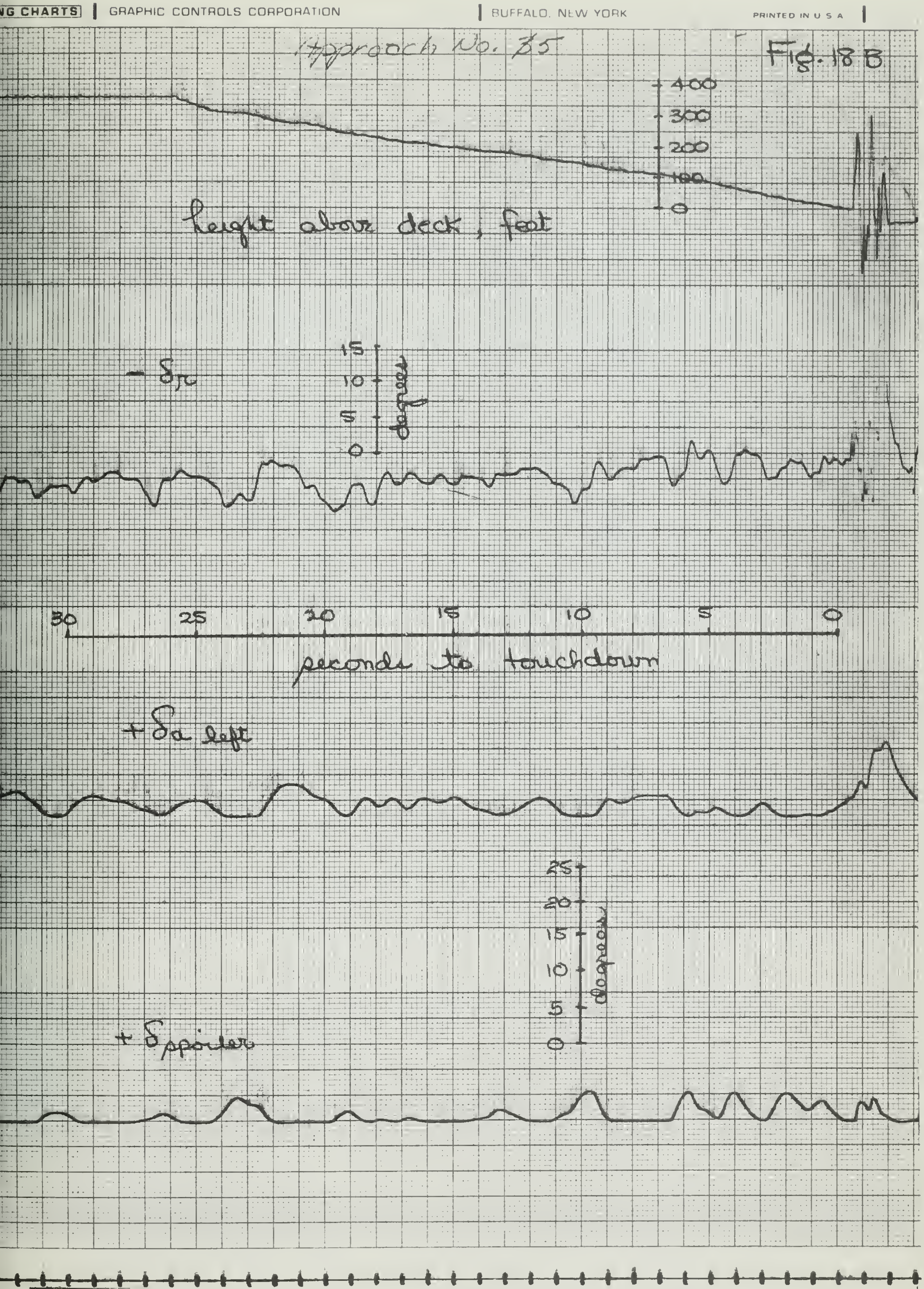
NG CHARTS
GRAPHIC CONTROLS CORPORATION
BUFFALO, NEW YORK
PRINTED IN U S A
Approach No. 35
400
300
200
100
0
height above deck, feet
− δr
15
10
5
0
degrees
30
25
20
15
10
5
0
seconds to touchdown
+ δa left
25
20
15
10
5
0
degrees
+ δspoiler

TS | GRAPHIC CONTROLS CORPORATION PRINTED IN U S A

Approach No. 35

Fig. 18 C

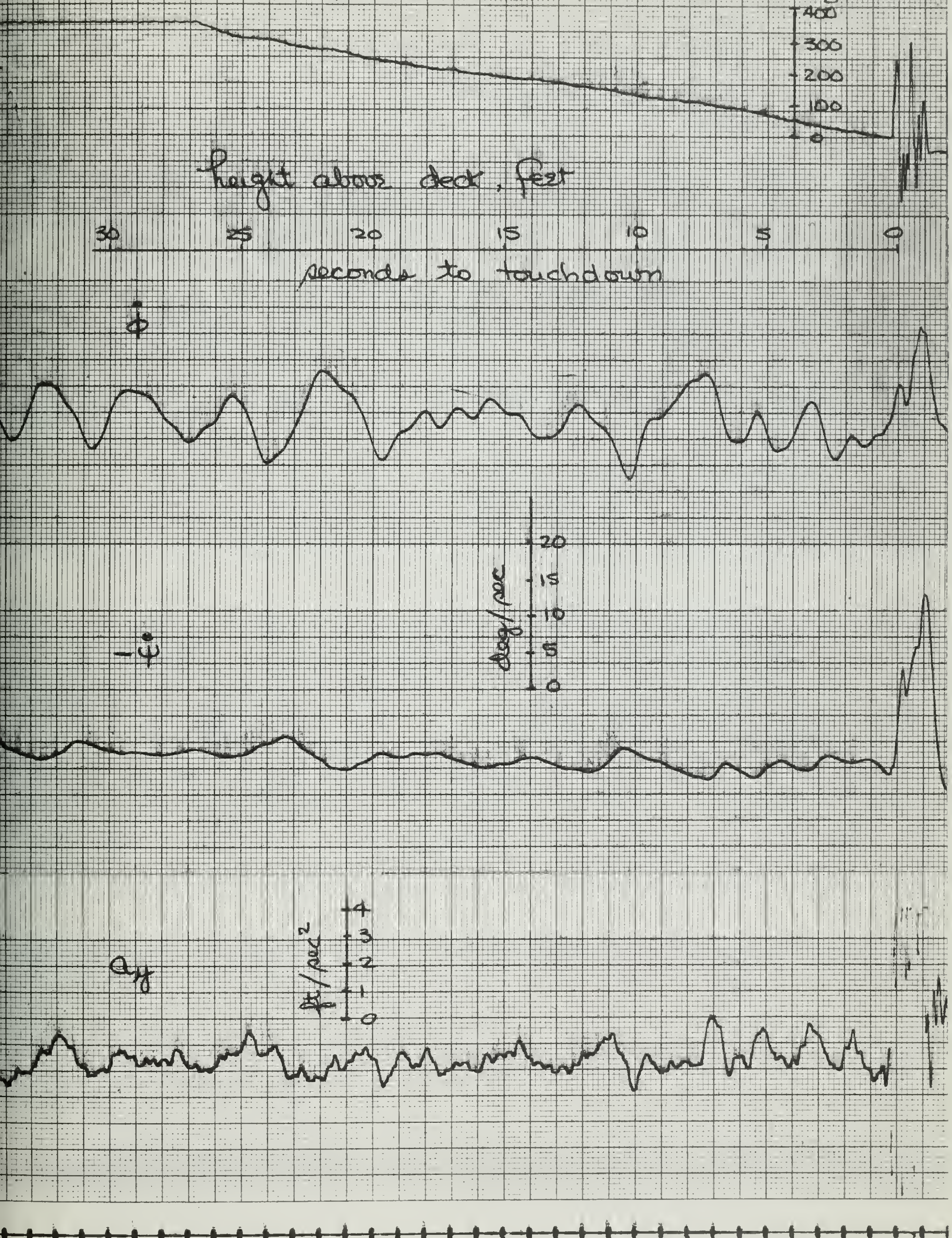

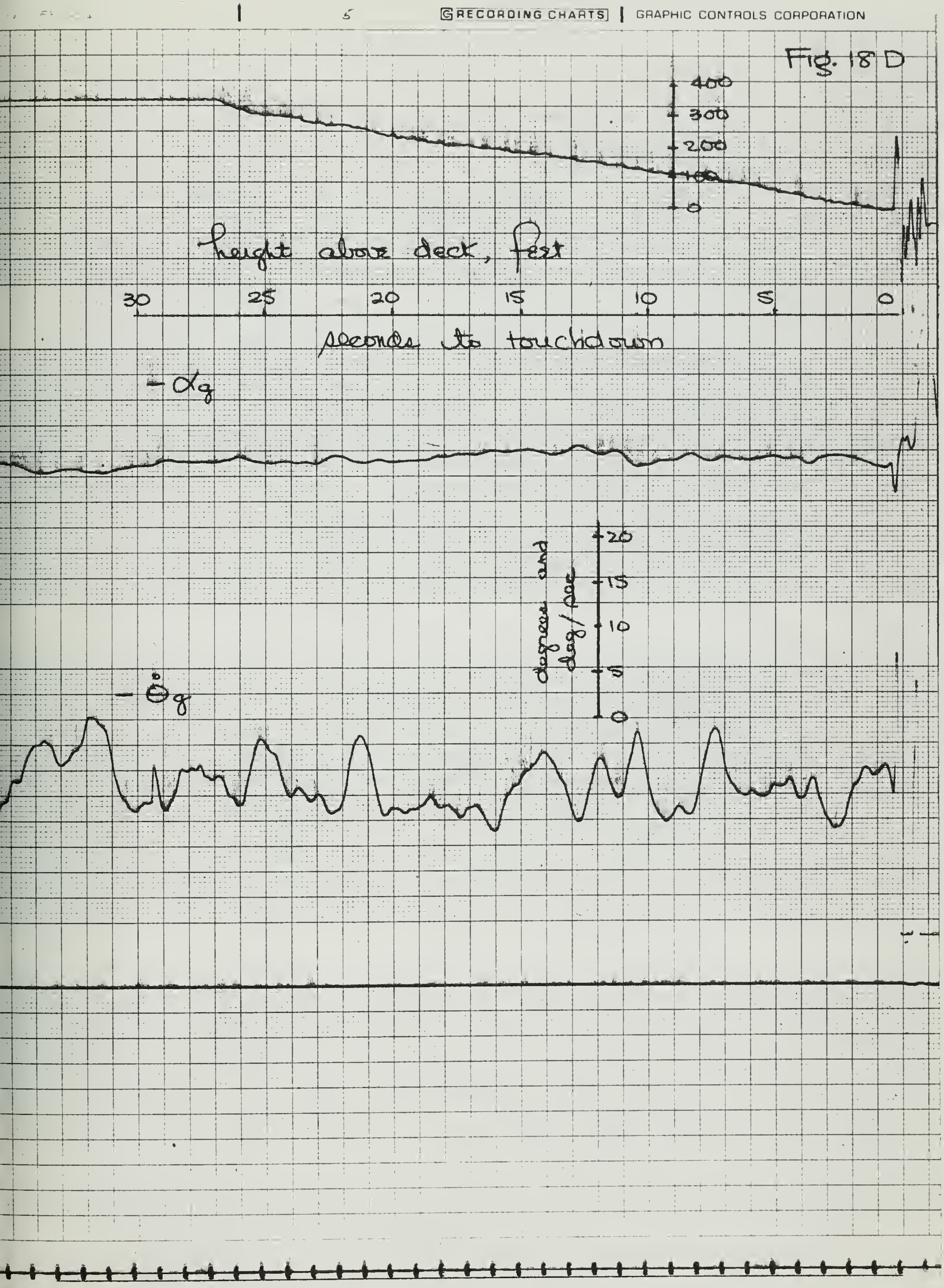

Fig. 18 D

5
RECORDING CHARTS | GRAPHIC CONTROLS CORPORATION
400
300
200
100
0
height above deck, feet
30
25
20
15
10
5
0
seconds to touchdown
$-\alpha_g$
20
15
10
5
0
degrees and deg/sec
$-\dot{\theta}_g$

Fig. 18E

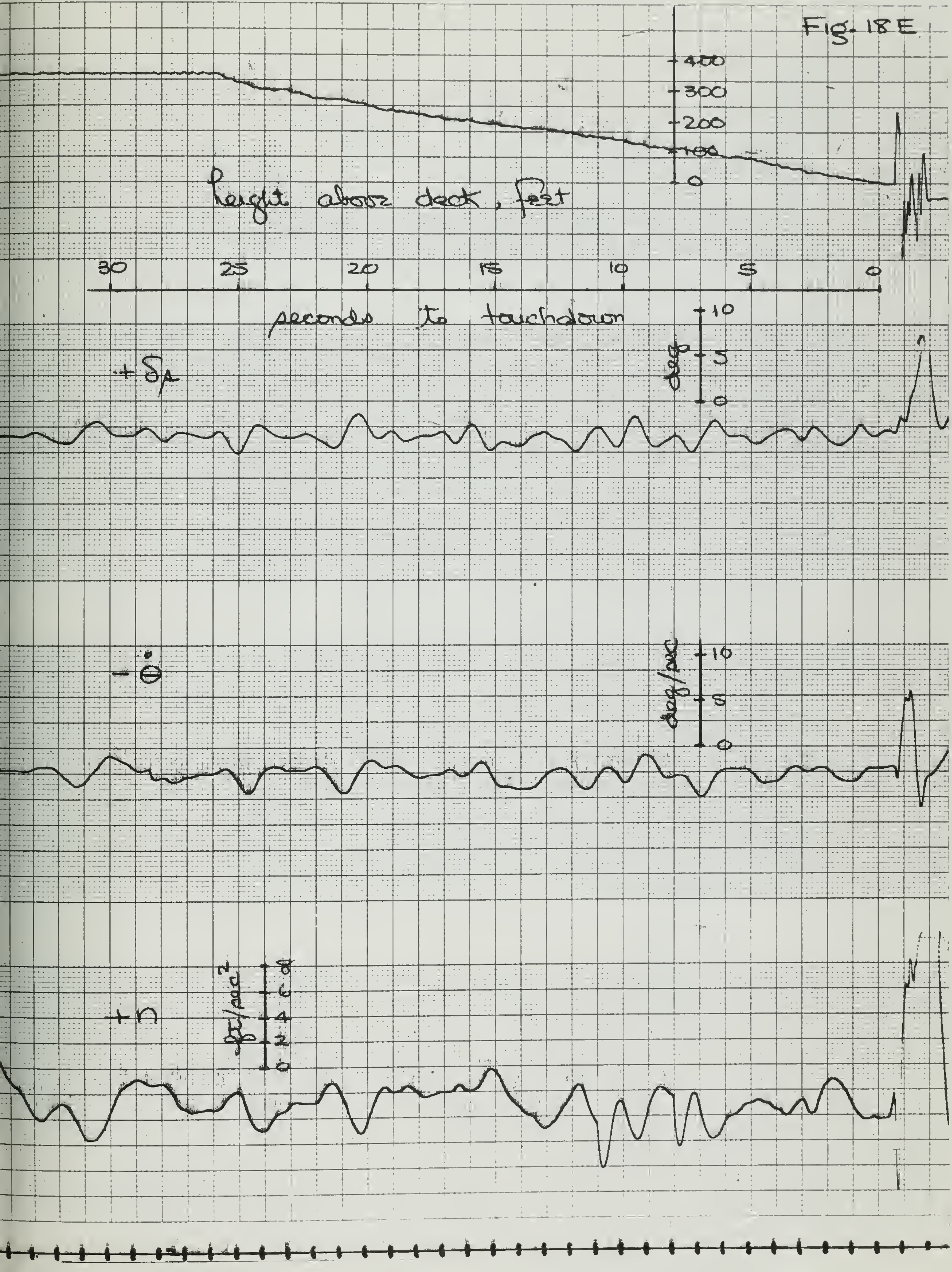
400
300
200
100
0
height above deck, feet
30
25
20
15
10
5
0
seconds to touchdown
+δp
deg
10
5
0
−θ̇
deg/sec
10
5
0
+n
ft/sec²
8
6
4
2
0

PRINTED IN U S A

Lateral and Longitudinal Gust Quantities

Approach No 6

G RECORDING CHARTS

Fig. 19 A

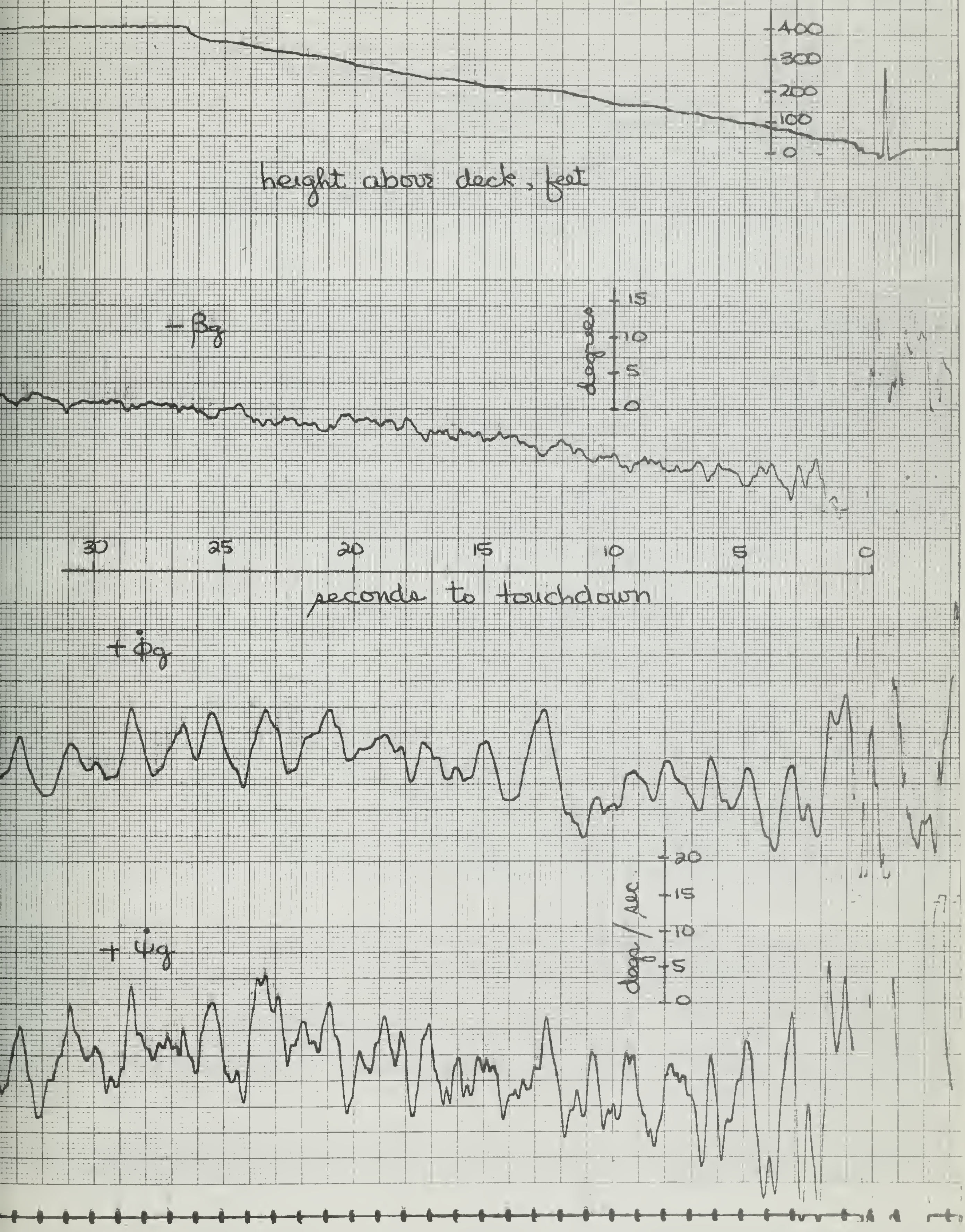

CHARTS | GRAPHIC CONTROLS CORPORATION | BUFFALO NEW YORK PRINTED IN U S A

Approach No. 6

Fig. 19B

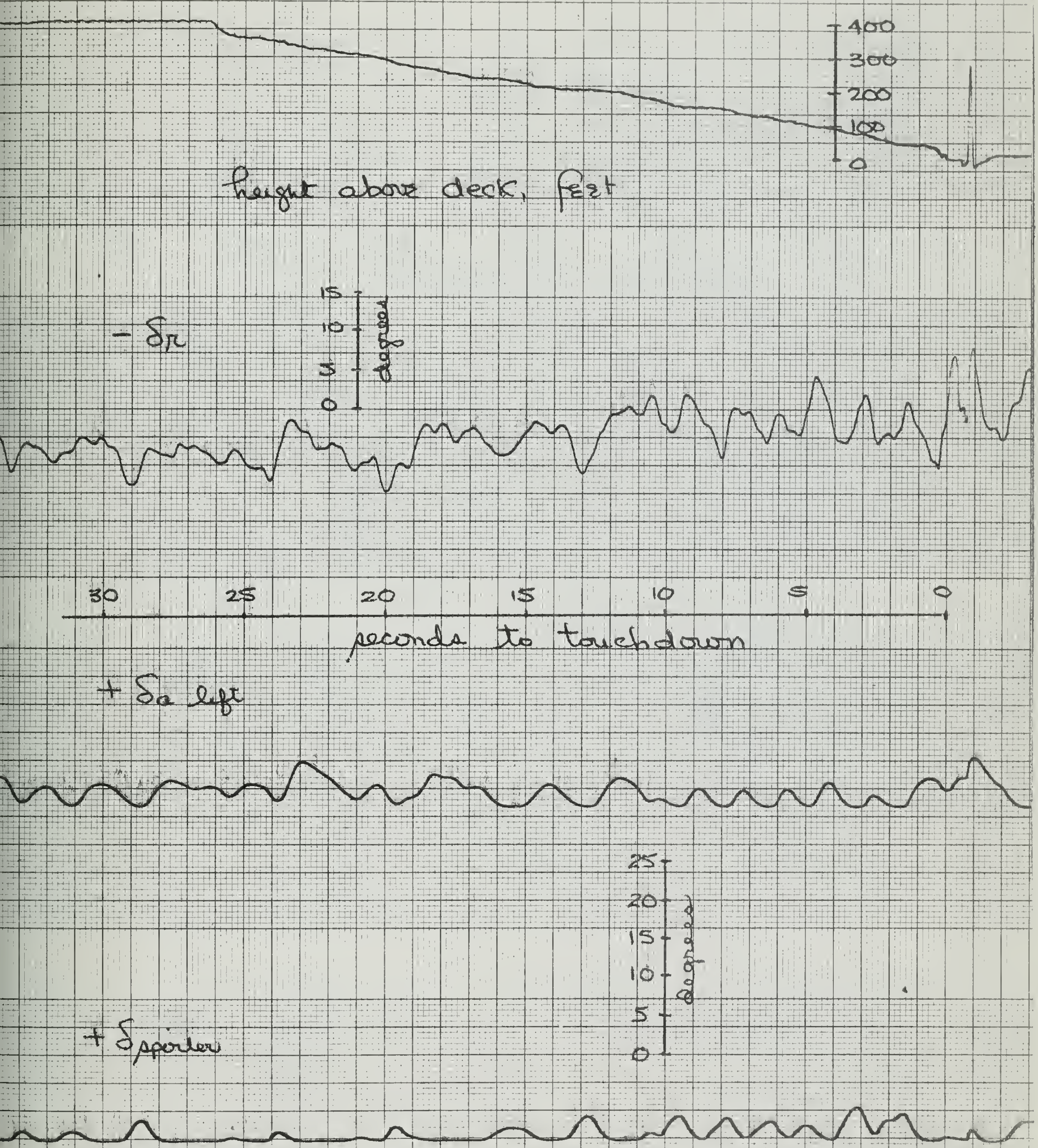

GRAPHIC CONTROLS CORPORATION | BUFFALO NEW YORK | PRINTED IN U S A

Approach No. 26

Fig. 19 C

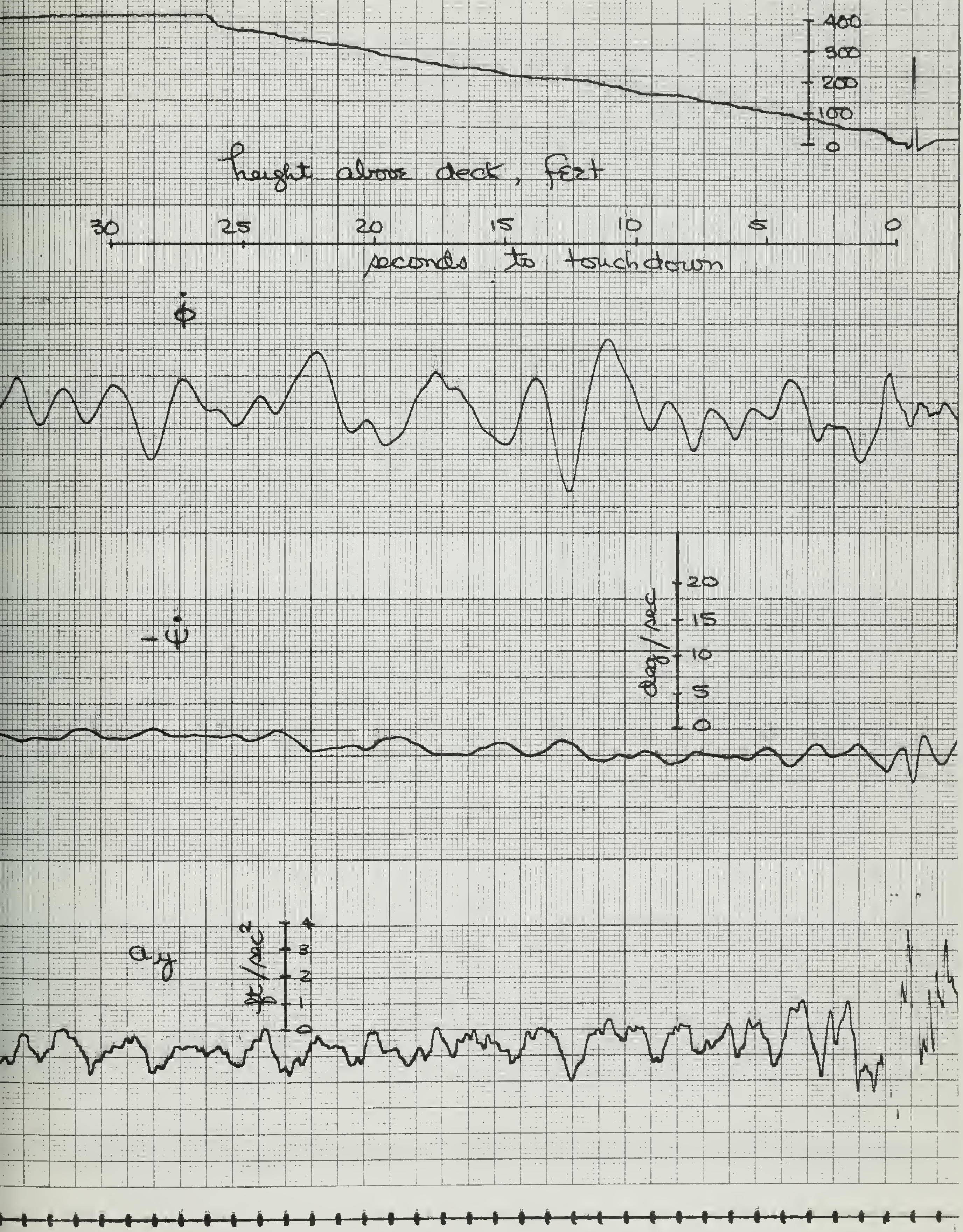

RECORDING CHARTS | GRAPHIC CONTROLS CORPORATION

Fig. 19D

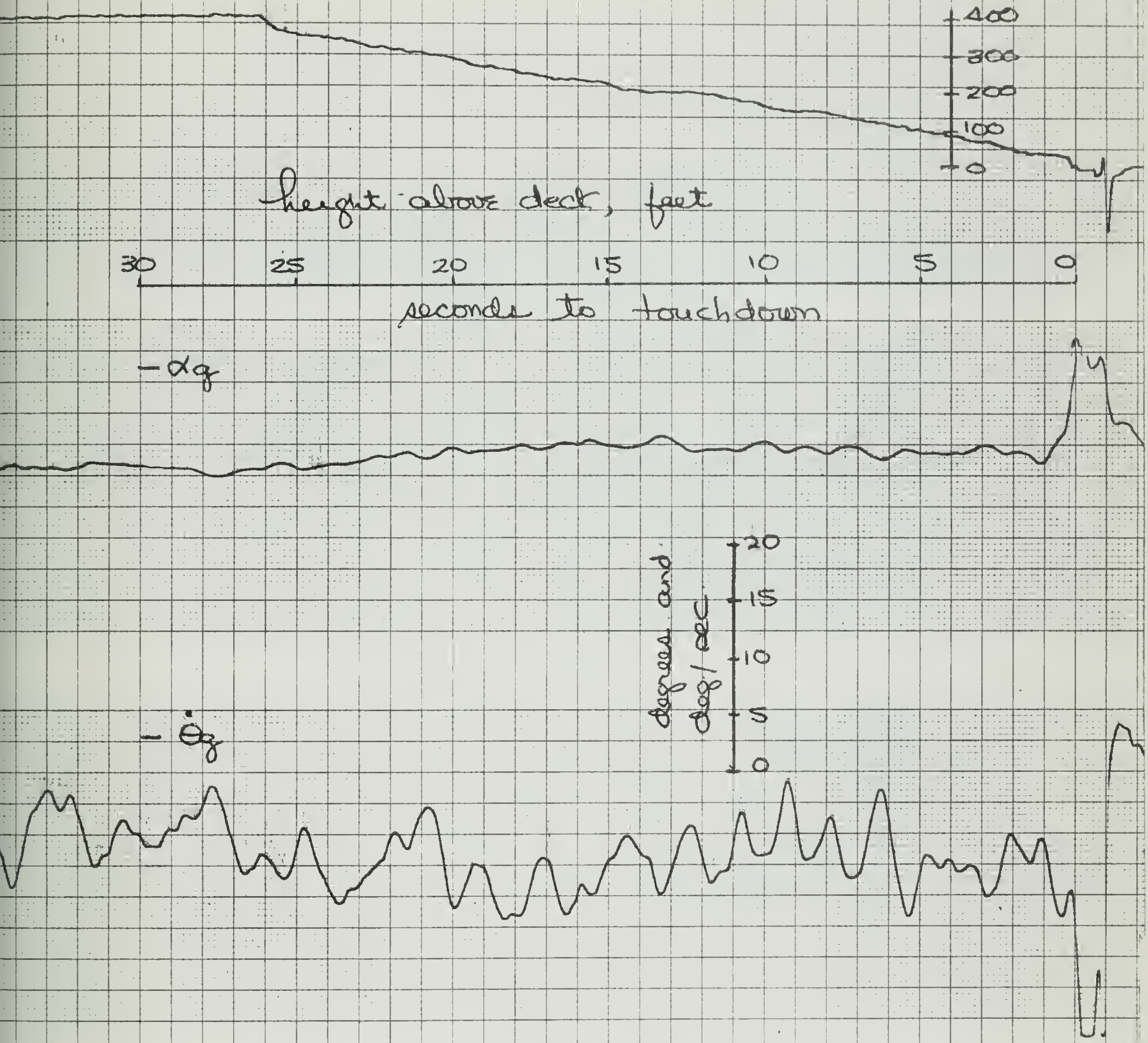

Fig. 19 E

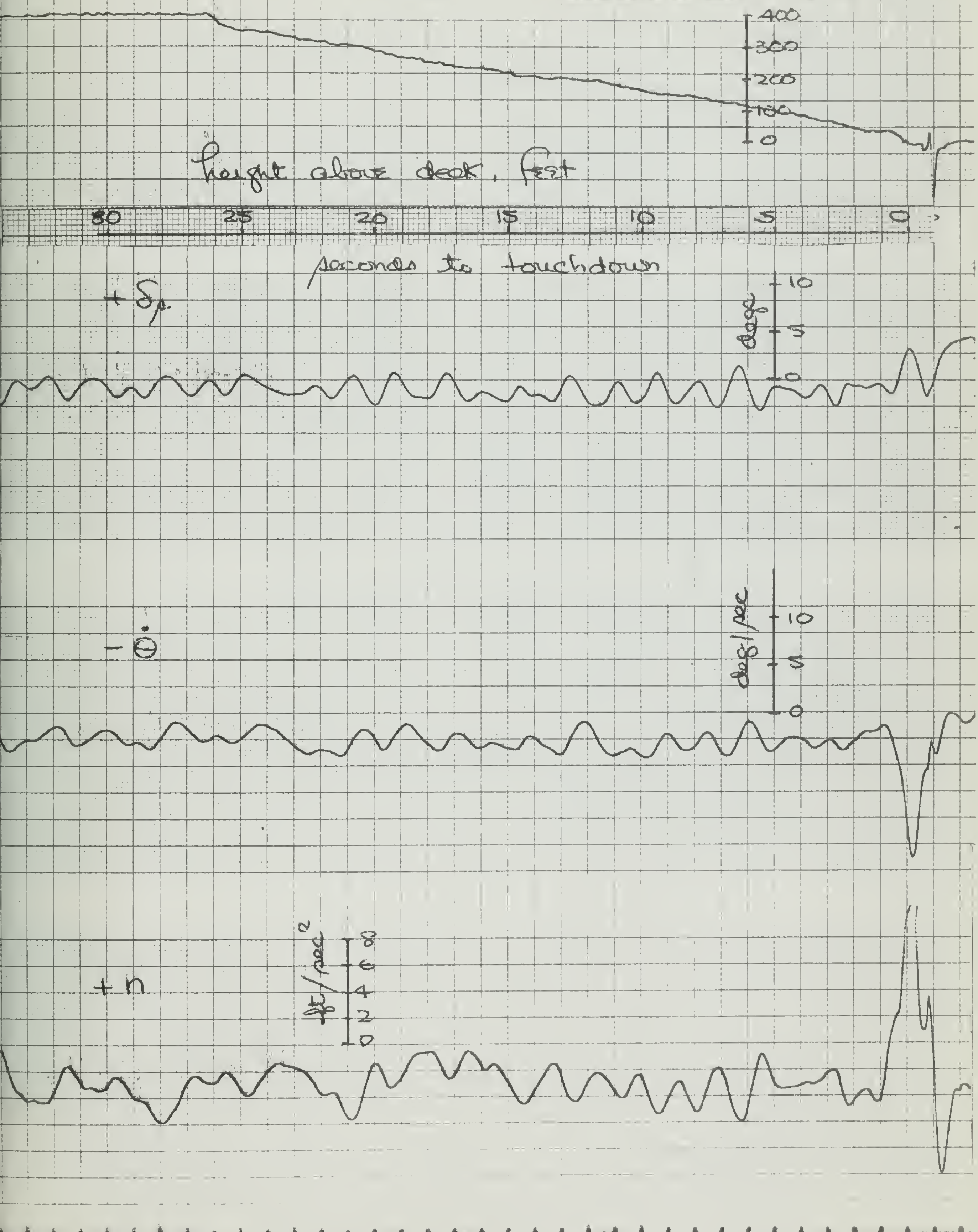
400
300
200
100
0
height above deck, feet
30
25
20
15
10
5
0
seconds to touchdown
$+\delta_p$
degs
10
5
0
$-\dot{\Theta}$
deg/sec
10
5
0
$+n$
ft/sec²
8
6
4
2
0

PRINTED IN U S A

# Lateral and Longitudinal Gust Quantities

Approach No. 7

Fig. 20A

RECORDING CHARTS

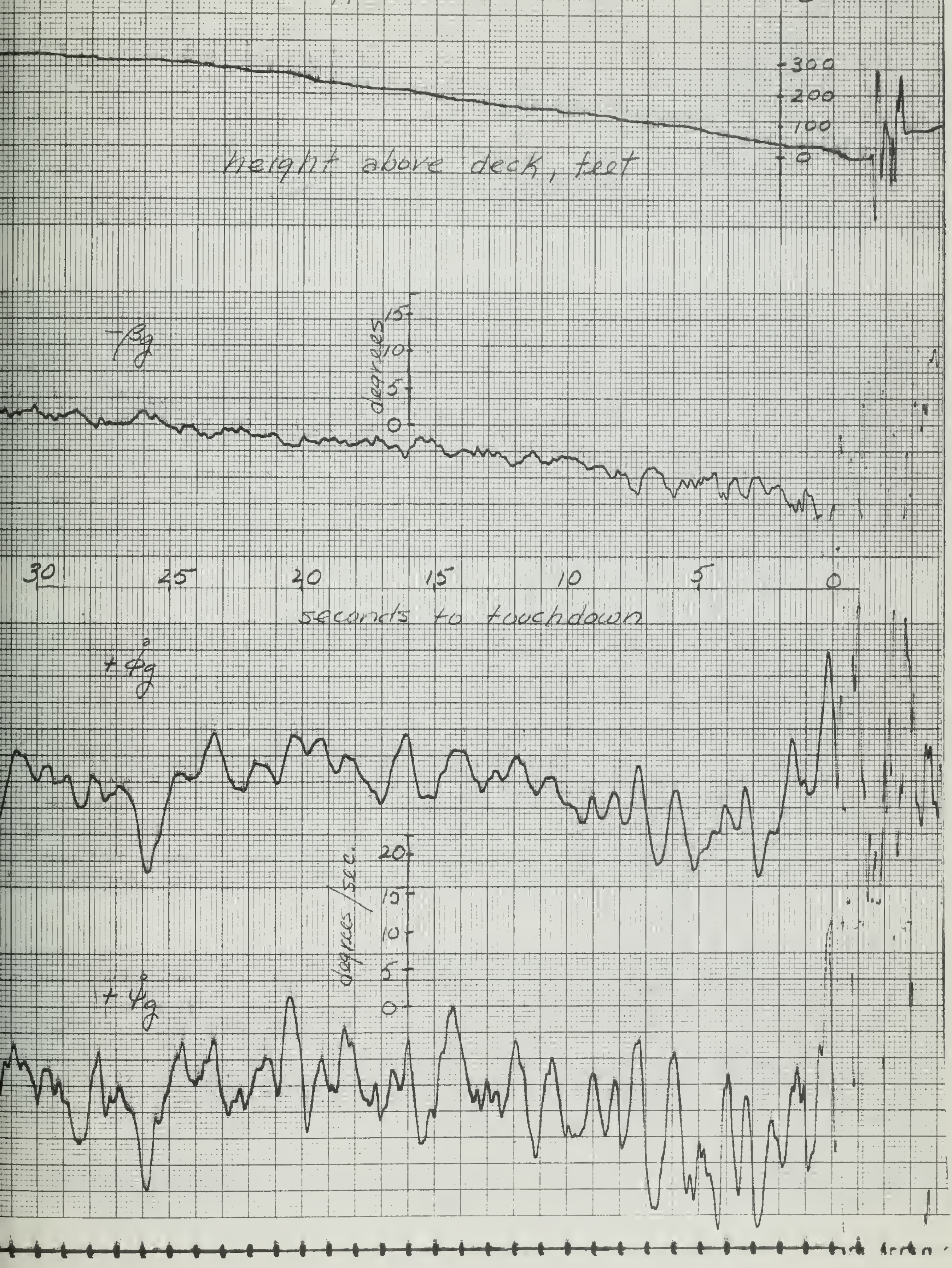

Fig. 20B

Approach No. 7

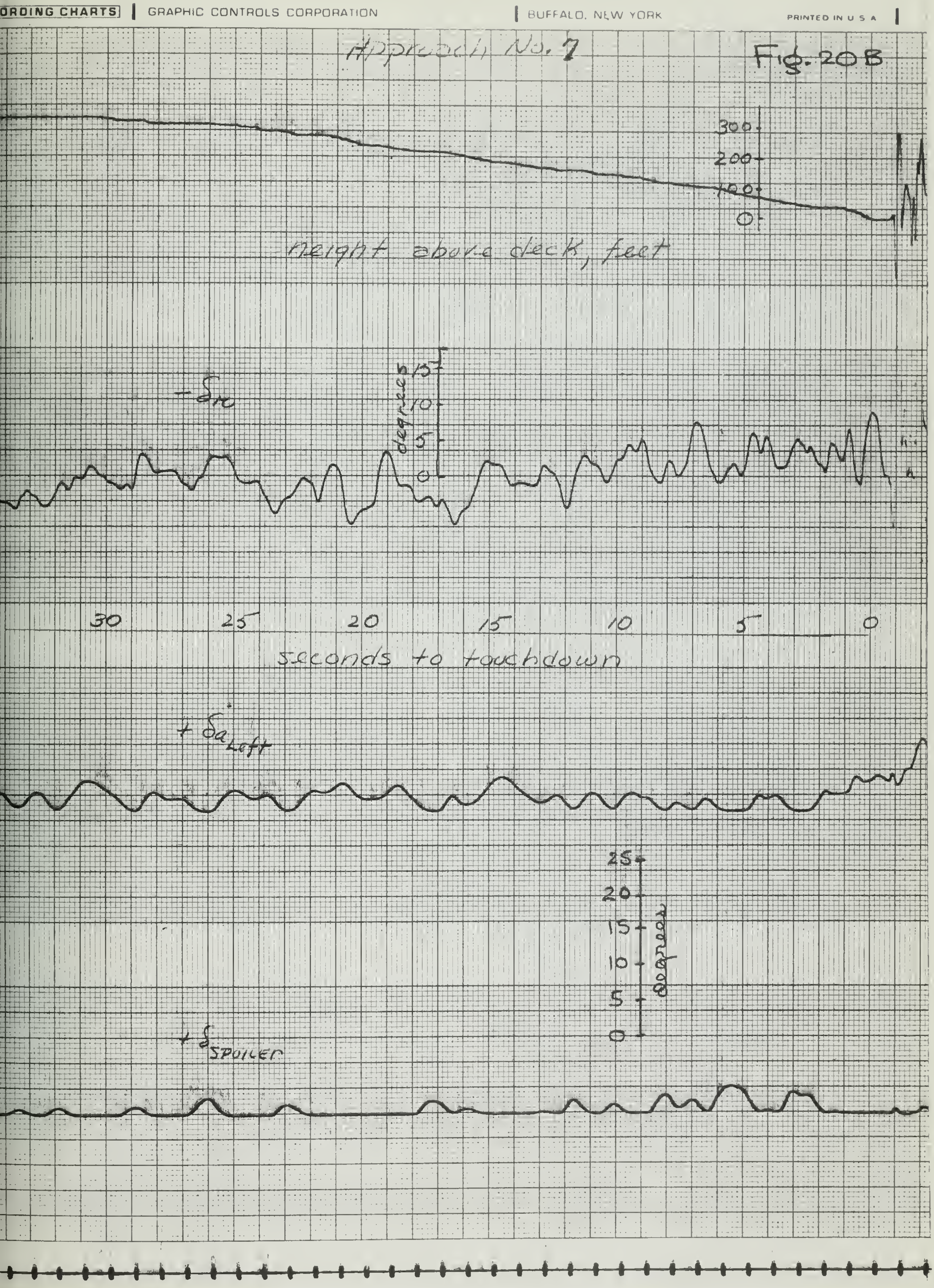

TS | GRAPHIC CONTROLS CORPORATION | NEW YORK PRINTED IN U S A |

Approach No. 7

Fig 20 C

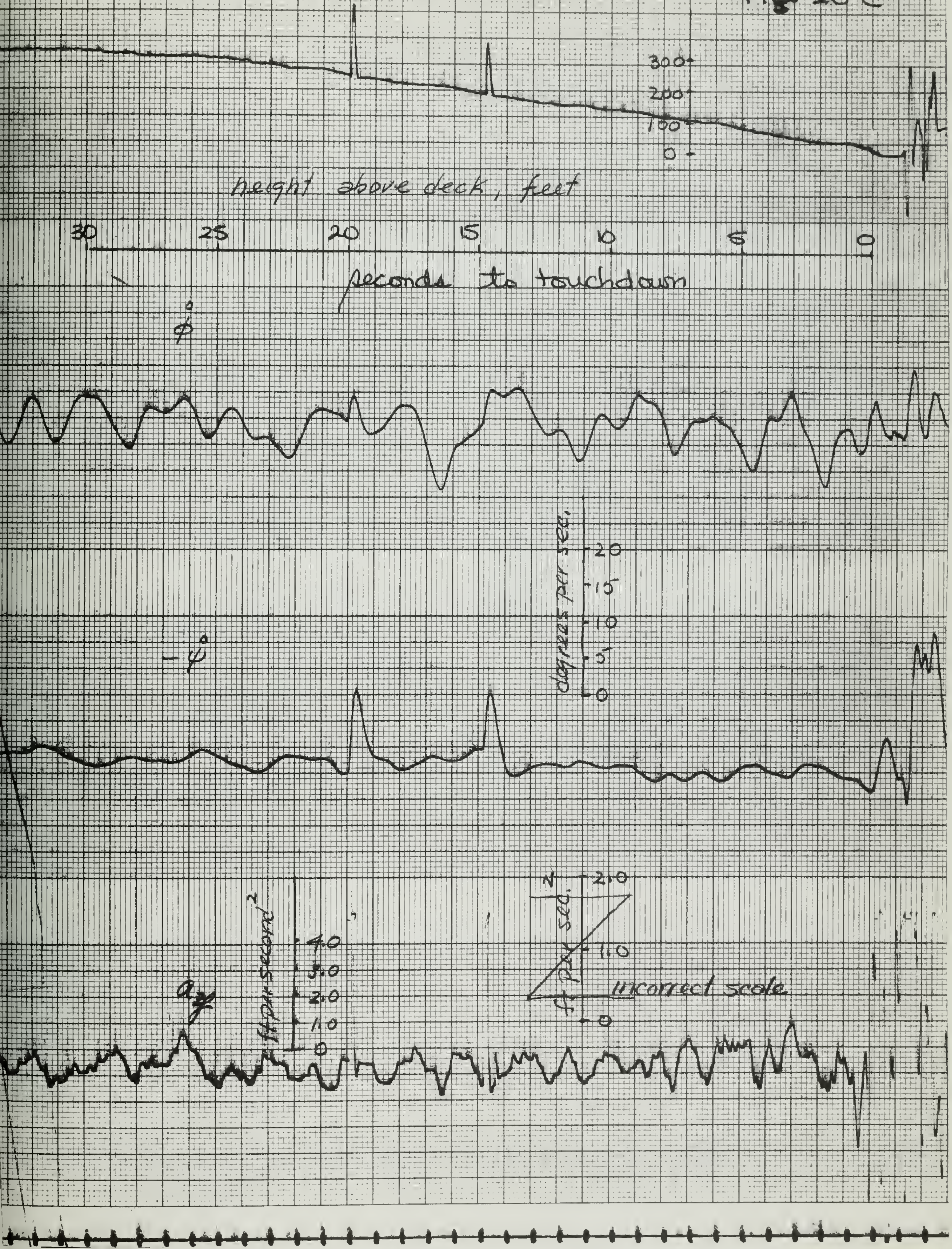

RECORDING CHARTS | GRAPHIC CONTROLS CORPORATION

Fig. 20 D

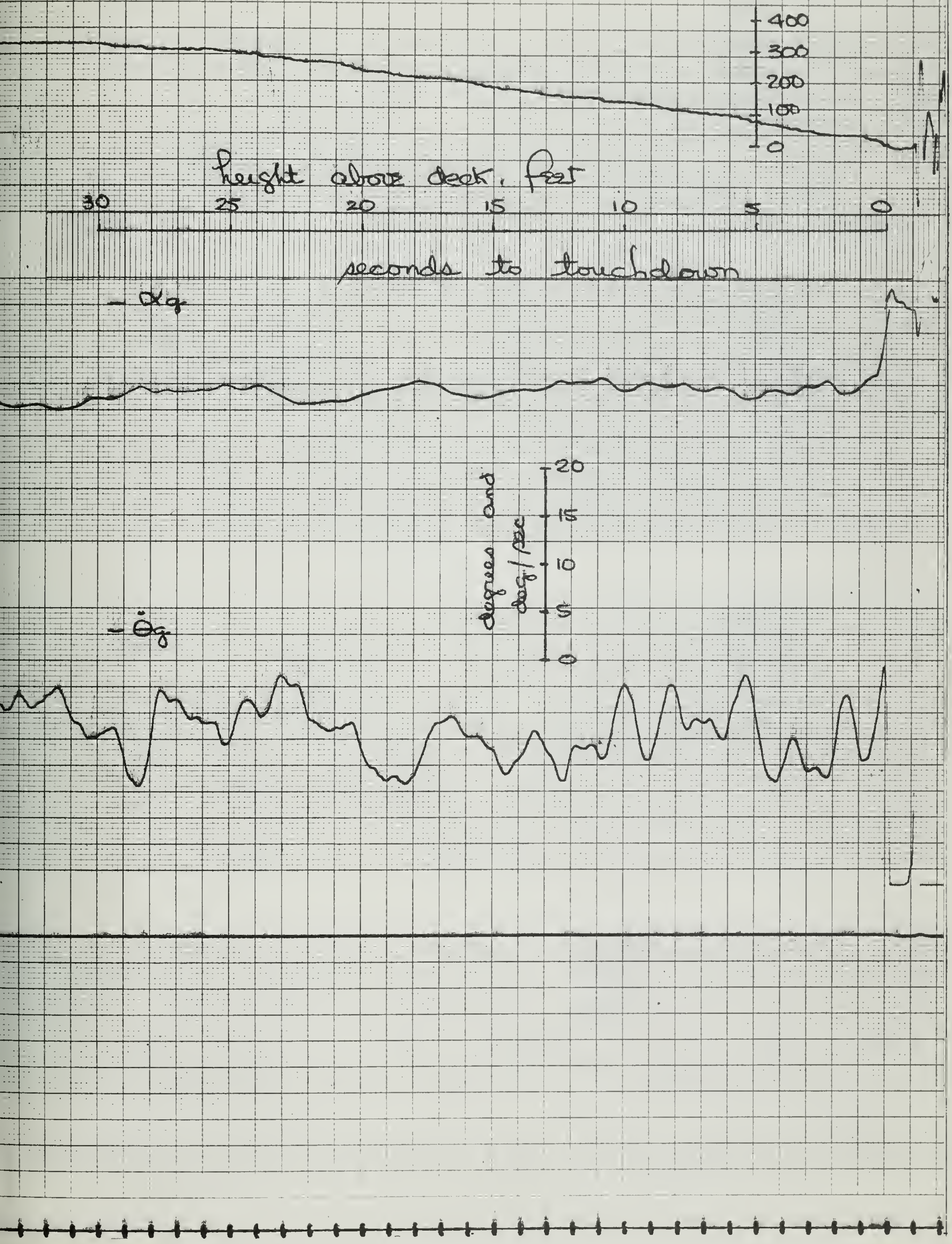

Fig. 20 E

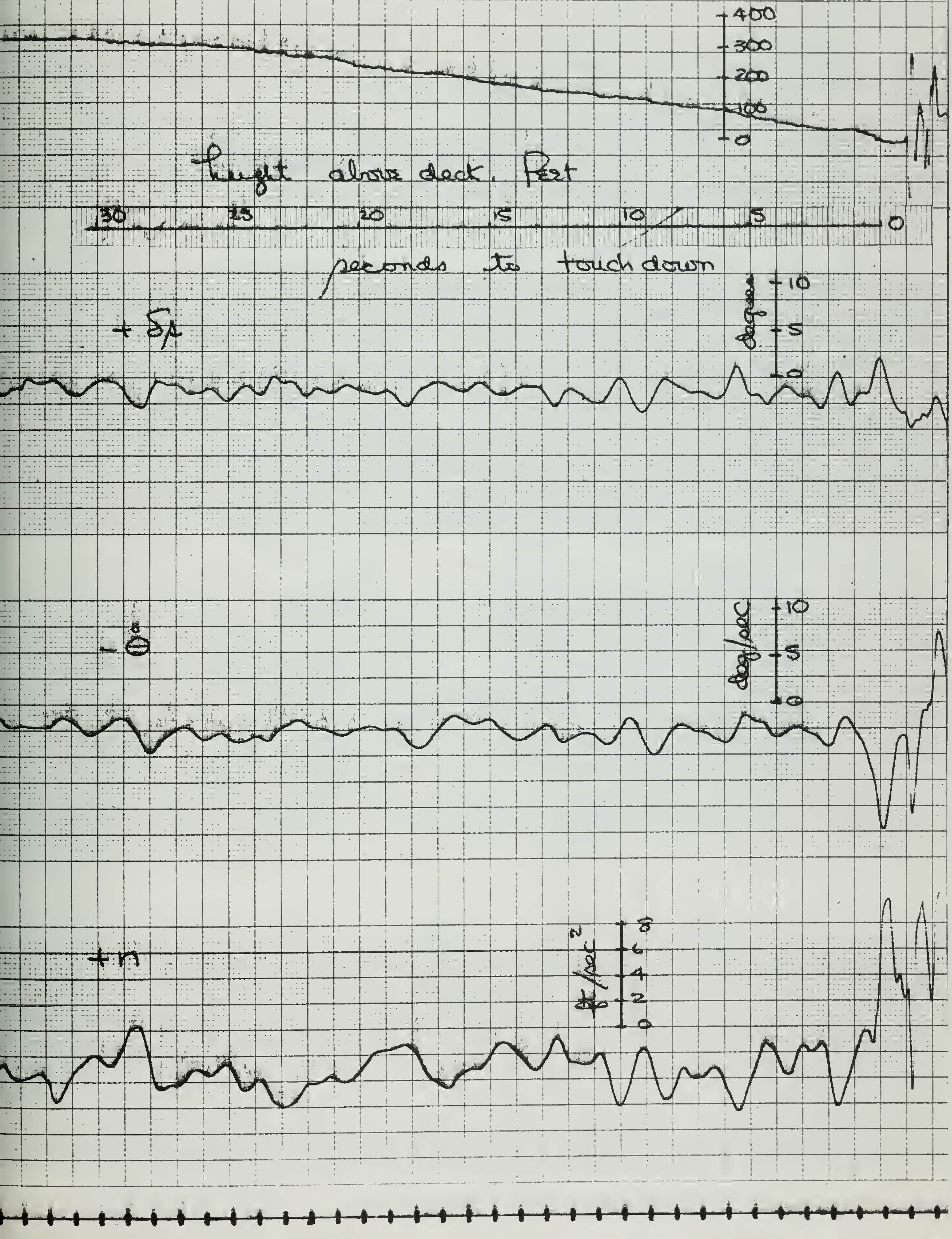
400
300
200
100
0
height above deck, feet
30
25
20
15
10
5
0
seconds to touch down
+δp
degrees
10
5
0
−θ̇
deg/sec
10
5
0
+n
ft/sec²
8
6
4
2
0

TION BUFFALO, NEW YORK PRINTED IN U.S.A.

Lateral and Longitudinal Gust Quantities
Approach No 15

Fig. 21A

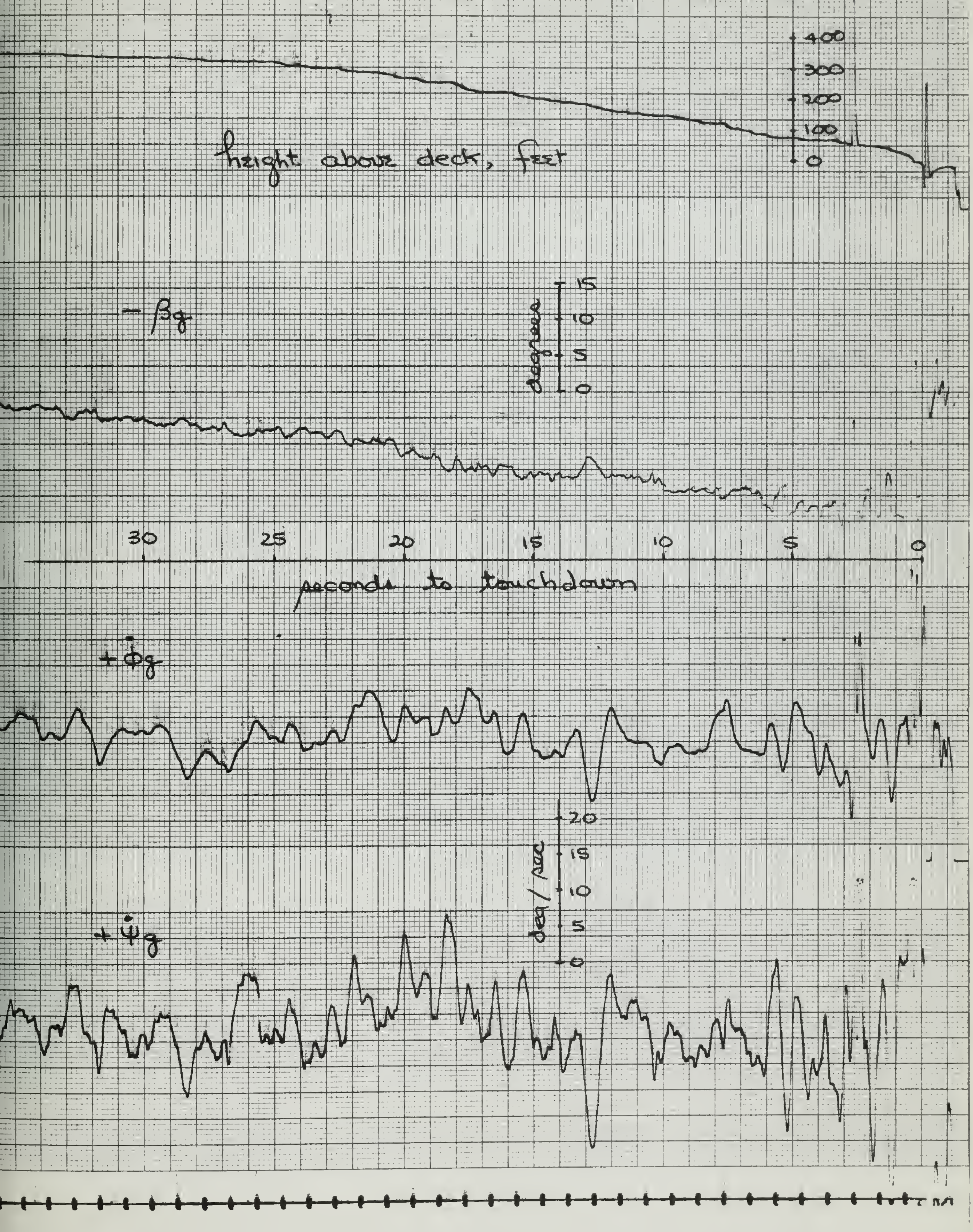

Approach No 15

Fig. 21 B

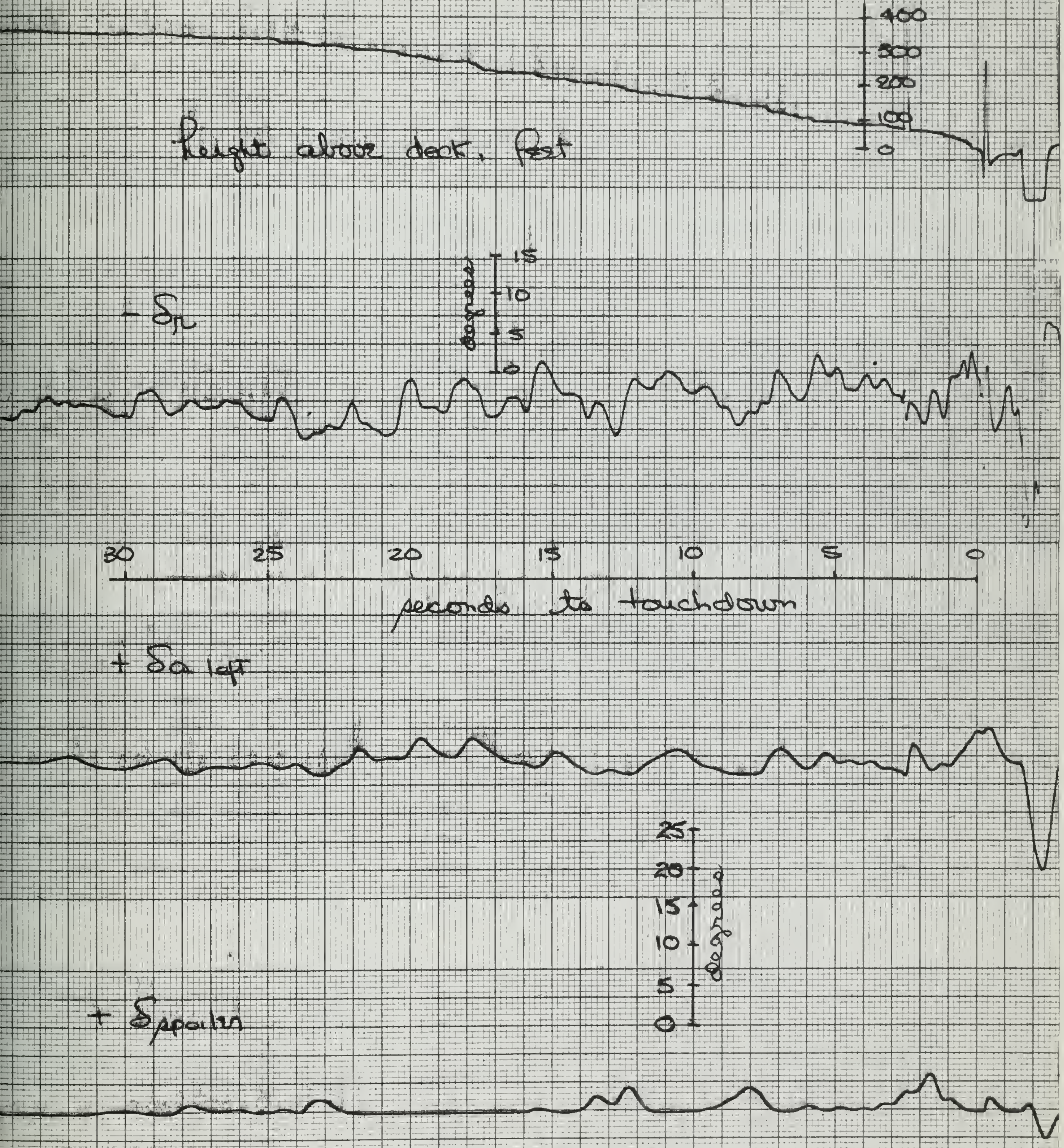

G RECORDING CHARTS | GRAPHIC CONTROLS CORPORATION | BUFFALO, NEW YORK

Approach No 15

Fig. 21 C

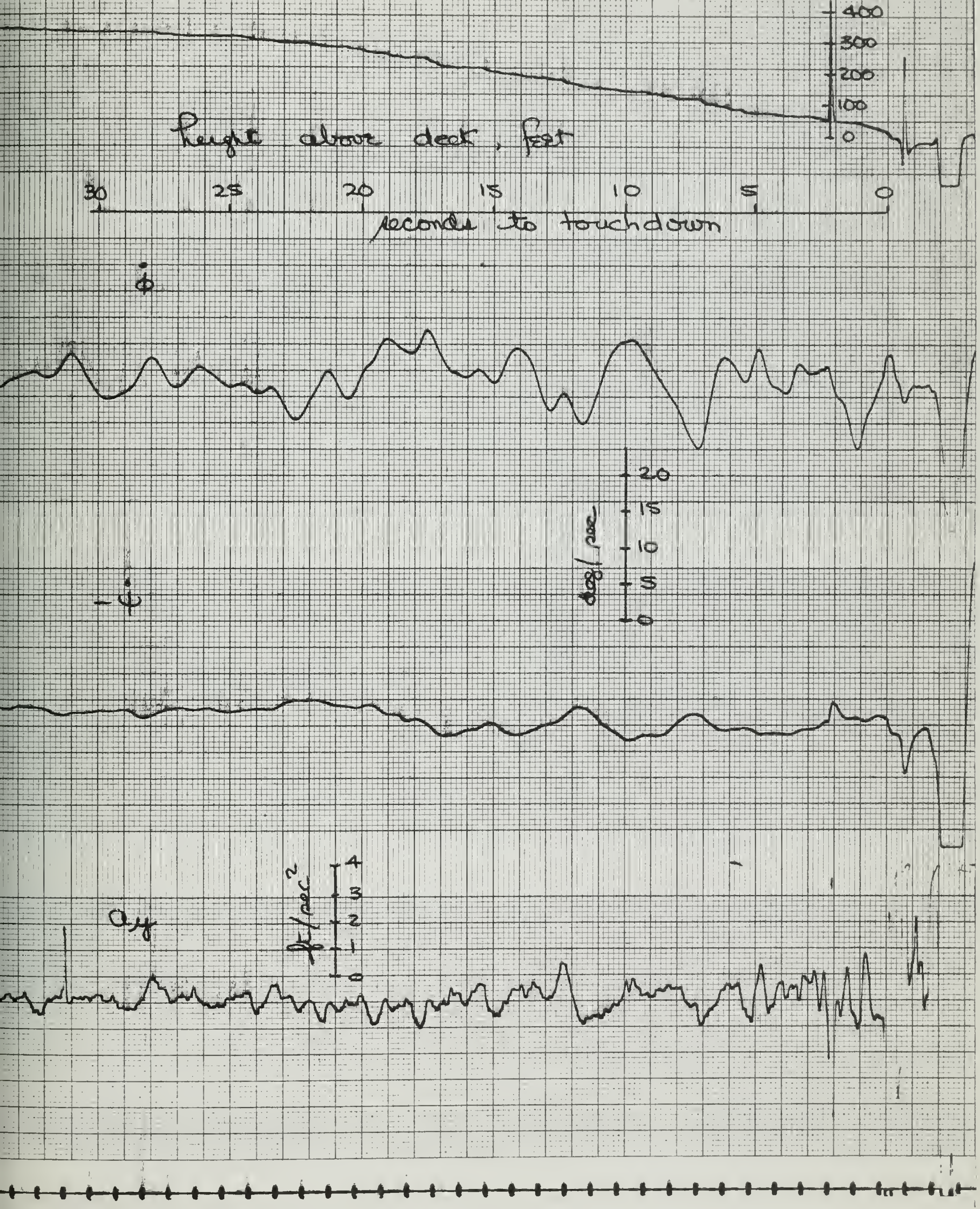

PRINTED IN U S A

G RECORDING CHARTS

No. 15

Fig. 21 D

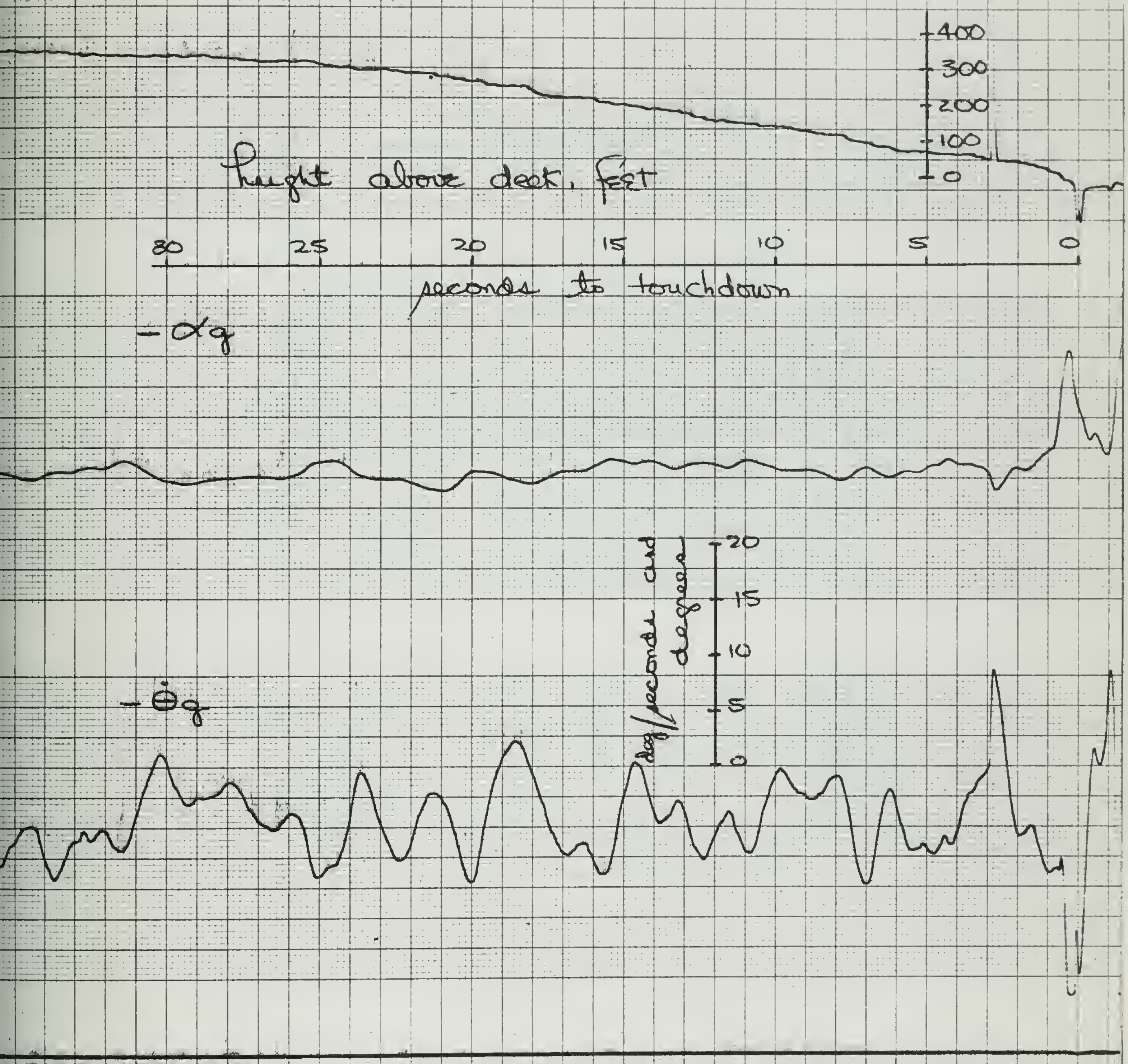

S | GRAPHIC CONTROLS CORPORATION | BUFFALO, NEW YORK | PRINTED IN U.S.A.

No. 15

Fig. 21 E

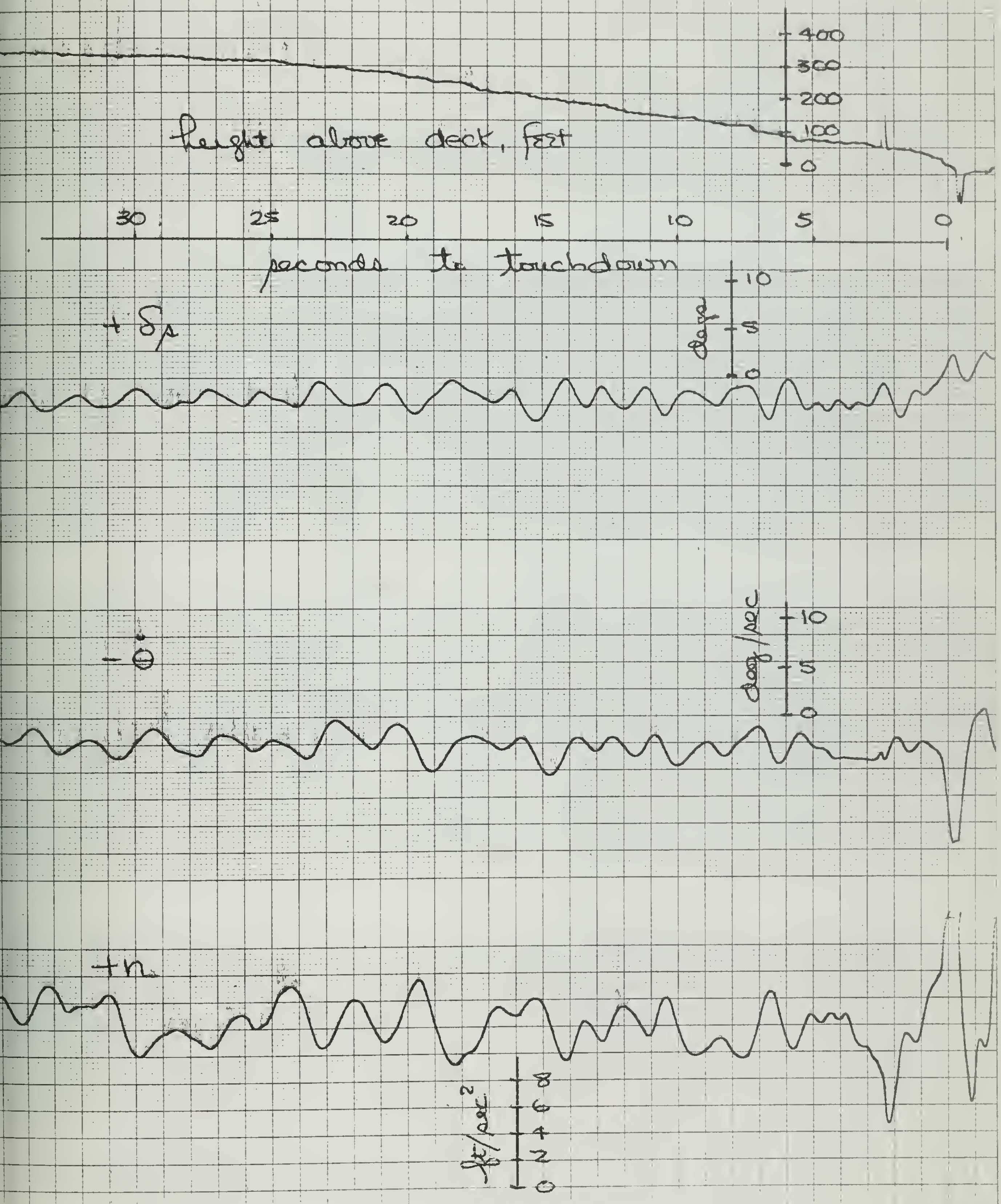

RAPHIC CONTROLS CORPORATION | BUFFALO, NEW YORK | PRINTED IN U.S.A.

Lateral and Longitudinal Gust Quantities
Approach NO 16

Fig. 22 A

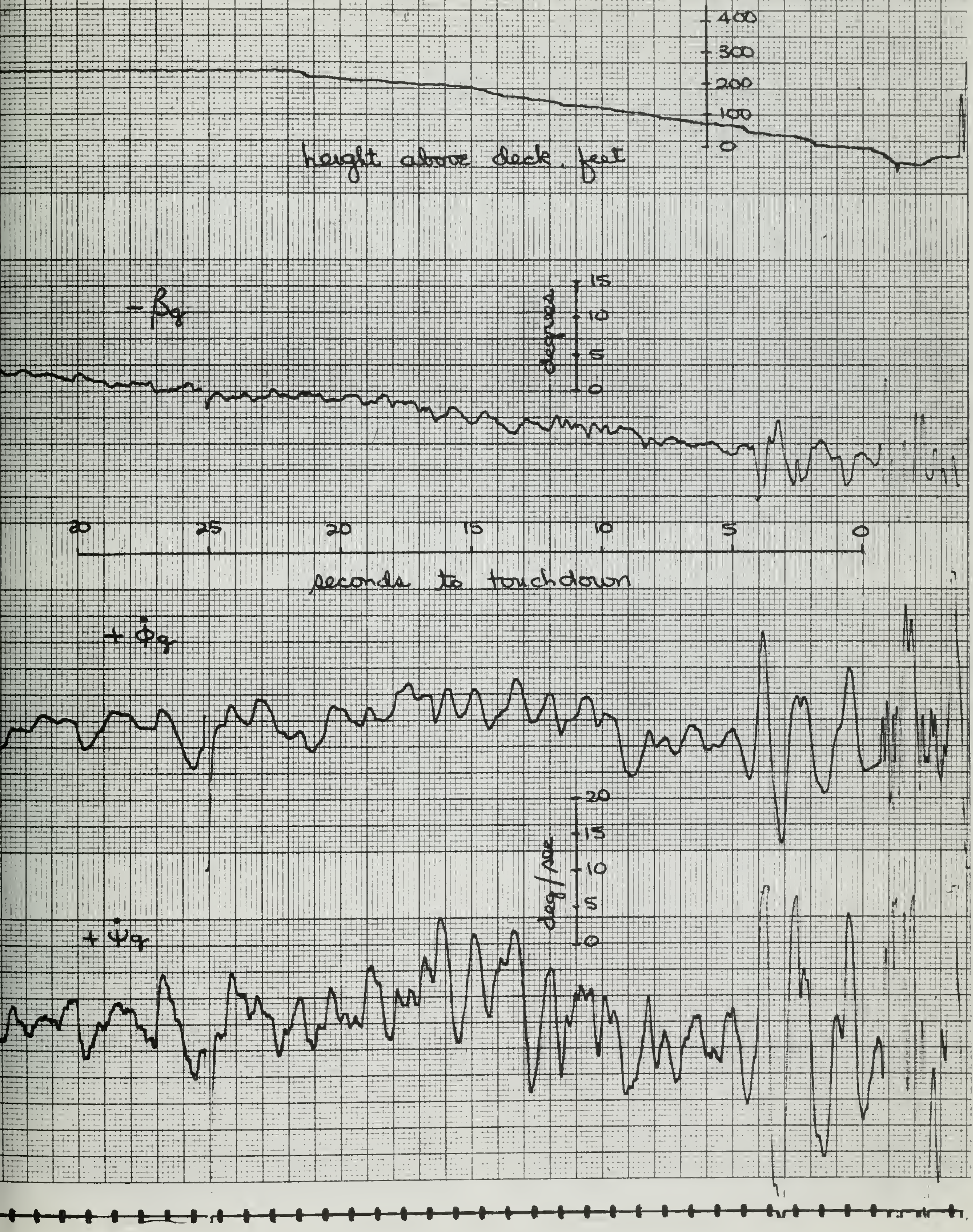

CHARTS | GRAPHIC CONTROLS CORPORATION | BUFFALO NEW YORK PRINTED IN U S A

No 16

Fig. 22B

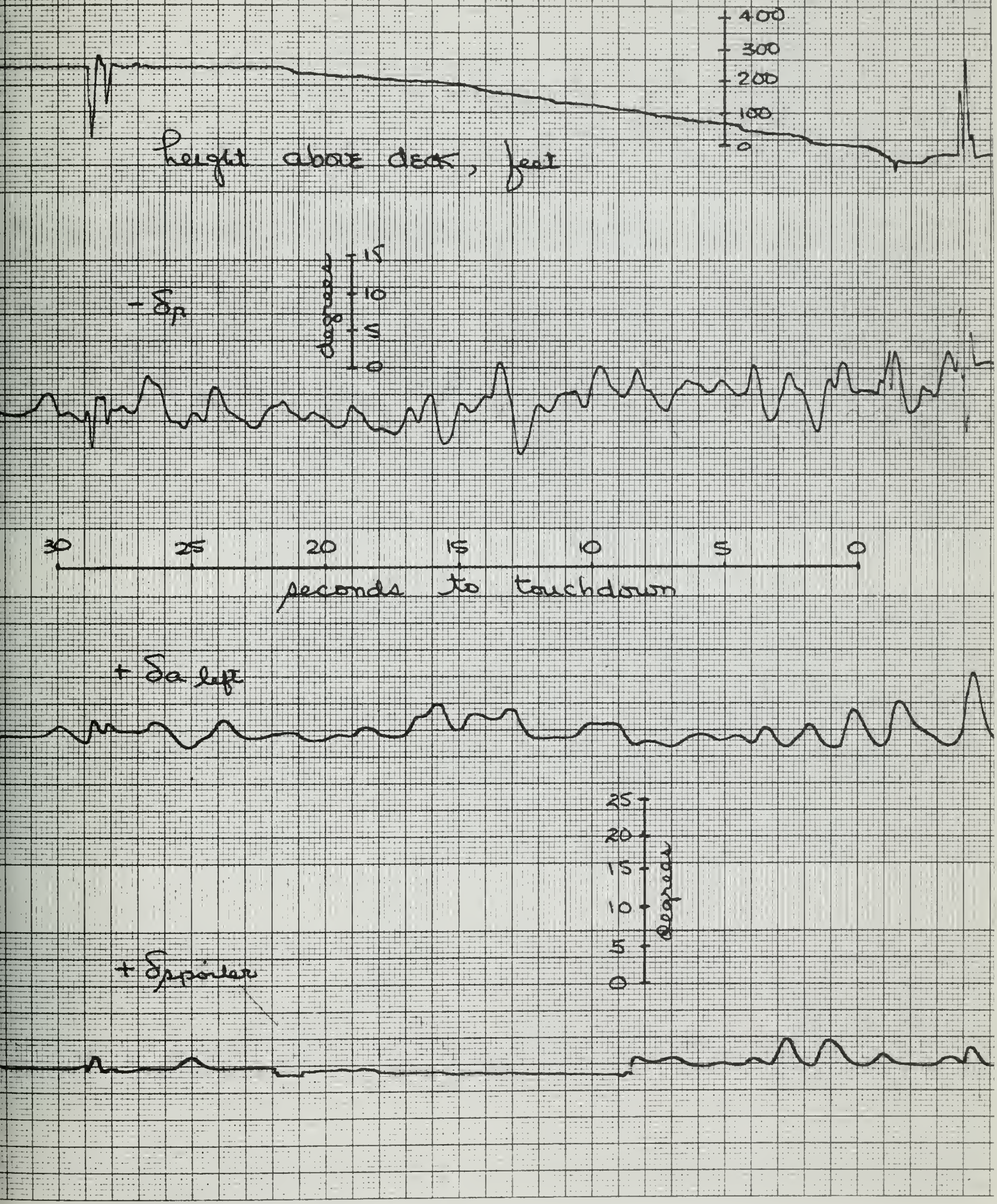

RECORDING CHARTS | GRAPHIC CONTROLS CORPORATION | BUFFAL

No ~~17~~ 16

Fig. 22 C

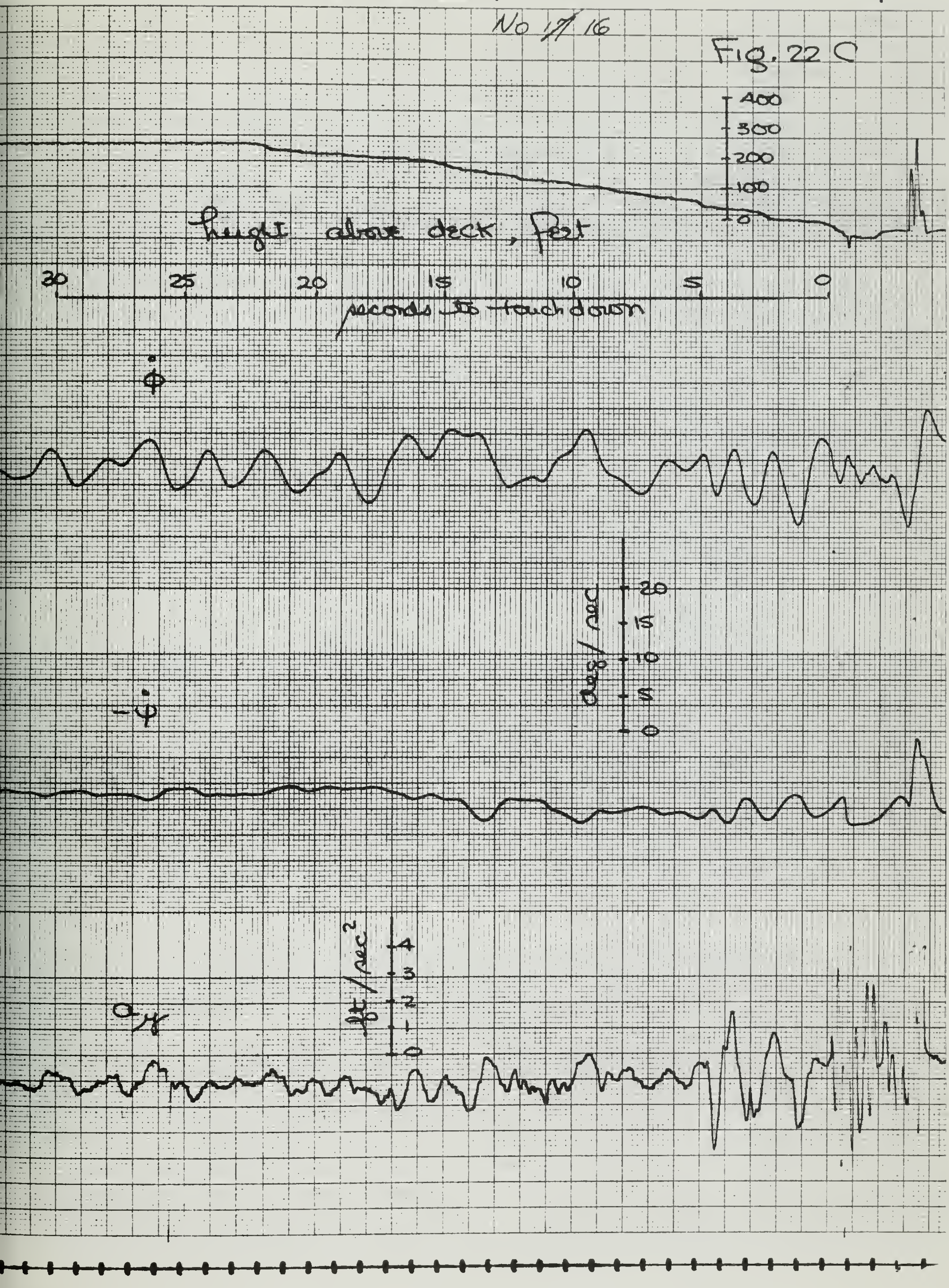

BUFFALO, NEW YORK PRINTED IN U.S.A.

No. 16

Fig. 22 D

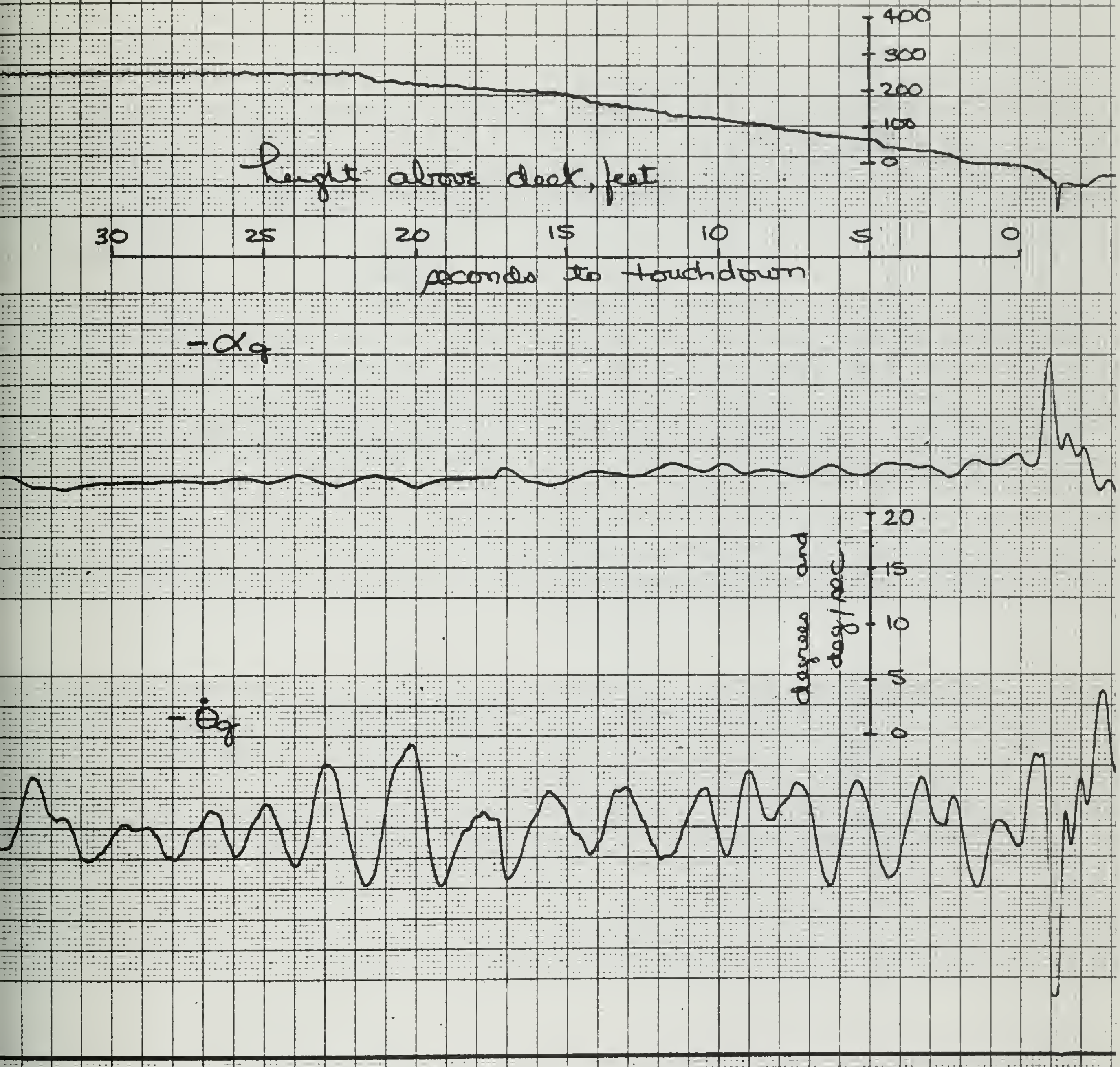

G RECORDING CHARTS | GRAPHIC CONTROLS CORPORATION | BUFFALO, NEW YORK PRINTED

No. 16

Fig. 22E

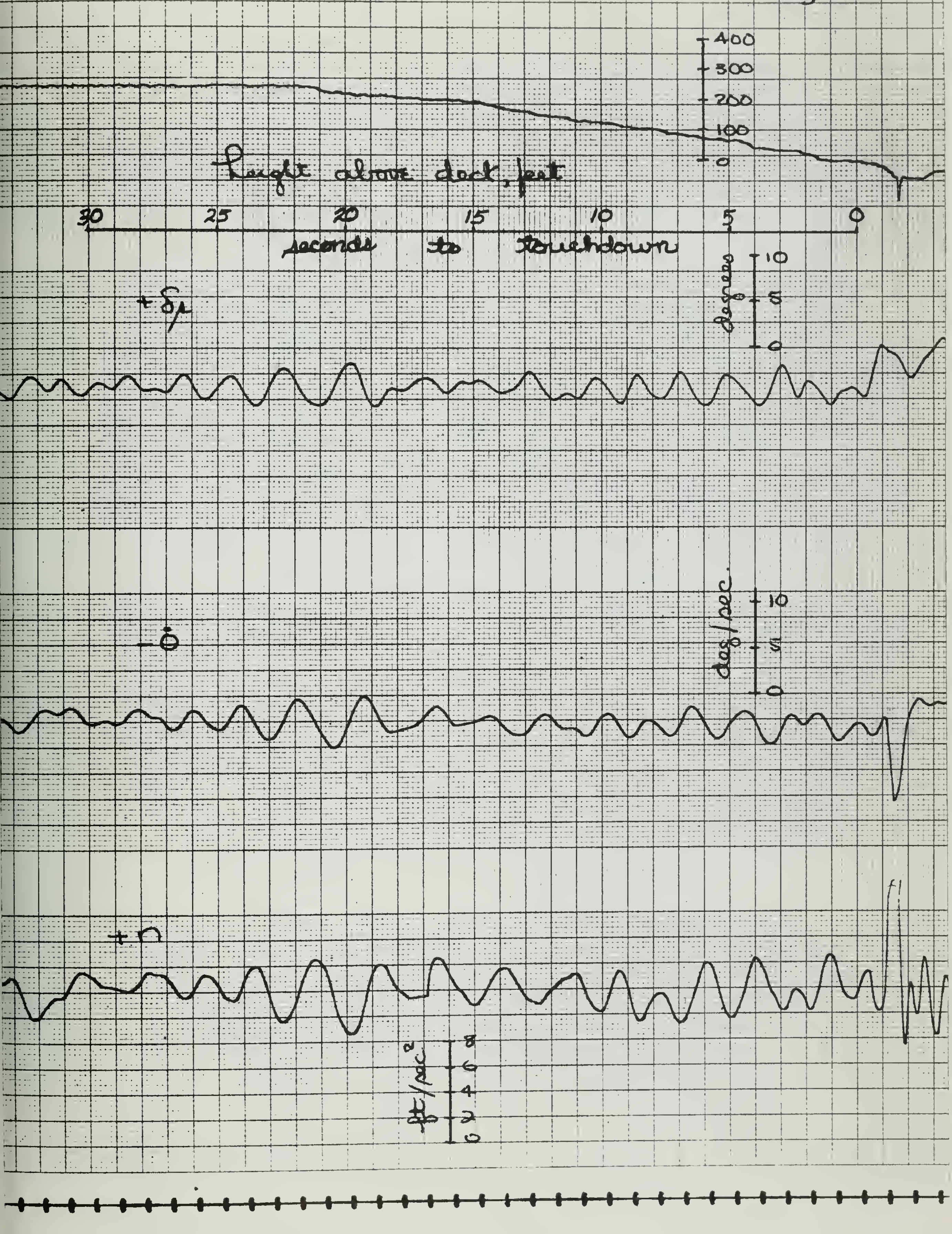

RECORDING CHARTS GRAPHIC CONTROLS CORPORATION BUFFALO N.Y. PRINTED IN U.S.

Lateral and Longitudinal Gust Quantities
No 18
Fig-23A

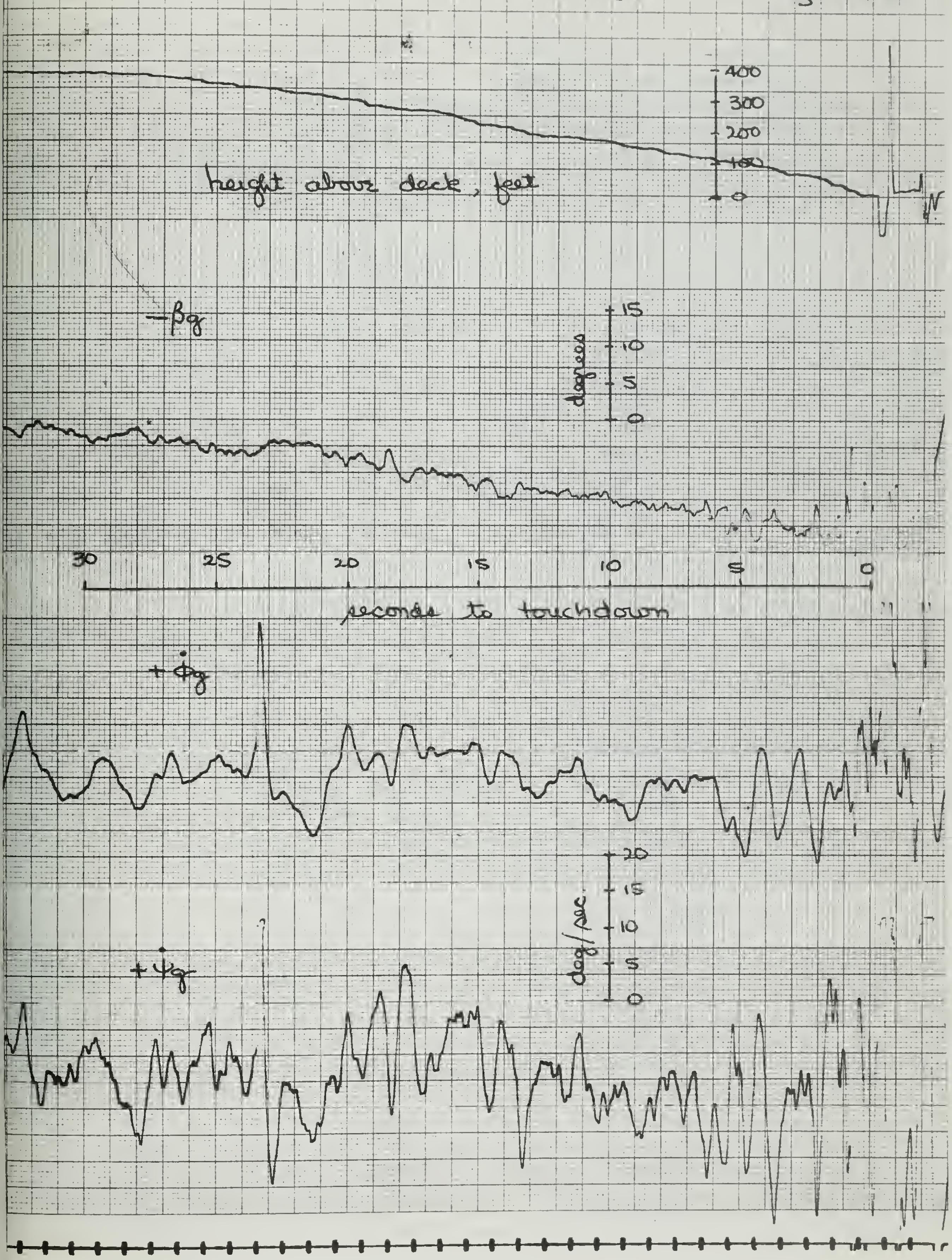

RECORDING CHARTS | GRAPHIC CONTROLS CORPORATION | BUFFALO NEW YORK

No. 18

Fig. 23 B

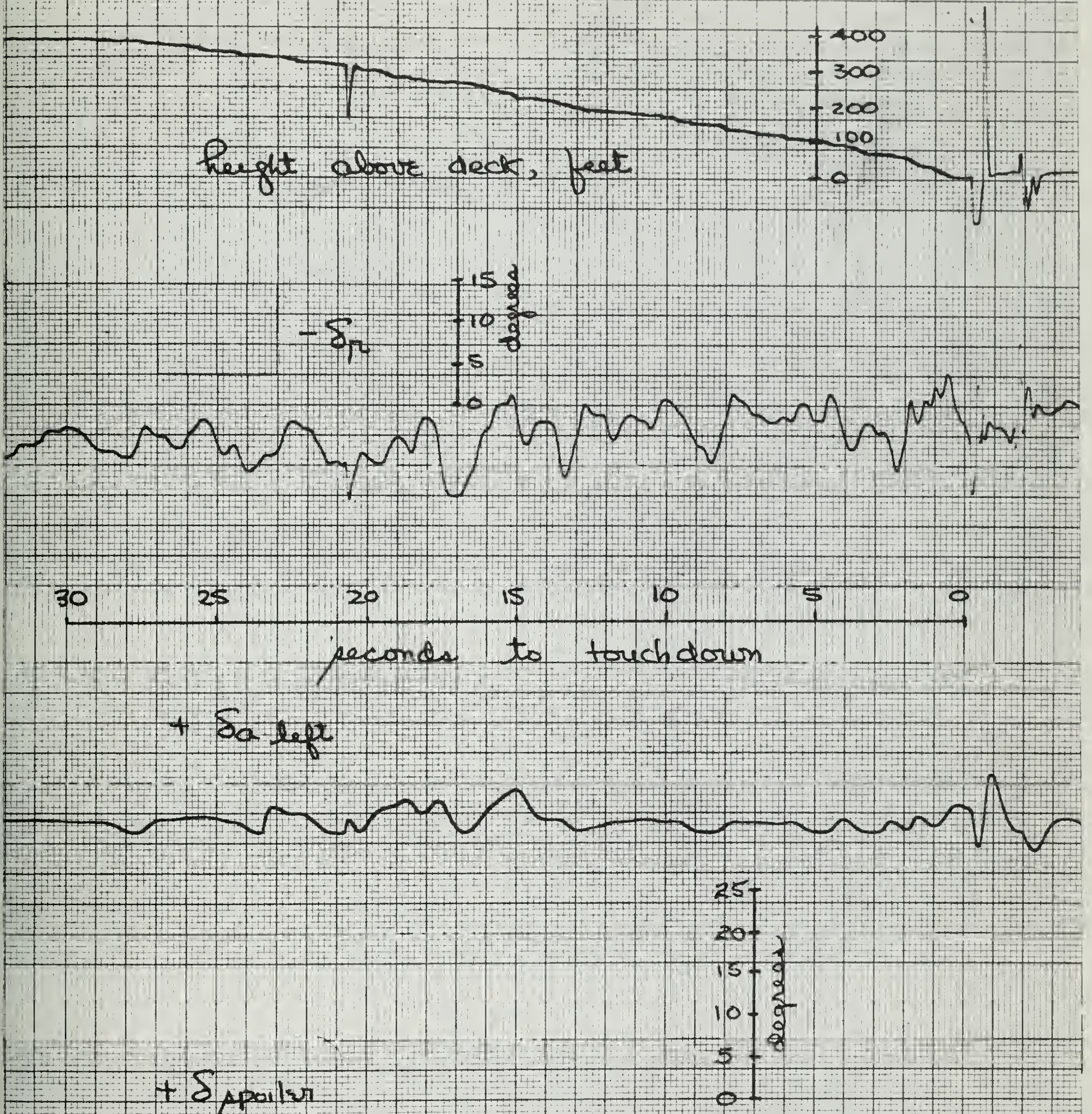

Fig. 23 C

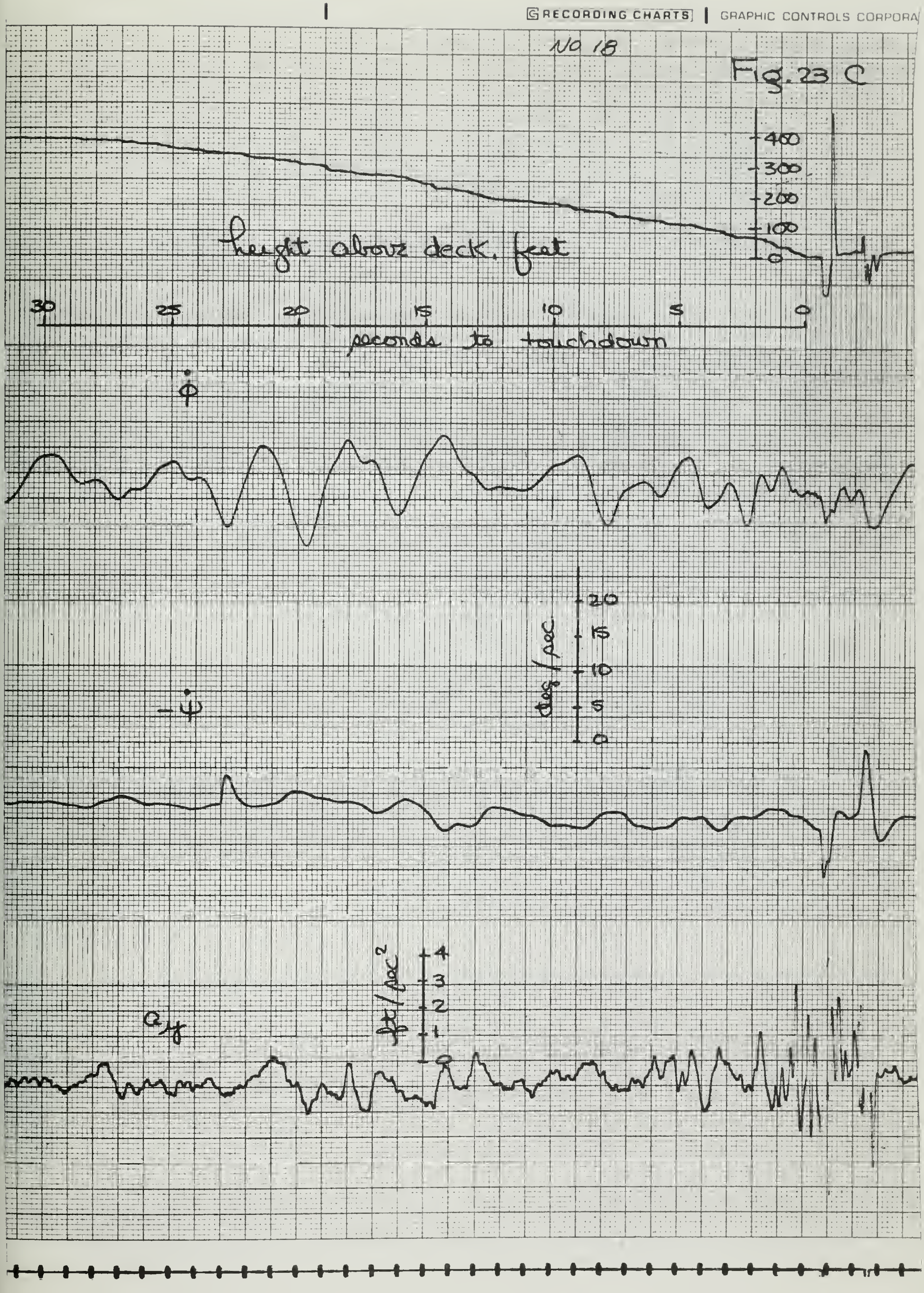
RECORDING CHARTS
GRAPHIC CONTROLS CORPORA
NO 18
400
300
200
100
0
height above deck, feet
30
25
20
15
10
5
0
seconds to touchdown
$\dot{\phi}$
20
15
10
5
0
deg / sec
$-\dot{\psi}$
4
3
2
1
0
ft / sec$^2$
$a_y$

PORATION | BUFFALO, NEW YORK PRINTED IN U.S.A.

No. 13

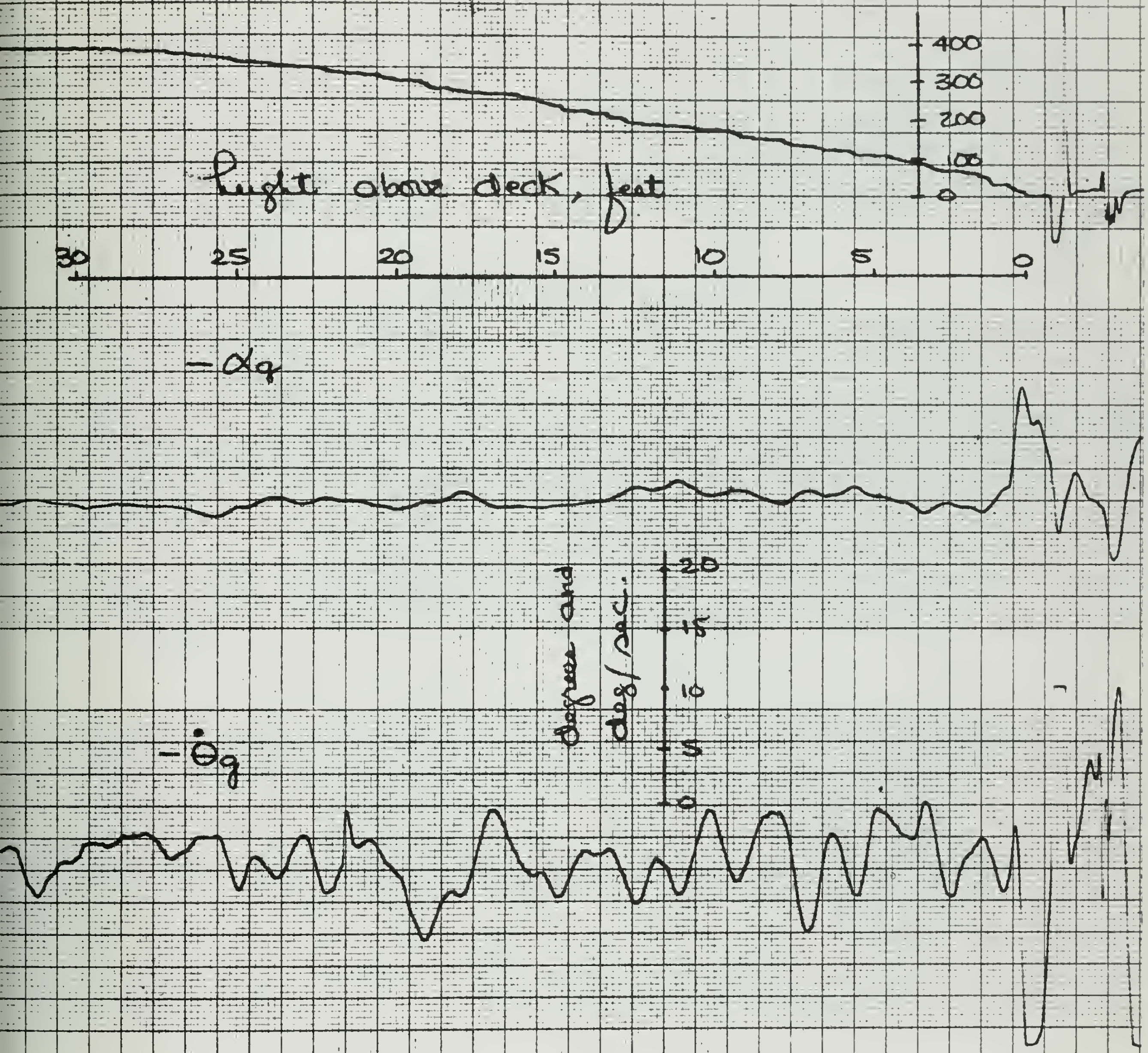

Fig. 23 D

RPORATION | BUFFALO, NEW YORK PRINTED IN U.S.A.

No. 18

Fig. 23 D

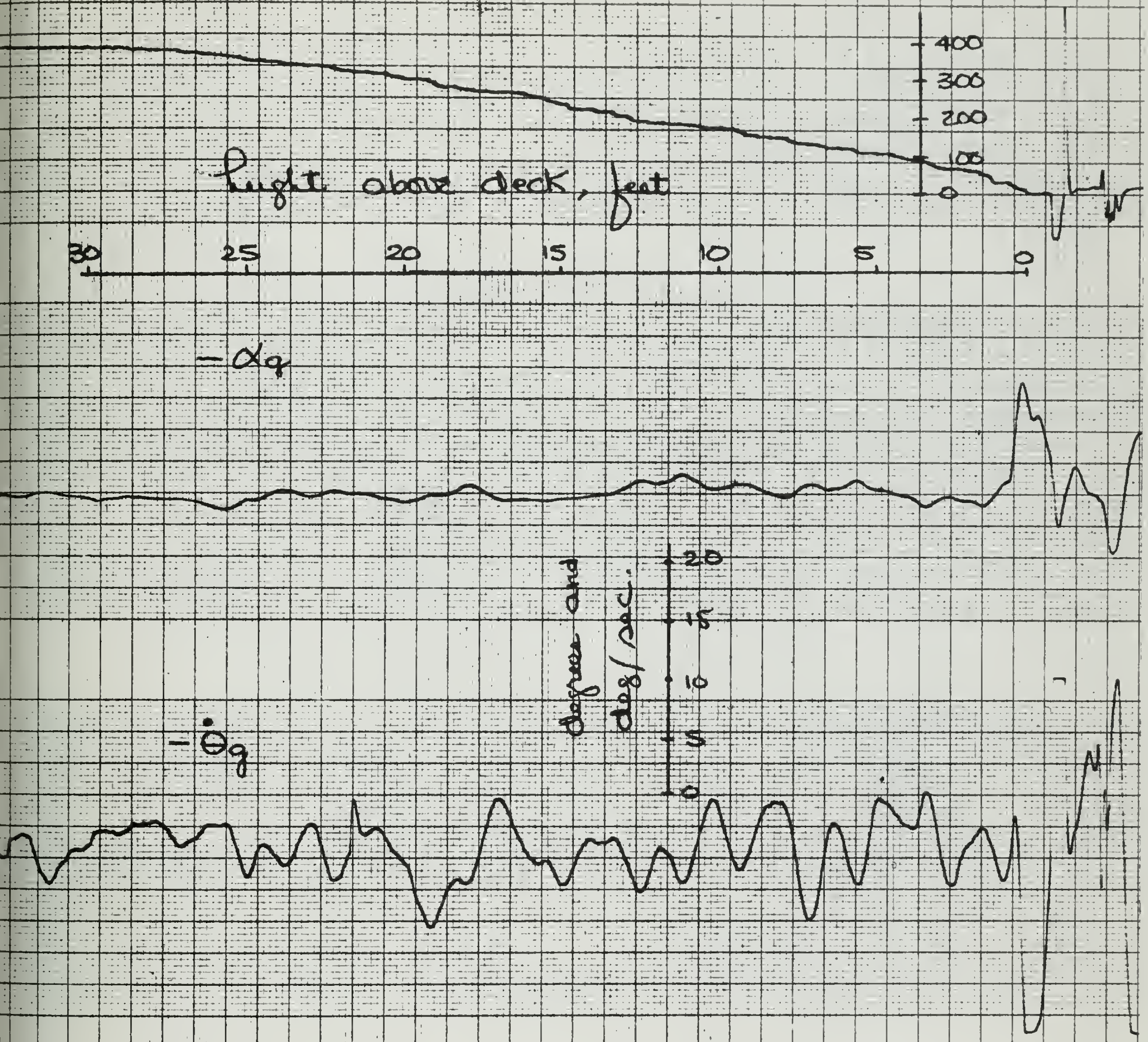

No. 1B

Fig. 23E

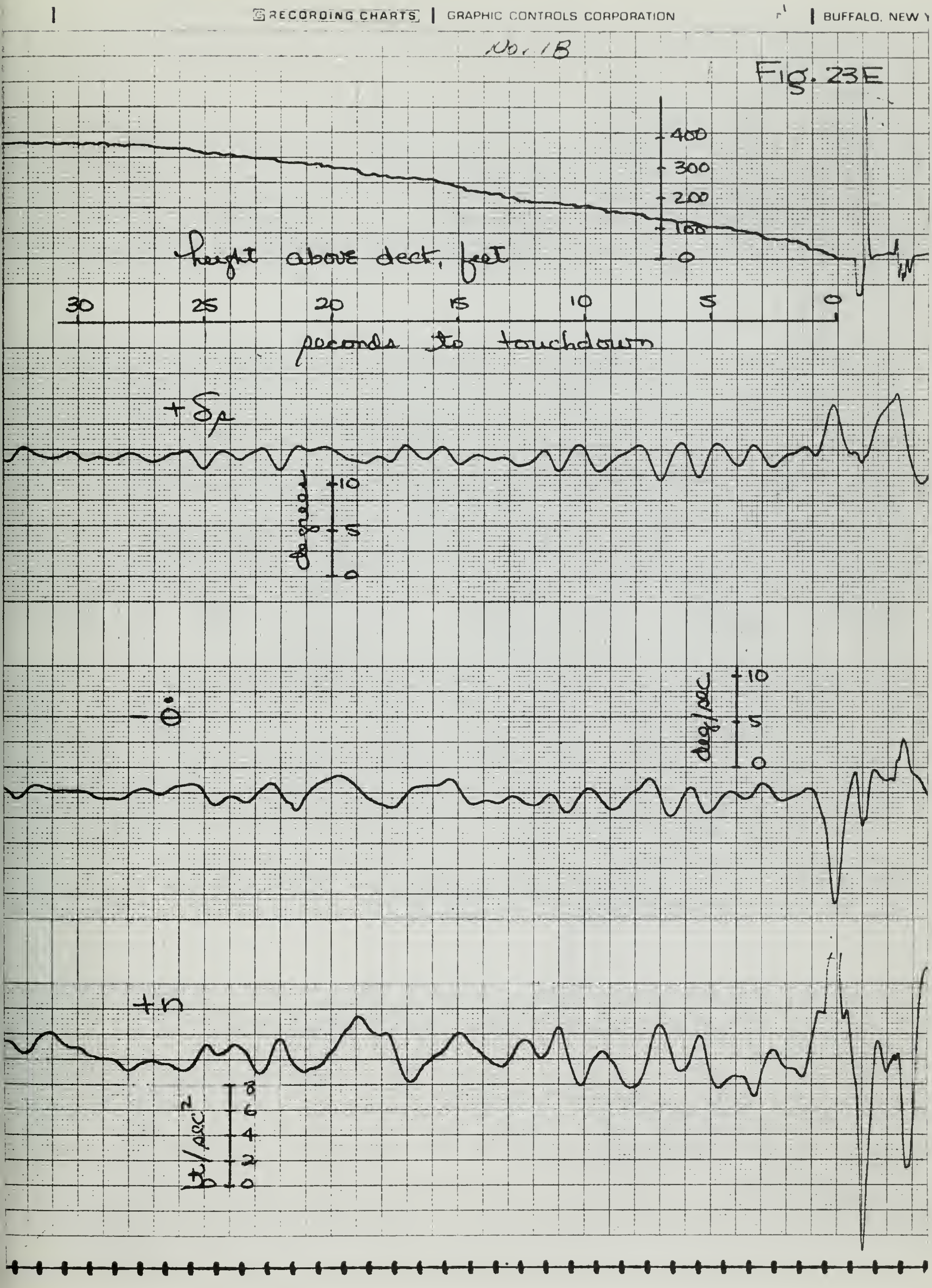
RECORDING CHARTS
GRAPHIC CONTROLS CORPORATION
BUFFALO, NEW Y
height above deck, feet
400
300
200
100
0
30
25
20
15
10
5
0
seconds to touchdown
+δp
degrees
+10
5
0
−θ̇
deg/sec
10
5
0
+n
ft/sec²
8
6
4
2
0

RECORDING CHARTS | GRAPHIC CONTROLS CORPORATION | BUFFALO, NEW YORK

Lateral and Longitudinal Gust Quantities no. 13

Fig. 24A

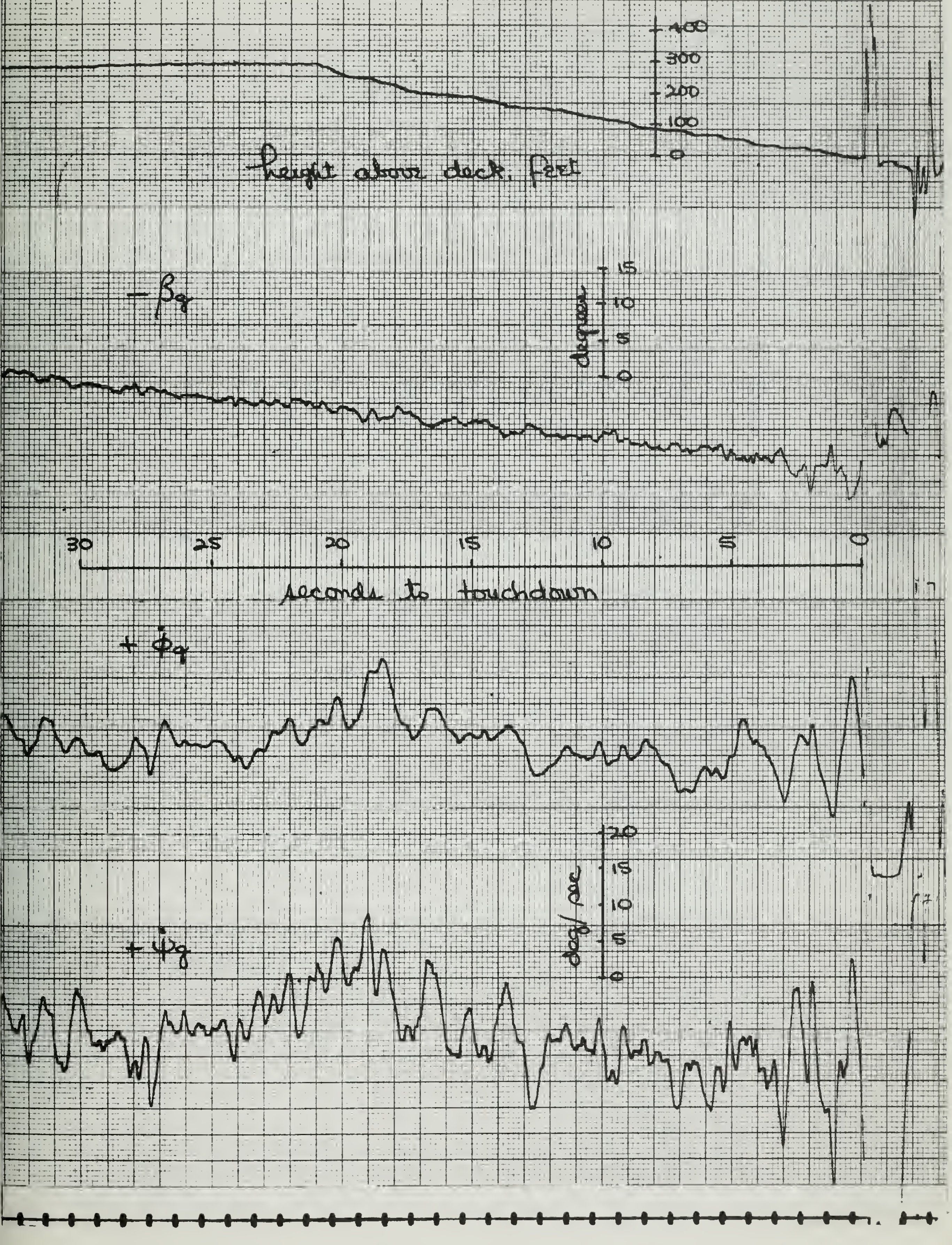

Fig. 24B

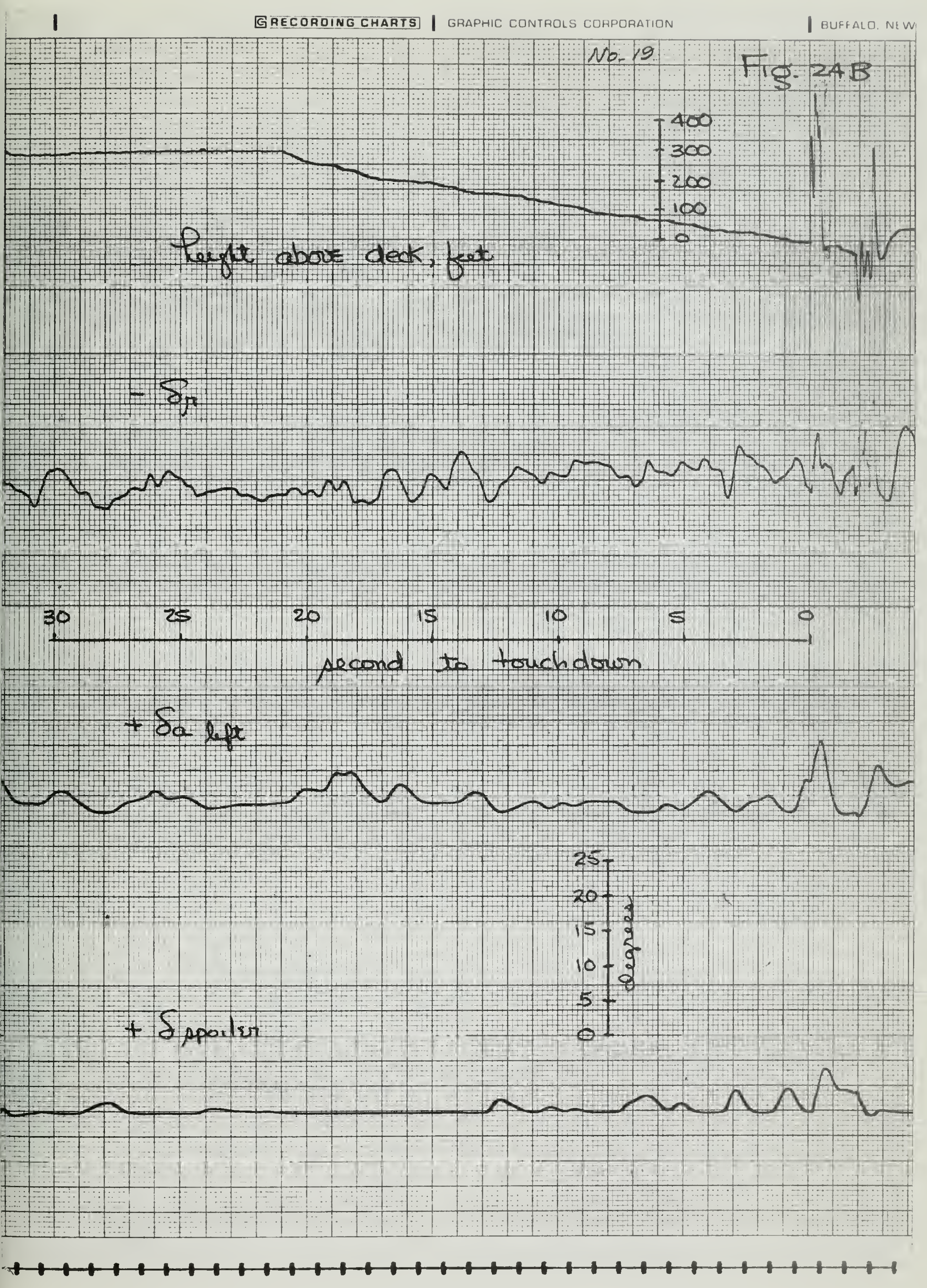
RECORDING CHARTS
GRAPHIC CONTROLS CORPORATION
BUFFALO, NEW
No. 19
400
300
200
100
0
Height above deck, feet
− δr
30
25
20
15
10
5
0
second to touchdown
+ δa left
25
20
15
10
5
0
degrees
+ δ spoiler

No 19

Fig. 24C

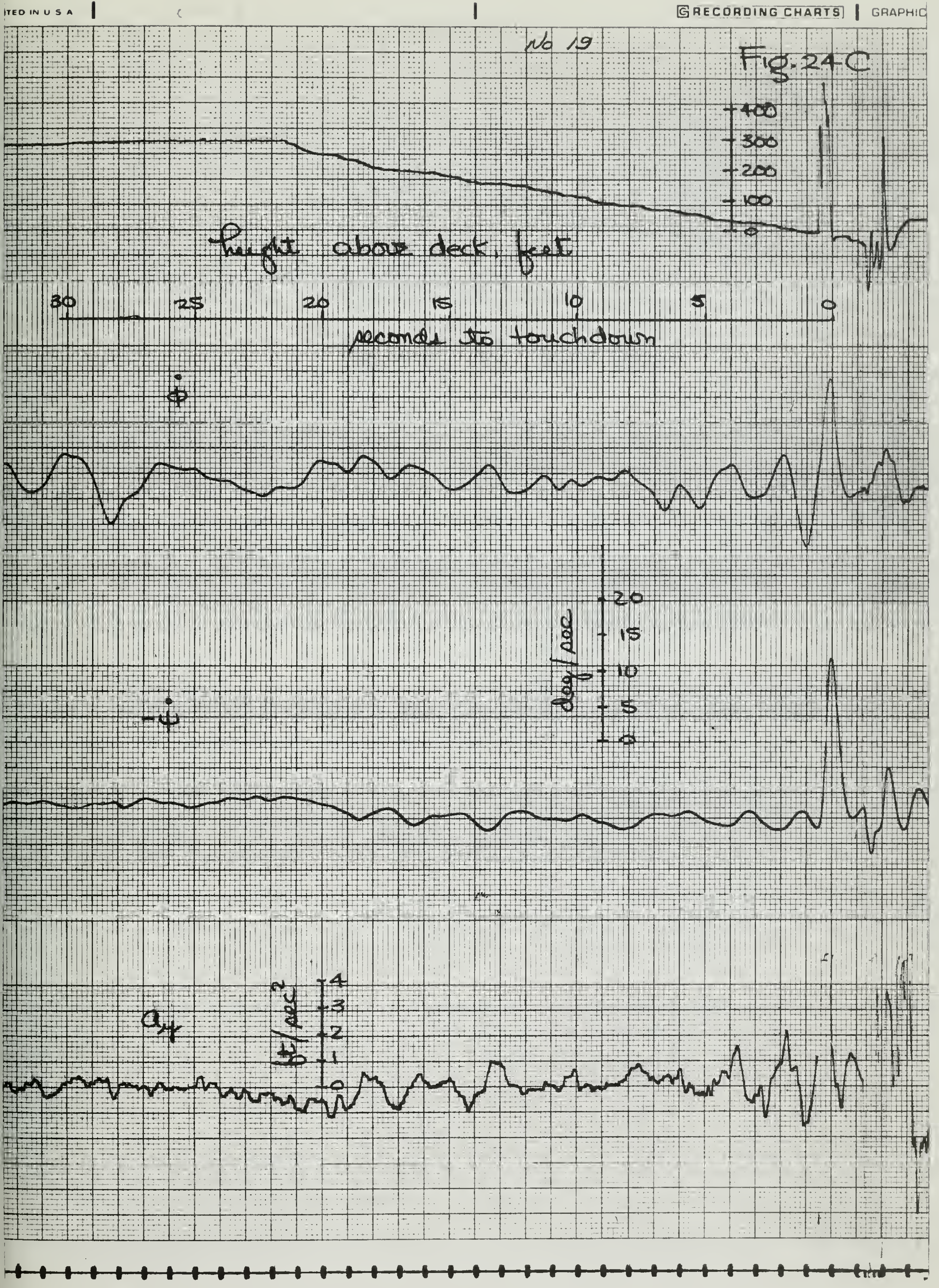
TED IN U S A
RECORDING CHARTS
GRAPHIC
400
300
200
100
0
height above deck, feet
30
25
20
15
10
5
0
seconds to touchdown
$\dot{\phi}$
20
15
10
5
0
deg/sec
$-\dot{\psi}$
$a_y$
4
3
2
1
0
ft/sec²

PHIC CONTROLS CORPORATION | BUFFALO, NEW YORK PRINTED IN U.S.A

Fig. 24 D

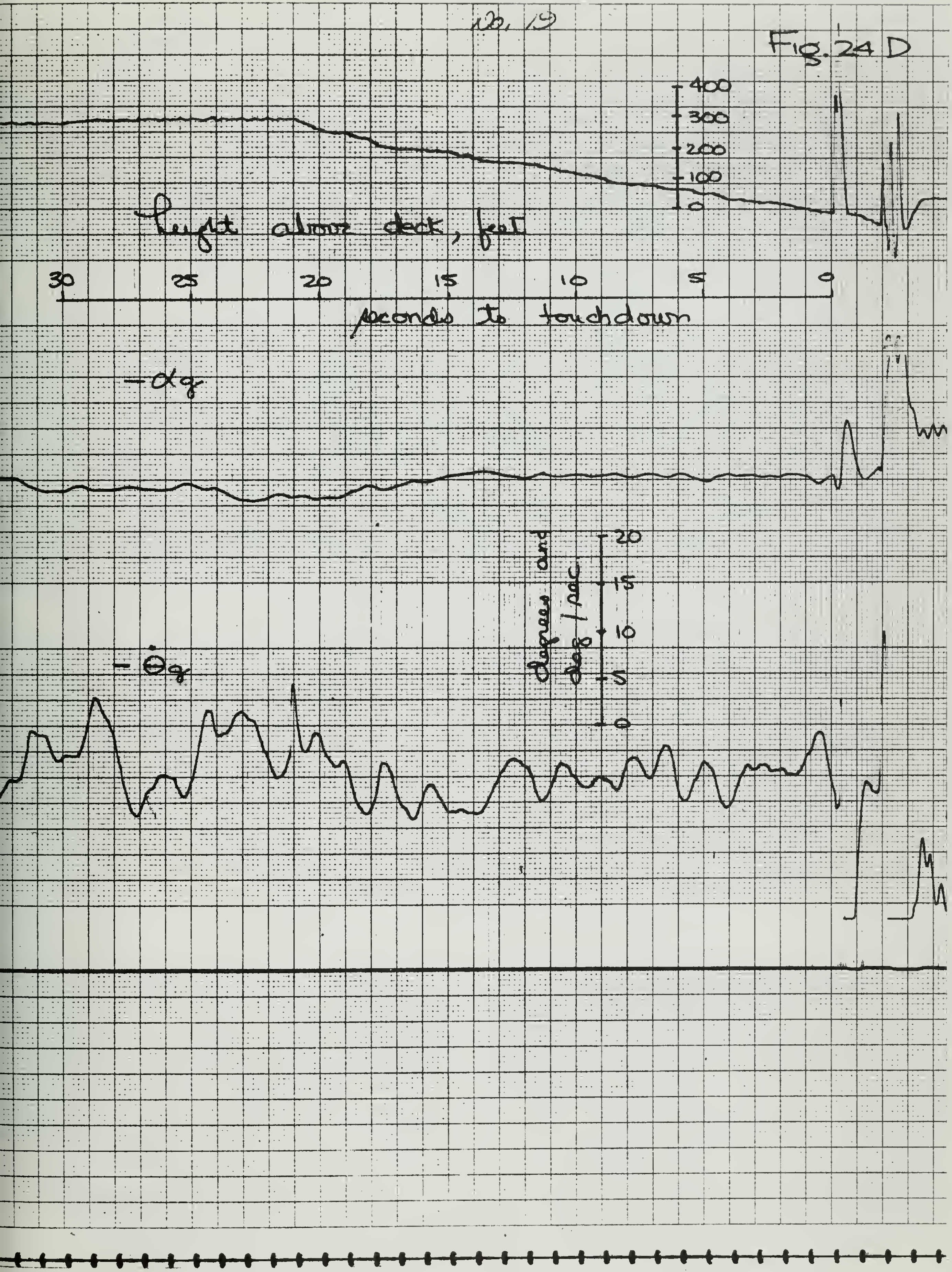

no. 19

Fig. 24 E

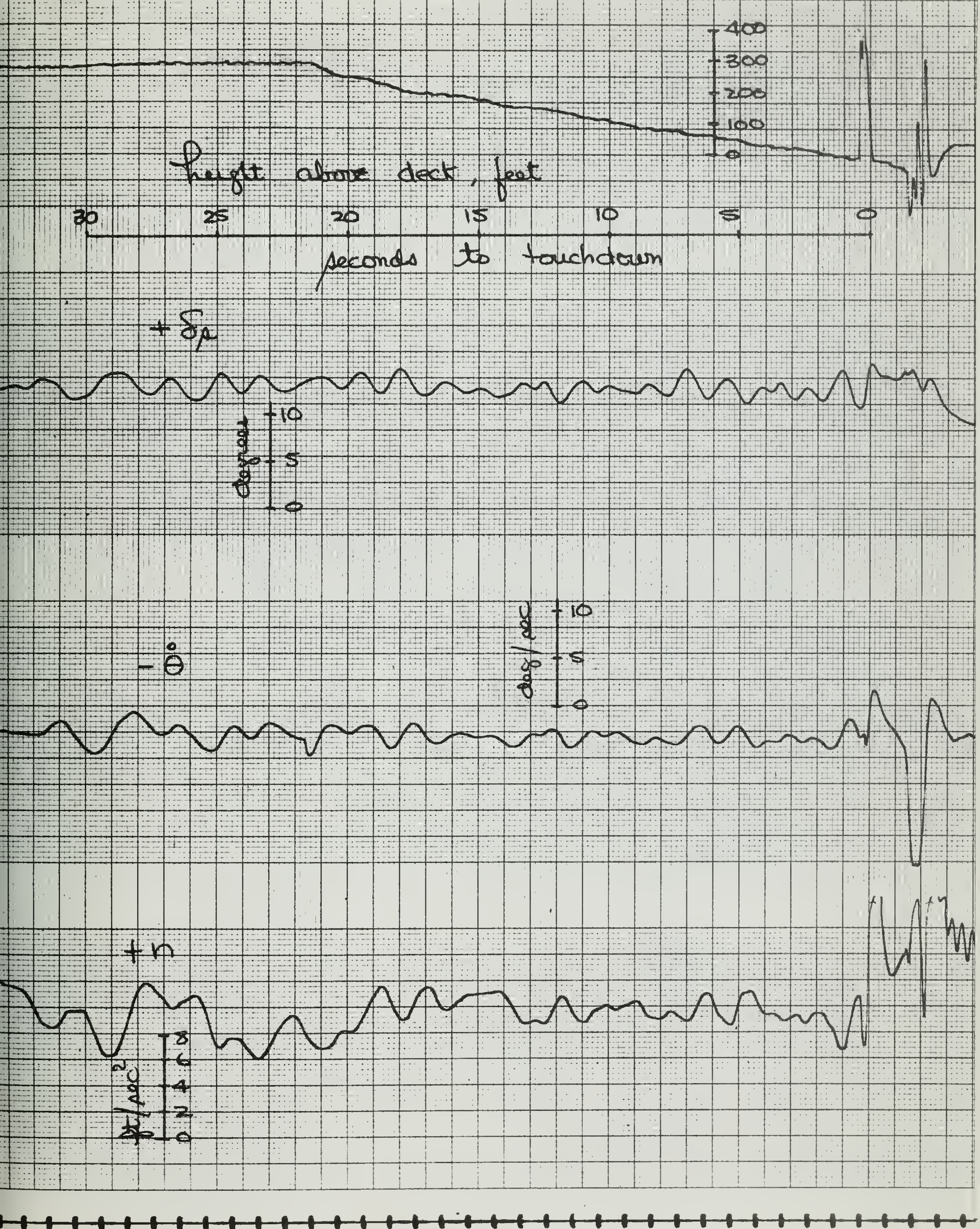
51-54
RECORDING CHARTS
GRAPHIC CONTROLS CORPORATION
400
300
200
100
0
height above deck, feet
30
25
20
15
10
5
0
seconds to touchdown
+ δp
degrees
10
5
0
− θ̇
deg/sec
10
5
0
+ n
ft/sec²
8
6
4
2
0

Lateral and Longitudinal Gust Quantities
No. 21

Fig. 25 A

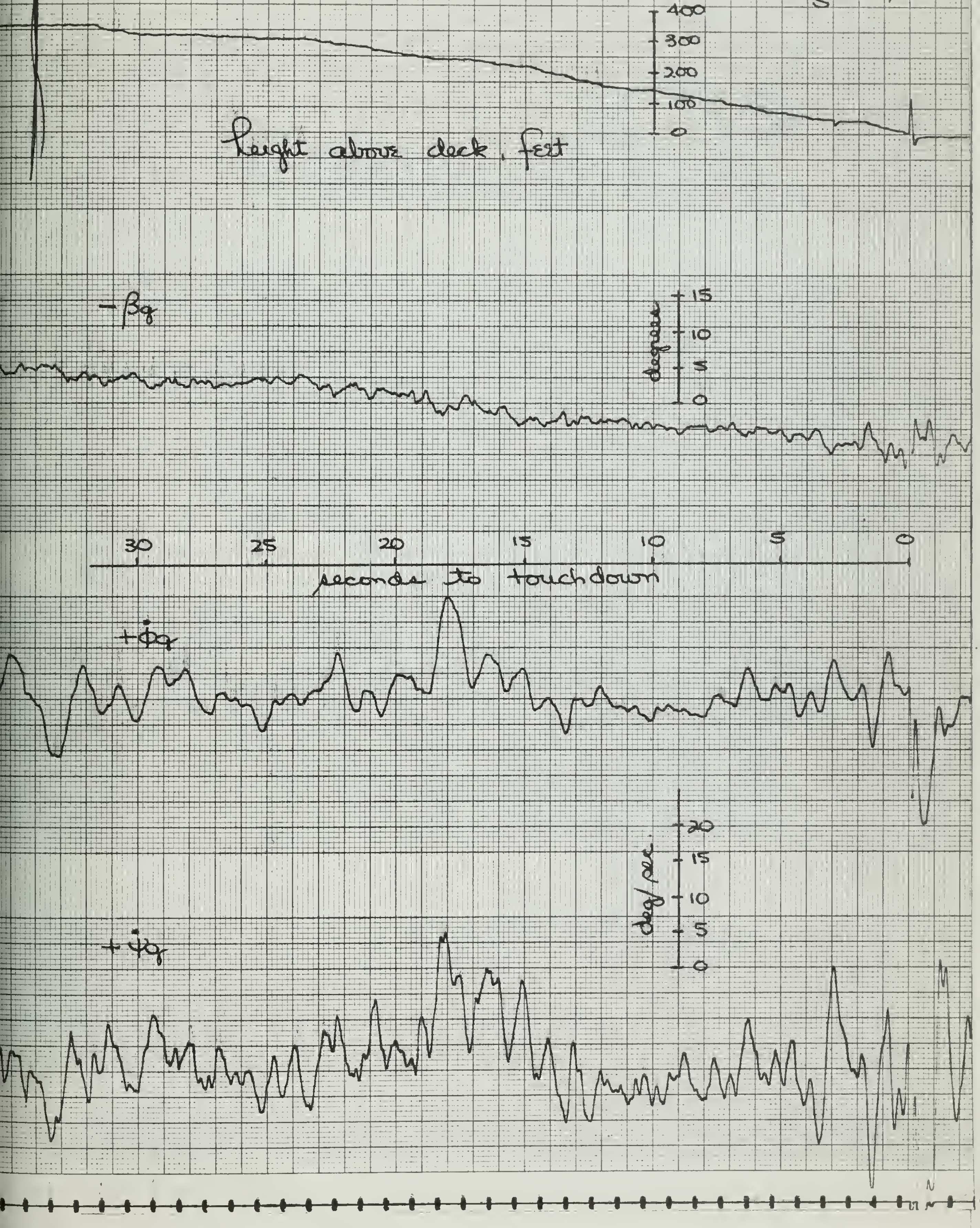

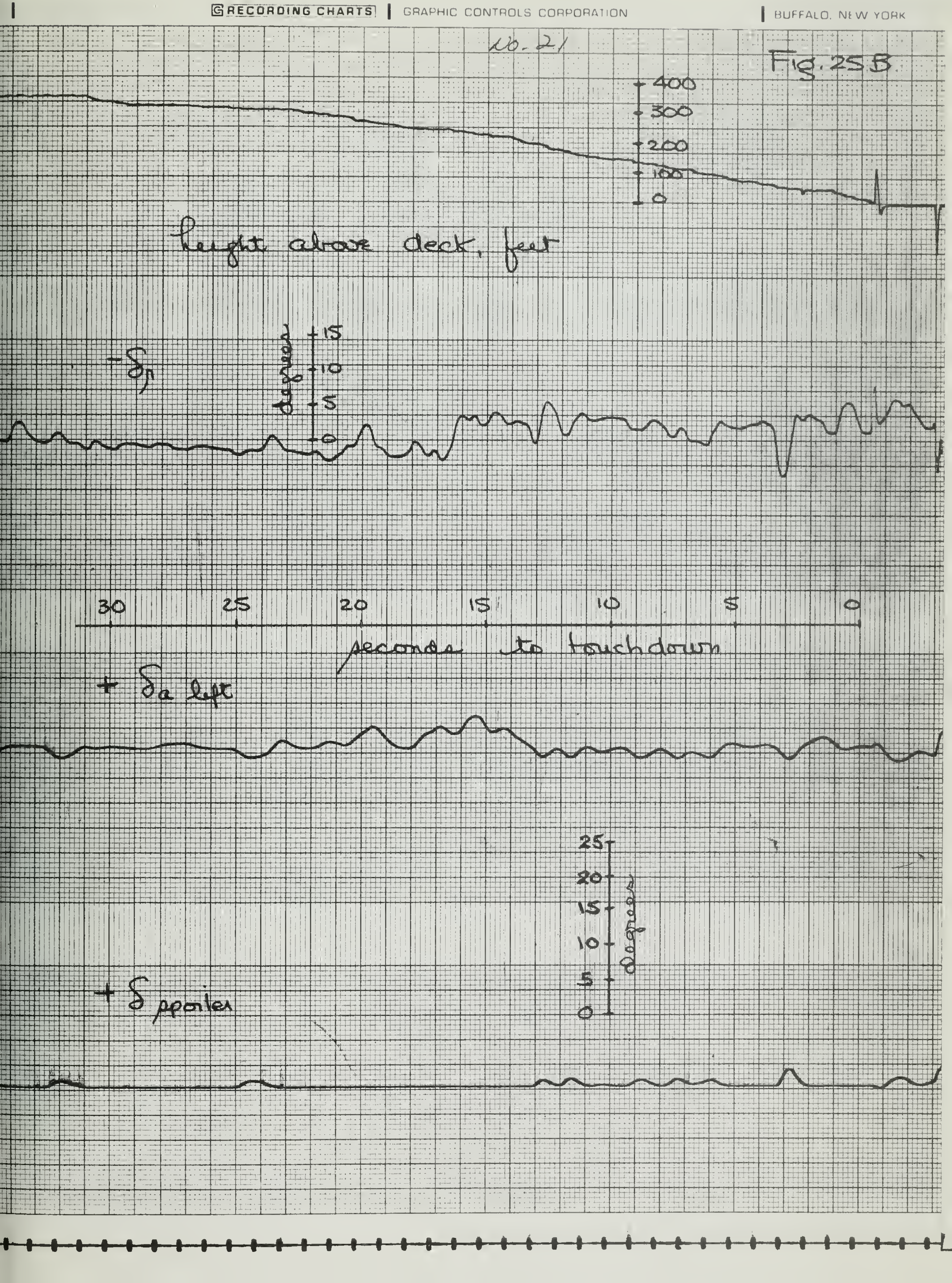
RECORDING CHARTS
GRAPHIC CONTROLS CORPORATION
BUFFALO, NEW YORK
No. 21
400
300
200
100
0
height above deck, feet
$-\delta_r$
degrees
15
10
5
0
30
25
20
15
10
5
0
seconds to touchdown
$+\delta_a$ left
25
20
15
10
5
0
degrees
$+\delta$ spoiler

Fig. 25B

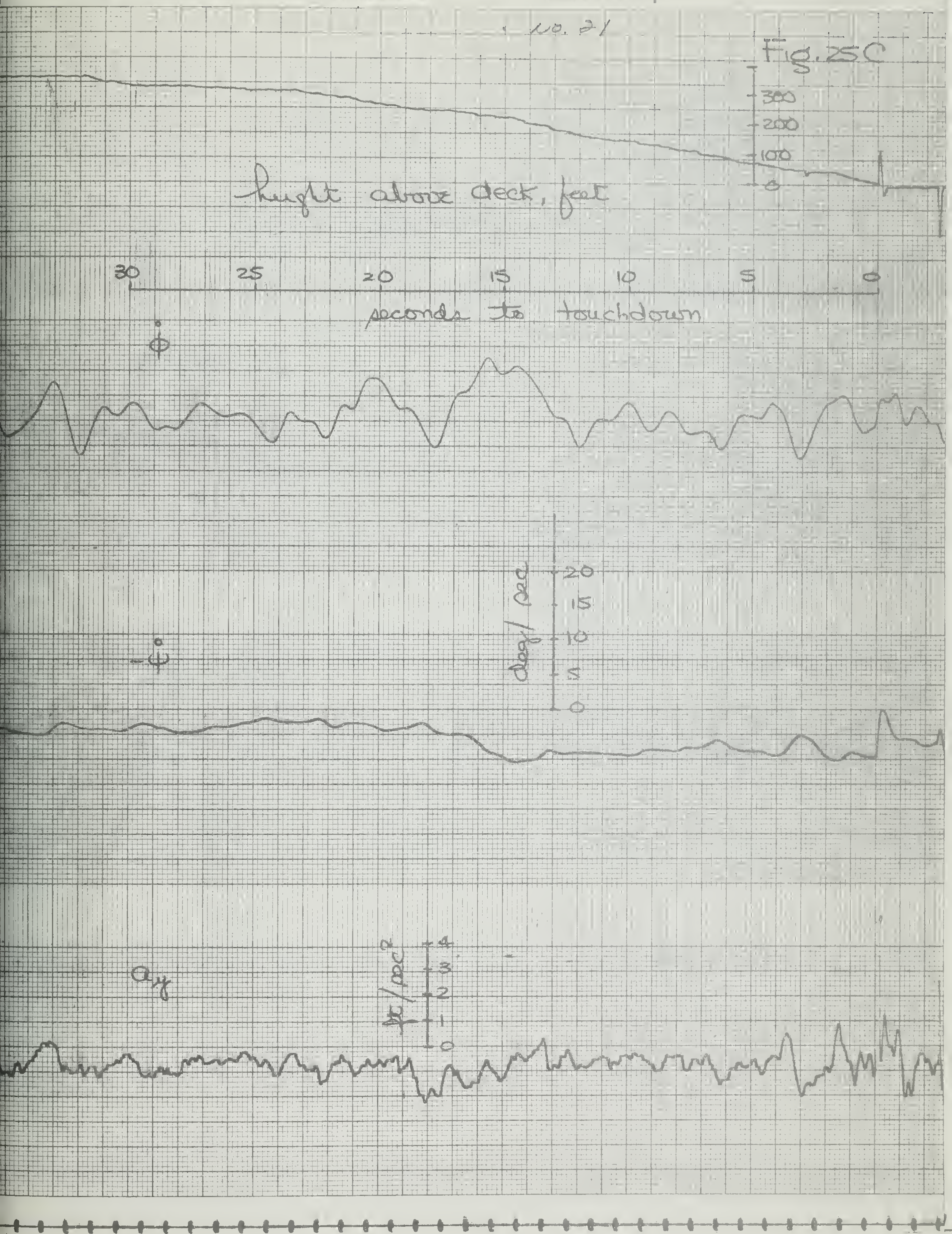
no. 21

Fig. 25C

300
200
100
0
height above deck, feet
30
25
20
15
10
5
0
seconds to touchdown
$\dot{\phi}$
deg/sec
20
15
10
5
0
$-\dot{\psi}$
$a_y$
ft/sec²
4
3
2
1
0

BUFFALO, NEW YORK PRINTED IN U.S.A.

100.21.

Fig. 25D

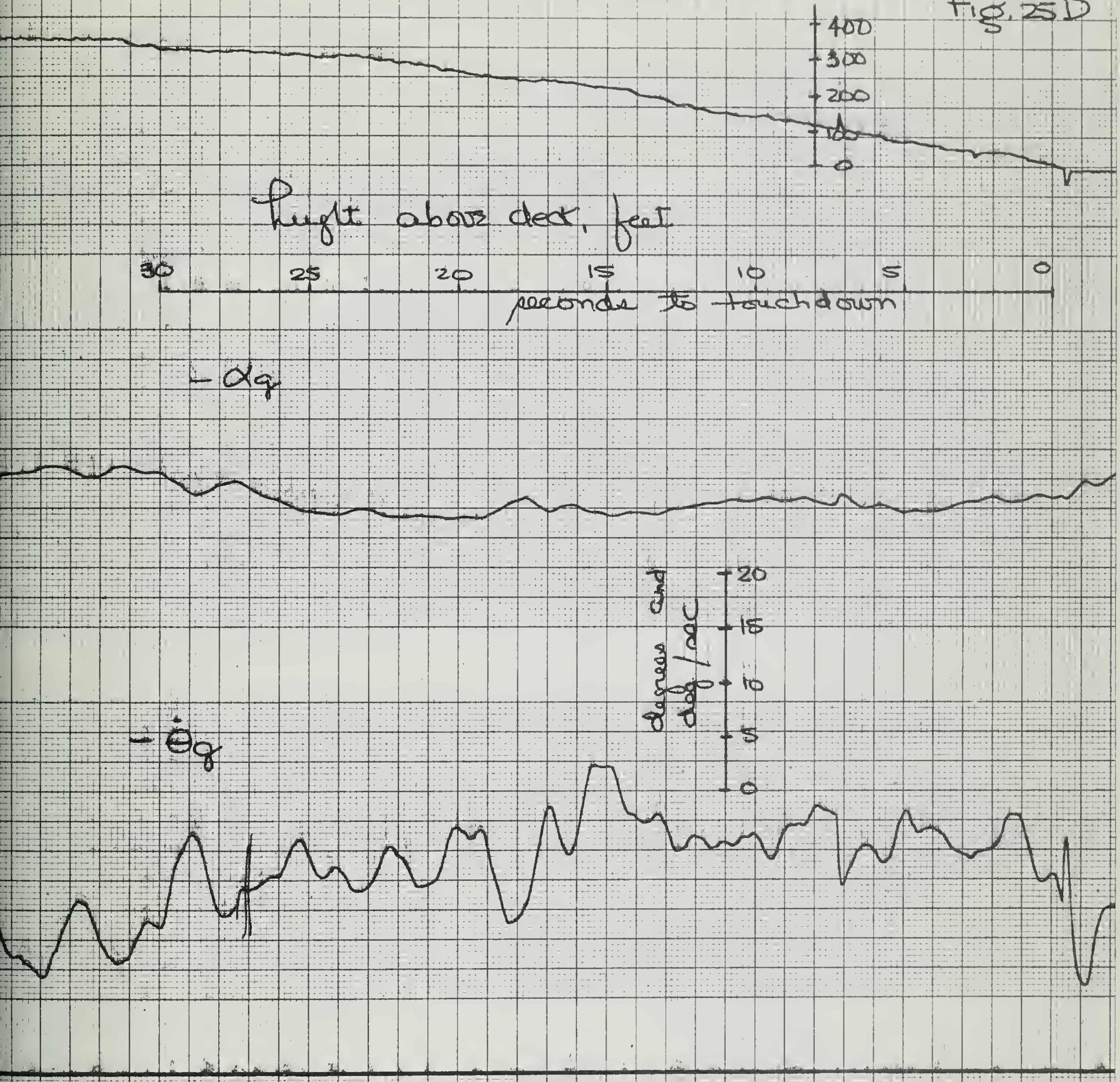

RECORDING CHARTS | GRAPHIC CONTROLS CORPORATION | BUFFALO, NEW YORK

No. 21

Fig. 25 E

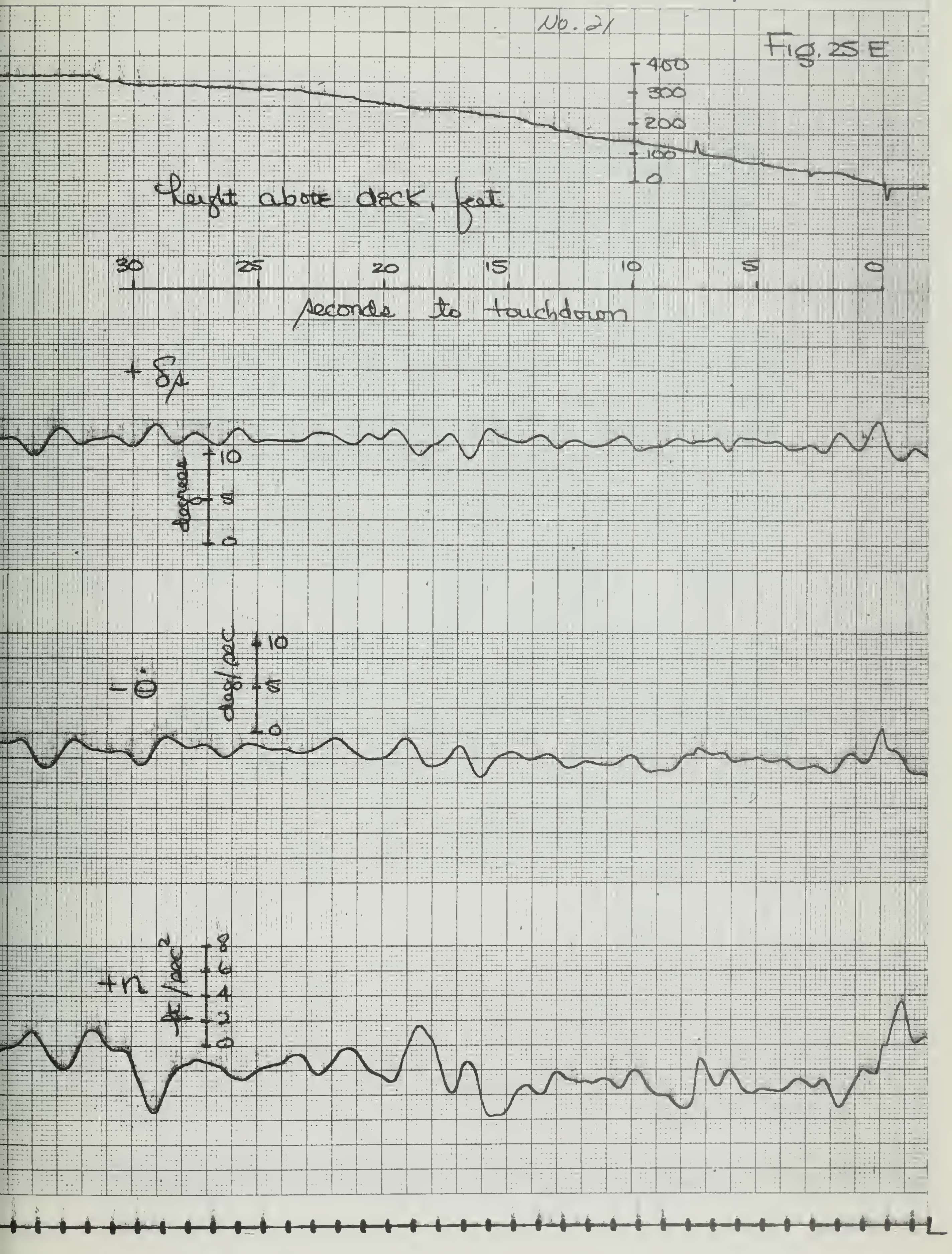

ARTS | GRAPHIC CONTROLS CORPORATION | BUFFALO, N.Y.

Lateral and Longitudinal Gust Quantities
no 23

Fig. 26A

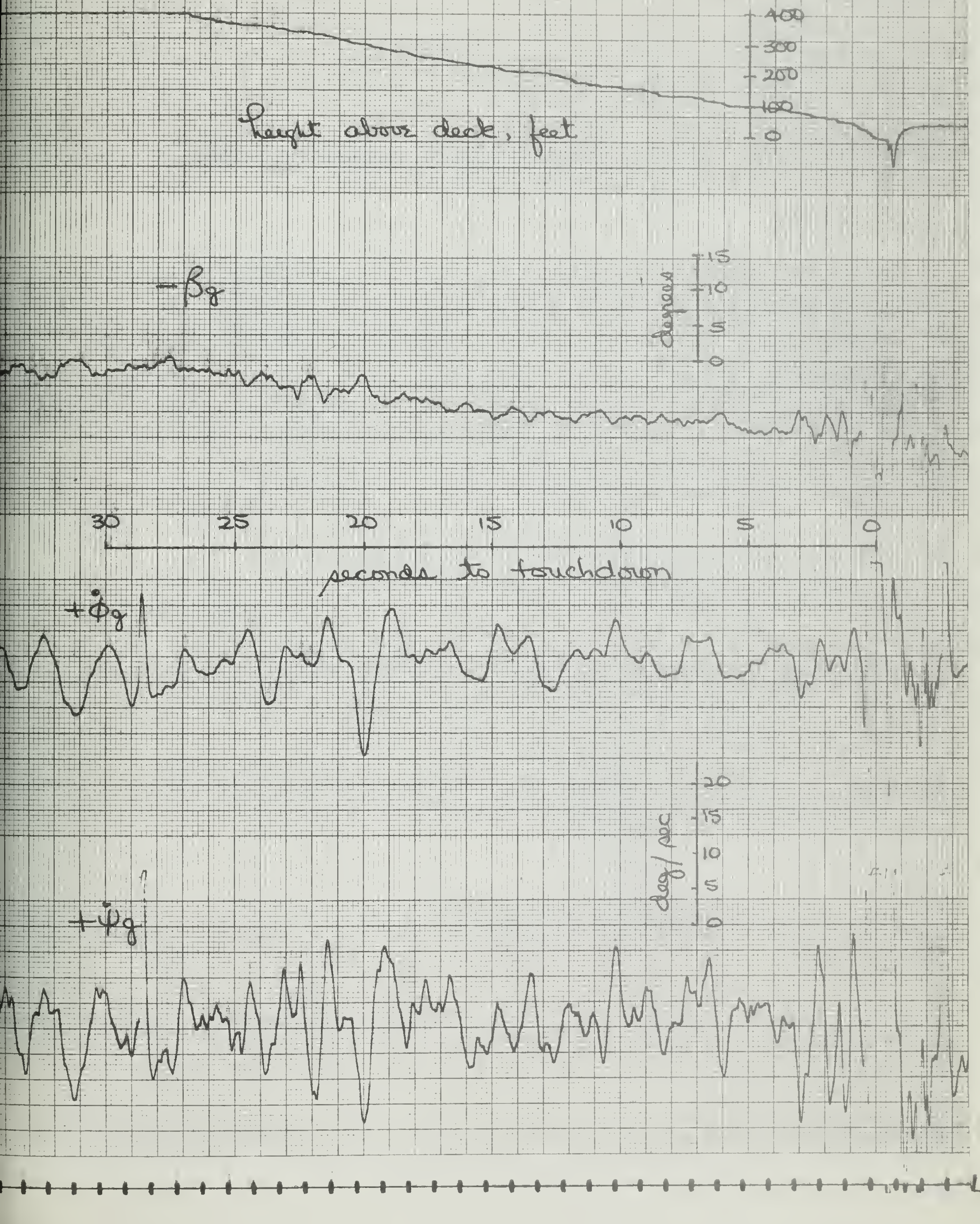

RECORDING CHARTS | GRAPHIC CONTROLS CORPORATION

No. 23

Fig. 26B

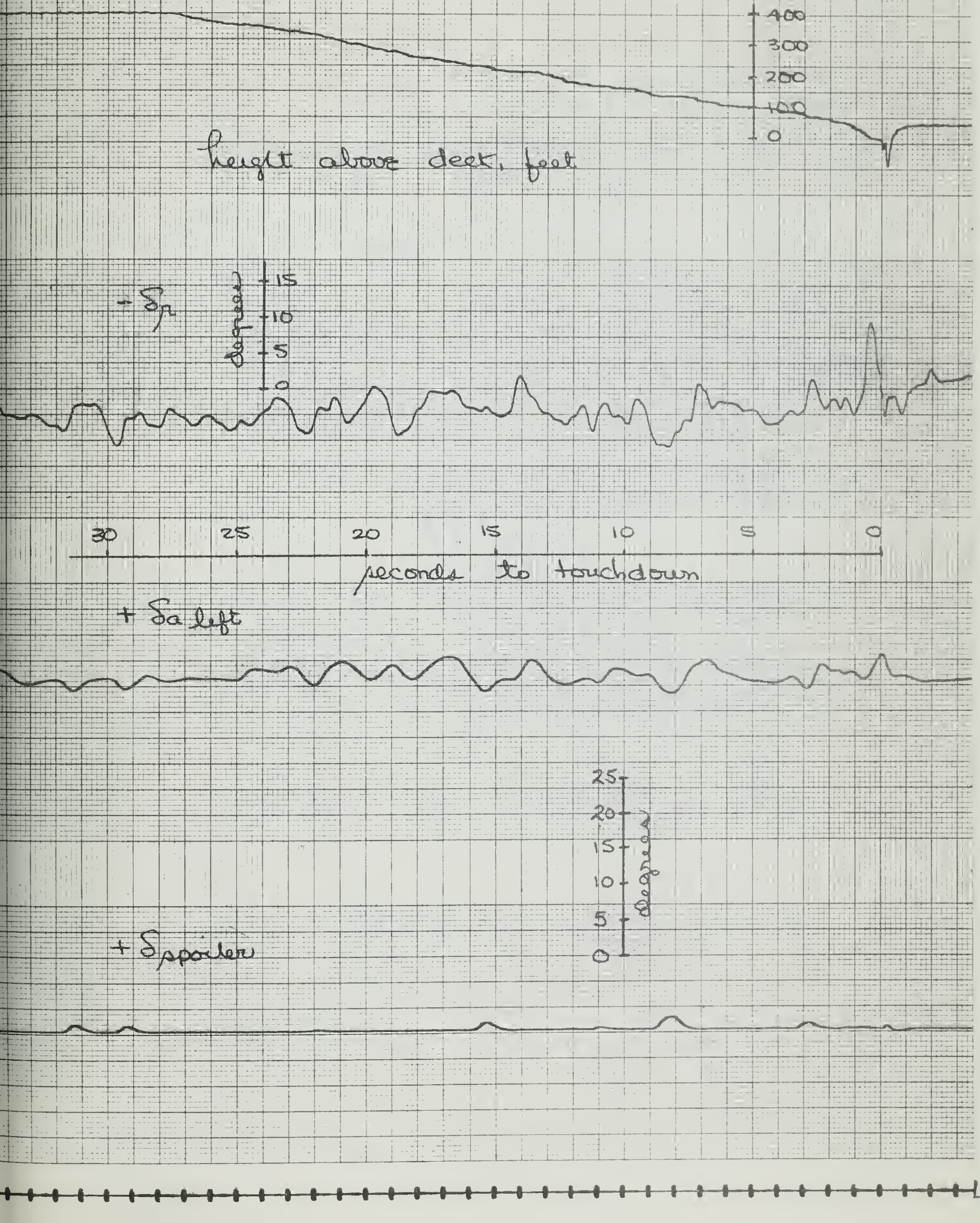

RECORDING CHARTS | GRAPHIC CONTROLS CORPORATION | BUFFALO NEW YORK PRINTED IN U S A

No. 23

Fig. 26 C

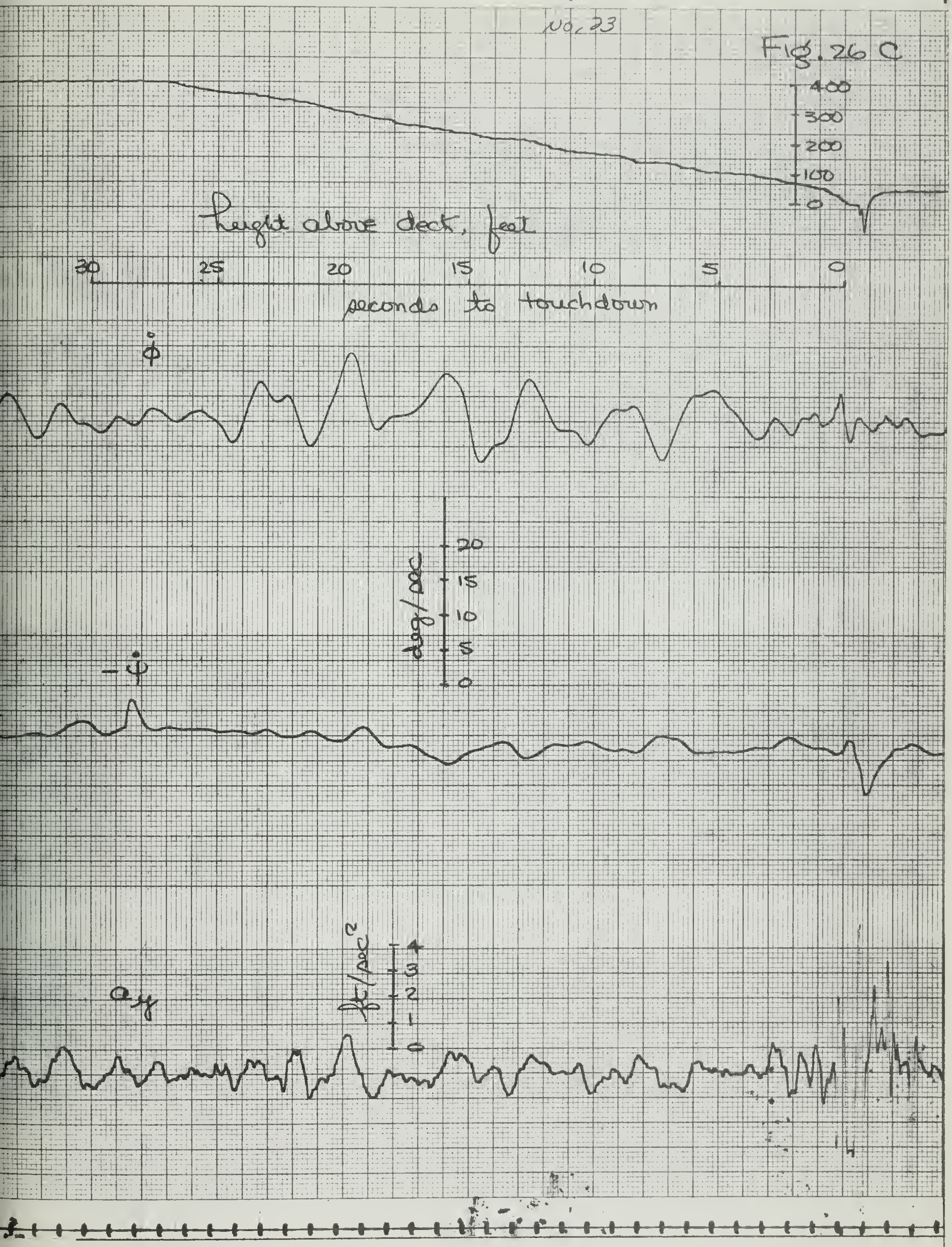

No. 23

Fig. 26D

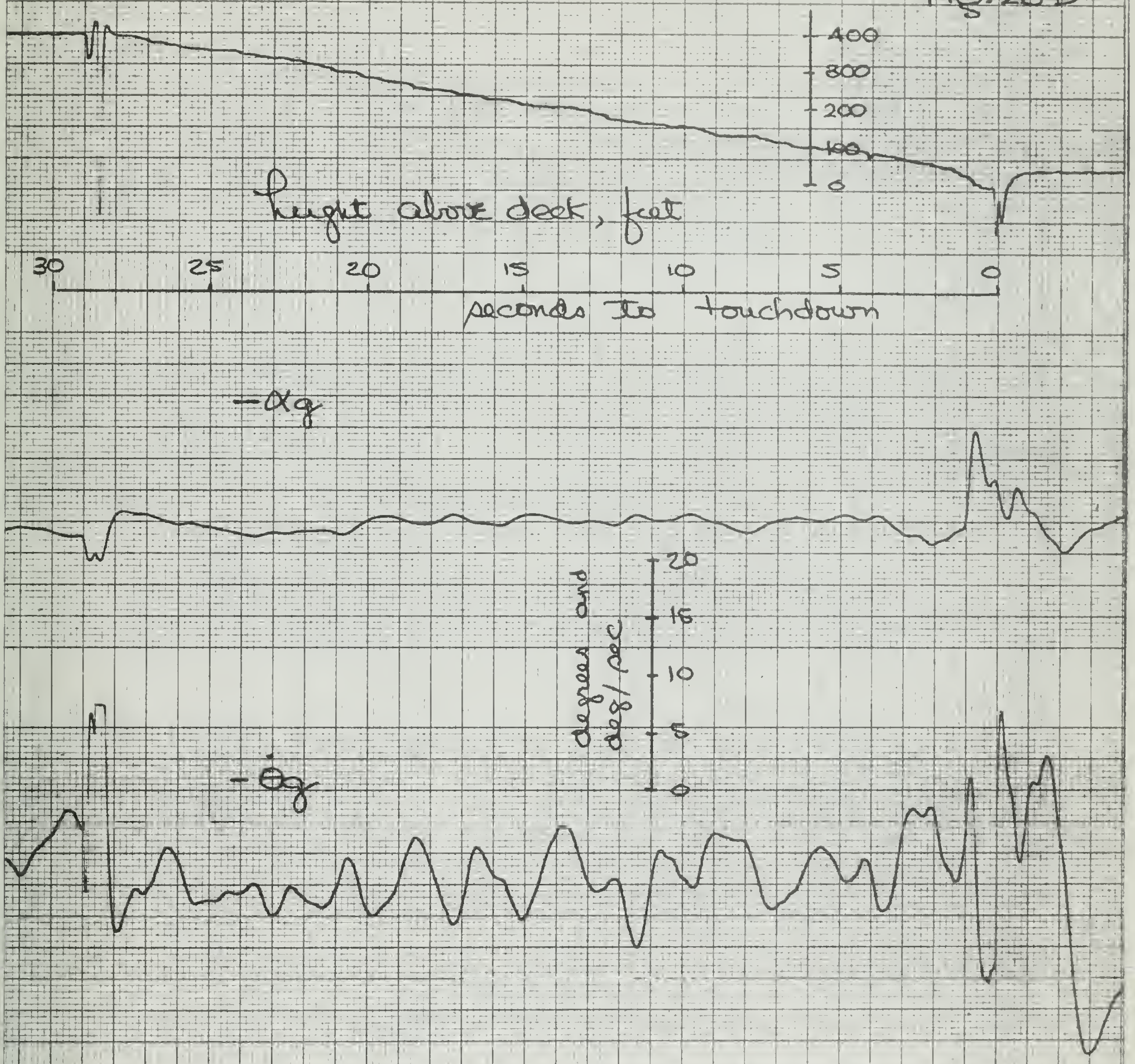
400
300
200
100
0
height above deck, feet
30
25
20
15
10
5
0
seconds to touchdown
$-\alpha_g$
20
15
10
5
0
degrees and deg/sec
$-\dot{\theta}_g$

651-54 RECORDING CHARTS | GRAPHIC CONTROLS CORPORATION

No. 23

Fig. 26 E

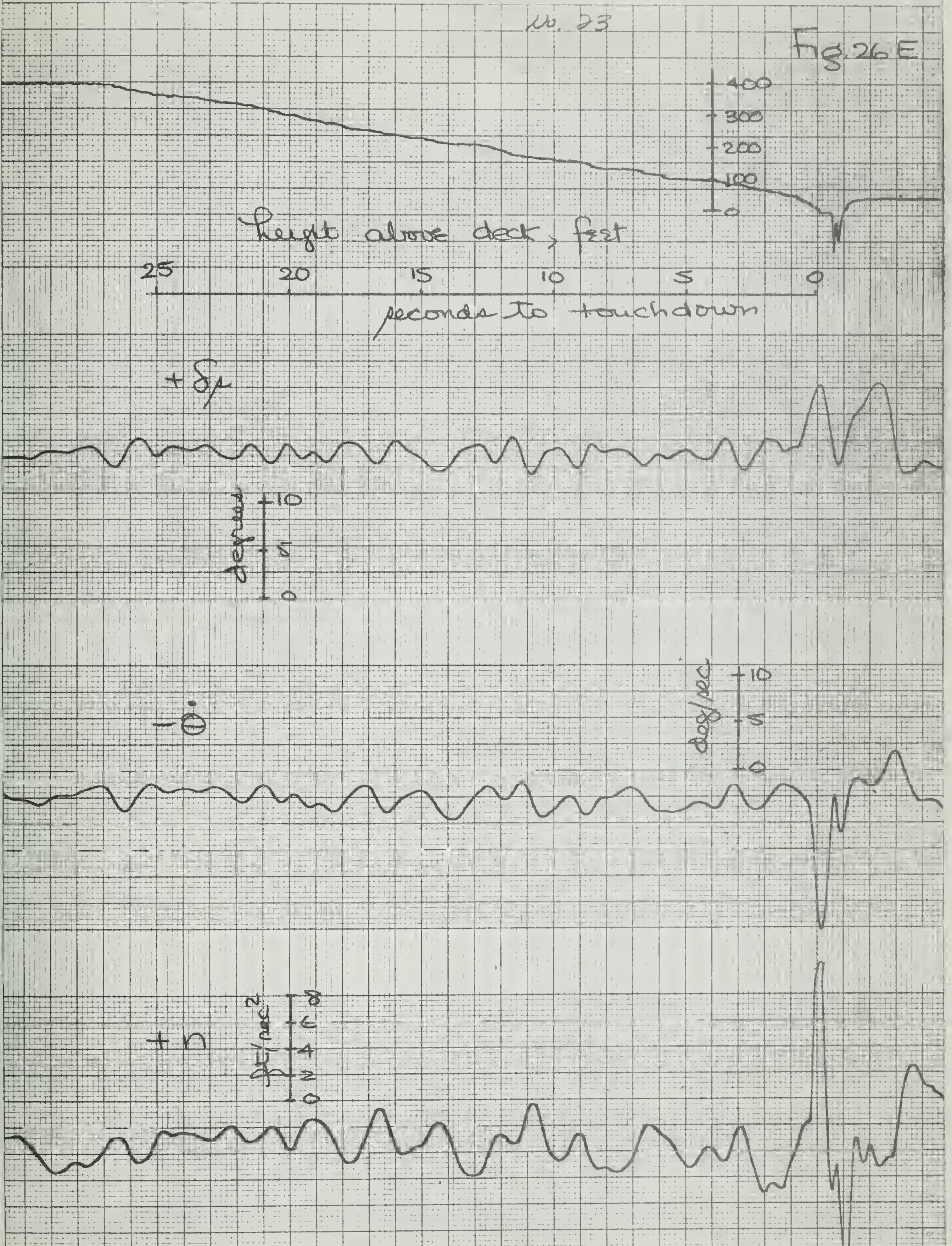

Lateral and Longitudinal Gust Quantities

No. 24

Fig. 27A

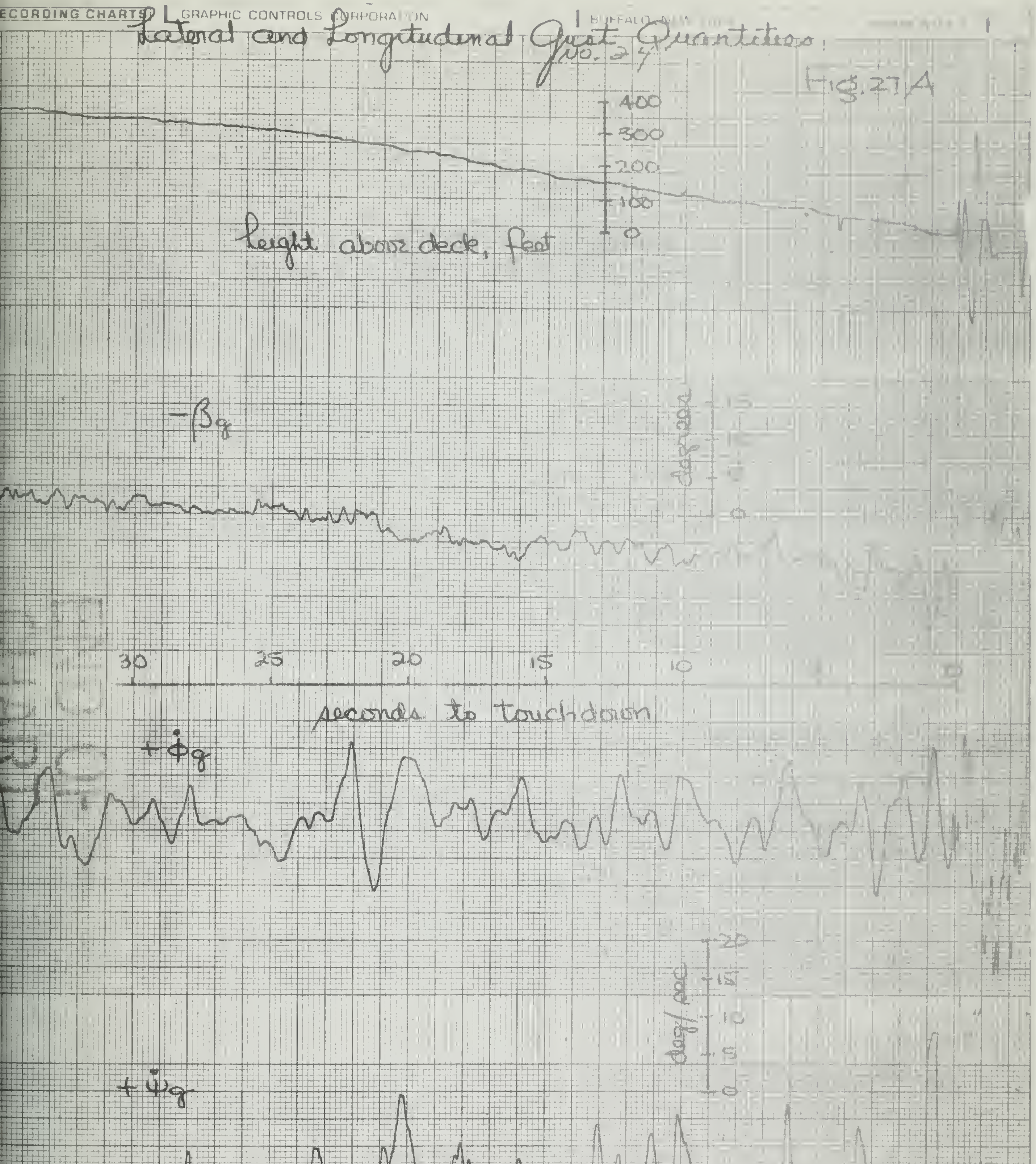

Fig 27B

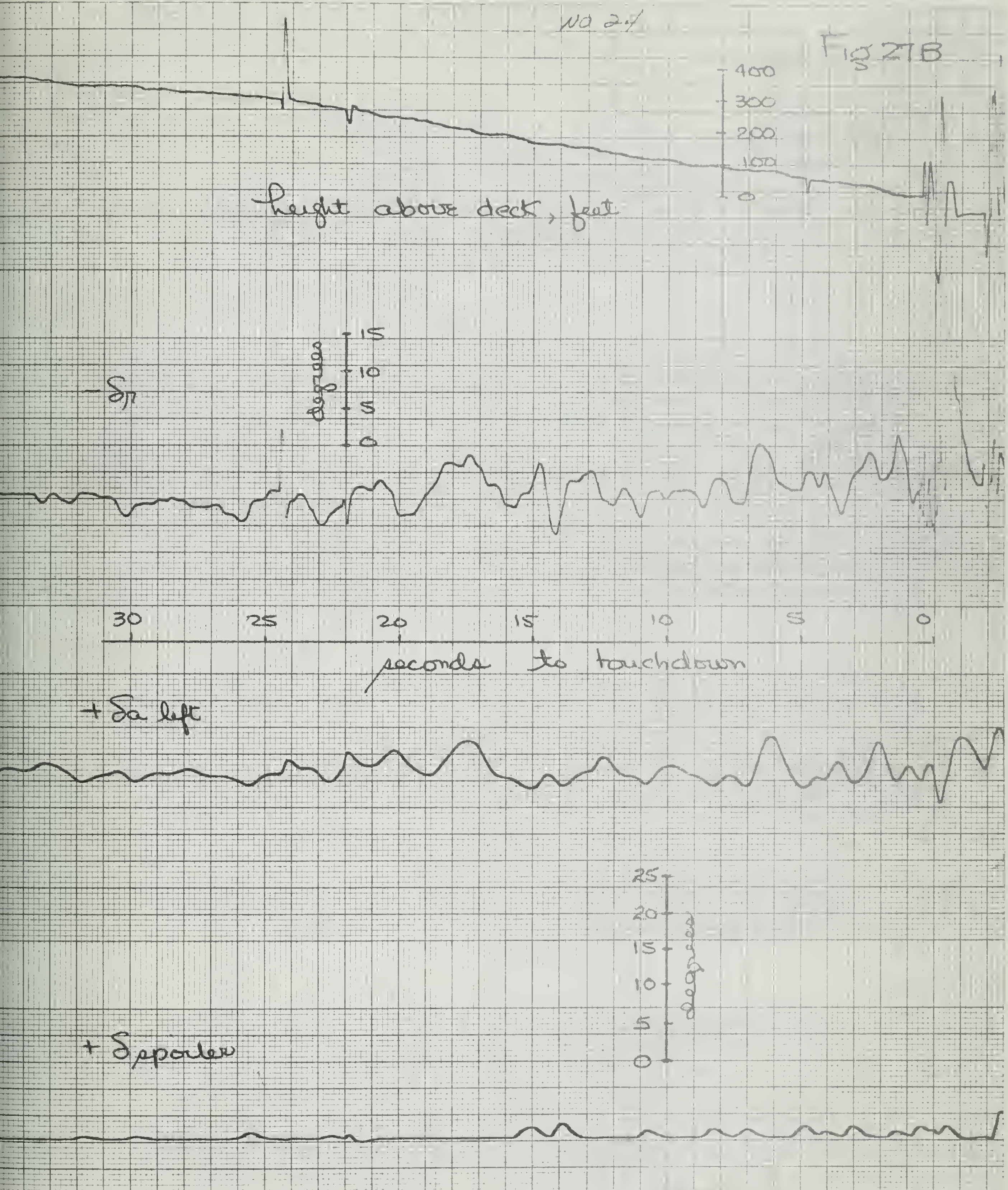
No 24
400
300
200
100
0
height above deck, feet
$-\delta_r$
degrees
15
10
5
0
30
25
20
15
10
5
0
seconds to touchdown
$+\delta_a$ left
$+\delta_{spoiler}$
25
20
15
10
5
0
degrees

RECORDING CHARTS | GRAPHIC CONTROLS CORPORATION | BUFFALO NEW YORK

no. 24

Fig. 27C

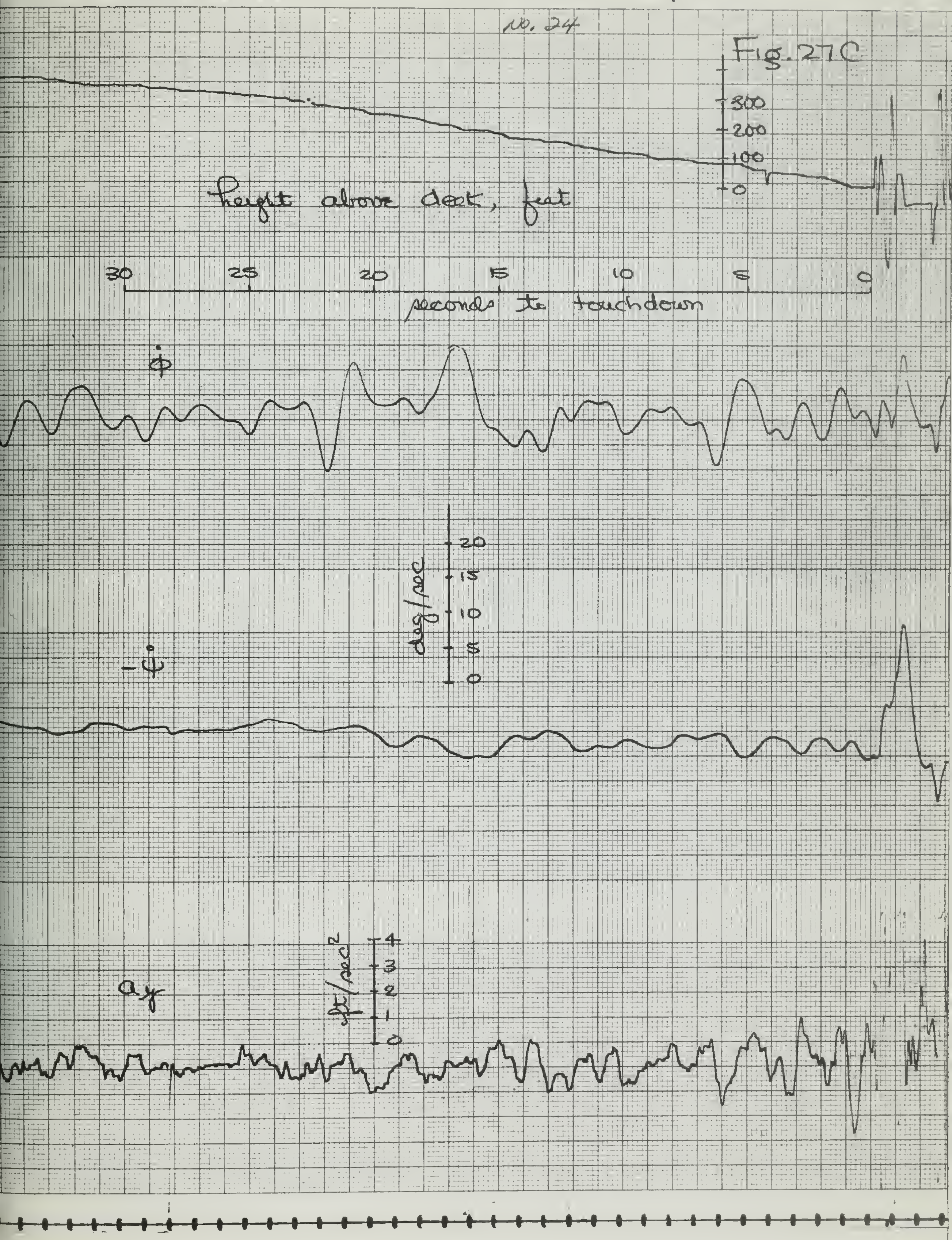

CHARTS | GRAPHIC CONTROLS CORPORATION | BUFFALO, NEW YORK PRINTED IN U.S.A.

No. 24.

Fig. 27D

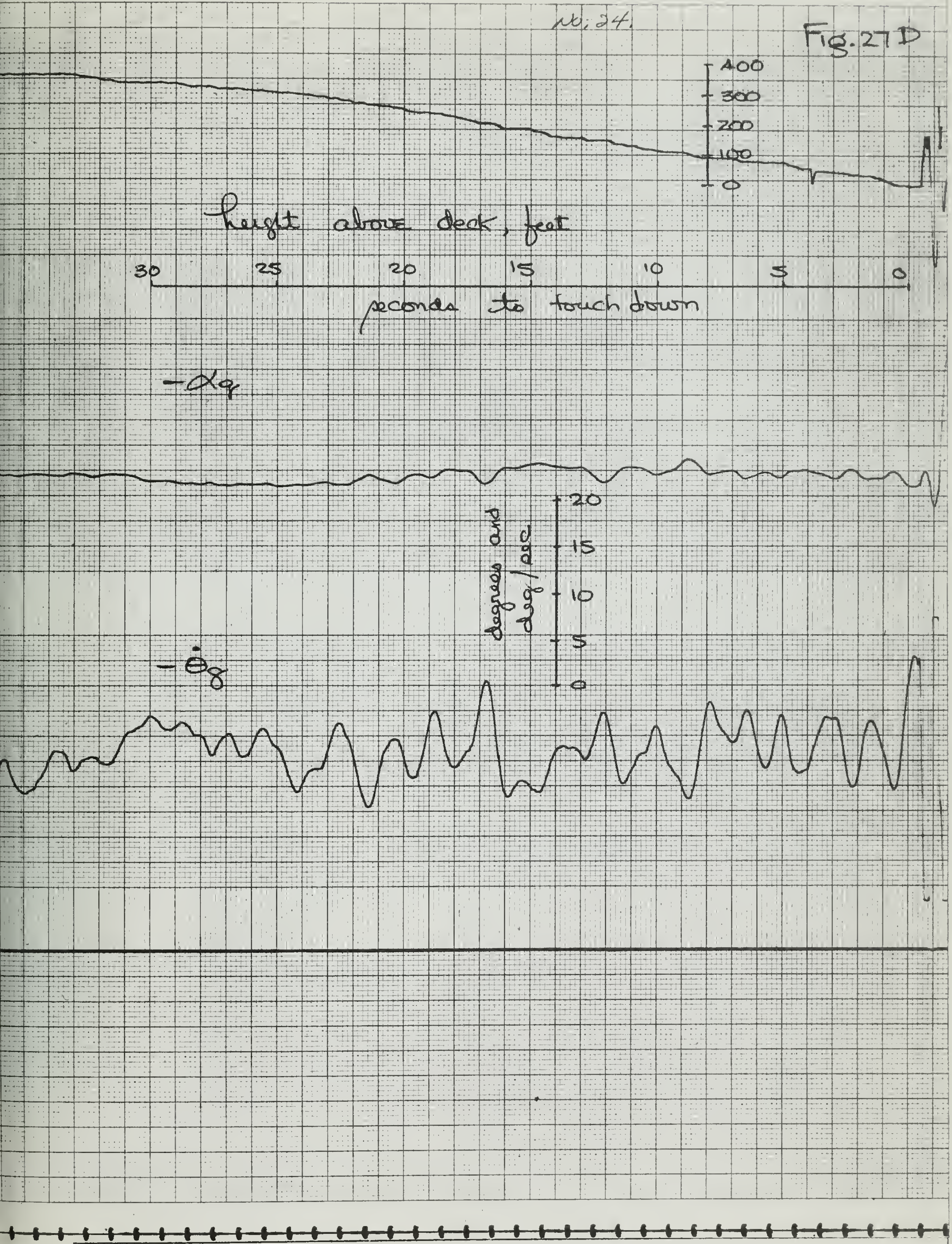

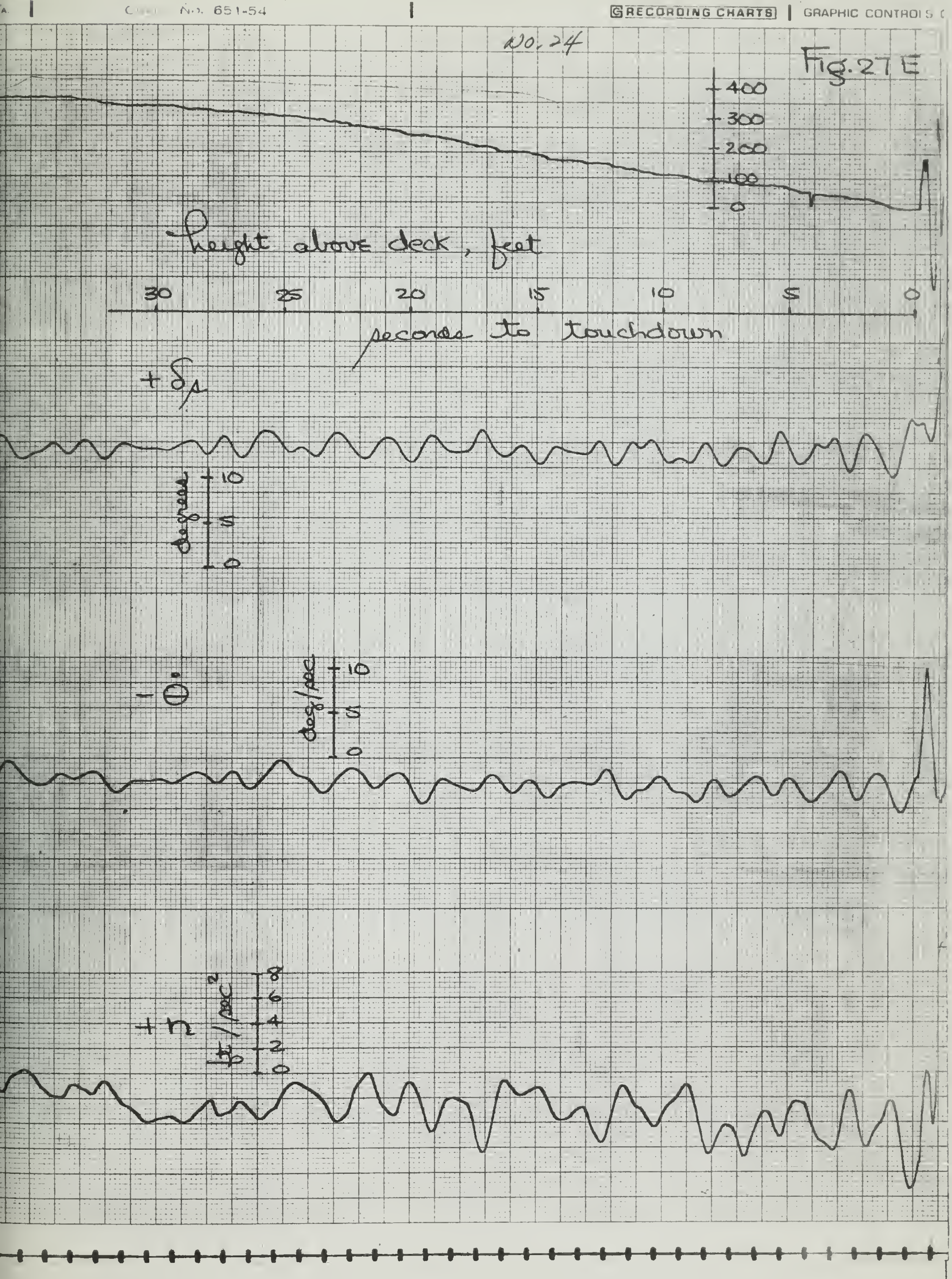
CHART NO. 651-54
RECORDING CHARTS
GRAPHIC CONTROLS
400
300
200
100
0
Height above deck, feet
30
25
20
15
10
5
0
seconds to touchdown
$+\delta_s$
degrees
10
5
0
$-\dot{\theta}$
deg/sec
10
5
0
$+n$
ft/sec$^2$
8
6
4
2
0

No. 24

Fig. 27E

RECORDING CHARTS | GRAPHIC CONTROLS CORPORATION | BUFFALO, NEW YORK | PRINTED IN U.S.A.

Lateral and Longitudinal Gust Quantities
no 25

Fig. 28 A

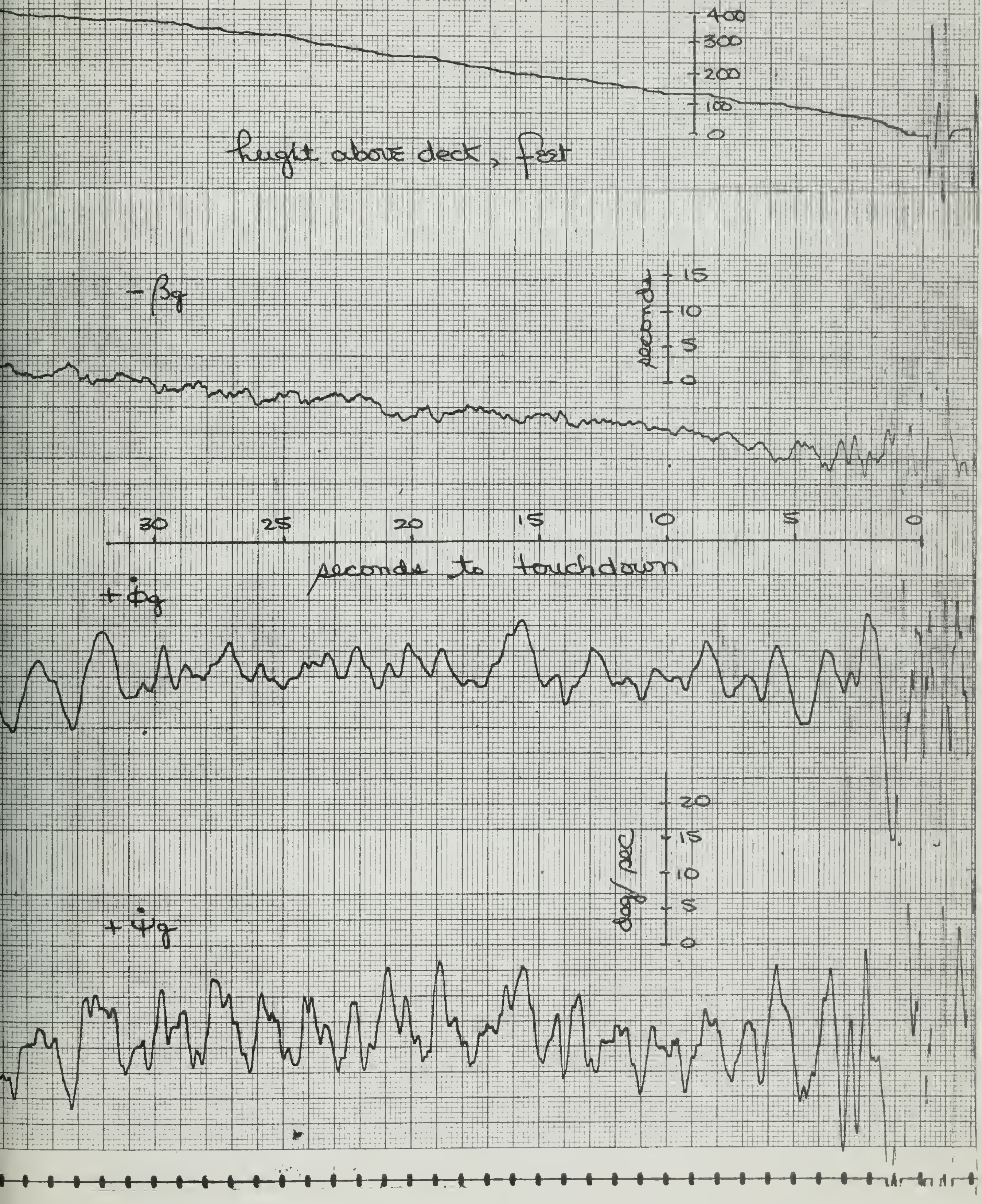

USA

RECORDING CHARTS | GRAPHIC CONTROLS

No. 25

Fig. 28 B

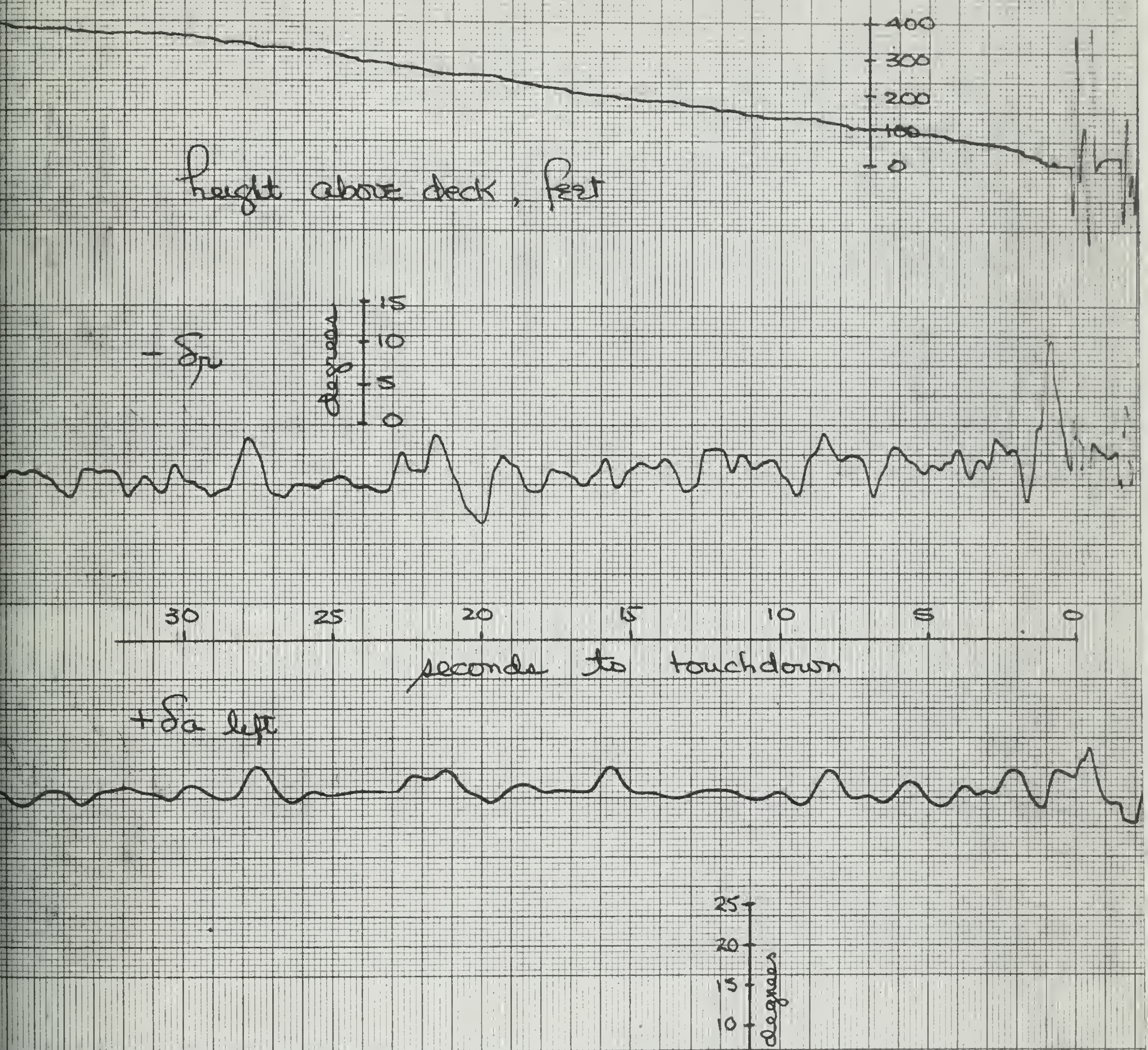

RECORDING CHARTS | GRAPHIC CONTROLS CORPORATION | BUFFALO, NEW YORK

no. 25

Fig. 28C

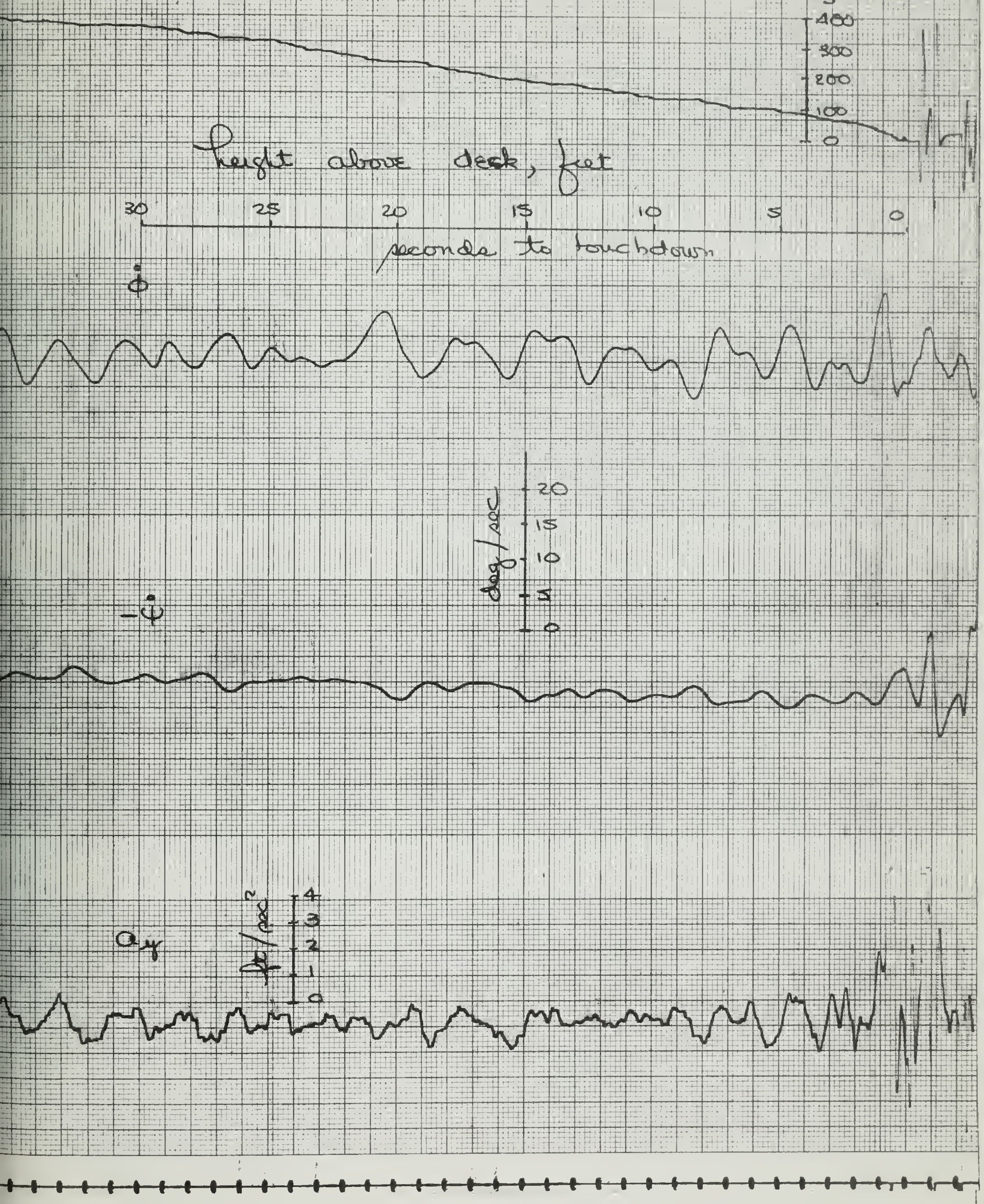

GRAPHIC CONTROLS CORPORATION | BUFFALO, NEW YORK | PRINTED IN U.S.A.

No. 25

Fig. 28 D

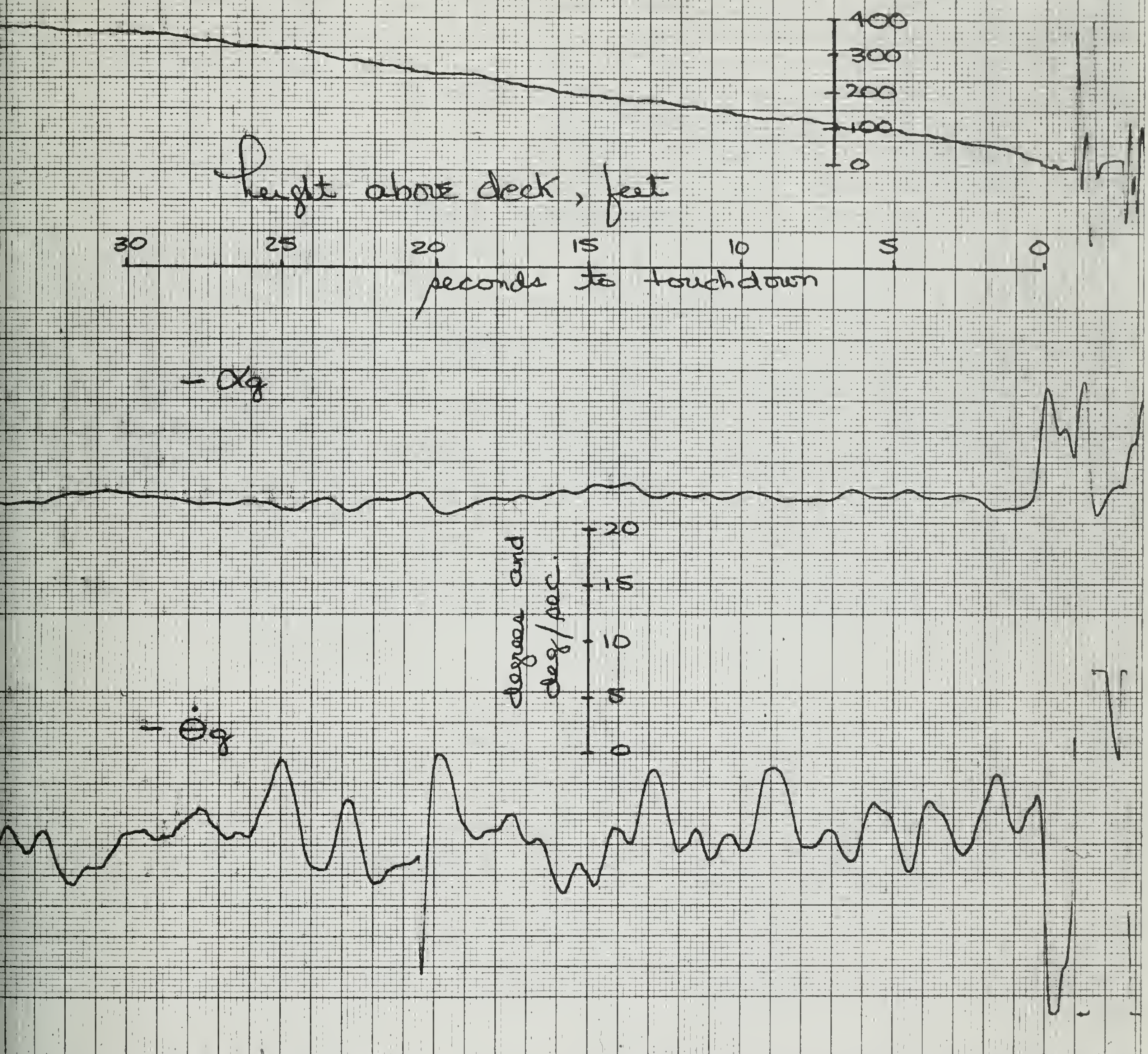

RECORDING CHARTS | GRAPHIC CONTROLS CORPO

No. 25

Fig. 28 E

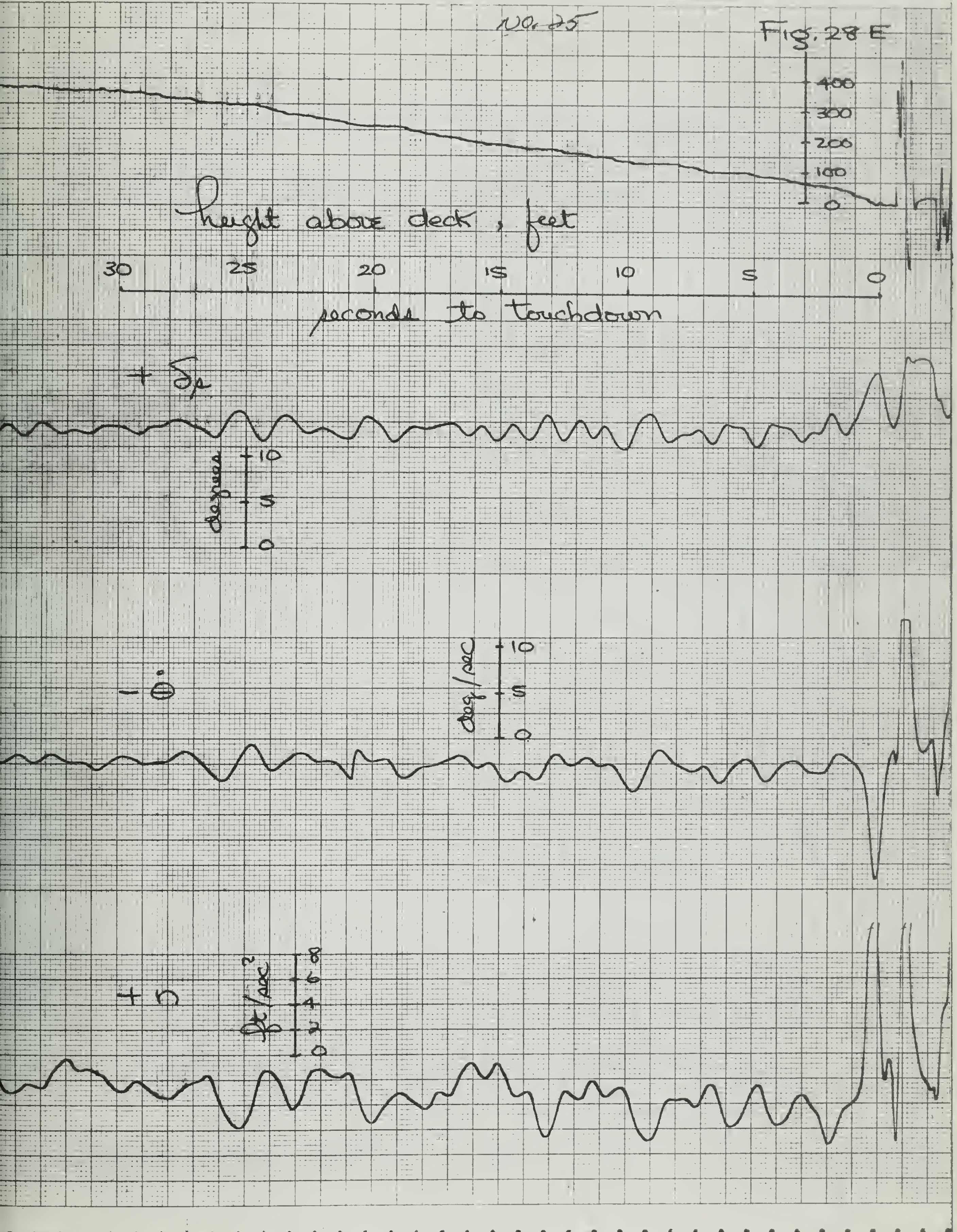

RECORDING CHARTS GRAPHIC CONTROLS

Lateral and Longitudinal Gust Quantities

10:27

Fig. 29A

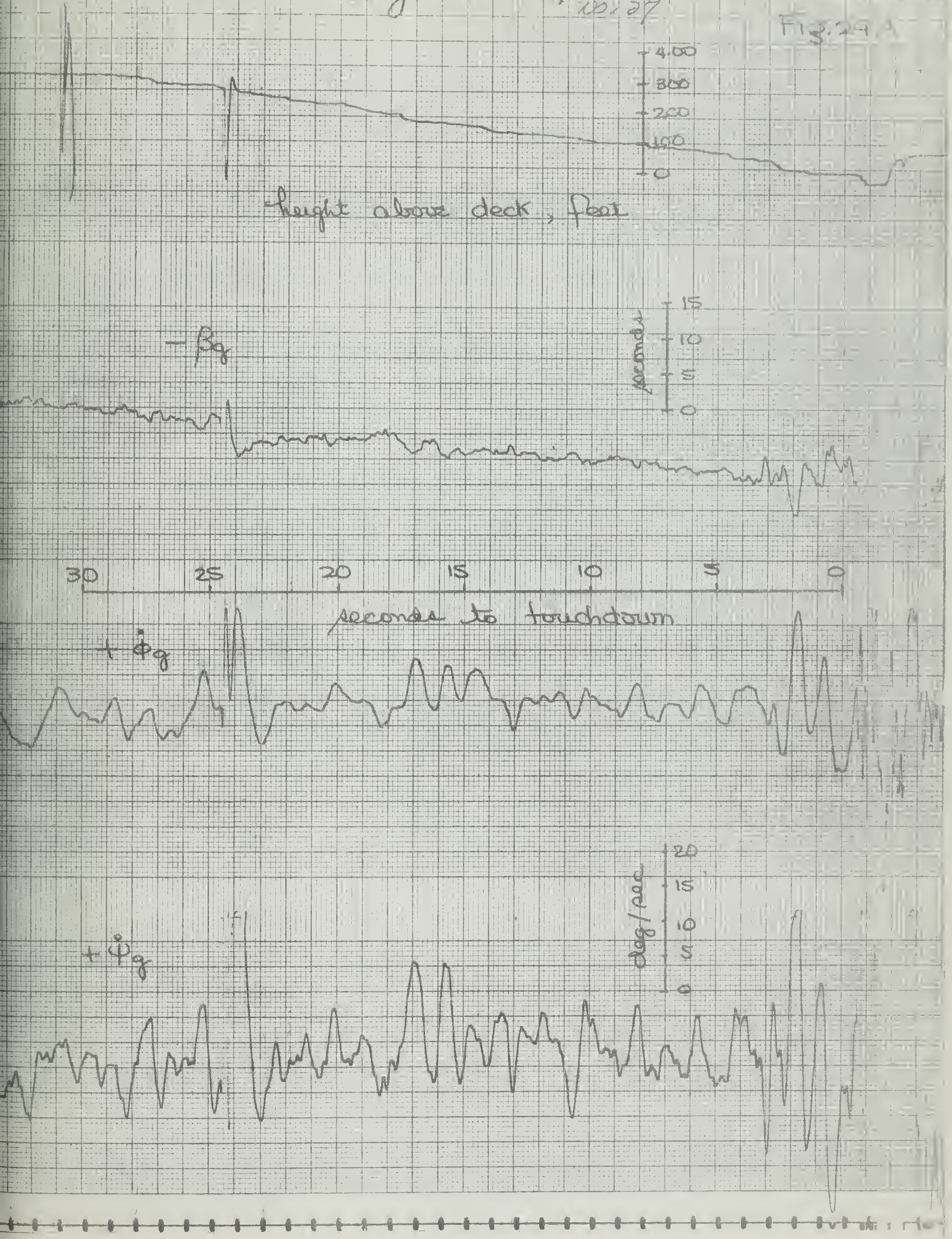

BUFFALO, NEW YORK PRINTED IN U S A

Fig. 29 B

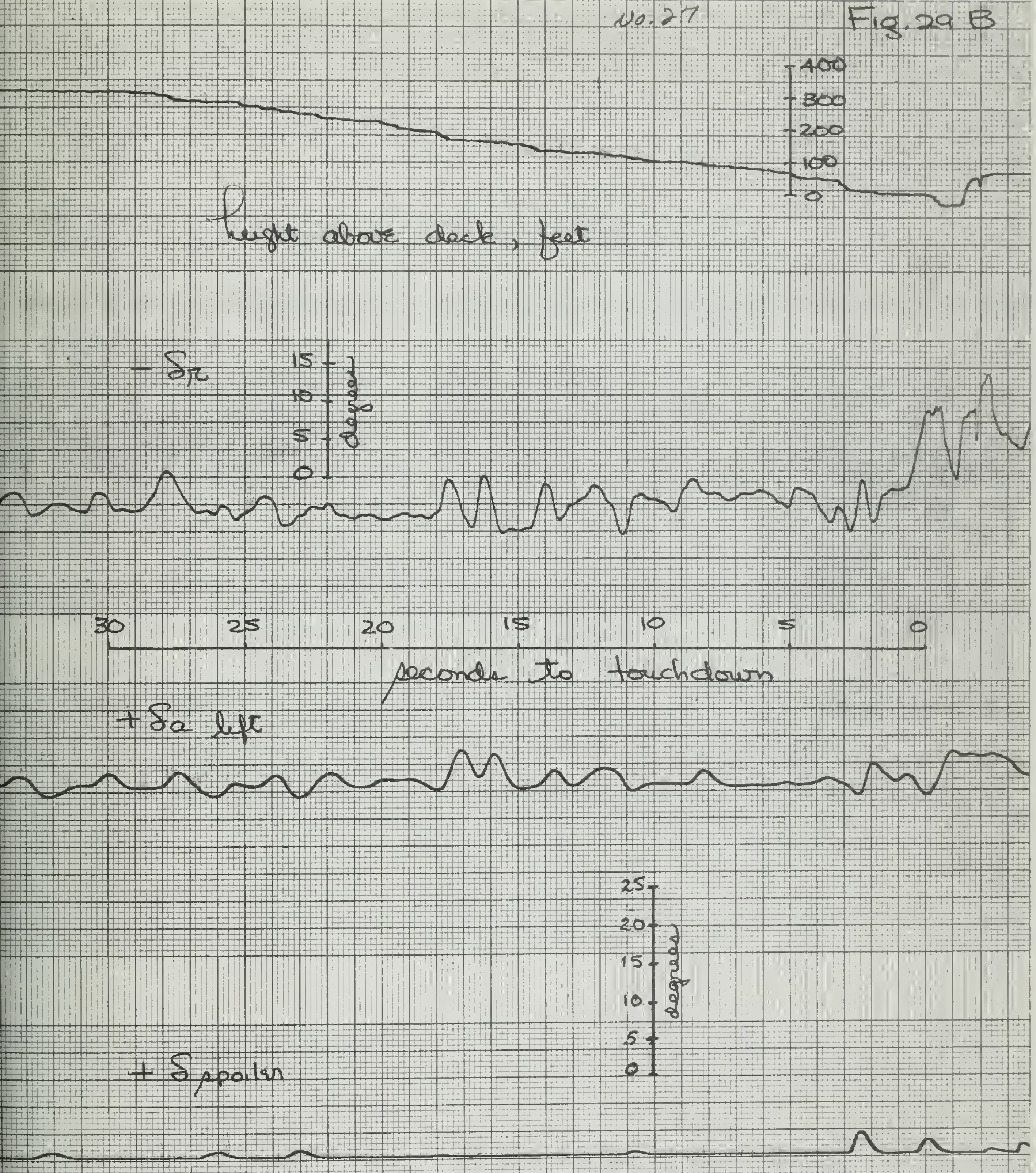

RT-No. 651-54

GRECORDING CHARTS | GRAPHIC CONTROLS CORPORATION

No. 27

Fig. 29 C

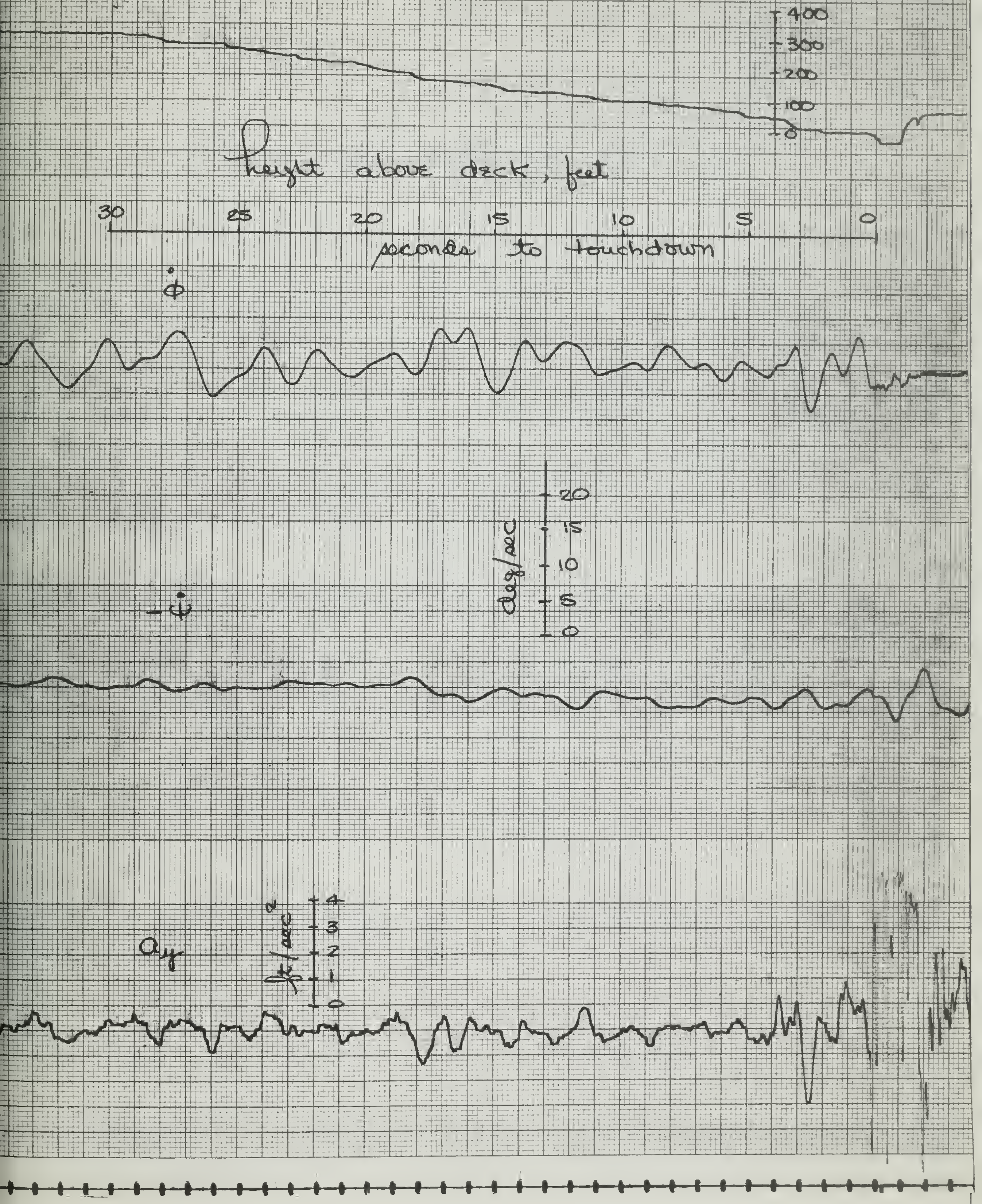

G RECORDING CHARTS | GRAPHIC CONTROLS CORPORATION | BUFFALO, NEW YORK

No. 27

Fig. 29D

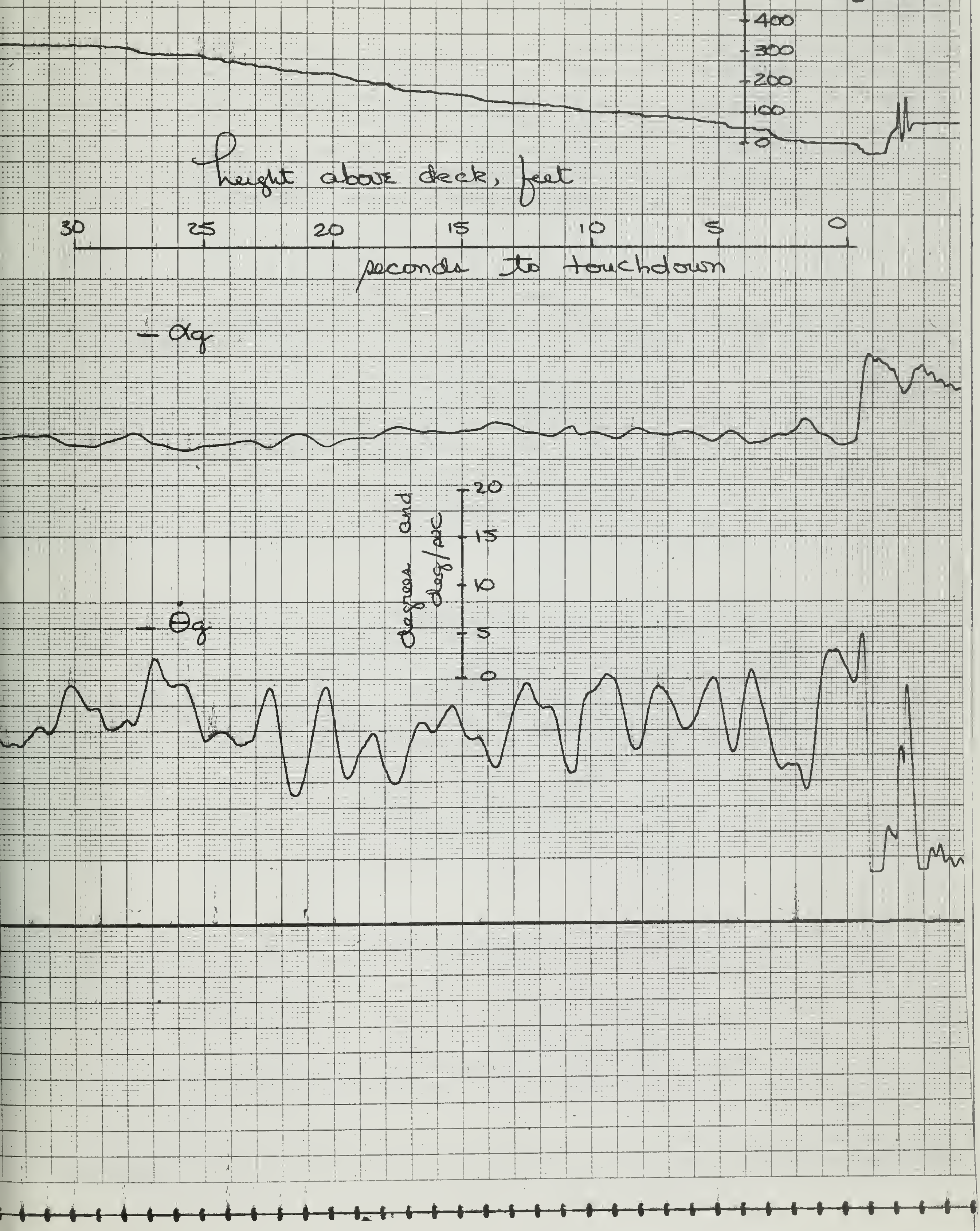

D, NEW YORK PRINTED IN U.S.A 651-14 RECO

NO. 27

Fig. 29E

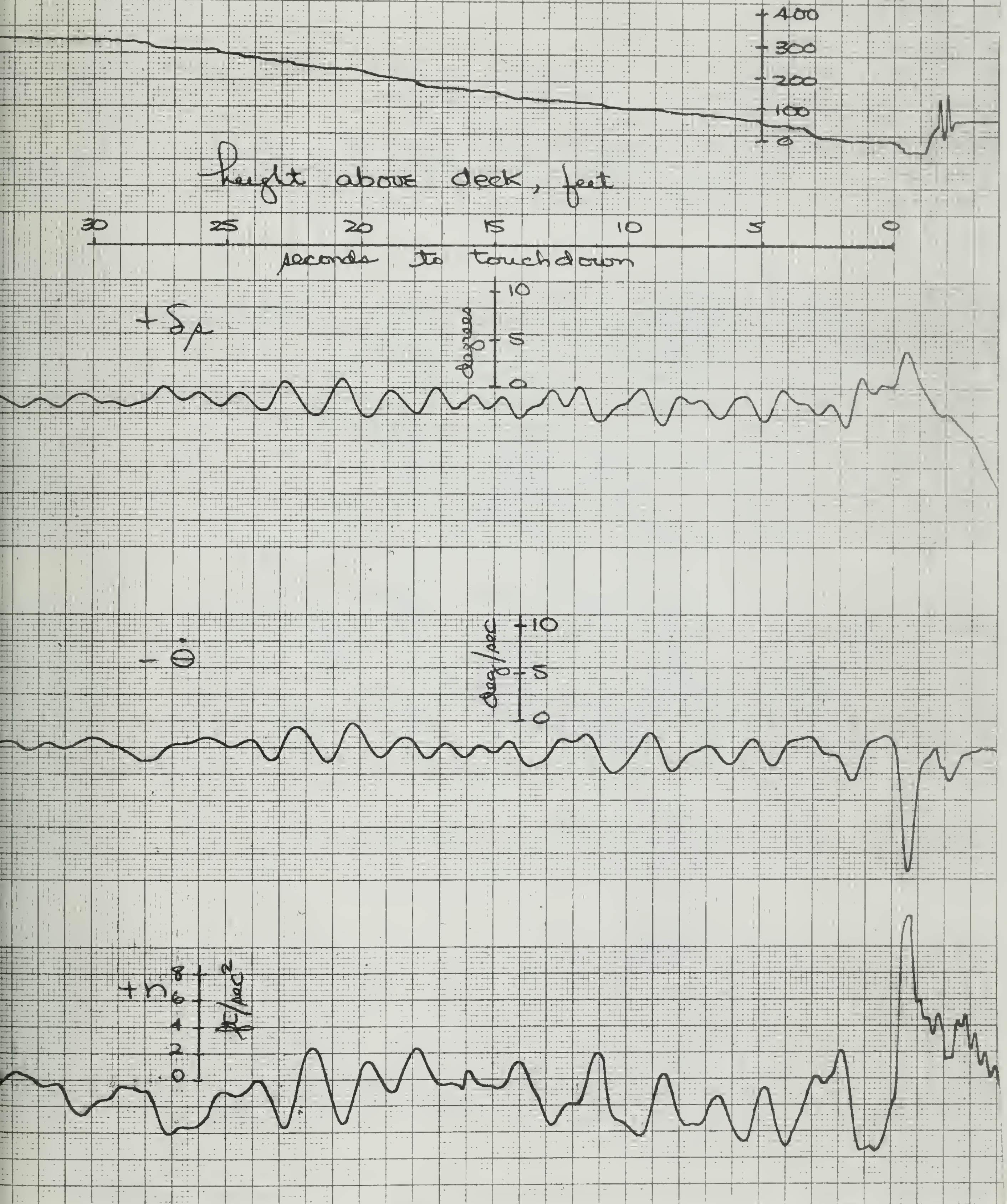

Lateral and Longitudinal Gust Quantities

Fig. 30A

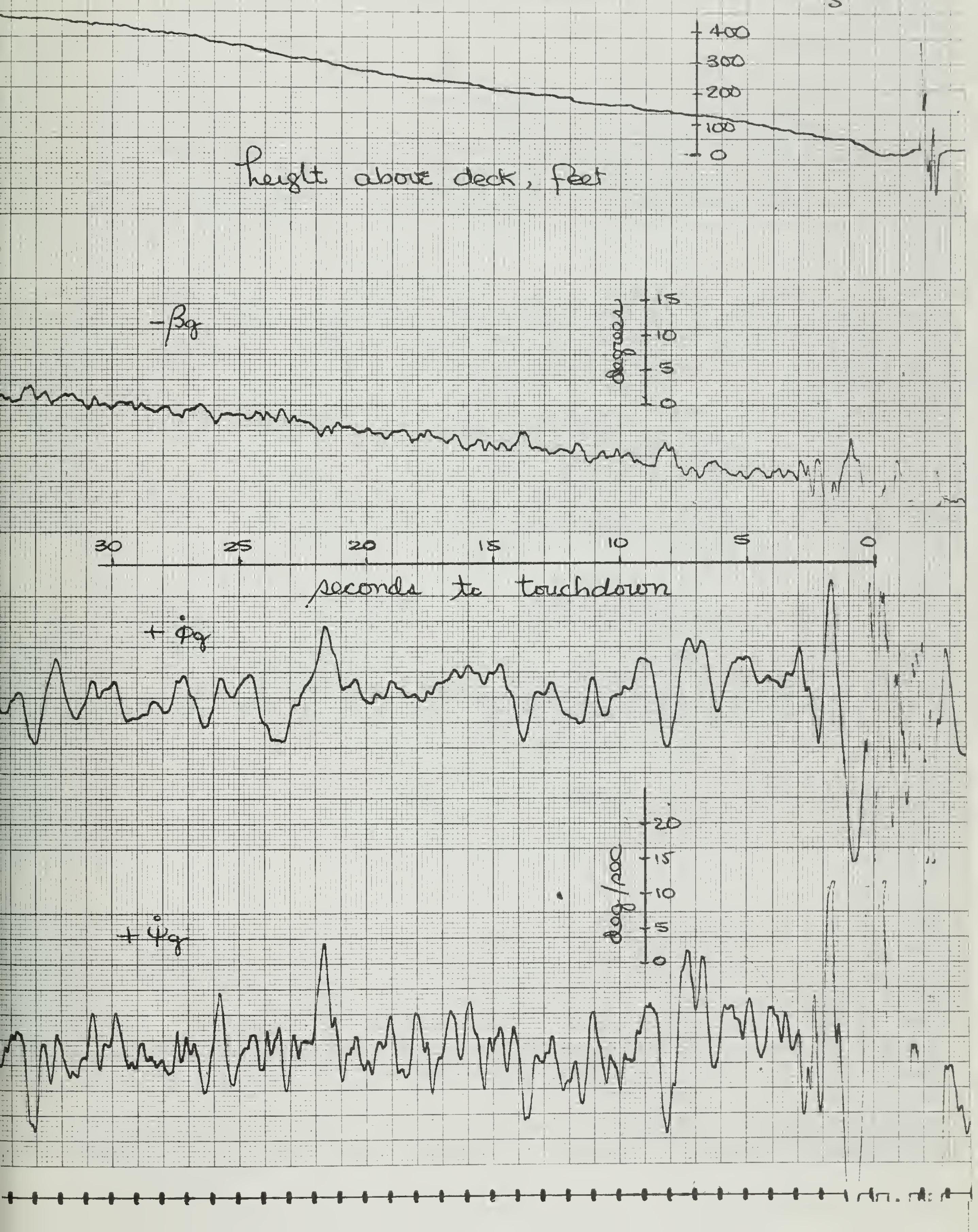

D IN U S A RECORDING CHARTS GRAPHIC CONTR

no. 30

Fig. 30 B

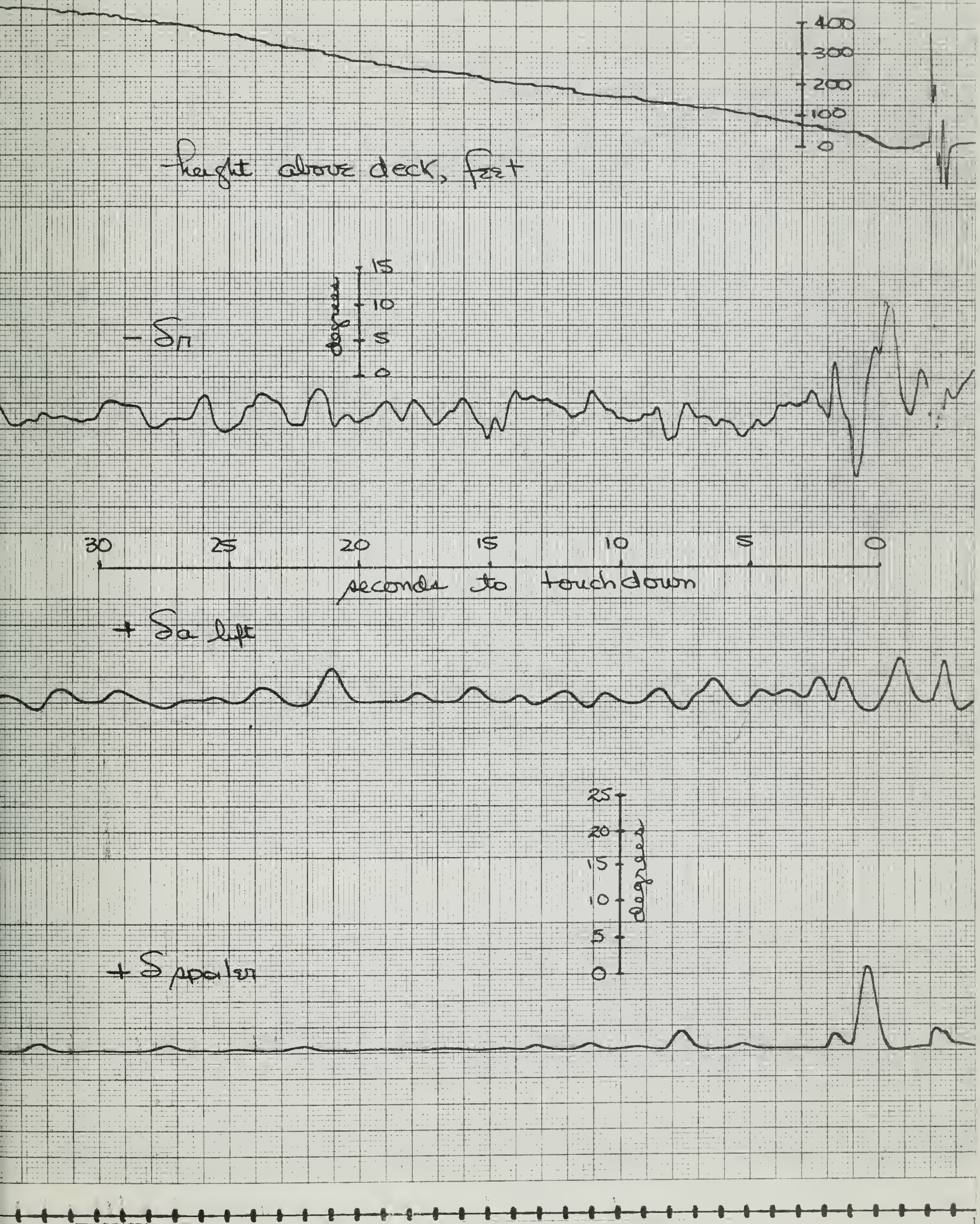

RECORDING CHARTS | GRAPHIC CONTROLS CORPORATION | BUFFALO, NEW YORK | PRINTED IN U.S.A.

No. 32

Fig. 30C

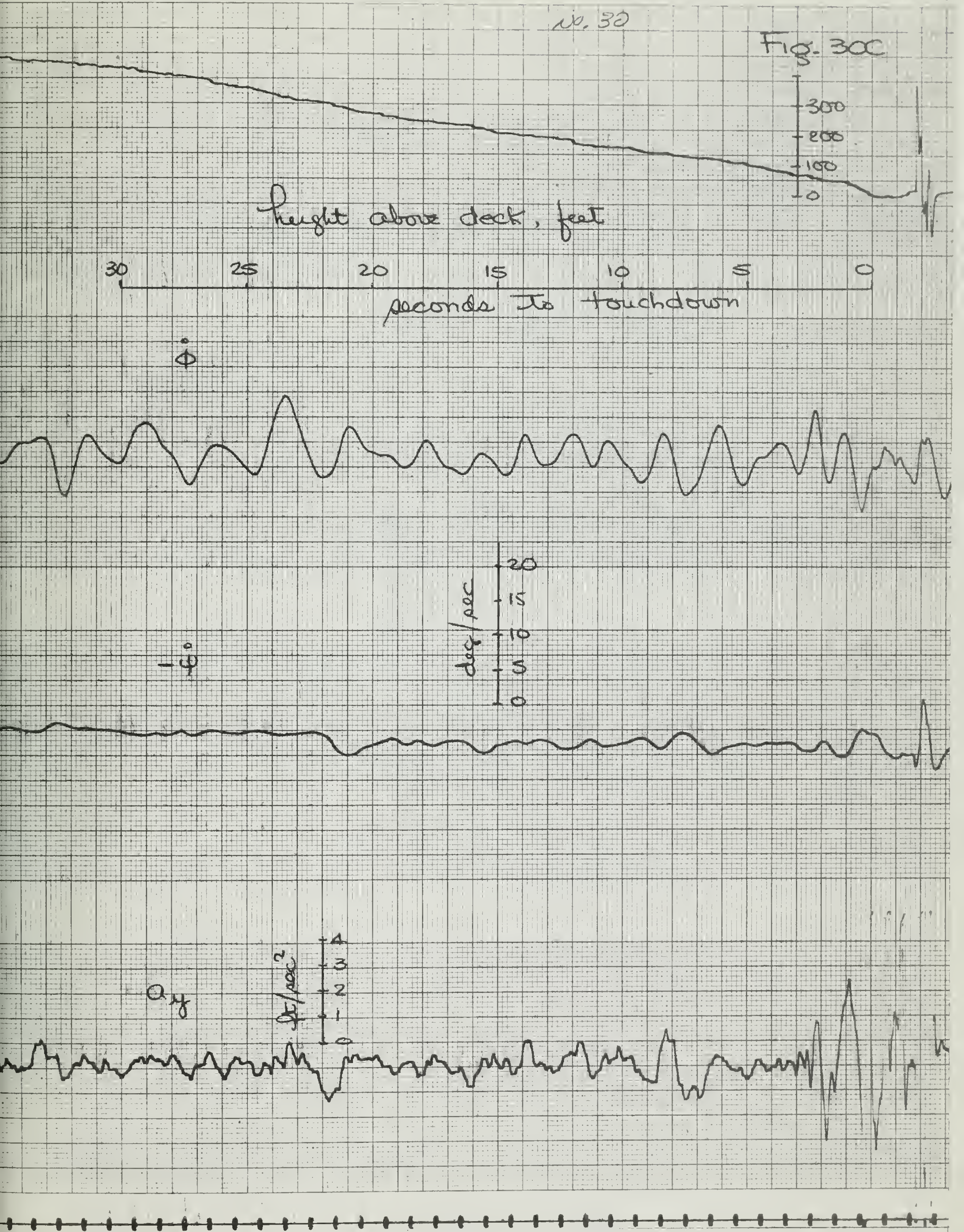

Fig. 30D

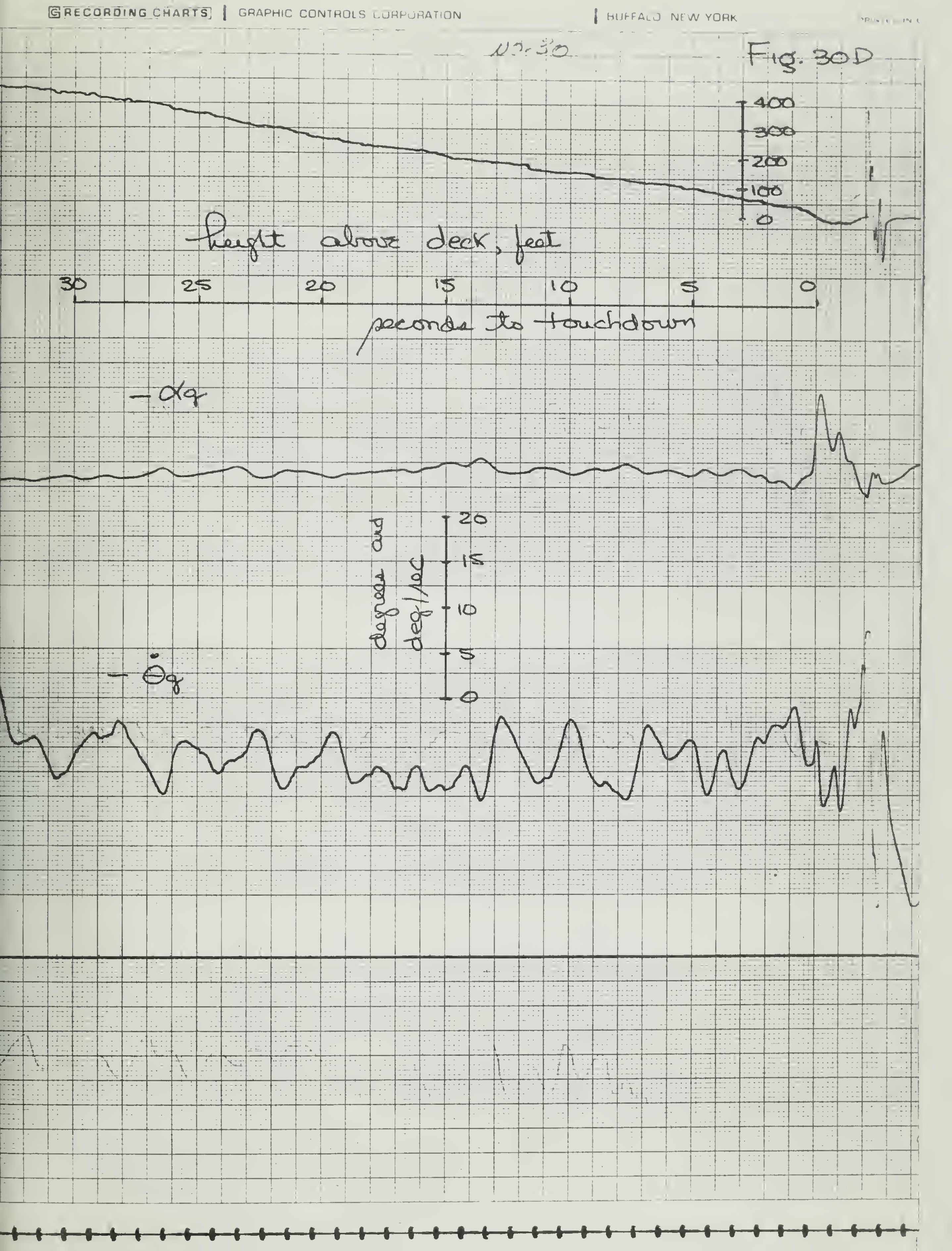
RECORDING CHARTS | GRAPHIC CONTROLS CORPORATION | BUFFALO NEW YORK
No. 30
400
300
200
100
0
height above deck, feet
30
25
20
15
10
5
0
seconds to touchdown
$-\alpha_q$
20
15
10
5
0
degrees and deg/sec
$-\dot{\theta}_q$

Fig. 30E

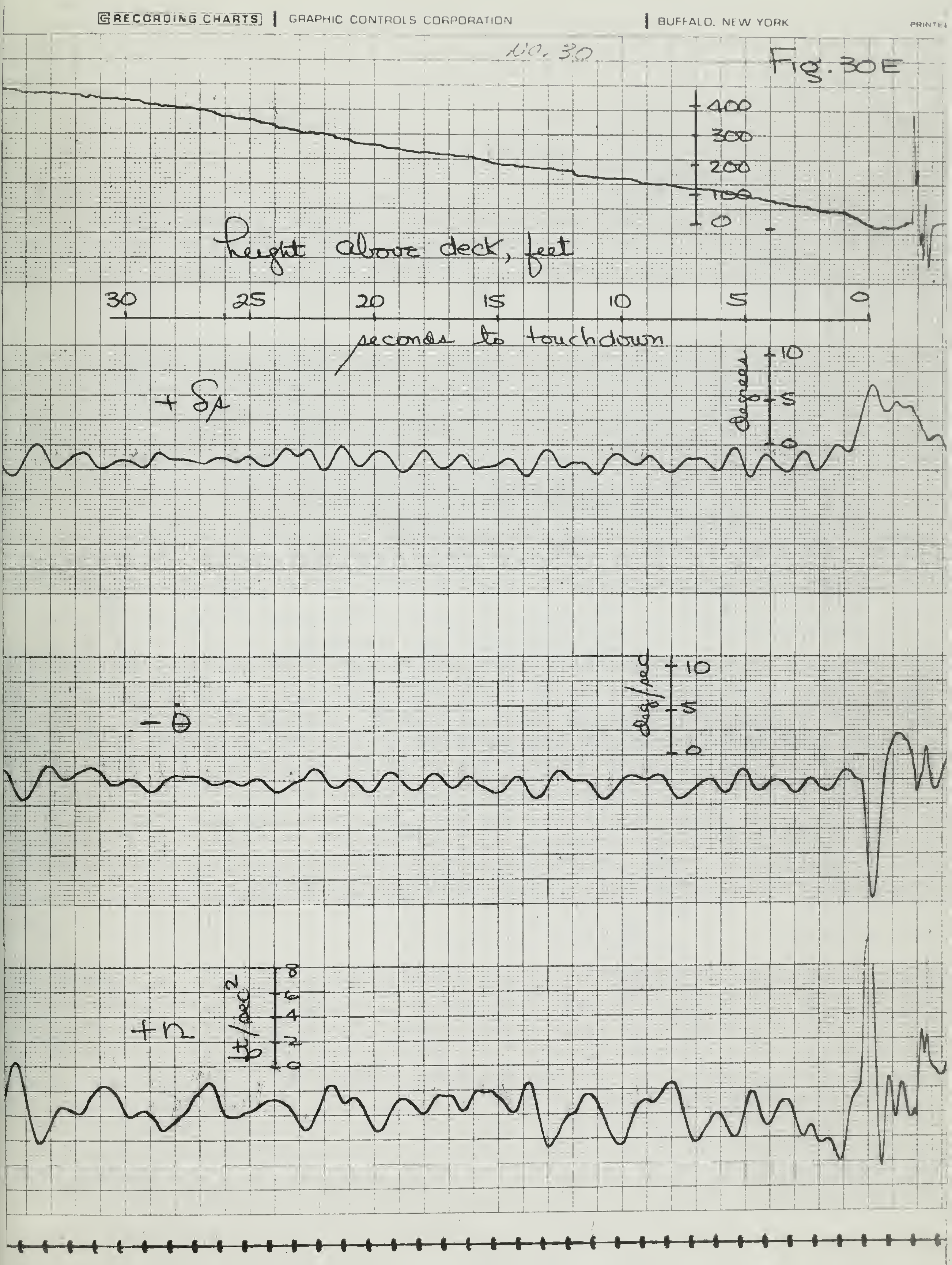
RECORDING CHARTS | GRAPHIC CONTROLS CORPORATION | BUFFALO, NEW YORK
NO. 30
400
300
200
100
0
height above deck, feet
30
25
20
15
10
5
0
seconds to touchdown
+ δs
degrees
10
5
0
− θ̇
deg/sec
10
5
0
+n
ft/sec²
8
6
4
2
0

© RECORDING CHARTS | GRAPHIC CONTROLS CORPORATION | BUFFALO N

Lateral and Longitudinal Gust Quantities

no. 31

Fig. 31 A

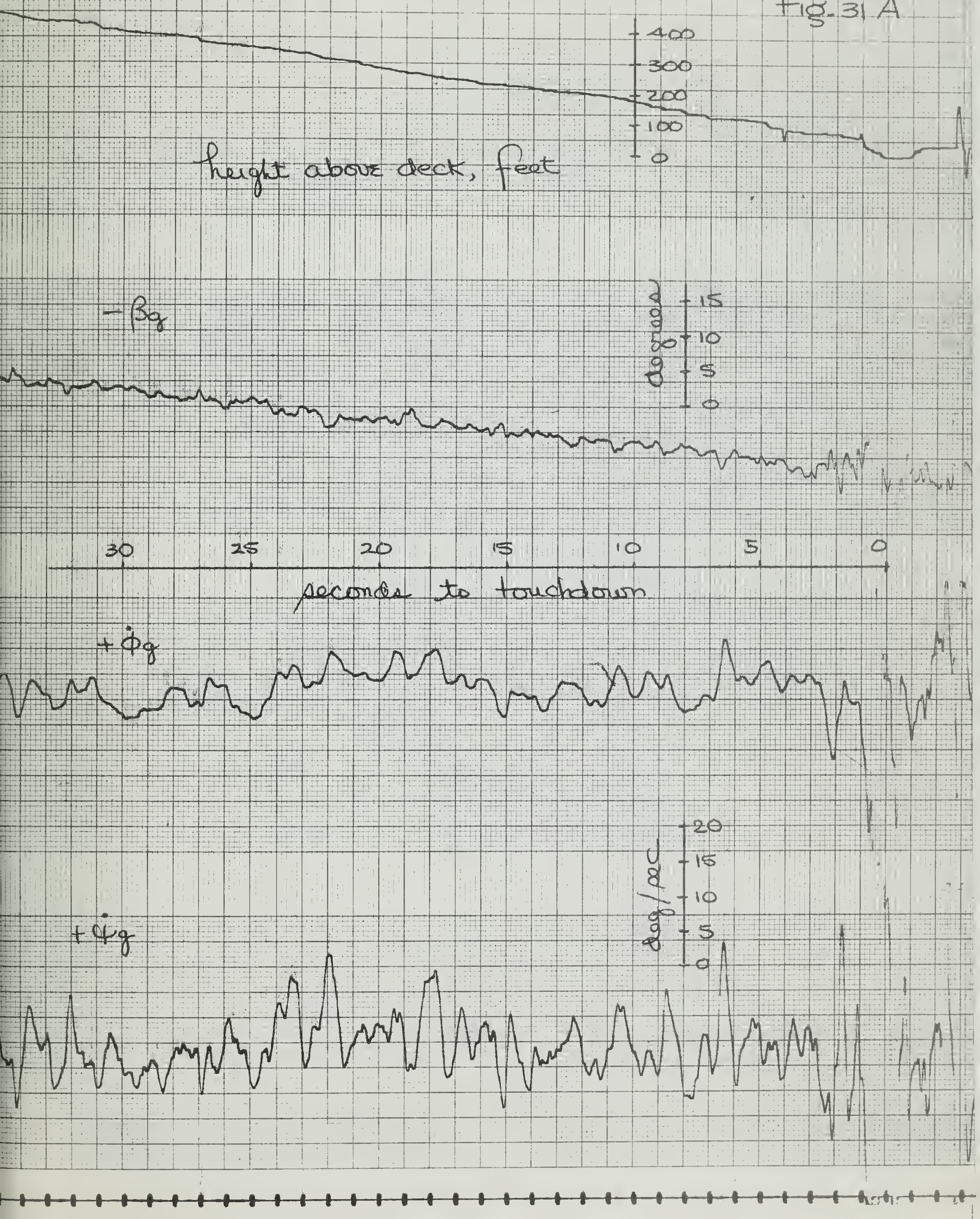

Fig. 31B

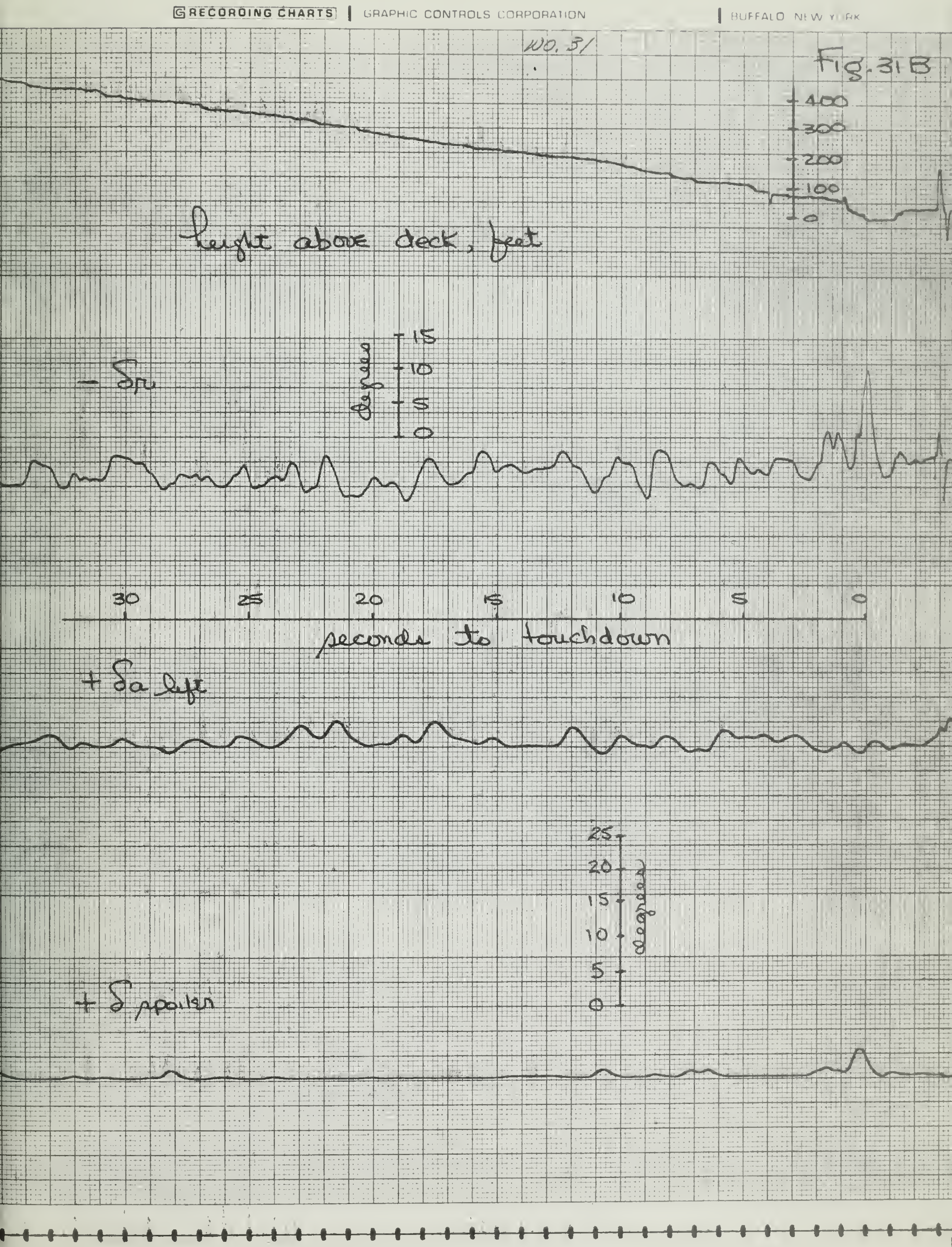
RECORDING CHARTS
GRAPHIC CONTROLS CORPORATION
BUFFALO NEW YORK
WO. 31
400
300
200
100
0
height above deck, feet
$-\delta_{ru}$
degrees
15
10
5
0
30
25
20
15
10
5
0
seconds to touchdown
$+\delta_a$ left
25
20
15
10
5
0
degrees
$+\delta$ spoiler

BUFFALO, NEW YORK PRINTED IN U S A

NO. 31

Fig. 31 C

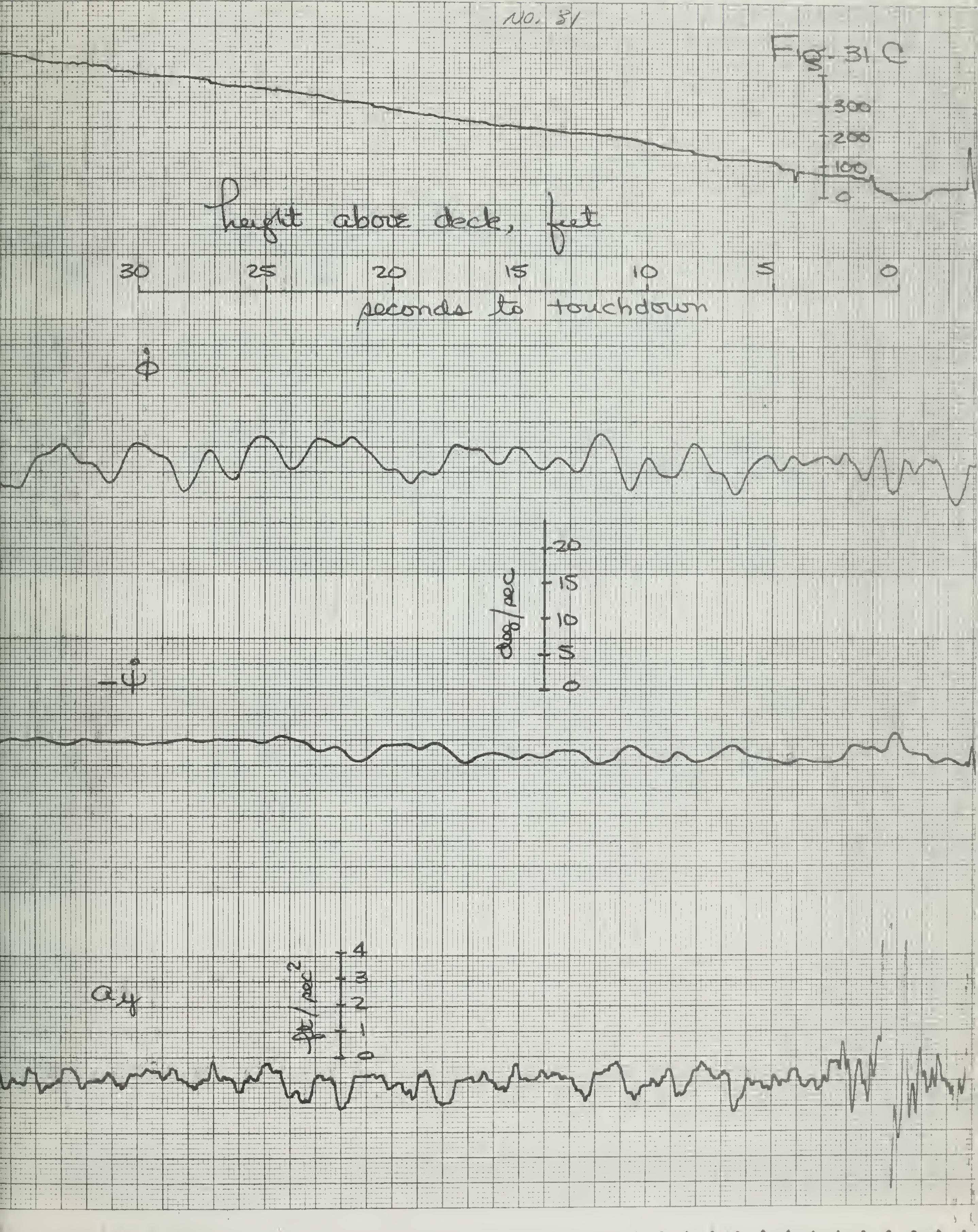

BUFFALO, NEW YORK PRINTED IN U.S.A.

No. 31

Fig. 31 D

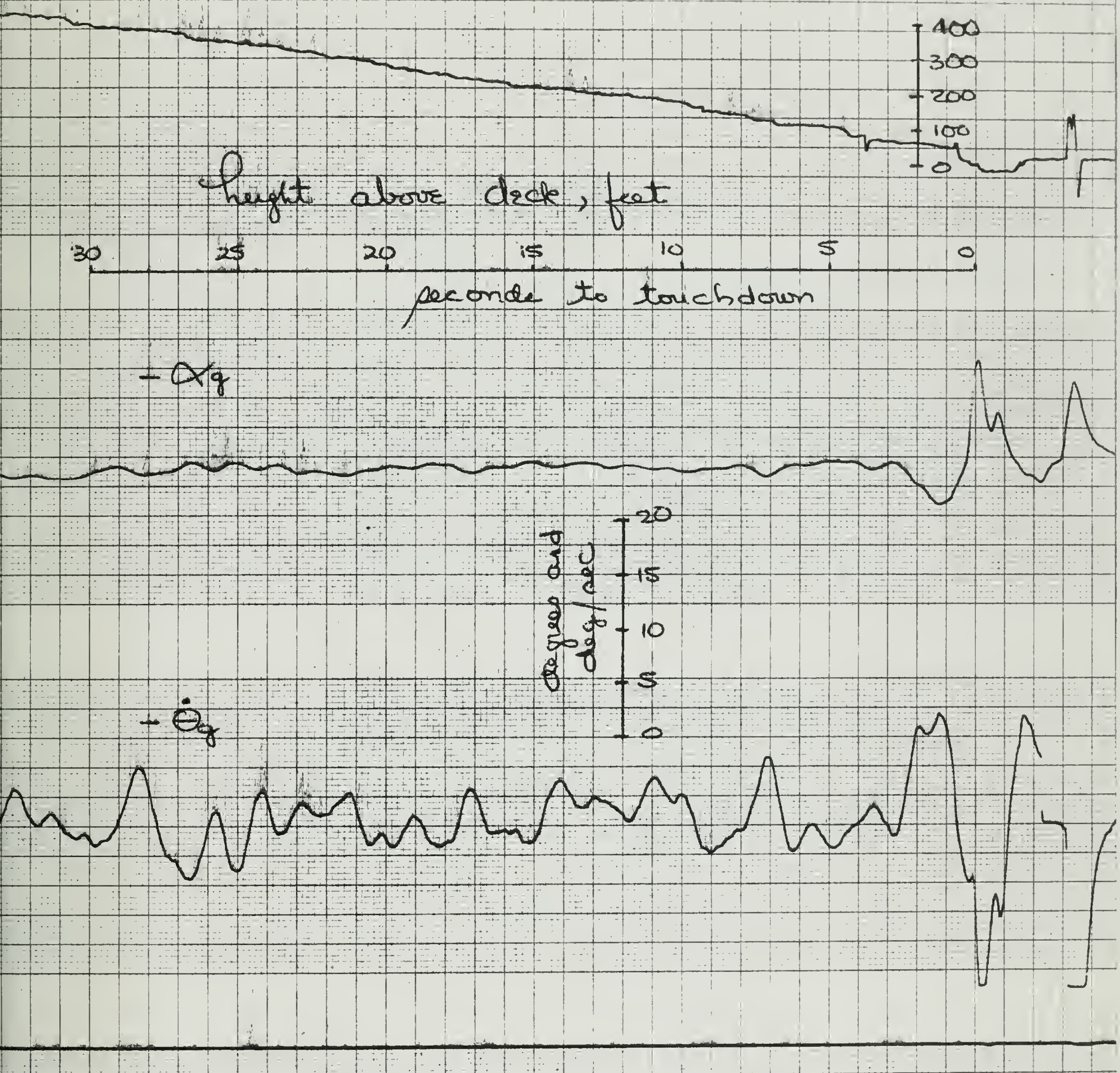

BUFFALO NEW YORK PRINTED IN U.S.A.

no. 31

Fig. 31 E

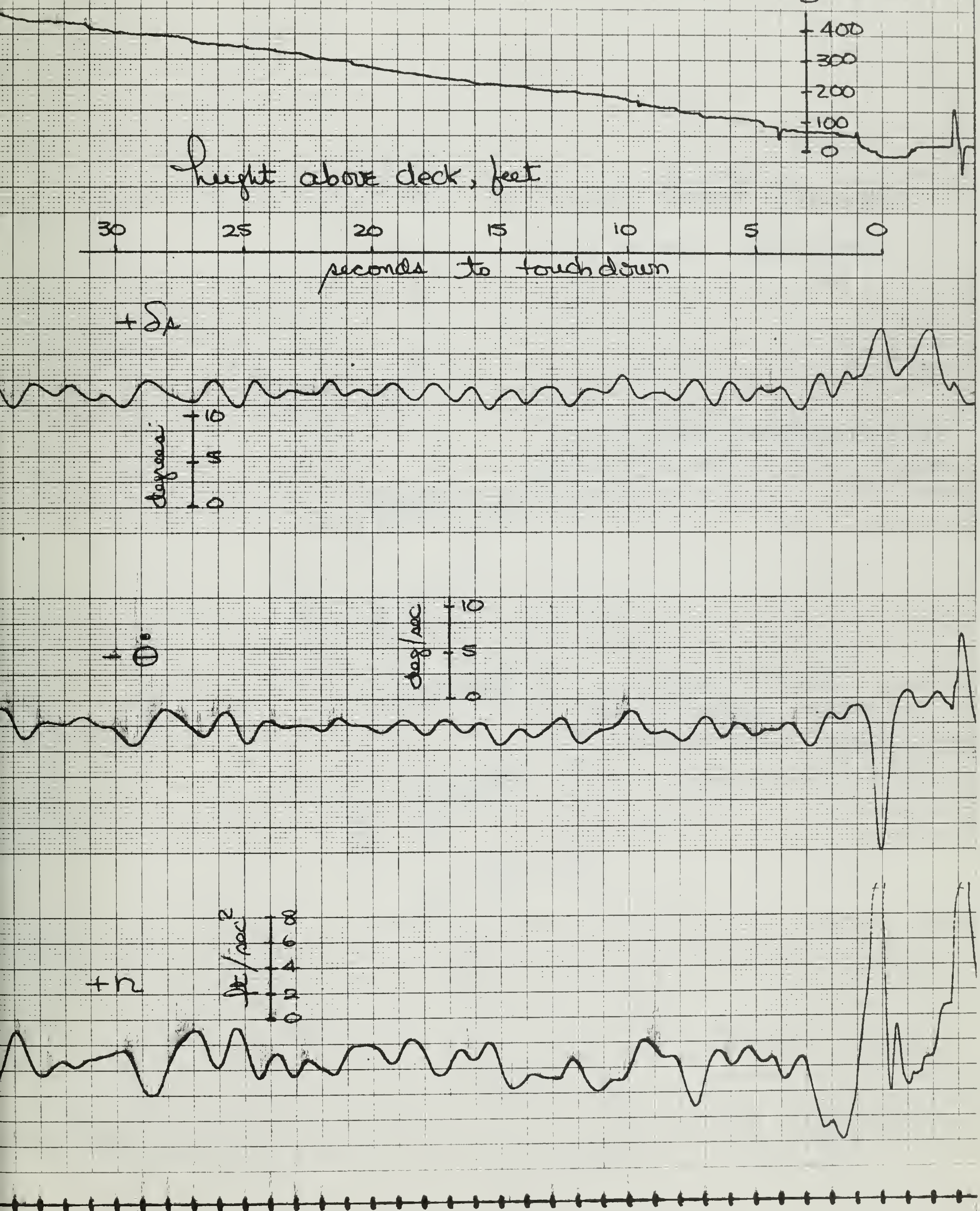

FIG. 32
Initial Burble Encounter for Various Approaches.

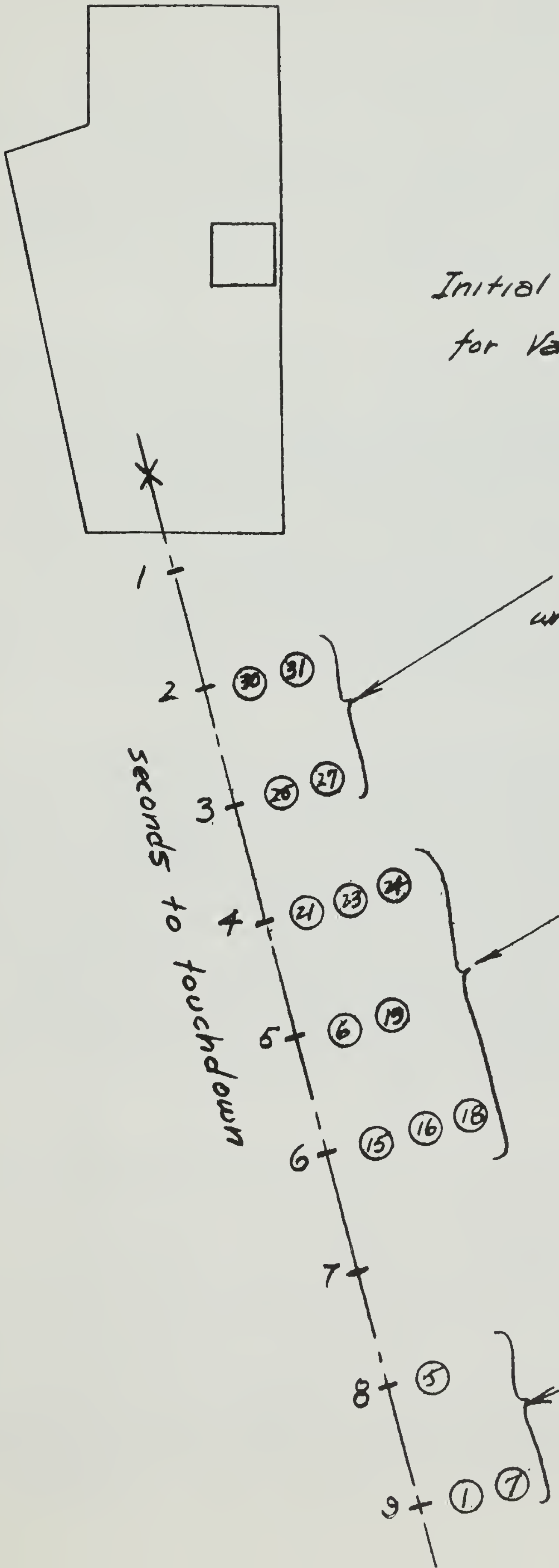
1
2 ㉚ ㉛
3 ㉖ ㉗
4 ㉑ ㉓ ㉔
5 ⑥ ⑲
6 ⑮ ⑯ ⑱
7
8 ⑤
9 ① ⑦
seconds to touchdown

These four approaches with right to left X-wind.

zero X-wind, normal relative wind along flight path. (23 to 28 knots)

zero X-wind, strong relative wind along flight path. (36 Knots).

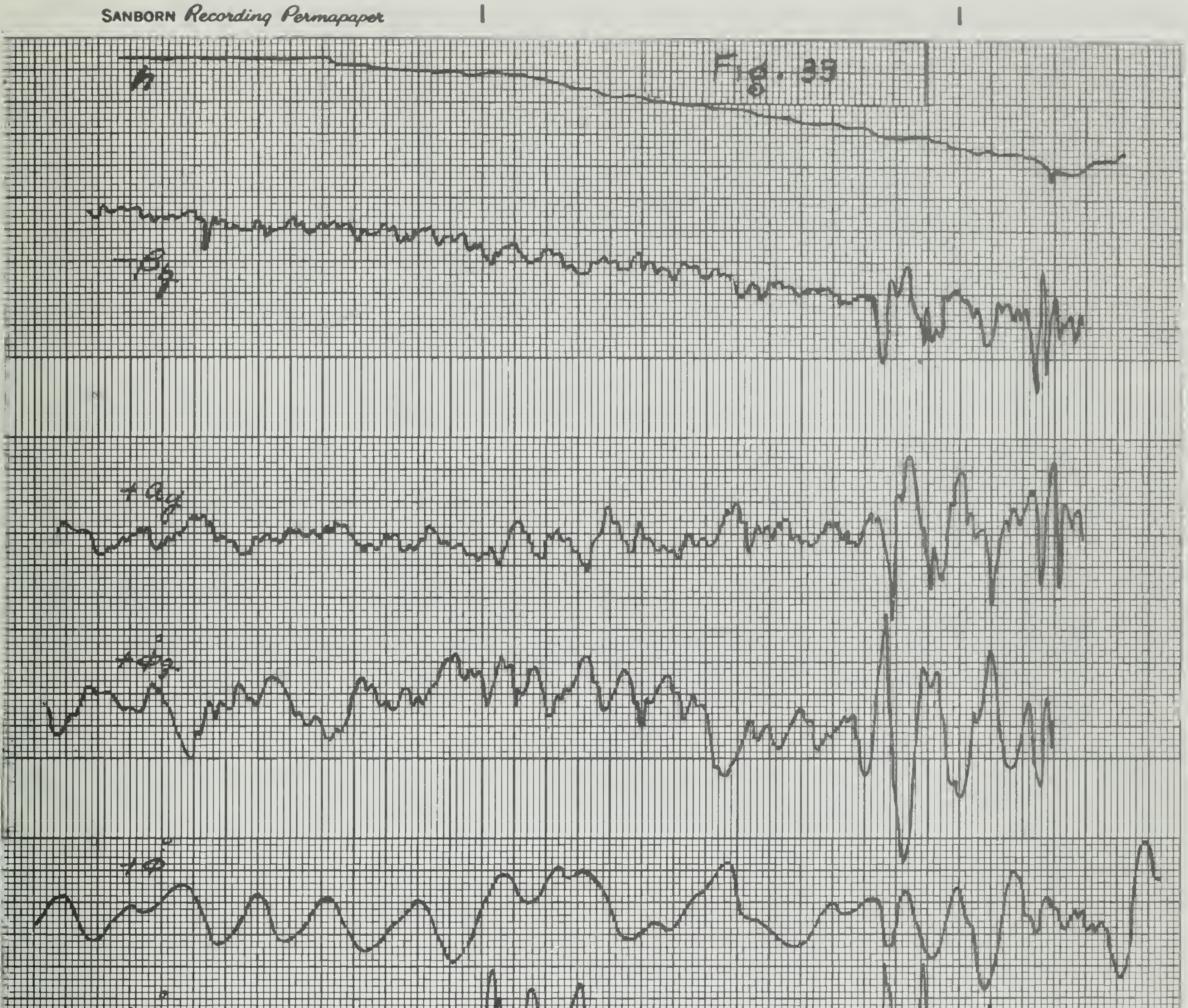

Fig. 33 Lateral and Longitudinal Gust Plot

thesO37
The acquisition, reductin, and analysis
3 2768 001 97477 7
DUDLEY KNOX LIBRARY